Distribution Agreement

In presenting this thesis or dissertation as a partial fulfillment of the requirements for an advanced degree from Emory University, I hereby grant to Emory University and its agents the non-exclusive license to archive, make accessible, and display my thesis or dissertation in whole or in part in all forms of media, now or hereafter known, including display on the world wide web. I understand that I may select some access restrictions as part of the online submission of this thesis or dissertation. I retain all ownership rights to the copyright of the thesis or dissertation. I also retain the right to use in future works (such as articles or books) all or part of this thesis or dissertation.

Signature:

_____ _____

Roxana M. Rodríguez Stewart Date

Non-canonical Triple-negative Breast Cancer Cell Death Induction by Reassortant Oncolytic Reovirus Generated by Forward Genetics

By

Roxana M. Rodríguez Stewart
Doctor of Philosophy

Graduate Division of Biological and Biomedical Sciences
Microbiology and Molecular Genetics

_____
Bernardo Mainou, Ph.D. Advisor

_____
Lawrence Boise, Ph.D. Committee Member

_____
Anice Lowen, Ph.D. Committee Member

_____
Carlos Moreno, Ph.D. Committee Member

_____
David Steinhauer, Ph.D. Committee Member

Accepted:

_____
Lisa A. Tedesco, Ph.D.
Dean of the James T. Laney School of Graduate Studies

_____
Date

Non-canonical Triple-negative Breast Cancer Cell Death Induction by Reassortant Oncolytic Reovirus Generated by Forward Genetics

By

Roxana M. Rodríguez Stewart
B.S., University of Puerto Rico-Río Piedras, 2015

Advisor: Bernardo A. Mainou, Ph.D.

An abstract of
A dissertation submitted to the Faculty of the James T. Laney School of Graduate Studies of Emory University in partial fulfillment of the requirements for the degree of Doctor of Philosophy in the Graduate Division of Biological and Biomedical Sciences in Microbiology and Molecular Genetics
2020

Abstract

Non-canonical Triple-negative Breast Cancer Cell Death Induction by Reassortant Oncolytic Reovirus Generated by Forward Genetics
By Roxana M. Rodríguez Stewart

Triple-negative breast cancer (TNBC) constitutes 10-15% of all breast cancer and is associated with worse prognosis when compared to other subtypes of breast cancer. Because of limited current therapy options, there is a need for targeted therapeutics to improve outcomes for TNBC patients. Mammalian orthoreovirus (reovirus) is a non-enveloped, segmented, dsRNA virus in the *Reoviridae* family. Reovirus selectively kills transformed cells and a serotype 3 reovirus is in clinical trials to assess its efficacy as an oncolytic agent against several cancers. To engineer reovirus with enhanced infective and cytopathic properties against TNBC cells, we coinfected TNBC MDA-MB-231 cells with prototype strains from three reovirus serotypes, Type 1 Lang (T1L), Type 2 Jones (T2J), and Type 3 Dearing (T3D). Following serial passage, we isolated two reassortant reoviruses, r1Reovirus and r2Reovirus, which contain gene segments predominately from T1L, with one (r2Reovirus) or three (r1Reovirus) gene segments from T3D and synonymous and nonsynonymous point mutations. Both reassortant reoviruses display enhanced infective and cytotoxic properties in TNBC cells. Additionally, combinatorial treatment with DNA damaging topoisomerase inhibitors enhances reovirus infectivity and cytotoxicity of TNBC cells. In a second study, we found that r2Reovirus infection of TNBC cells of a mesenchymal-stem like (MSL) lineage downregulates MAPK/ERK signaling and induces non-canonical cell death that is caspase-dependent, but caspase 3-independent. Furthermore, r2Reovirus blocks caspase 3 activity in a replication-dependent manner. Infection of other MSL lineage TNBC cells with r2Reovirus results in caspase 3-dependent cell death. We mapped the enhanced oncolytic properties of r2Reovirus in both TNBC cells to the T3D M2 gene segment in an otherwise T1L virus. Together, our findings suggest that the genetic composition of the host cell and interactions between host and viral gene products impact the mechanism of reovirus-induced cell death in TNBC cells. These studies identify a reassortant reovirus engineered by forward genetics with enhanced non-canonical, cell-dependent oncolytic properties in TNBC cells. Understanding how reovirus induces cell death will help define host and viral factors that promote enhanced oncolysis against TNBC, which will help generate a more effective and targeted viral oncolytic therapy that enhances the prognosis of TNBC patients.

Unconventional Triple-negative Breast Cancer Cell Death Induction by Reassortant Oncolytic Reovirus Generated by Forward Genetics

By

Roxana M. Rodríguez Stewart
B.S., University of Puerto Rico-Río Piedras, 2015

Advisor: Bernardo A. Mainou, Ph.D.

A dissertation submitted to the Faculty of the
James T. Laney School of Graduate Studies of Emory University
in partial fulfillment of the requirements for the degree of
Doctor of Philosophy
in the Graduate Division of Biological and Biomedical Sciences
in Microbiology and Molecular Genetics
2020

Acknowledgements

In addition to **God**, there are way too many people to thank for helping me before and throughout my graduate school journey. I believe that all the encounters I have had throughout my life have made me the person I am today and have helped me achieve all I have achieved. However, there's definitely people that have a more prominent and persistent impact. And these are…

1. **Mi familia,** who -on top of everything- instilled my faith and love for God. I would not be here without Him.
    a. My dad, Pablo, my mom, Marjorie, my sisters, Marjorie and Viviana, and my brother-in-law, Matt, have always been my biggest supporters. If I ever doubt myself, they always have the perfect words to help me start believing in myself again and their desire to help is endless. I really don't think I would've gotten so far in life without their love and support.
    b. My grandfather, Pablo, who is frequently calling and asking me about how my cells and viruses are doing and who always has great life and professional/academic advice for me.
    c. My niece and nephew, Emilia and Paul, who haven't been in my life as long, but have brought so much love and joy to my life. They've definitely made the not-so-good days a lot better!
    d. My extended family for their continued love, support, and investment in my success.
2. **My lab** (or my second family).
    a. Bernardo is definitely the best graduate school P.I. I could've asked for. Thank you for always striving to be the best mentor you can be, whether it is lab related or giving life advice. Jameson and I have always felt supported by you. Thank you for handling difficult conversations gracefully and always having pep talks after a not-so-great presentation, lab meeting, or a non-funded grant (sometimes even while I was crying). And of course, your constant jokes always made the lab a happy environment. Thank you for being such a great mentor!
    b. Jameson, my favorite lab mate! (Not only because you're the only one, haha). After years of being the only constant people in the lab, our science conversations turned into conversations on life decisions, faith, and too many "your face" jokes. You're definitely more of a friend than a lab mate and I can always rely on you for advice!
    c. Both, along with Angela, made the lab a great environment full of jokes (no non-mutilated banter, though!), laughter, and support. I've definitely been spoiled with my graduate school experience! Becoming influencers would've just been the icing on the cake..! #MainouLab #BestLabEver #SuperSeriousScience #BAMfam
3. **My committee**: Anice, Carlos, Dave, and Larry: thank you for all your helpful ideas, constructive criticism, and support. I really appreciate your help during my committee meetings and being available for additional one-on-one meetings. This project would definitely not be the same without your continued guidance!
4. The "**Party People**" who turned into more of "Sedentary People" after a few years in graduate school. Caro, Edgar, Elda, Jackie, Jessie, Luis (thank you for your edits!), and Seyi, I cannot imagine graduate school without you! Thank you for all the advice, girls' nights, laughs, parties in the multiple manors (and Buckhead), Tin Lizzy's margarita nights, and venting sessions.
5. My **best friends** since high school, Alexandra, Lorena, and Natasha. We have been through so much together and I really cannot remember a conversation that hasn't ended in laughter.

Even though our interests could not be more different, our sense of humor, advice, and support always gets us through our toughest times!

6. My **boyfriend**, Nick, who in the past few months has extended his role to editor. Thank you so much for your constant love and support and for cooking me dinner while I worked on this dissertation! I love being able to switch between talking about science and getting on a climb with you. Graduate school would've been so much harder without you in it and I am so thankful to have you in my life! ¡Te amo!

Table of Contents

List of Figures and Tables

Authorship Contributions

I co-first authored the publication in chapter II, which was published in Journal of Virology in November of 2019. I contributed by genotypic characterization of reassortant reoviruses through high-throughput sequencing experimentation and analysis and phenotypic characterization by assessment of reovirus attachment, infectivity, replication, and cytotoxicity. Data from these experiments are featured in Figures 1-5 and supplemental table 1. I wrote the introduction section of the manuscript in addition to methods and discussion for experiments I performed. I also participated in editing and review of the final draft.

I am the first author on the manuscript in chapter III. I contributed to project development, experimental design, data collection, interpretation, and statistical analyses. I designed all the experiments, generated all data, and performed statistical analyses for experiments featured in Figures 1-8. I designed and performed statistical analyses for all experiments in Figure 9 and generated one of the two recombinant viruses used in this figure. I wrote the original draft of all sections of the manuscript and participated in editing and review of the final draft.

I designed all the experiments, generated all data, and performed statistical analyses for all experiments featured in chapter V.

Chapter I. Introduction

Overview

Triple-negative breast cancer (TNBC) accounts for 10-20% of breast cancer cases and is associated with worse prognosis than other subtypes of breast cancer (1). Hormone therapies are not effective against TNBC, so treatment is largely limited to chemotherapy, surgery, and radiation therapy (2, 3). Infection with mammalian orthoreovirus (reovirus) is generally asymptomatic and preferentially kills transformed cells (4-11). Reovirus is currently in Phase I-III clinical trials to assess its efficacy as an oncolytic agent against a variety of cancers (https://clinicaltrials.gov). However, little is known about the oncolytic efficacy of reovirus against TNBC or the contribution of specific host and viral factors in inhibiting growth of TNBC cells during infection.

This work centers on understanding host and viral factors that drive oncolysis of reovirus in TNBC cells. The generation of a reassortant reovirus with enhanced infective and cytotoxic capacities in TNBC cells in chapter II showed that genetic reassortment between different reovirus strains and arising mutations can lead to an enhanced oncolytic virus in TNBC cells. This discovery raised questions of what host factors make TNBC cells susceptible to reovirus-induced cell death and what viral factors are involved in this enhanced cell death induction. Studies conducted in chapter III showed that even though a reassortant reovirus induces cell death with enhanced kinetics in various cell lines, its mode of cell death induction varies upon genetic makeup of the host cell. Additionally, the third chapter maps enhanced induction of cell death in TNBC cells to a specific viral genetic composition.

Understanding host cell and virus determinants that regulate cell death induction can be used to identify virus-host interactions that drive reovirus oncolysis in TNBC. This knowledge can be exploited in the development of improved viral oncolytics. Together, results from these studies will

help generate a more effective and targeted viral oncolytic therapy that enhances the prognosis of patients affected with TNBC.

Breast cancer

Breast cancer is the most common cancer and second most common cause of cancer-related deaths in women in the United States (https://seer.cancer.gov/). The National Cancer Institute estimates 279,100 new cases and 45,690 deaths caused by breast cancer in 2020. Based on 2018 NCI's Surveillance, Epidemiology, and End Results (SEER) data, approximately 12.8 percent of women born in the United States will be diagnosed with breast cancer at some point during their lifetime (https://seer.cancer.gov/csr/1975_2016/). Treatment against breast cancer include chemotherapy, hormone therapy, immunotherapy, radiation, surgery, and targeted therapy. The type of treatment a breast cancer patient undergoes is dependent on the type of cancer, disease stage, and presence of hormone receptors. Breast cancer is classified as one of three subtypes on the basis of estrogen receptor (ER), progesterone receptor (PR), and human epidermal growth factor receptor 2 (HER2)/neu expression: hormone-receptor positive (ER and PR positive), HER2/neu positive, or triple-negative (ER, PR, and HER2/neu negative). ER, PR, and HER2 status are important in determining prognosis and in predicting response to targeted hormone and HER2-directed therapies (12, 13).

Triple-negative breast cancer

Triple-negative breast cancer (TNBC) constitutes 10-15% of breast cancers and is known to have a higher rate of relapse and shorter overall survival after metastasis than other subtypes of breast cancer (1). TNBCs more frequently affect younger people, are more prevalent in African-American women, are generally larger in size, and are biologically more aggressive. Less than 30% of women with metastatic triple-negative breast cancer survive 5 years (14). TNBCs are highly diverse and are grouped into six subtypes based on differential gene expression and ontologies: basal-like 1

(BL1), basal-like 2 (BL2), immunomodulatory (IM), mesenchymal (M), mesenchymal stem-like (MSL), and luminal androgen receptor (LAR). BL1 subtype TNBCs are enriched in cell cycle and cell division components, while BL2 subtype displays unique gene expression of growth factor receptors and signaling. IM subtype TNBCs are enriched for genes involved in immune cell processes. M subtype TNBCs are heavily enriched in components and pathways involved in cell motility, extracellular matrix receptor interaction, and cell differentiation pathways, while MSL subtype TNBCs share with M subtype enrichment of genes involved in cell motility, cellular differentiation, and growth pathways in addition to genes linked to growth factor signaling pathways. Lastly, LAR subtype TNBCs are the most unique among TNBC subtypes, with gene expression heavily enriched in hormonally regulated pathways including steroid synthesis, porphyrin metabolism, and androgen/estrogen metabolism (14). The high level of diversity in TNBC complicates the development of targeted therapies. Currently, TNBC treatment is limited to cytotoxic chemotherapy, radiation, and surgery (2, 3). Among chemotherapeutic drugs used against TNBC are topoisomerase inhibitors, which cause DNA double-strand breaks during DNA replication (15). This class of drugs are effective against TNBC because although double-strand breaks can be repaired by homologous recombination, many cells belonging to the TNBC subtype have defects in proteins needed for this type of repair, such as BRCA1 protein (15). Because these treatments target replicating cells, they can be detrimental to both healthy and malignant cells.

Among the most studied TNBC cell lines are MSL subtype MDA-MB-231 cells (16). This cell line has mutations in *BRAF, CDKN2A, KRAS, NF2, TP53,* and *PDGFRA* genes (14). Germline *BRCA1* and *BRCA2* mutations are more frequent in TNBC (affecting up to 30% of TNBCs) than in other breast cancer subtypes (17). *BRCA1* dysfunction is associated with deficient DNA repair (18). For studies seeking to address the role of *BRCA1* mutations in breast cancer, BL1 subtype HCC1937 cells and MSL subtype MDA-MB-436 cells are widely used (19, 20). In addition to

BRCA1 mutation, HCC1937 cells also have mutations in *TP53, MAPK13,* and *MDC1* genes while MDA-MB-436 cells have mutations in *TP53* genes (14). The wide array of different mutations present in cells belonging to the TNBC subtype make this subtype highly heterogeneous and greatly impact the treatment response of each cell line. This makes the development of targeted therapies more challenging.

Oncolytic viruses

The concept of oncolytic virotherapy dates back to clinical reports of cancer regression that coincided with natural viral infections (21). Oncolytic viruses have selective tropism for cancerous cells and tissues through the exploitation of deregulated metabolic processes that characterize cancerous transformation (22). Oncolytic viruses preferentially infect and replicate in cancer cells due to their increased expression of viral receptors, increased expression of endocytic uptake molecules and proteases, altered metabolic states, and impaired antiviral innate immunity (22-24). Oncolytic viruses are grouped into wild-type viruses or their attenuated derivatives, or genetically modified viruses containing heterologous transgenes. For example, viruses have been engineered to encode efficacy-enhancing proteins, including cytokines such as such as granulocyte–macrophage colony-stimulating factor (GM-CSF), interferons (IFNs), and tumor necrosis factor (TNF) or prodrug-activating enzymes, such as β-glucuronidase, nitroreductase, and purine-nucleoside phosphorylase (9, 22, 23, 25, 26). In addition to having a direct effect on cancer cells, some oncolytic viruses can elicit an anti-tumor immune response or serve as adjuvants for other anti-cancer therapies (27). IMLYGIC, a genetically modified herpes simplex virus type 1 that replicates inside tumors and produces the immunostimulatory protein GM-CSF to induce an anti-tumor immune response, was the first viral oncolytic to gain FDA approval for treatment of melanoma (28). Various additional viruses, including vaccinia, herpes simplex virus type 1, reovirus, and Newcastle disease virus are under study to assess their oncolytic properties against several cancers (29, 30).

Despite the potential of oncolytic viruses, there are still many limitations, such as pre-existing antiviral immunity and non-specific viral tropism (31). We can exploit our understanding of tumor and virus biology to provide more targeted oncolytics by engineering viruses to specifically replicate in and kill cancer cells.

Overview of Reoviruses

The *Reoviridae* family includes 15 genera of dsRNA viruses that infect a wide variety of plants, animals, fungi, and protozoa (4). Mammalian orthoreovirus (reovirus) belongs to the *Orthoreovirus* genus, which contains viruses that infect birds, reptiles, and mammals. Reovirus was discovered in the early 1950's by Albert Sabin, Leon Rosen, and their colleagues from stool specimens of healthy and sick children (4, 32, 33). Although not generally associated with illness, reovirus has been found in children and adults with respiratory and gastrointestinal illnesses (34). Reovirus is an "orphan" due to its association with minimal or no disease, giving rise to the name respiratory enteric orphan virus (reovirus) (4).

Although reovirus is associated with minimal or no disease, some members of the *Reoviridae* family are pathogenic. Rotaviruses cause gastroenteritis in animals and humans. Rotaviruses are a leading cause of viral gastroenteritis among children younger than 5 and a major cause of infant illness and death (35). Four effective live-attenuated oral rotavirus vaccines (LAORoVs) (Rotarix®, RotaTeq®, Rotavac®, and RotaSIIL®) have been developed and licensed to be used against all forms of rotavirus-associated infection. However, vaccine implementation is limited in low-income countries partly due to the vaccine access and cost (36). Bluetongue virus, belonging to the orbivirus genus, infects cows, goats, and sheep. Severe animal morbidity and mortality and imposition of trade restrictions on animals from blue-tongue affected regions result in significant economic impact (37, 38). Colorado tick fever virus, belonging to the coltivirus genus, can cause neurologic disease in humans (39). Recent studies have associated reovirus infection with disruption of intestinal immune

homeostasis and initiation of loss of oral tolerance and T helper 1 (T_H1) immunity to dietary antigen, triggering development of celiac disease (5).

Reovirus structure and serotypes

Reovirus is a non-enveloped segmented double-stranded RNA virus (4). Reovirus virions have an icosahedral structure formed by two concentric protein shells, the outer capsid and inner core (40). The inner core encapsulates 10 gene segments, categorized based on size, that encode 8 structural and 3 non-structural proteins (33, 41). The three large (L) gene segments L1, L2, and L3 encode for the RNA-dependent RNA polymerase (RdRp) λ3, core spike λ2, and major inner-capsid λ1 proteins, respectively (4, 42-44). The three medium (M) gene segments M1, M2, and M3, encode for minor inner-capsid μ2, major outer-capsid μ1, and non-structural replication μNS proteins, respectively (4, 45, 46). The four small (S) gene segments S1, S2, S3, and S4 encode the attachment σ1 and nonstructural replication σ1s, major inner-capsid σ2, nonstructural replication σNS, and major outer-capsid σ3 proteins, respectively (4, 44, 47).

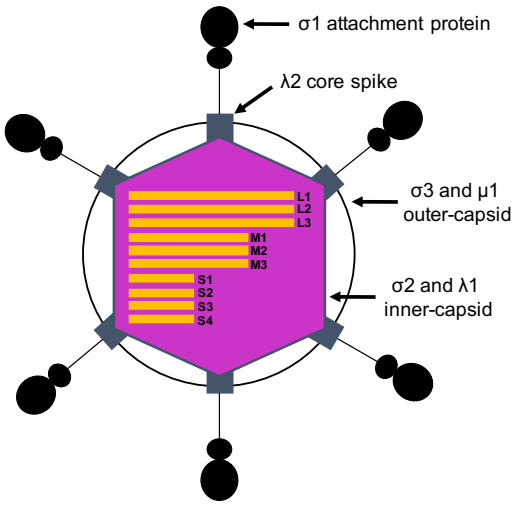

Fig. 1. Schematic representation of the reovirus virion. Reovirus particles are formed from two concentric protein shells, the outer and inner (core) capsid. The attachment protein (σ1; black), core

(σ2 and λ1; pink), core spike protein (λ2; gray), and outer capsid (σ3 and μ1; white) are indicated. The core encapsulates the viral genome, which consists of ten dsRNA gene segments (orange).

There are three different reovirus serotypes: Type 1, Type 2, and Type 3 based on the neutralization ability of antibodies raised against the σ1 attachment protein (4, 32, 33, 41). Prototype strains for each serotype refer to the children from whom the strain was initially isolated. Type 1 Lang (T1L) was isolated from a healthy child, whereas Type 2 Jones (T2J) and Type 3 Dearing (T3D) were isolated from children experiencing diarrheal disease (32, 48, 49). A fourth serotype, Type 4 Ndelle (T4N), has also been proposed (50). Despite extensive genetic and phenotypic similarities between reovirus serotypes, each serotype has distinct infective, replicative, and cell-killing properties (51-60). Cell surface carbohydrate binding varies from T1L to T3D, as well as primary cell death induction mechanism, strength of immune responses induced, and disease induction. Initial binding of reovirus to a host cell is driven by low affinity binding of σ1 attachment protein to cell-surface carbohydrates. T1L attaches to GM2 glycans on the cell surface while T3D interacts with α-2,3–linked sialic acid (61, 62). Differences in carbohydrate binding can lead to different cell tropism. Interestingly, a high expression level of α 2,3-sialic acid in breast cancer is associated with greater metastatic potential (63). T3D is more efficient at inducing apoptosis in a variety of cell lines (4), although T1L induces cell death with faster kinetics in some contexts (64, 65). Innate immune responses raised against reovirus also vary by serotype. T1L poorly induces Type I interferon (IFN) and strongly represses IFN signaling (66). Conversely, T3D strongly induces Type I IFN and a poorly represses IFN signaling (66). Differences in interferon repression have been attributed to the M1-enconded μ2 protein (67, 68). Reovirus has been shown to induce neurological disease in newborn mice. T1L and T3D reovirus strains invade the central nervous system (CNS) but use different routes of dissemination and produce distinct pathologic

consequences. T1L induces hydrocephalus, whereas T3D induces encephalitis (69-72). The S1-encoded σ1 protein is hypothesized to mediate tropism differences in the CNS by binding distinct receptors on the surfaces of ependyma and neurons (73). Routes of viral dissemination also differ between strains. T1L spreads by strictly hematogenous mechanisms, whereas T3D disseminates by both hematogenous and neural pathways (74). The differing properties between T1L and T3D make them useful for studying different aspects of reovirus biology.

Reovirus replication

The reovirus infectious cycle is mainly cytoplasmic and mostly occurs in viral factories (4). Reovirus attachment is mediated through low affinity binding of σ1 attachment protein to cell-surface carbohydrates which facilitates high affinity binding to its receptor junctional adhesion molecule-A (JAM-A)(62, 75). In neurons, reovirus attaches to Nogo receptor 1 NgR1 (76). Following attachment, virions enter cells by receptor-mediated and β1 integrin-dependent endocytosis (77, 78). Following endocytic uptake, activation of Src kinase is required for correct trafficking of virions to an endocytic compartment (79). Within acidified endosomes, virions are exposed to cathepsin proteases, cathepsin B, L, and S, which facilitate virion disassembly events (80, 81). The first disassembly intermediate is an infectious subvirion particle (ISVP), which is characterized by outer capsid modifications through loss of S4-encoded outer-capsid σ3 protein and cleavage of M2-encoded μ1 protein into μ1N and particle-associated fragments δ and φ derived from μ1C (80, 82). The ISVP subsequently turns into an ISVP* through further conformational changes, in which the viral particle loses σ1 and μ1 goes through further cleavage (83, 84). The μ1 cleavage fragments penetrate the endosomal membrane and viral core is released into the cytoplasm (85, 86). Once in the cytoplasm, the cores synthesize viral mRNAs using the negative-sense genomic RNA as a template (4). Viral nonstructural proteins μNS and σNS, encoded by M3 and S3 gene segments, respectively, form viral factories (VFs) or inclusions, which serve as sites for reovirus

transcription, translation, and assembly of progeny virions (46, 47, 87, 88). Reovirus egress from cells is poorly understood. Although it was hypothesized to occur mainly via cell lysis, it has been recently suggested reovirus can exit cells via nonlytic mechanisms (4, 89-91)

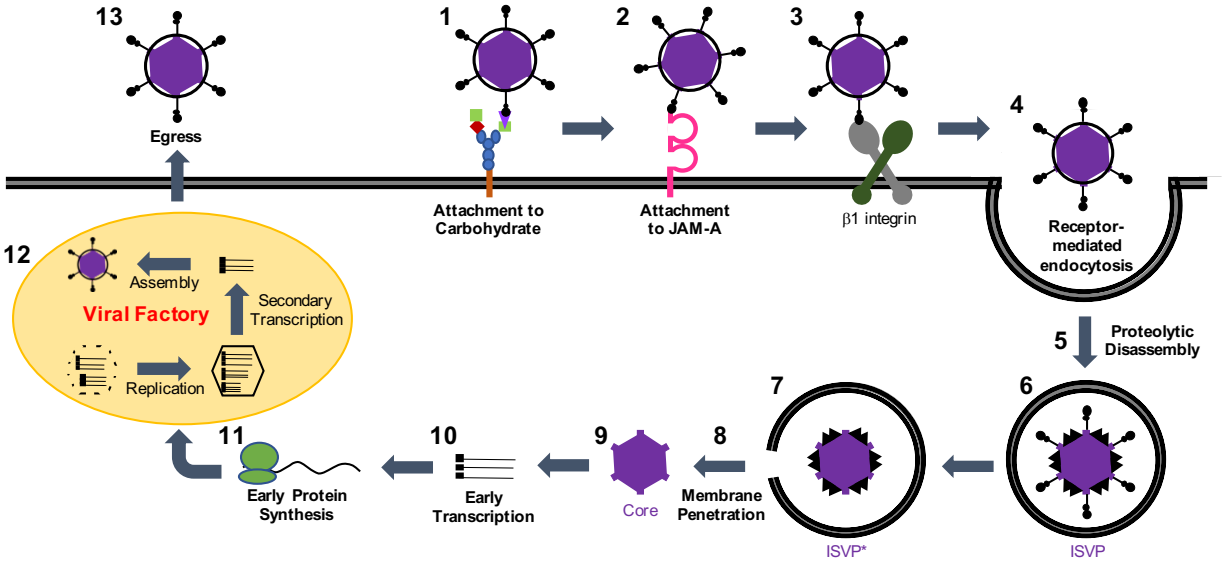

Fig 2. Schematic of reovirus replication cycle. Following attachment to (1) cell-surface carbohydrates and (2) JAM-A, virions enter cells by (3) β1 integrin-dependent, (4) receptor-mediated endocytosis. Following endocytic uptake, activation of Src is required for correct trafficking of virions to an endocytic compartment where virions undergo various (5) acid-dependent disassembly events. First, the virion turns into an (6) ISVP by outer capsid proteolytic processing. The ISVP subsequently turns into an (7) ISVP* through further conformational changes (8). The μ1 cleavage fragments penetrate the endosomal membrane and (9) the transcriptionally active viral core is released into the cytoplasm. Once in the cytoplasm, (10) early transcription and (11) translation occurs. Viral nonstructural proteins μNS and σNS form (12) viral factories, which serve as sites for reovirus replication and assembly of progeny virions. (13) Reovirus egress from cells is poorly understood.

Reovirus reassortment

Viruses with segmented genomes can undergo exchange of gene segments upon co-infection of the same cell through a process known as genetic reassortment. The progeny of these mixed infections are called reassortant viruses. The segmented nature of reovirus allows the generation of reassortant viruses with novel genotypic and phenotypic properties. Although all reoviruses have the same number gene segments, gene segments display high sequence variability between strains (92). Reovirus strains can be distinguished by the molecular weight of their gene segments in polyacrylamide gels, facilitating the determination of the parental origin of each gene segment following electrophoresis of genomic dsRNA of progeny virions (33). Because reovirus VFs are dynamic and individual VFs can interact transiently and undergo fusion events, reovirus reassortment has been partly attributed to fusion between viral factories within co-infected cells (93, 94).

Reovirus reassortment occurs in nature. However, the frequency of reassortment is unknown. Nonrandom associations of parental alleles observed in the L1–L2, L1–M1, L1–S1, and L3–S1 gene segment pairs shows reassortment is not entirely random, which may influence the evolution of reoviruses in nature (51). It is hypothesized that reassortant reoviruses obtained from co-infection of T1L and T3D commonly contain mutations that improve their fitness for independent replication. Reassortment of reovirus gene segments has been documented *in vitro* and *in vivo* (4). Co-infection of cells with different reovirus strains can yield new progeny virions with distinct genotypic and phenotypic characteristics from parental strains.

The process by which a virus is put under selective pressure, thereby driving evolution, is termed "forward genetics". This method is useful for identifying genes and mutations responsible for phenotypes of interest (95). Selection by forward genetics has been used for multiple studies and the generation of reassortant viruses with adaptations to host cells has been useful in studying

various aspects of reovirus biology (4). Forward genetics has been used for the generation of temperature-sensitive mutants, deletions mutants, cell-adapted mutants, and mutants resistant to denaturants (4). Forward genetics is useful to understand the genetic changes that yield a virus with specific host adaptations. Reverse genetics allows the engineering of recombinant viruses with specific genetic modifications and the identification of phenotypes as a consequence of these modifications (96, 97). The reovirus plasmid-based reverse genetics uses plasmids with a gene segment cDNA flanked by the bacteriophage T7 RNA polymerase promoter and hepatitis delta virus (HDV) ribozyme sequences (96, 98, 99). The 10 plasmids are transfected into baby hamster kidney (BHK) cells expressing T7 RNA polymerase. Transcription generates mRNA synthesis of reovirus genes with their authentic 5' ends. The HDV ribozyme undergoes self-cleavage to generate native 3' ends. The mRNAs are translated and launch reovirus replication. After a 2-5 day incubation period, cells are harvested by freeze-thaw lysis, viable viral clones are selected by plaque purification, and amplified using L929 cells (96, 98, 99).

Studies with reassortant and recombinant viruses are useful in mapping strain-specific phenotypic differences to specific viral gene segments. Studies using a T1L reovirus with a T3D M2 gene segment (T1L-T3M2) have shown interactions between T3D μ1 protein and T1L σ1 protein likely result in enhanced viral stability, attachment, and infectivity in L929 cells and HeLa cells (53, 100, 101). Additionally, the S1 and M2 gene segments have been implicated in strain-specific differences in reovirus-induced inhibition of cellular DNA synthesis and programmed cell death (56, 58, 59, 102, 103). More so, a recombinant reovirus with mutant μ1 ϕ domain is less efficient in inducing apoptosis, showing the ϕ domain of the μ1 protein plays an important regulatory role in reovirus-induced apoptosis and disease (103, 104). Studies using T1L × T3D reassortant viruses mapped the major determinant of CNS pathology to the viral S1 gene (105, 106). The use of forward and reverse genetics are useful techniques in the study of reovirus as an oncolytic.

Reovirus as an oncolytic

Reoviruses exhibit an inherent preference to replicate in tumor cells, which makes them ideally suited for use in oncolytic virotherapies (8, 9). Reovirus induces cell death in tumor cells with little cytotoxicity in normal, diploid cells (9). Of the three serotypes, type 3 reovirus has been the most studied as an oncolytic and a type 3 reovirus, T3C$, is the strain currently undergoing Phase I and II clinical trials against a variety of cancers (https://clinicaltrials.gov). However, the mechanism by which reovirus preferentially targets cancer cells is not fully understood. Overexpression of the reovirus proteinaceous receptor junction adhesion molecule-A (JAM-A) in cancer cells (75, 107), defective Ras/EGFR and Ras/Ral guanine exchange factor (RalGEF)/p38, Ras-driven protein kinase R (PKR) downregulation, and impaired type I IFN pathways positively influence reovirus tropism for some cancer cells (11, 108-114). Various aspects of reovirus biology, including virus uncoating, infectivity, replication, and apoptosis-dependent release from infected cells are regulated by Ras signaling (10, 11, 24, 111, 113-118). The K-Ras G13D and B-Raf G464V mutations found in MDA-MB-231 cells result in an upregulated Ras signaling, which increases tumor cell proliferation and survival in some cancers (119-124). Constitutively active Ras mutations have been identified in approximately 30% of all human cancers and mutations of elements upstream and downstream of Ras are prevalent in the majority of cancers (125). B-Raf regulates the Raf–mitogen-activated protein kinase (MAPK)/extracellular signal-regulated kinase (ERK) pathway through phosphorylation of MEK 1/2 (126). MAPK/ERK signaling promotes cancer cell proliferation, survival, and metastasis (127).

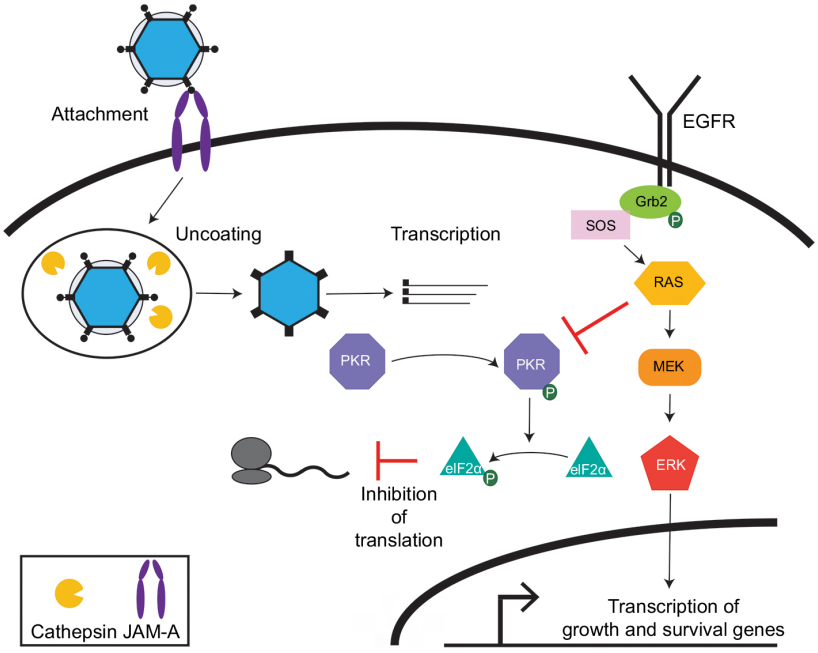

Fig. 3. Effect of Ras transformation on reovirus oncolysis. In normal cells, viral dsRNA is recognized by PKR, triggering its auto-phosphorylation and activation. Activated PKR phosphorylates eIF2α resulting in inhibition of protein synthesis. In Ras-transformed cells, viral uncoating during cell entry is enhanced by higher levels of cathepsins, viral protein synthesis is boosted by Ras inhibition of PKR, and programmed cell death is impaired. Ras also stimulates growth and survival of tumor cells. Signaling through EGFR can also activate Ras and enhance the oncolytic effects of reovirus. From Phillips MB, Stuart JD, Rodríguez Stewart RM, Berry JTL, et. al., 2018. (24)

Reovirus can also infect and kill cancer cells independent of Ras activation (65, 128-130). In some cells, expression of mutated Ras increases the sensitivity of tumor cells to reovirus-induced apoptosis, but is not required (131). In other cells, reovirus induces programmed cell death through the downregulation of Ras signaling (132). Reovirus can induce cellular cytotoxicity indirectly through activation of anti-tumor immune responses. Reovirus induces various immunological events that can overturn tumor-induced immunosuppressive mechanisms and promote antitumor immune

responses, such as secretion of proinflammatory cytokines and chemokines like interferon (IFN)-β and interleukin (IL)-8 and activation of dendritic cells, which in turn results in priming of tumor antigen-specific T cells and increase of the cytolytic activity of natural killer (NK) cells (133-139). This cell-mediated immunity triggered by reovirus makes it a good potential immunotherapy agent (140). Induction of cell death by reovirus is linked to p53-dependent NF-κB activation (141, 142) and activation of the IFN-stimulated response element (ISRE) in an interferon-independent manner and upregulation of IFN-stimulated genes (ISGs) via the PI3K/Akt/EMSY pathway (143).

Oncolytic reovirus pre-clinical studies and clinical trials

Pre-clinical studies performed with reovirus have shown it is an effective oncolytic against brain (144-146), breast (147, 148), colon (149, 150), ovarian (149), prostate (151, 152), bladder (153, 154), pancreatic (155-157), lung (158), and lymphoid (159) malignancies. Various pre-clinical studies have also shown reovirus oncolytic efficiency in combination with radiation and a variety of chemotherapeutic agents (160-163).

T3C$, a Type 3 reovirus, is being developed as an oncolytic by Oncolytics Biotech® under the name Reolysin® and can be delivered via intra-tumoral and intravenous administration (164). Although it has shown great potential as an oncolytic in preclinical studies, clinical trials have indicated that reovirus has limited oncolytic efficacy as a monotherapy (21). However, the proficiency of reovirus to sensitize cancer cells to chemotherapeutic drugs and radiation treatment makes it a good candidate for combination treatment (140). Reovirus has been shown to be more effective in preliminary studies in combination therapy than in monotherapy (164). All the current 10 clinical trials are testing Reolysin® in combination with various drugs. Of the mentioned clinical trials, six are in phase I and four are in phase II. Three of these clinical trials are being performed in patients with breast cancer (one phase I study and two phase II studies) at the time this dissertation is being written (https://clinicaltrials.gov).

Types of cell death induction by reovirus

Reovirus induces programmed cell death in a host cell-dependent manner. While the two major mechanisms of reovirus cell death induction are apoptosis and necroptosis, reovirus also induces cell cycle arrest and autophagy (56, 57, 102, 115, 165-175). Apoptosis is a cellular homeostatic mechanism that occurs normally during development and aging (176). Apoptosis is also a major cellular defense mechanism during cellular damage and pathogen infection (177, 178). Reovirus-induced apoptosis requires activation of transcription factors IFN regulatory factor 3 (IRF3) and nuclear factor–κB (NF-κB), suggesting that apoptosis is an essential component of innate immunity (165, 171, 179). Reovirus disassembly, but not subsequent replication steps, is required for NF-κB activation (180). Reovirus-induced apoptosis is mediated by TNF-related apoptosis-inducing ligand (TRAIL) (181, 182). Reovirus can trigger apoptosis through recognition of viral nucleic acid by cellular pattern recognition receptors and subsequent activation of caspase 8, Bid cleavage, and disruption of the mitochondrial membrane (182-184). This results in cytochrome c release, caspase 9 activation, and activation of executioner caspases 3 and 7, which cleave poly (ADP-ribose) polymerase (PARP). PARP cleavage inhibits DNA repair and results in apoptosis induction (4, 56-59, 102, 165, 166, 169, 171, 181, 185-191).

Alternately, reovirus induces caspase-independent cell death through induction of receptor interacting protein kinase 3 (RIPK3) and mixed lineage kinase domain like pseudokinase (MLKL)-dependent necroptosis (167, 168, 173). Necroptosis is a regulated necrosis that can occur in cells where apoptosis has been inhibited and exhibits morphological features of both apoptosis and necrosis (192). As observed in all types of necrosis, cells undergoing necroptosis are characterized by cell swelling and rupturing of plasma membrane (193). Additionally, necroptosis is activated through signaling from death receptors (e.g. Fas, tumor necrosis factor (TNF), and TRAIL), is not dependent on caspase activity, and requires kinase activity of RIPK1 or RIPK3 (194), (168, 195). Inhibition of

caspase 8 can shift cell death induction from extrinsic apoptosis to necrosis by activating RIPK3 and MLKL (196), (193, 197-200). Reovirus induction of necroptosis requires sensing of incoming viral dsRNA by retinoic-acid inducible gene I (RIG-I) and melanoma differentiation-associated protein 5 (MDA5) to produce type I IFN in a mitochondrial antiviral signaling protein (MAVS)-dependent manner (167, 168). During late stages of reovirus infection, newly synthesized genomic dsRNA is detected by an unknown interferon stimulated gene (ISG), which elicits RIPK3 and MLKL-dependent necrotic cell death (167).

Apoptotic signaling can be elicited by non-replicating virions while induction of necroptosis requires late synthesis of viral dsRNA produced during viral replication (167, 201). Cell death induction varies among reovirus serotypes. T3D activates initiator caspases and effector caspases to a significantly greater extent than T1L in several cell lines (168). Additionally, T3D has increased cytotoxic effects (168) and elicits an enhanced antiviral immune response (202) compared to T1L. Serotype-specific differences in apoptosis induction between T1L and T3D segregate genetically with the S1 gene-encoded σ1 attachment protein and nonstructural protein σ1s and the M2 gene-encoded μ1 outer capsid protein (56-59, 169). T3D also induces necroptosis with faster kinetics than T1L (168). Induction of cell death in TNBC by different reovirus strains has not been thoroughly characterized.

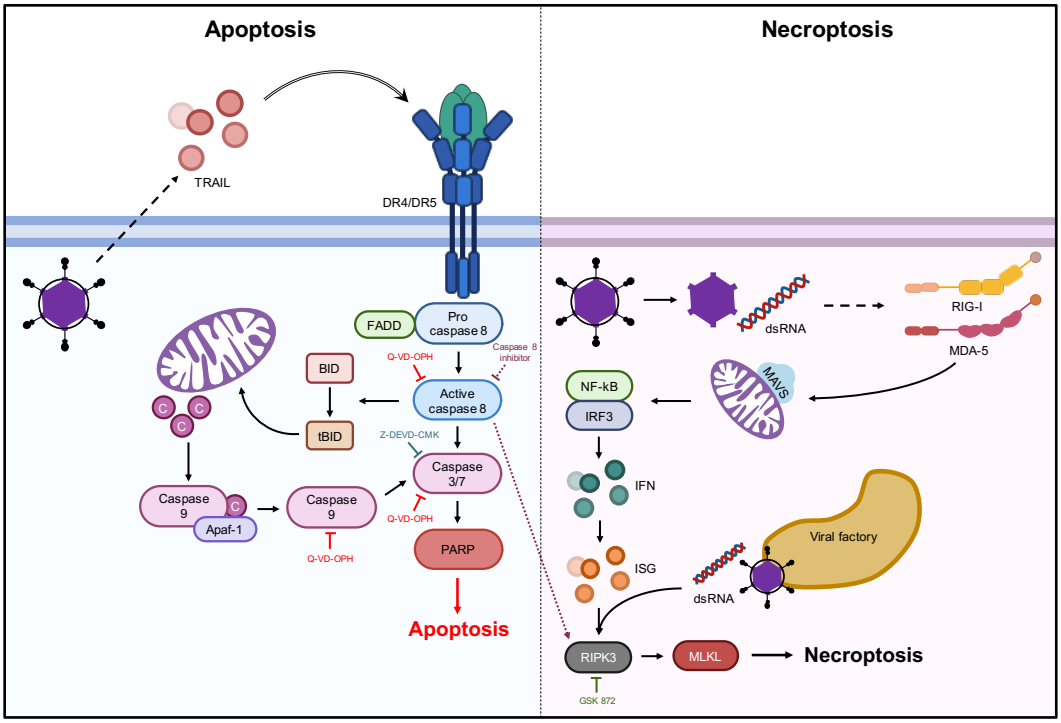

Fig. 4. Reovirus induction of programmed cell death by apoptosis and necroptosis. Upon infection, reovirus activates extrinsic apoptosis pathway through secretion of TRAIL, which attaches to DR4/DR5, resulting in caspase 8 activation. Activated caspase-8 cleaves Bid into t-Bid, which translocates to the mitochondria, resulting in the subsequent release of cytochrome c. Cytochrome c induces oligomerization of apoptotic protease activating factor-1 (Apaf-1), assembly of the apoptosome (composed of cytochrome c, Apaf-1, and deoxy adenosine triphosphate (dATP)), and activation of caspase-9. Both caspases 8 and 9 can activate caspase 3/7, which cleaves PARP and results in apoptosis. Alternatively, reovirus infection can result in necroptosis induction through RIG-I and MDA-5 sensing of incoming viral dsRNA resulting in production of type I IFN in a MAVS-dependent manner. Newly synthesized genomic dsRNA is detected by an unknown ISG, which elicits RIPK3 and MLKL-dependent necrotic cell death.

Introduction to dissertation project

The goal of this project was to use reovirus to make a more efficient and targeted oncolytic

therapy against TNBC to address limited treatment options available to TNBC patients. We engineered a reassortant reovirus with enhanced oncolytic capacities in TNBC and characterized the virus genotypically and phenotypically. In the first study, we engineered reoviruses with enhanced replicative and cytotoxic properties in TNBC cells by serially passaging prototypic strains from three reovirus serotypes (T1L, T2J, and T3D) in TNBC MDA-MB-231 cells. We isolated two reassortant viruses, r1Reovirus and r2Reovirus, which have reassorted gene segments from parental reoviruses T1L and T3D and several synonymous and non-synonymous point mutations. Both reassortant reoviruses have enhanced infective and cytotoxic properties in TNBC cells. Furthermore, combination of r2Reovirus with topoisomerase inhibitors enhances viral infectivity and cytotoxicity in these cells. This work identified a less cytotoxic, more targeted, and more efficacious therapeutic against TNBC using a reassortant reovirus in combination with topoisomerase inhibitors.

In the second study, we describe key aspects of cell death mechanisms of r2Reovirus in TNBC cells. We show the genetic composition of the host cell greatly impacts the type of cell death induced by reovirus. Infection with r2Reovirus downregulates the MAPK/ERK pathway in TNBC MDA-MB-231 cells and induces a non-conventional cell death that is caspase dependent, but independent of mitochondrial membrane potential disruption, cytochrome c release from the mitochondria, and caspase 3 activation. In TNBC MDA-MB-436 cells, r2Reovirus infection results in mitochondrial membrane potential disruption and caspase 3-dependent cell death. We also mapped the enhanced oncolytic properties of r2Reovirus in TNBC to the T3D M2 gene segment in the context of an otherwise T1L virus. Together, these studies identify an engineered reassortant reovirus with enhanced non-canonical, cell-dependent oncolytic properties in TNBC cells that segregate with specific viral factors. Results from these studies will aid in the development of an improved viral oncolytic therapeutic against TNBC.

References

1. Abramson VG, Lehmann BD, Ballinger TJ, Pietenpol JA. 2015. Subtyping of triple-negative breast cancer: implications for therapy. Cancer 121:8-16.
2. Wahba HA, El-Hadaad HA. 2015. Current approaches in treatment of triple-negative breast cancer. Cancer Biol Med 12:106-16.
3. Zeichner SB, Terawaki H, Gogineni K. 2016. A Review of Systemic Treatment in Metastatic Triple-Negative Breast Cancer. Breast Cancer (Auckl) 10:25-36.
4. Sherry TSDJSLPB. 2013. Orthoreoviruses. Fields Virology, 6th Edition 2.
5. Bouziat R, Hinterleitner R, Brown JJ, Stencel-Baerenwald JE, Ikizler M, Mayassi T, Meisel M, Kim SM, Discepolo V, Pruijssers AJ, Ernest JD, Iskarpatyoti JA, Costes LM, Lawrence I, Palanski BA, Varma M, Zurenski MA, Khomandiak S, McAllister N, Aravamudhan P, Boehme KW, Hu F, Samsom JN, Reinecker HC, Kupfer SS, Guandalini S, Semrad CE, Abadie V, Khosla C, Barreiro LB, Xavier RJ, Ng A, Dermody TS, Jabri B. 2017. Reovirus infection triggers inflammatory responses to dietary antigens and development of celiac disease. Science 356:44-50.
6. Tai JH, Williams JV, Edwards KM, Wright PF, Crowe JE, Jr., Dermody TS. 2005. Prevalence of reovirus-specific antibodies in young children in Nashville, Tennessee. J Infect Dis 191:1221-4.
7. Ouattara LA, Barin F, Barthez MA, Bonnaud B, Roingeard P, Goudeau A, Castelnau P, Vernet G, Paranhos-Baccala G, Komurian-Pradel F. 2011. Novel human reovirus isolated from children with acute necrotizing encephalopathy. Emerg Infect Dis 17:1436-44.
8. Duncan MR, Stanish SM, Cox DC. 1978. Differential sensitivity of normal and transformed human cells to reovirus infection. J Virol 28:444-9.
9. Kemp V, Hoeben RC, van den Wollenberg DJ. 2015. Exploring Reovirus Plasticity for Improving Its Use as Oncolytic Virus. Viruses 8.
10. Coffey MC, Strong JE, Forsyth PA, Lee PW. 1998. Reovirus therapy of tumors with activated Ras pathway. Science 282:1332-4.
11. Strong JE, Coffey MC, Tang D, Sabinin P, Lee PW. 1998. The molecular basis of viral oncolysis: usurpation of the Ras signaling pathway by reovirus. EMBO J 17:3351-62.
12. Hammond ME, Hayes DF, Dowsett M, Allred DC, Hagerty KL, Badve S, Fitzgibbons PL, Francis G, Goldstein NS, Hayes M, Hicks DG, Lester S, Love R, Mangu PB, McShane L, Miller K, Osborne CK, Paik S, Perlmutter J, Rhodes A, Sasano H, Schwartz JN, Sweep FC, Taube S, Torlakovic EE, Valenstein P, Viale G, Visscher D, Wheeler T, Williams RB, Wittliff JL, Wolff AC. 2010. American Society of Clinical Oncology/College of American Pathologists guideline recommendations for immunohistochemical testing of estrogen and progesterone receptors in breast cancer. Arch Pathol Lab Med 134:907-22.
13. Wolff AC, Hammond ME, Hicks DG, Dowsett M, McShane LM, Allison KH, Allred DC, Bartlett JM, Bilous M, Fitzgibbons P, Hanna W, Jenkins RB, Mangu PB, Paik S, Perez EA, Press MF, Spears PA, Vance GH, Viale G, Hayes DF, American Society of Clinical O, College of American P. 2013. Recommendations for human epidermal growth factor receptor 2 testing in breast cancer: American Society of Clinical Oncology/College of American Pathologists clinical practice guideline update. J Clin Oncol 31:3997-4013.
14. Lehmann BD, Bauer JA, Chen X, Sanders ME, Chakravarthy AB, Shyr Y, Pietenpol JA. 2011. Identification of human triple-negative breast cancer subtypes and preclinical models for selection of targeted therapies. J Clin Invest 121:2750-67.
15. Coussy F, El-Botty R, Chateau-Joubert S, Dahmani A, Montaudon E, Leboucher S, Morisset L, Painsec P, Sourd L, Huguet L, Nemati F, Servely JL, Larcher T, Vacher S, Briaux A,

Reyes C, La Rosa P, Lucotte G, Popova T, Foidart P, Sounni NE, Noel A, Decaudin D, Fuhrmann L, Salomon A, Reyal F, Mueller C, Ter Brugge P, Jonkers J, Poupon MF, Stern MH, Bieche I, Pommier Y, Marangoni E. 2020. BRCAness, SLFN11, and RB1 loss predict response to topoisomerase I inhibitors in triple-negative breast cancers. Sci Transl Med 12.

16. Holliday DL, Speirs V. 2011. Choosing the right cell line for breast cancer research. Breast Cancer Res 13:215.
17. Szekely B, Silber AL, Pusztai L. 2017. New Therapeutic Strategies for Triple-Negative Breast Cancer. Oncology (Williston Park) 31.
18. Tanino H, Kosaka Y, Nishimiya H, Tanaka Y, Minatani N, Kikuchi M, Shida A, Waraya M, Katoh H, Enomoto T, Sengoku N, Kajita S, Hoffman RM, Watanabe M. 2016. BRCAness and Prognosis in Triple-Negative Breast Cancer Patients Treated with Neoadjuvant Chemotherapy. PLoS One 11:e0165721.
19. Elstrodt F, Hollestelle A, Nagel JH, Gorin M, Wasielewski M, van den Ouweland A, Merajver SD, Ethier SP, Schutte M. 2006. BRCA1 mutation analysis of 41 human breast cancer cell lines reveals three new deleterious mutants. Cancer Res 66:41-5.
20. Chavez KJ, Garimella SV, Lipkowitz S. 2010. Triple negative breast cancer cell lines: one tool in the search for better treatment of triple negative breast cancer. Breast Dis 32:35-48.
21. Miest TS, Cattaneo R. 2014. New viruses for cancer therapy: meeting clinical needs. Nat Rev Microbiol 12:23-34.
22. Bell J, McFadden G. 2014. Viruses for tumor therapy. Cell Host Microbe 15:260-5.
23. Cattaneo R, Miest T, Shashkova EV, Barry MA. 2008. Reprogrammed viruses as cancer therapeutics: targeted, armed and shielded. Nat Rev Microbiol 6:529-40.
24. Phillips MB, Stuart JD, Rodriguez Stewart RM, Berry JT, Mainou BA, Boehme KW. 2018. Current understanding of reovirus oncolysis mechanisms. Oncolytic Virother 7:53-63.
25. Palmer DH, Mautner V, Mirza D, Oliff S, Gerritsen W, van der Sijp JR, Hubscher S, Reynolds G, Bonney S, Rajaratnam R, Hull D, Horne M, Ellis J, Mountain A, Hill S, Harris PA, Searle PF, Young LS, James ND, Kerr DJ. 2004. Virus-directed enzyme prodrug therapy: intratumoral administration of a replication-deficient adenovirus encoding nitroreductase to patients with resectable liver cancer. J Clin Oncol 22:1546-52.
26. Karaman R. 2014. Using predrugs to optimize drug candidates. Expert Opin Drug Discov 9:1405-19.
27. El-Sherbiny YM, Holmes TD, Wetherill LF, Black EV, Wilson EB, Phillips SL, Scott GB, Adair RA, Dave R, Scott KJ, Morgan RS, Coffey M, Toogood GJ, Melcher AA, Cook GP. 2015. Controlled infection with a therapeutic virus defines the activation kinetics of human natural killer cells in vivo. Clin Exp Immunol 180:98-107.
28. Lawler SE, Chiocca EA. 2015. Oncolytic Virus-Mediated Immunotherapy: A Combinatorial Approach for Cancer Treatment. J Clin Oncol 33:2812-4.
29. Saha D, Ahmed SS, Rabkin SD. 2015. Exploring the Antitumor Effect of Virus in Malignant Glioma. Drugs Future 40:739-749.
30. Javier RT, Butel JS. 2008. The history of tumor virology. Cancer Res 68:7693-706.
31. Zheng M, Huang J, Tong A, Yang H. 2019. Oncolytic Viruses for Cancer Therapy: Barriers and Recent Advances. Mol Ther Oncolytics 15:234-247.
32. Sabin AB. 1959. Reoviruses. A new group of respiratory and enteric viruses formerly classified as ECHO type 10 is described. Science 130:1387-9.
33. Shatkin AJ, Sipe JD, Loh P. 1968. Separation of ten reovirus genome segments by polyacrylamide gel electrophoresis. J Virol 2:986-91.
34. Norman KL, Lee PW. 2000. Reovirus as a novel oncolytic agent. J Clin Invest 105:1035-8.

35. Amadori F, Terracciano E, Gennaio I, Mita V, Gargano D, Zaratti L, Franco E, Arigliani R. 2020. Opinions and attitudes of Italian healthcare workers towards recommended but not compulsory rotavirus vaccination. Hum Vaccin Immunother doi:10.1080/21645515.2020.1776546:1-6.
36. Folorunso OS, Sebolai OM. 2020. Overview of the Development, Impacts, and Challenges of Live-Attenuated Oral Rotavirus Vaccines. Vaccines (Basel) 8.
37. MacLachlan NJ, Osburn BI. 2006. Impact of bluetongue virus infection on the international movement and trade of ruminants. J Am Vet Med Assoc 228:1346-9.
38. Coetzee P, Stokstad M, Venter EH, Myrmel M, Van Vuuren M. 2012. Bluetongue: a historical and epidemiological perspective with the emphasis on South Africa. Virol J 9:198.
39. Attoui H, Mohd Jaafar F, de Micco P, de Lamballerie X. 2005. Coltiviruses and seadornaviruses in North America, Europe, and Asia. Emerg Infect Dis 11:1673-9.
40. Nibert ML. 1998. Structure of mammalian orthoreovirus particles. Curr Top Microbiol Immunol 233:1-30.
41. Millward S, Graham AF. 1970. Structural studies on reovirus: discontinuities in the genome. Proc Natl Acad Sci U S A 65:422-9.
42. Starnes MC, Joklik WK. 1993. Reovirus protein lambda 3 is a poly(C)-dependent poly(G) polymerase. Virology 193:356-66.
43. Cleveland DR, Zarbl H, Millward S. 1986. Reovirus guanylyltransferase is L2 gene product lambda 2. J Virol 60:307-11.
44. Reinisch KM, Nibert ML, Harrison SC. 2000. Structure of the reovirus core at 3.6 A resolution. Nature 404:960-7.
45. Yin P, Cheang M, Coombs KM. 1996. The M1 gene is associated with differences in the temperature optimum of the transcriptase activity in reovirus core particles. J Virol 70:1223-7.
46. Broering TJ, Parker JS, Joyce PL, Kim J, Nibert ML. 2002. Mammalian reovirus nonstructural protein microNS forms large inclusions and colocalizes with reovirus microtubule-associated protein micro2 in transfected cells. J Virol 76:8285-97.
47. Miller CL, Broering TJ, Parker JS, Arnold MM, Nibert ML. 2003. Reovirus sigma NS protein localizes to inclusions through an association requiring the mu NS amino terminus. J Virol 77:4566-76.
48. Ramos-Alvarez M, Sabin AB. 1954. Characteristics of poliomyelitis and other enteric viruses recovered in tissue culture from healthy American children. Proc Soc Exp Biol Med 87:655-61.
49. Ramos-Alvarez M, Sabin AB. 1958. Enteropathogenic viruses and bacteria; role in summer diarrheal diseases of infancy and early childhood. J Am Med Assoc 167:147-56.
50. Attoui H, Biagini P, Stirling J, Mertens PP, Cantaloube JF, Meyer A, de Micco P, de Lamballerie X. 2001. Sequence characterization of Ndelle virus genome segments 1, 5, 7, 8, and 10: evidence for reassignment to the genus Orthoreovirus, family Reoviridae. Biochem Biophys Res Commun 287:583-8.
51. Nibert ML, Margraf RL, Coombs KM. 1996. Nonrandom segregation of parental alleles in reovirus reassortants. J Virol 70:7295-300.
52. Wenske EA, Chanock SJ, Krata L, Fields BN. 1985. Genetic reassortment of mammalian reoviruses in mice. J Virol 56:613-6.
53. Snyder AJ, Wang JC, Danthi P. 2019. Components of the Reovirus Capsid Differentially Contribute to Stability. J Virol 93.
54. Roner MR, Mutsoli C. 2007. The use of monoreassortants and reverse genetics to map reovirus lysis of a ras-transformed cell line. J Virol Methods 139:132-42.

55. Sharpe AH, Fields BN. 1982. Reovirus inhibition of cellular RNA and protein synthesis: role of the S4 gene. Virology 122:381-91.
56. Tyler KL, Squier MK, Rodgers SE, Schneider BE, Oberhaus SM, Grdina TA, Cohen JJ, Dermody TS. 1995. Differences in the capacity of reovirus strains to induce apoptosis are determined by the viral attachment protein sigma 1. J Virol 69:6972-9.
57. Danthi P, Hansberger MW, Campbell JA, Forrest JC, Dermody TS. 2006. JAM-A-independent, antibody-mediated uptake of reovirus into cells leads to apoptosis. J Virol 80:1261-70.
58. Rodgers SE, Barton ES, Oberhaus SM, Pike B, Gibson CA, Tyler KL, Dermody TS. 1997. Reovirus-induced apoptosis of MDCK cells is not linked to viral yield and is blocked by Bcl-2. J Virol 71:2540-6.
59. Connolly JL, Barton ES, Dermody TS. 2001. Reovirus binding to cell surface sialic acid potentiates virus-induced apoptosis. J Virol 75:4029-39.
60. Kim M, Garant KA, zur Nieden NI, Alain T, Loken SD, Urbanski SJ, Forsyth PA, Rancourt DE, Lee PW, Johnston RN. 2011. Attenuated reovirus displays oncolysis with reduced host toxicity. Br J Cancer 104:290-9.
61. Reiss K, Stencel JE, Liu Y, Blaum BS, Reiter DM, Feizi T, Dermody TS, Stehle T. 2012. The GM2 glycan serves as a functional coreceptor for serotype 1 reovirus. PLoS Pathog 8:e1003078.
62. Barton ES, Connolly JL, Forrest JC, Chappell JD, Dermody TS. 2001. Utilization of sialic acid as a coreceptor enhances reovirus attachment by multistep adhesion strengthening. J Biol Chem 276:2200-11.
63. Cui H, Lin Y, Yue L, Zhao X, Liu J. 2011. Differential expression of the alpha2,3-sialic acid residues in breast cancer is associated with metastatic potential. Oncol Rep 25:1365-71.
64. Rodriguez Stewart RM, Berry JTL, Berger AK, Yoon SB, Hirsch AL, Guberman JA, Patel NB, Tharp GK, Bosinger SE, Mainou BA. 2019. Enhanced Killing of Triple-Negative Breast Cancer Cells by Reassortant Reovirus and Topoisomerase Inhibitors. J Virol 93.
65. Simon EJ, Howells MA, Stuart JD, Boehme KW. 2017. Serotype-Specific Killing of Large Cell Carcinoma Cells by Reovirus. Viruses 9.
66. Sherry B, Torres J, Blum MA. 1998. Reovirus induction of and sensitivity to beta interferon in cardiac myocyte cultures correlate with induction of myocarditis and are determined by viral core proteins. J Virol 72:1314-23.
67. Zurney J, Kobayashi T, Holm GH, Dermody TS, Sherry B. 2009. Reovirus mu2 protein inhibits interferon signaling through a novel mechanism involving nuclear accumulation of interferon regulatory factor 9. J Virol 83:2178-87.
68. Irvin SC, Zurney J, Ooms LS, Chappell JD, Dermody TS, Sherry B. 2012. A single-amino-acid polymorphism in reovirus protein mu2 determines repression of interferon signaling and modulates myocarditis. J Virol 86:2302-11.
69. Tyler KL, McPhee DA, Fields BN. 1986. Distinct pathways of viral spread in the host determined by reovirus S1 gene segment. Science 233:770-4.
70. Weiner HL, Drayna D, Averill DR, Jr., Fields BN. 1977. Molecular basis of reovirus virulence: role of the S1 gene. Proc Natl Acad Sci U S A 74:5744-8.
71. Weiner HL, Powers ML, Fields BN. 1980. Absolute linkage of virulence and central nervous system cell tropism of reoviruses to viral hemagglutinin. J Infect Dis 141:609-16.
72. Morrison LA, Sidman RL, Fields BN. 1991. Direct spread of reovirus from the intestinal lumen to the central nervous system through vagal autonomic nerve fibers. Proc Natl Acad Sci U S A 88:3852-6.

73. Sutherland DM, Aravamudhan P, Dietrich MH, Stehle T, Dermody TS. 2018. Reovirus Neurotropism and Virulence Are Dictated by Sequences in the Head Domain of the Viral Attachment Protein. J Virol 92.
74. Dermody TS, Nibert ML, Bassel-Duby R, Fields BN. 1990. Sequence diversity in S1 genes and S1 translation products of 11 serotype 3 reovirus strains. J Virol 64:4842-50.
75. Barton ES, Forrest JC, Connolly JL, Chappell JD, Liu Y, Schnell FJ, Nusrat A, Parkos CA, Dermody TS. 2001. Junction adhesion molecule is a receptor for reovirus. Cell 104:441-51.
76. Konopka-Anstadt JL, Mainou BA, Sutherland DM, Sekine Y, Strittmatter SM, Dermody TS. 2014. The Nogo receptor NgR1 mediates infection by mammalian reovirus. Cell Host Microbe 15:681-91.
77. Maginnis MS, Forrest JC, Kopecky-Bromberg SA, Dickeson SK, Santoro SA, Zutter MM, Nemerow GR, Bergelson JM, Dermody TS. 2006. Beta1 integrin mediates internalization of mammalian reovirus. J Virol 80:2760-70.
78. Maginnis MS, Mainou BA, Derdowski A, Johnson EM, Zent R, Dermody TS. 2008. NPXY motifs in the beta1 integrin cytoplasmic tail are required for functional reovirus entry. J Virol 82:3181-91.
79. Mainou BA, Dermody TS. 2011. Src kinase mediates productive endocytic sorting of reovirus during cell entry. J Virol 85:3203-13.
80. Ebert DH, Deussing J, Peters C, Dermody TS. 2002. Cathepsin L and cathepsin B mediate reovirus disassembly in murine fibroblast cells. J Biol Chem 277:24609-17.
81. Johnson EM, Doyle JD, Wetzel JD, McClung RP, Katunuma N, Chappell JD, Washington MK, Dermody TS. 2009. Genetic and pharmacologic alteration of cathepsin expression influences reovirus pathogenesis. J Virol 83:9630-40.
82. Guglielmi KM, Johnson EM, Stehle T, Dermody TS. 2006. Attachment and cell entry of mammalian orthoreovirus. Curr Top Microbiol Immunol 309:1-38.
83. Chandran K, Farsetta DL, Nibert ML. 2002. Strategy for nonenveloped virus entry: a hydrophobic conformer of the reovirus membrane penetration protein micro 1 mediates membrane disruption. J Virol 76:9920-33.
84. Chandran K, Parker JS, Ehrlich M, Kirchhausen T, Nibert ML. 2003. The delta region of outer-capsid protein micro 1 undergoes conformational change and release from reovirus particles during cell entry. J Virol 77:13361-75.
85. Ivanovic T, Agosto MA, Zhang L, Chandran K, Harrison SC, Nibert ML. 2008. Peptides released from reovirus outer capsid form membrane pores that recruit virus particles. EMBO J 27:1289-98.
86. Zhang L, Agosto MA, Ivanovic T, King DS, Nibert ML, Harrison SC. 2009. Requirements for the formation of membrane pores by the reovirus myristoylated micro1N peptide. J Virol 83:7004-14.
87. Tenorio R, Fernandez de Castro I, Knowlton JJ, Zamora PF, Lee CH, Mainou BA, Dermody TS, Risco C. 2018. Reovirus sigmaNS and muNS Proteins Remodel the Endoplasmic Reticulum to Build Replication Neo-Organelles. mBio 9.
88. Broering TJ, Kim J, Miller CL, Piggott CD, Dinoso JB, Nibert ML, Parker JS. 2004. Reovirus nonstructural protein mu NS recruits viral core surface proteins and entering core particles to factory-like inclusions. J Virol 78:1882-92.
89. Excoffon KJ, Guglielmi KM, Wetzel JD, Gansemer ND, Campbell JA, Dermody TS, Zabner J. 2008. Reovirus preferentially infects the basolateral surface and is released from the apical surface of polarized human respiratory epithelial cells. J Infect Dis 197:1189-97.
90. Lai CM, Mainou BA, Kim KS, Dermody TS. 2013. Directional release of reovirus from the apical surface of polarized endothelial cells. mBio 4:e00049-13.

91. Fernandez de Castro I, Tenorio R, Ortega-Gonzalez P, Knowlton JJ, Zamora PF, Lee CH, Fernandez JJ, Dermody TS, Risco C. 2020. A modified lysosomal organelle mediates nonlytic egress of reovirus. J Cell Biol 219.
92. Breun LA, Broering TJ, McCutcheon AM, Harrison SJ, Luongo CL, Nibert ML. 2001. Mammalian reovirus L2 gene and lambda2 core spike protein sequences and whole-genome comparisons of reoviruses type 1 Lang, type 2 Jones, and type 3 Dearing. Virology 287:333-48.
93. Bussiere LD, Choudhury P, Bellaire B, Miller CL. 2017. Characterization of a Replicating Mammalian Orthoreovirus with Tetracysteine-Tagged muNS for Live-Cell Visualization of Viral Factories. J Virol 91.
94. Lowen AC. 2018. It's in the mix: Reassortment of segmented viral genomes. PLoS Pathog 14:e1007200.
95. Schneeberger K. 2014. Using next-generation sequencing to isolate mutant genes from forward genetic screens. Nat Rev Genet 15:662-76.
96. Kobayashi T, Antar AA, Boehme KW, Danthi P, Eby EA, Guglielmi KM, Holm GH, Johnson EM, Maginnis MS, Naik S, Skelton WB, Wetzel JD, Wilson GJ, Chappell JD, Dermody TS. 2007. A plasmid-based reverse genetics system for animal double-stranded RNA viruses. Cell Host Microbe 1:147-57.
97. Komoto S, Kawagishi T, Kobayashi T, Ikizler M, Iskarpatyoti J, Dermody TS, Taniguchi K. 2014. A plasmid-based reverse genetics system for mammalian orthoreoviruses driven by a plasmid-encoded T7 RNA polymerase. J Virol Methods 196:36-9.
98. Kobayashi T, Ooms LS, Ikizler M, Chappell JD, Dermody TS. 2010. An improved reverse genetics system for mammalian orthoreoviruses. Virology 398:194-200.
99. Boehme KW, Ikizler M, Kobayashi T, Dermody TS. 2011. Reverse genetics for mammalian reovirus. Methods 55:109-13.
100. Thete D, Snyder AJ, Mainou BA, Danthi P. 2016. Reovirus mu1 Protein Affects Infectivity by Altering Virus-Receptor Interactions. J Virol 90:10951-10962.
101. Thete D, Danthi P. 2018. Protein Mismatches Caused by Reassortment Influence Functions of the Reovirus Capsid. J Virol 92.
102. Tyler KL, Squier MK, Brown AL, Pike B, Willis D, Oberhaus SM, Dermody TS, Cohen JJ. 1996. Linkage between reovirus-induced apoptosis and inhibition of cellular DNA synthesis: role of the S1 and M2 genes. J Virol 70:7984-91.
103. Danthi P, Coffey CM, Parker JS, Abel TW, Dermody TS. 2008. Independent regulation of reovirus membrane penetration and apoptosis by the mu1 phi domain. PLoS Pathog 4:e1000248.
104. Danthi P, Kobayashi T, Holm GH, Hansberger MW, Abel TW, Dermody TS. 2008. Reovirus apoptosis and virulence are regulated by host cell membrane penetration efficiency. J Virol 82:161-72.
105. Dichter MA, Weiner HL. 1984. Infection of neuronal cell cultures with reovirus mimics in vitro patterns of neurotropism. Ann Neurol 16:603-10.
106. Tardieu M, Weiner HL. 1982. Viral receptors on isolated murine and human ependymal cells. Science 215:419-21.
107. Lai CM, Boehme KW, Pruijssers AJ, Parekh VV, Van Kaer L, Parkos CA, Dermody TS. 2015. Endothelial JAM-A promotes reovirus viremia and bloodstream dissemination. J Infect Dis 211:383-93.
108. Marcato P, Shmulevitz M, Lee PW. 2005. Connecting reovirus oncolysis and Ras signaling. Cell Cycle 4:556-9.

109. Strong JE, Tang D, Lee PW. 1993. Evidence that the epidermal growth factor receptor on host cells confers reovirus infection efficiency. Virology 197:405-11.
110. Shmulevitz M, Marcato P, Lee PW. 2005. Unshackling the links between reovirus oncolysis, Ras signaling, translational control and cancer. Oncogene 24:7720-8.
111. Shmulevitz M, Pan LZ, Garant K, Pan D, Lee PW. 2010. Oncogenic Ras promotes reovirus spread by suppressing IFN-beta production through negative regulation of RIG-I signaling. Cancer Res 70:4912-21.
112. Shmulevitz M, Marcato P, Lee PW. 2010. Activated Ras signaling significantly enhances reovirus replication and spread. Cancer Gene Ther 17:69-70.
113. Marcato P, Shmulevitz M, Pan D, Stoltz D, Lee PW. 2007. Ras transformation mediates reovirus oncolysis by enhancing virus uncoating, particle infectivity, and apoptosis-dependent release. Mol Ther 15:1522-30.
114. Norman KL, Hirasawa K, Yang AD, Shields MA, Lee PW. 2004. Reovirus oncolysis: the Ras/RalGEF/p38 pathway dictates host cell permissiveness to reovirus infection. Proc Natl Acad Sci U S A 101:11099-104.
115. Maitra R, Seetharam R, Tesfa L, Augustine TA, Klampfer L, Coffey MC, Mariadason JM, Goel S. 2014. Oncolytic reovirus preferentially induces apoptosis in KRAS mutant colorectal cancer cells, and synergizes with irinotecan. Oncotarget 5:2807-19.
116. Kelly KR, Espitia CM, Mahalingam D, Oyajobi BO, Coffey M, Giles FJ, Carew JS, Nawrocki ST. 2012. Reovirus therapy stimulates endoplasmic reticular stress, NOXA induction, and augments bortezomib-mediated apoptosis in multiple myeloma. Oncogene 31:3023-38.
117. Garant KA, Shmulevitz M, Pan L, Daigle RM, Ahn DG, Gujar SA, Lee PW. 2016. Oncolytic reovirus induces intracellular redistribution of Ras to promote apoptosis and progeny virus release. Oncogene 35:771-82.
118. Gong J, Mita MM. 2014. Activated ras signaling pathways and reovirus oncolysis: an update on the mechanism of preferential reovirus replication in cancer cells. Front Oncol 4:167.
119. Daud A, Bastian BC. 2012. Beyond BRAF in melanoma. Curr Top Microbiol Immunol 355:99-117.
120. Calvo F, Agudo-Ibanez L, Crespo P. 2010. The Ras-ERK pathway: understanding site-specific signaling provides hope of new anti-tumor therapies. Bioessays 32:412-21.
121. Malumbres M, Barbacid M. 2003. RAS oncogenes: the first 30 years. Nat Rev Cancer 3:459-65.
122. Gou HF, Li X, Qiu M, Cheng K, Li LH, Dong H, Chen Y, Tang Y, Gao F, Zhao F, Men HT, Ge J, Su JM, Xu F, Bi F, Gao JJ, Liu JY. 2013. Epidermal growth factor receptor (EGFR)-RAS signaling pathway in penile squamous cell carcinoma. PLoS One 8:e62175.
123. Hollestelle A, Elstrodt F, Nagel JH, Kallemeijn WW, Schutte M. 2007. Phosphatidylinositol-3-OH kinase or RAS pathway mutations in human breast cancer cell lines. Mol Cancer Res 5:195-201.
124. Yao Z, Torres NM, Tao A, Gao Y, Luo L, Li Q, de Stanchina E, Abdel-Wahab O, Solit DB, Poulikakos PI, Rosen N. 2015. BRAF Mutants Evade ERK-Dependent Feedback by Different Mechanisms that Determine Their Sensitivity to Pharmacologic Inhibition. Cancer Cell 28:370-83.
125. Clements D, Helson E, Gujar SA, Lee PW. 2014. Reovirus in cancer therapy: an evidence-based review. Oncolytic Virother 3:69-82.
126. Catling AD, Schaeffer HJ, Reuter CW, Reddy GR, Weber MJ. 1995. A proline-rich sequence unique to MEK1 and MEK2 is required for raf binding and regulates MEK function. Mol Cell Biol 15:5214-25.

127. Guo YJ, Pan WW, Liu SB, Shen ZF, Xu Y, Hu LL. 2020. ERK/MAPK signalling pathway and tumorigenesis. Exp Ther Med 19:1997-2007.
128. Song L, Ohnuma T, Gelman IH, Holland JF. 2009. Reovirus infection of cancer cells is not due to activated Ras pathway. Cancer Gene Ther 16:382.
129. Twigger K, Roulstone V, Kyula J, Karapanagiotou EM, Syrigos KN, Morgan R, White C, Bhide S, Nuovo G, Coffey M, Thompson B, Jebar A, Errington F, Melcher AA, Vile RG, Pandha HS, Harrington KJ. 2012. Reovirus exerts potent oncolytic effects in head and neck cancer cell lines that are independent of signalling in the EGFR pathway. BMC Cancer 12:368.
130. Thirukkumaran CM, Shi ZQ, Luider J, Kopciuk K, Gao H, Bahlis N, Neri P, Pho M, Stewart D, Mansoor A, Morris DG. 2012. Reovirus as a viable therapeutic option for the treatment of multiple myeloma. Clin Cancer Res 18:4962-72.
131. Smakman N, van den Wollenberg DJ, Borel Rinkes IH, Hoeben RC, Kranenburg O. 2005. Sensitization to apoptosis underlies KrasD12-dependent oncolysis of murine C26 colorectal carcinoma cells by reovirus T3D. J Virol 79:14981-5.
132. Hwang CC, Igase M, Okuda M, Coffey M, Noguchi S, Mizuno T. 2019. Reovirus changes the expression of anti-apoptotic and proapoptotic proteins with the c-kit downregulation in canine mast cell tumor cell lines. Biochem Biophys Res Commun 517:233-237.
133. Gujar SA, Marcato P, Pan D, Lee PW. 2010. Reovirus virotherapy overrides tumor antigen presentation evasion and promotes protective antitumor immunity. Mol Cancer Ther 9:2924-33.
134. Prestwich RJ, Ilett EJ, Errington F, Diaz RM, Steele LP, Kottke T, Thompson J, Galivo F, Harrington KJ, Pandha HS, Selby PJ, Vile RG, Melcher AA. 2009. Immune-mediated antitumor activity of reovirus is required for therapy and is independent of direct viral oncolysis and replication. Clin Cancer Res 15:4374-4381.
135. Prestwich RJ, Errington F, Ilett EJ, Morgan RS, Scott KJ, Kottke T, Thompson J, Morrison EE, Harrington KJ, Pandha HS, Selby PJ, Vile RG, Melcher AA. 2008. Tumor infection by oncolytic reovirus primes adaptive antitumor immunity. Clin Cancer Res 14:7358-66.
136. Gujar SA, Pan DA, Marcato P, Garant KA, Lee PW. 2011. Oncolytic virus-initiated protective immunity against prostate cancer. Mol Ther 19:797-804.
137. Gujar S, Dielschneider R, Clements D, Helson E, Shmulevitz M, Marcato P, Pan D, Pan LZ, Ahn DG, Alawadhi A, Lee PW. 2013. Multifaceted therapeutic targeting of ovarian peritoneal carcinomatosis through virus-induced immunomodulation. Mol Ther 21:338-47.
138. Errington F, Steele L, Prestwich R, Harrington KJ, Pandha HS, Vidal L, de Bono J, Selby P, Coffey M, Vile R, Melcher A. 2008. Reovirus activates human dendritic cells to promote innate antitumor immunity. J Immunol 180:6018-26.
139. Errington F, White CL, Twigger KR, Rose A, Scott K, Steele L, Ilett LJ, Prestwich R, Pandha HS, Coffey M, Selby P, Vile R, Harrington KJ, Melcher AA. 2008. Inflammatory tumour cell killing by oncolytic reovirus for the treatment of melanoma. Gene Ther 15:1257-70.
140. Zhao X, Chester C, Rajasekaran N, He Z, Kohrt HE. 2016. Strategic Combinations: The Future of Oncolytic Virotherapy with Reovirus. Mol Cancer Ther 15:767-73.
141. Knowlton JJ, Dermody TS, Holm GH. 2012. Apoptosis induced by mammalian reovirus is beta interferon (IFN) independent and enhanced by IFN regulatory factor 3- and NF-kappaB-dependent expression of Noxa. J Virol 86:1650-60.
142. Pan D, Pan LZ, Hill R, Marcato P, Shmulevitz M, Vassilev LT, Lee PW. 2011. Stabilisation of p53 enhances reovirus-induced apoptosis and virus spread through p53-dependent NF-kappaB activation. Br J Cancer 105:1012-22.

143. Tian J, Zhang X, Wu H, Liu C, Li Z, Hu X, Su S, Wang LF, Qu L. 2015. Blocking the PI3K/AKT pathway enhances mammalian reovirus replication by repressing IFN-stimulated genes. Front Microbiol 6:886.
144. Forsyth P, Roldan G, George D, Wallace C, Palmer CA, Morris D, Cairncross G, Matthews MV, Markert J, Gillespie Y, Coffey M, Thompson B, Hamilton M. 2008. A phase I trial of intratumoral administration of reovirus in patients with histologically confirmed recurrent malignant gliomas. Mol Ther 16:627-32.
145. Wilcox ME, Yang W, Senger D, Rewcastle NB, Morris DG, Brasher PM, Shi ZQ, Johnston RN, Nishikawa S, Lee PW, Forsyth PA. 2001. Reovirus as an oncolytic agent against experimental human malignant gliomas. J Natl Cancer Inst 93:903-12.
146. Gong J, Sachdev E, Mita AC, Mita MM. 2016. Clinical development of reovirus for cancer therapy: An oncolytic virus with immune-mediated antitumor activity. World J Methodol 6:25-42.
147. Norman KL, Coffey MC, Hirasawa K, Demetrick DJ, Nishikawa SG, DiFrancesco LM, Strong JE, Lee PW. 2002. Reovirus oncolysis of human breast cancer. Hum Gene Ther 13:641-52.
148. Yang WQ, Senger DL, Lun XQ, Muzik H, Shi ZQ, Dyck RH, Norman K, Brasher PM, Rewcastle NB, George D, Stewart D, Lee PW, Forsyth PA. 2004. Reovirus as an experimental therapeutic for brain and leptomeningeal metastases from breast cancer. Gene Ther 11:1579-89.
149. Hirasawa K, Nishikawa SG, Norman KL, Alain T, Kossakowska A, Lee PW. 2002. Oncolytic reovirus against ovarian and colon cancer. Cancer Res 62:1696-701.
150. Smakman N, van der Bilt JD, van den Wollenberg DJ, Hoeben RC, Borel Rinkes IH, Kranenburg O. 2006. Immunosuppression promotes reovirus therapy of colorectal liver metastases. Cancer Gene Ther 13:815-8.
151. Thirukkumaran CM, Nodwell MJ, Hirasawa K, Shi ZQ, Diaz R, Luider J, Johnston RN, Forsyth PA, Magliocco AM, Lee P, Nishikawa S, Donnelly B, Coffey M, Trpkov K, Fonseca K, Spurrell J, Morris DG. 2010. Oncolytic viral therapy for prostate cancer: efficacy of reovirus as a biological therapeutic. Cancer Res 70:2435-44.
152. Gupta-Saraf P, Miller CL. 2014. HIF-1alpha downregulation and apoptosis in hypoxic prostate tumor cells infected with oncolytic mammalian orthoreovirus. Oncotarget 5:561-74.
153. Kilani RT, Tamimi Y, Hanel EG, Wong KK, Karmali S, Lee PW, Moore RB. 2003. Selective reovirus killing of bladder cancer in a co-culture spheroid model. Virus Res 93:1-12.
154. Hanel EG, Xiao Z, Wong KK, Lee PW, Britten RA, Moore RB. 2004. A novel intravesical therapy for superficial bladder cancer in an orthotopic model: oncolytic reovirus therapy. J Urol 172:2018-22.
155. Etoh T, Himeno Y, Matsumoto T, Aramaki M, Kawano K, Nishizono A, Kitano S. 2003. Oncolytic viral therapy for human pancreatic cancer cells by reovirus. Clin Cancer Res 9:1218-23.
156. Himeno Y, Etoh T, Matsumoto T, Ohta M, Nishizono A, Kitano S. 2005. Efficacy of oncolytic reovirus against liver metastasis from pancreatic cancer in immunocompetent models. Int J Oncol 27:901-6.
157. Hirano S, Etoh T, Okunaga R, Shibata K, Ohta M, Nishizono A, Kitano S. 2009. Reovirus inhibits the peritoneal dissemination of pancreatic cancer cells in an immunocompetent animal model. Oncol Rep 21:1381-4.
158. Hirasawa K, Nishikawa SG, Norman KL, Coffey MC, Thompson BG, Yoon CS, Waisman DM, Lee PW. 2003. Systemic reovirus therapy of metastatic cancer in immune-competent mice. Cancer Res 63:348-53.

159. Alain T, Hirasawa K, Pon KJ, Nishikawa SG, Urbanski SJ, Auer Y, Luider J, Martin A, Johnston RN, Janowska-Wieczorek A, Lee PW, Kossakowska AE. 2002. Reovirus therapy of lymphoid malignancies. Blood 100:4146-53.
160. Harrington KJ, Karapanagiotou EM, Roulstone V, Twigger KR, White CL, Vidal L, Beirne D, Prestwich R, Newbold K, Ahmed M, Thway K, Nutting CM, Coffey M, Harris D, Vile RG, Pandha HS, Debono JS, Melcher AA. 2010. Two-stage phase I dose-escalation study of intratumoral reovirus type 3 dearing and palliative radiotherapy in patients with advanced cancers. Clin Cancer Res 16:3067-77.
161. Harrington KJ, Vile RG, Melcher A, Chester J, Pandha HS. 2010. Clinical trials with oncolytic reovirus: moving beyond phase I into combinations with standard therapeutics. Cytokine Growth Factor Rev 21:91-8.
162. Heinemann L, Simpson GR, Boxall A, Kottke T, Relph KL, Vile R, Melcher A, Prestwich R, Harrington KJ, Morgan R, Pandha HS. 2011. Synergistic effects of oncolytic reovirus and docetaxel chemotherapy in prostate cancer. BMC Cancer 11:221.
163. Hingorani P, Zhang W, Lin J, Liu L, Guha C, Kolb EA. 2011. Systemic administration of reovirus (Reolysin) inhibits growth of human sarcoma xenografts. Cancer 117:1764-74.
164. Rajani K, Parrish C, Kottke T, Thompson J, Zaidi S, Ilett L, Shim KG, Diaz RM, Pandha H, Harrington K, Coffey M, Melcher A, Vile R. 2016. Combination Therapy With Reovirus and Anti-PD-1 Blockade Controls Tumor Growth Through Innate and Adaptive Immune Responses. Mol Ther 24:166-74.
165. Connolly JL, Rodgers SE, Clarke P, Ballard DW, Kerr LD, Tyler KL, Dermody TS. 2000. Reovirus-induced apoptosis requires activation of transcription factor NF-kappaB. J Virol 74:2981-9.
166. Clarke P, Debiasi RL, Goody R, Hoyt CC, Richardson-Burns S, Tyler KL. 2005. Mechanisms of reovirus-induced cell death and tissue injury: role of apoptosis and virus-induced perturbation of host-cell signaling and transcription factor activation. Viral Immunol 18:89-115.
167. Berger AK, Hiller BE, Thete D, Snyder AJ, Perez E, Jr., Upton JW, Danthi P. 2017. Viral RNA at Two Stages of Reovirus Infection Is Required for the Induction of Necroptosis. J Virol 91.
168. Berger AK, Danthi P. 2013. Reovirus activates a caspase-independent cell death pathway. MBio 4:e00178-13.
169. Boehme KW, Hammer K, Tollefson WC, Konopka-Anstadt JL, Kobayashi T, Dermody TS. 2013. Nonstructural protein sigma1s mediates reovirus-induced cell cycle arrest and apoptosis. J Virol 87:12967-79.
170. Igase M, Shibutani S, Kurogouchi Y, Fujiki N, Hwang CC, Coffey M, Noguchi S, Nemoto Y, Mizuno T. 2019. Combination Therapy with Reovirus and ATM Inhibitor Enhances Cell Death and Virus Replication in Canine Melanoma. Mol Ther Oncolytics 15:49-59.
171. Holm GH, Zurney J, Tumilasci V, Leveille S, Danthi P, Hiscott J, Sherry B, Dermody TS. 2007. Retinoic acid-inducible gene-I and interferon-beta promoter stimulator-1 augment proapoptotic responses following mammalian reovirus infection via interferon regulatory factor-3. J Biol Chem 282:21953-61.
172. Hansberger MW, Campbell JA, Danthi P, Arrate P, Pennington KN, Marcu KB, Ballard DW, Dermody TS. 2007. IkappaB kinase subunits alpha and gamma are required for activation of NF-kappaB and induction of apoptosis by mammalian reovirus. J Virol 81:1360-71.
173. Roebke KE, Danthi P. 2019. Cell Entry-Independent Role for the Reovirus mu1 Protein in Regulating Necroptosis and the Accumulation of Viral Gene Products. J Virol 93.

174. Chiu HC, Richart S, Lin FY, Hsu WL, Liu HJ. 2014. The interplay of reovirus with autophagy. Biomed Res Int 2014:483657.
175. Clarke P, Tyler KL. 2003. Reovirus-induced apoptosis: A minireview. Apoptosis 8:141-50.
176. Elmore S. 2007. Apoptosis: a review of programmed cell death. Toxicol Pathol 35:495-516.
177. Norbury CJ, Hickson ID. 2001. Cellular responses to DNA damage. Annu Rev Pharmacol Toxicol 41:367-401.
178. Rudel T, Kepp O, Kozjak-Pavlovic V. 2010. Interactions between bacterial pathogens and mitochondrial cell death pathways. Nat Rev Microbiol 8:693-705.
179. O'Donnell SM, Hansberger MW, Connolly JL, Chappell JD, Watson MJ, Pierce JM, Wetzel JD, Han W, Barton ES, Forrest JC, Valyi-Nagy T, Yull FE, Blackwell TS, Rottman JN, Sherry B, Dermody TS. 2005. Organ-specific roles for transcription factor NF-kappaB in reovirus-induced apoptosis and disease. J Clin Invest 115:2341-50.
180. Connolly JL, Dermody TS. 2002. Virion disassembly is required for apoptosis induced by reovirus. J Virol 76:1632-41.
181. Clarke P, Meintzer SM, Gibson S, Widmann C, Garrington TP, Johnson GL, Tyler KL. 2000. Reovirus-induced apoptosis is mediated by TRAIL. J Virol 74:8135-9.
182. Luo X, Budihardjo I, Zou H, Slaughter C, Wang X. 1998. Bid, a Bcl2 interacting protein, mediates cytochrome c release from mitochondria in response to activation of cell surface death receptors. Cell 94:481-90.
183. Joza N, Susin SA, Daugas E, Stanford WL, Cho SK, Li CY, Sasaki T, Elia AJ, Cheng HY, Ravagnan L, Ferri KF, Zamzami N, Wakeham A, Hakem R, Yoshida H, Kong YY, Mak TW, Zuniga-Pflucker JC, Kroemer G, Penninger JM. 2001. Essential role of the mitochondrial apoptosis-inducing factor in programmed cell death. Nature 410:549-54.
184. Li H, Zhu H, Xu CJ, Yuan J. 1998. Cleavage of BID by caspase 8 mediates the mitochondrial damage in the Fas pathway of apoptosis. Cell 94:491-501.
185. Iordanov MS, Ryabinina OP, Schneider P, Magun BE. 2005. Two mechanisms of caspase 9 processing in double-stranded RNA- and virus-triggered apoptosis. Apoptosis 10:153-66.
186. Beckham JD, Tuttle KD, Tyler KL. 2010. Caspase-3 activation is required for reovirus-induced encephalitis in vivo. J Neurovirol 16:306-17.
187. Danthi P, Pruijssers AJ, Berger AK, Holm GH, Zinkel SS, Dermody TS. 2010. Bid regulates the pathogenesis of neurotropic reovirus. PLoS Pathog 6:e1000980.
188. Kominsky DJ, Bickel RJ, Tyler KL. 2002. Reovirus-induced apoptosis requires both death receptor- and mitochondrial-mediated caspase-dependent pathways of cell death. Cell Death Differ 9:926-33.
189. Kominsky DJ, Bickel RJ, Tyler KL. 2002. Reovirus-induced apoptosis requires mitochondrial release of Smac/DIABLO and involves reduction of cellular inhibitor of apoptosis protein levels. J Virol 76:11414-24.
190. Chaitanya GV, Steven AJ, Babu PP. 2010. PARP-1 cleavage fragments: signatures of cell-death proteases in neurodegeneration. Cell Commun Signal 8:31.
191. Zou H, Li Y, Liu X, Wang X. 1999. An APAF-1.cytochrome c multimeric complex is a functional apoptosome that activates procaspase-9. J Biol Chem 274:11549-56.
192. Degterev A, Huang Z, Boyce M, Li Y, Jagtap P, Mizushima N, Cuny GD, Mitchison TJ, Moskowitz MA, Yuan J. 2005. Chemical inhibitor of nonapoptotic cell death with therapeutic potential for ischemic brain injury. Nat Chem Biol 1:112-9.
193. Dhuriya YK, Sharma D. 2018. Necroptosis: a regulated inflammatory mode of cell death. J Neuroinflammation 15:199.
194. Galluzzi L, Vitale I, Abrams JM, Alnemri ES, Baehrecke EH, Blagosklonny MV, Dawson TM, Dawson VL, El-Deiry WS, Fulda S, Gottlieb E, Green DR, Hengartner MO, Kepp O,

Knight RA, Kumar S, Lipton SA, Lu X, Madeo F, Malorni W, Mehlen P, Nunez G, Peter ME, Piacentini M, Rubinsztein DC, Shi Y, Simon HU, Vandenabeele P, White E, Yuan J, Zhivotovsky B, Melino G, Kroemer G. 2012. Molecular definitions of cell death subroutines: recommendations of the Nomenclature Committee on Cell Death 2012. Cell Death Differ 19:107-20.

195. Taylor RC, Cullen SP, Martin SJ. 2008. Apoptosis: controlled demolition at the cellular level. Nat Rev Mol Cell Biol 9:231-41.
196. Vercammen D, Beyaert R, Denecker G, Goossens V, Van Loo G, Declercq W, Grooten J, Fiers W, Vandenabeele P. 1998. Inhibition of caspases increases the sensitivity of L929 cells to necrosis mediated by tumor necrosis factor. J Exp Med 187:1477-85.
197. Holler N, Zaru R, Micheau O, Thome M, Attinger A, Valitutti S, Bodmer JL, Schneider P, Seed B, Tschopp J. 2000. Fas triggers an alternative, caspase-8-independent cell death pathway using the kinase RIP as effector molecule. Nat Immunol 1:489-95.
198. Cho YS, Challa S, Moquin D, Genga R, Ray TD, Guildford M, Chan FK. 2009. Phosphorylation-driven assembly of the RIP1-RIP3 complex regulates programmed necrosis and virus-induced inflammation. Cell 137:1112-23.
199. Zhang DW, Shao J, Lin J, Zhang N, Lu BJ, Lin SC, Dong MQ, Han J. 2009. RIP3, an energy metabolism regulator that switches TNF-induced cell death from apoptosis to necrosis. Science 325:332-6.
200. Sun X, Lee J, Navas T, Baldwin DT, Stewart TA, Dixit VM. 1999. RIP3, a novel apoptosis-inducing kinase. J Biol Chem 274:16871-5.
201. Hiller BE, Berger AK, Danthi P. 2015. Viral gene expression potentiates reovirus-induced necrosis. Virology 484:386-94.
202. Farone AL, O'Donnell SM, Brooks CS, Young KM, Pierce JM, Wetzel JD, Dermody TS, Farone MB. 2006. Reovirus strain-dependent inflammatory cytokine responses and replication patterns in a human monocyte cell line. Viral Immunol 19:546-57.

Chapter II: Enhanced Killing of Triple-Negative Breast Cancer Cells by Reassortant Reovirus and Topoisomerase Inhibitors

Roxana M. Rodríguez Stewart[1,2#], Jameson T.L. Berry[1,2^#], Angela K. Berger[2,3], Sung Bo Yoon[1], Aspen L. Hirsch[2,3], Jaime A. Guberman[1], Nirav B. Patel[4], Gregory K. Tharp[4], Steven E. Bosinger[4], and Bernardo A. Mainou[2,3*]

Emory University,[1] Department of Pediatrics,[2] Emory University School of Medicine, Atlanta, GA 30322, Children's Healthcare of Atlanta[3], Atlanta, GA, 30322, Emory Vaccine Center[4], Yerkes National Primate Research Center, Atlanta, GA 30322

# R.M.R.S. and J.T.L.B. contributed equally to this work.

* To whom correspondence should be addressed: Emory University School of Medicine, Department of Pediatrics, ECC 564, 2015 Uppergate Drive, Atlanta, GA 30322. Tel.: (404) 727-1605. Fax: (404) 727-9223. E-mail: bernardo.mainou@emory.edu.

The work of this chapter was published in the Journal of Virology in 2019.

Citation:

Rodríguez Stewart RM*, Berry JTL*, Berger AK, Yoon SB, Hirsch AL, Guberman JA, Patel NB, Tharp GK, Bosinger SE, Mainou BA. Enhanced killing of triple-negative breast cancer cells by reassortant reovirus and topoisomerase inhibitors. 13 November 2019. J Virol 93:e01411-19. https://doi.org/10.1128/JVI.01411-19.

Abstract

Breast cancer is the second-leading cause of cancer-related deaths in women in the United States. Triple-negative breast cancer constitutes a subset of breast cancer that is associated with higher rates of relapse, decreased survival, and limited therapeutic options for patients afflicted with this type of breast cancer. Mammalian orthoreovirus (reovirus) selectively infects and kills transformed cells and a serotype 3 reovirus is in clinical trials to assess its efficacy as an oncolytic agent against several cancers. It is unclear if reovirus serotypes differentially infect and kill triple-negative breast cancer cells and if reovirus-induced cytotoxicity of breast cancer cells can be enhanced by modulating the activity of host molecules and pathways. Here, we generated reassortant reoviruses by forward genetics with enhanced infective and cytotoxic properties in triple-negative breast cancer cells. From a high-throughput screen of small molecule inhibitors, we identified topoisomerase inhibitors as a class of drugs that enhance reovirus infectivity and cytotoxicity of triple-negative breast cancer cells. Treatment of triple-negative breast cancer cells with topoisomerase inhibitors activates DNA damage response pathways and reovirus infection induces robust production of Type III, but not Type I, interferon. Although Type I and Type III IFN can activate STAT1 and STAT2, triple-negative breast cancer cellular proliferation is only negatively affected by Type I IFN. Together, these data show that reassortant viruses with a novel genetic composition generated by forward genetics in combination with topoisomerase inhibitors more efficiently infect and kill triple-negative breast cancer cells.

Importance

Patients afflicted by triple-negative breast cancer have decreased survival and limited therapeutic options. Reovirus infection results in cell death of a variety of cancers, but it is unknown if different reovirus types lead to triple-negative breast cancer cell death. In this study, we generated two novel reoviruses that more efficiently infect and kill triple-negative breast cancer cells. We show that infection in the presence of DNA-damaging agents enhances infection and triple-negative breast cancer cell killing by reovirus. These data suggest that a combination of a genetically engineered oncolytic reovirus and topoisomerase inhibitors may provide a potent therapeutic option for patients afflicted with triple-negative breast cancer.

Introduction

Breast cancer is the leading cause of cancer and second leading cause of deaths by cancer in women in the United States (http://seer.cancer.gov/). Triple-negative breast cancer (TNBC) constitutes approximately 15% of breast cancers and has a higher rate of relapse and shorter overall survival after metastasis than other subtypes of breast cancer (1). In addition, compared to other forms of breast cancer, TNBC more frequently affects the young, is more prevalent in African American women, and tumors are larger in size and biologically more aggressive (2). TNBC is characterized by the lack of expression of estrogen receptor (ER), progesterone receptor (PR), and human epidermal growth factor receptor 2 (HER2/neu) and can be classified into seven subtypes based on their genetic signature (2). Although targeted therapies against hormone receptor-positive and HER2-positive breast cancer have been efficacious, the absence of these molecules on TNBC cells has limited treatment to cytotoxic chemotherapy, radiotherapy, and surgery (3, 4). This raises a need for targeted therapeutics against this type of cancer.

The concept that viruses can promote tumor regression is nearly as old as the discovery of viruses (5). The deregulated expression of viral receptors, endocytic uptake molecules, proteases, altered metabolic states, and impaired innate immunity make cancer cells ideally suitable for virus infection and replication (6-8). In addition to directly impacting cancer cell biology, oncolytic viruses can elicit anti-tumor immune responses and serve as adjuvants for other cancer therapies (9-11). Several viruses are under study to assess their oncolytic properties against several cancers (6, 7). Nonfusogenic mammalian orthoreovirus (reovirus) is a non-enveloped double-stranded RNA (dsRNA) virus in the *Reoviridae* family. A serotype 3 reovirus (Reolysin) is in Phase I and II clinical trials (clinicaltrials.gov: NCT01622543, NCT01656538) to assess its efficacy against a variety of cancers (12). Reovirus can be delivered to patients via intratumoral and intravenous administration and can be effective in combination therapy (13). Reovirus has an inherent preference to replicate in

tumor cells, making it ideally suited for use in oncolytic virotherapies (14, 15). However, the cellular and viral factors that promote preferential reovirus infection of cancer cells are not fully elucidated.

Reovirus has a segmented genome with three large (L), three medium (M), and four small (S) dsRNA gene segments (16). There are three different reovirus serotypes (Type 1, 2, and 3) based on the neutralization ability of antibodies raised against the σ1 attachment protein that is encoded by the S1 gene segment (17, 18). Reoviruses infect most mammals and although humans are infected during childhood, infection seldom results in disease (17, 19-21). Reovirus induces programmed cell death *in vitro* and *in vivo* (22-29). Although both Type 1 and Type 3 reovirus can induce apoptosis, Type 3 reoviruses induce apoptosis and necroptosis more efficiently in most cells (17, 22, 23). Serotype-dependent differences in apoptosis induction segregate with the S1 and M2 gene segments (30-32). However, there is a limited understanding of the viral factors that determine preferential replication and killing of cancer cells.

In this study, we show that co-infection and serial passaging of parental reoviruses in TNBC cells yields reassortant viruses with enhanced oncolytic capacities compared to parental reoviruses. Reassortant reoviruses have a predominant Type 1 genetic composition with some Type 3 gene segments as well as synonymous and non-synonymous point mutations. We show that reassortant reoviruses have enhanced infective and cytotoxic capacities in TNBC cells compared to parental viruses. To further enhance the oncolytic properties of these reassortant viruses, we used a high-throughput screen of small molecule inhibitors and identified DNA-damaging topoisomerase inhibitors as a class of drugs that reduces TNBC cell viability while enhancing reovirus infectivity. Infection of TNBC cells in the presence of topoisomerase inhibitors results in induction of DNA damage, increased levels of Type III but not Type I interferon, and enhanced cell killing. Although Type I and Type III IFN can activate STAT1 and STAT2, triple-negative breast cancer cellular proliferation is only negatively affected by Type I IFN. Together, we show that reassortant

reoviruses with a novel genetic composition have enhanced oncolytic properties and pairing of topoisomerase inhibitors with reovirus potentiates TNBC cell killing.

Results

Generation of reassortant viruses in triple-negative breast cancer cells by forward genetics.

Reovirus serotypes have distinct infective, replicative, and cell killing properties and the segmented nature of the reovirus genome allows the generation of viruses with novel properties through gene reassortment following co-infection (33, 34). To generate reoviruses with enhanced replicative properties in TNBC cells, MDA-MB-231 cells were co-infected with prototype laboratory strains T1L, T2J, and T3D and serially passaged in these cells ten or twenty times (FIG 1A). Following serial passage, individual viral clones were isolated by plaque assay and the gene segment identity for each clone (44 clones following 10 passages, 45 clones following 20 passages) was determined by SDS-gel electrophoresis (FIG 1B). Of the 44 isolates analyzed following 10 serial passages, 8 distinct electropherotypes were identified, with 23 isolates (52%) having the same electropherotype (r2Reovirus) (FIG 1C). Following 20 serial passages, 6 distinct isolates were identified, including two (r9 and r10) that were not observed after passage 10 (FIG 1D). The most predominant electropherotypes following 20 serial passages were r1Reovirus and r2Reovirus, constituting 33% and 27% respectively of all isolates. Illumina Next-Generation Sequencing (NGS) revealed that r1Reovirus is composed of seven gene segments from T1L and three from T3D (L2, M2, S2), while r2Reovirus is composed of nine gene segments from T1L and one from T3D (M2) (FIG 2). In addition, both viruses have previously unidentified nonsynonymous point mutations that result in an Ala to Thr substitution at amino acid 160 in L3, an Ile to Val substitution at amino acid 250 in S3, and Val to Ile substitution at amino acid 49 in S4. A Pro to Thr substitution at amino acid 161 is also found in r1Reovirus. In addition, r1Reovirus and r2Reovirus have several synonymous

point mutations (Table S1). Interestingly, the r1Reovirus S2 gene segment, but no other gene segment, has single residue variations that range from 35% to 65%. Sanger sequencing of the S2 gene segment from ten r1Reovirus plaque isolates showed a wide array of mutations distinct from the initial virus isolate (data not shown). These data suggest that the S2 gene segment of r1Reovirus is genetically unstable. We did not detect single residue variations in gene segments from either parental T1L, T2J, or T3D or r2Reovirus, suggesting this is not an intrinsic property of the S2 gene segment carried from parental viruses. Together, these data indicate that co-infection and serial passaging of reoviruses in MDA-MB-231 cells leads to the generation of reassortant reoviruses with novel genetic compositions.

Reassortant reoviruses infect MDA-MB-231cells more efficiently than parental reoviruses.

Reovirus attaches to cells via a strength-adhesion mechanism whereby the viral attachment fiber σ1 binds to cell-surface carbohydrate and proteinaceous receptors JAM-A or NgR1 (35-39). To determine the attachment efficiency of r1Reovirus and r2Reovirus in comparison to parental reoviruses, MDA-MB-231 cells were adsorbed with vehicle (mock) or Alexa 633 (A633)-labeled T1L, T3D, T3C$ (the reovirus strain currently in clinical trials), or reassortant reoviruses at an MOI of 5×10^4 particles/cell and assessed for cell surface reovirus by flow cytometry (FIG 3A). Reassortant reoviruses attach to cells with similar efficiency as T1L, but less efficiently than Type 3 reoviruses T3D and T3C$. As reassortant reoviruses contain a T1L S1 gene segment, it is not surprising that they attach to cells to similar levels as parental T1L. These data also indicate that other genetic changes found in r1Reovirus and r2Reovirus do not impact the ability of these viruses to attach to cells.

To determine how genetic changes in r1Reovirus and r2Reovirus affect reovirus infection of TNBC cells, MDA-MB-231 cells were pretreated with DMSO or the cysteine protease inhibitor

E64-d, which blocks reovirus cell entry by preventing proteolysis during endocytic uptake (40), adsorbed with mock, T1L, T3D, T3C$, or reassortant reoviruses at an MOI of 100 PFU/cell and assessed for infectivity after 18 h by indirect immunofluorescence using reovirus-specific antiserum (FIG 3B). In contrast to attachment, r1Reovirus and r2Reovirus infect MDA-MB-231 cells more efficiently than parental reoviruses or T3C$, with both reassortant viruses infecting cells over 2-fold more efficiently. Infection with all viruses tested was impaired by E64-d, indicating a similar requirement for proteolytic processing during entry. These data indicate that reassortant reoviruses establish infection more efficiently in MDA-MB-231 cells than parental reoviruses and that infection of these cells requires proteasomal processing of the virion during cell entry.

To determine if the increased infectivity of the reassortant viruses is limited to MDA-MB-231 cells, the infectivity of parental and reassortant reoviruses was assessed on murine L929 fibroblasts, which are highly susceptible to reovirus infection and are used to propagate the virus (FIG 3C). L929 cells were adsorbed with mock, T1L, T3D, T3C$, or reassortant reoviruses at an MOI of 5 PFU/cell and assessed for infectivity after 18 h by indirect immunofluorescence using reovirus-specific antiserum. In contrast to that observed in MDA-MB-231 cells, reassortant reoviruses infect L929 cells to similar levels as parental T1L, but less efficiently than both T3D and T3C$. These data indicate that r1Reovirus and r2Reovirus more efficiently infect TNBC cells, but not L929 cells. This suggests that the genetic changes found in the reassortant viruses confer enhanced infection in the TNBC cells used for serial passage at a step after attachment.

Replication kinetics of reassortant reoviruses are similar to T1L but faster than T3D.

To determine the replication efficiency of parental and reassortant reoviruses, MDA-MB-231 cells were adsorbed with mock, T1L, T3D, T3C$ or reassortant reoviruses at an MOI of 10 PFU/cell and assessed for viral replication over a 3 day course of infection (FIG 4). Despite the

differences observed in infectivity, all viruses except T3D replicated with similar kinetics, with T3C$ having faster replication kinetics by day 1 post infection (FIG 4B) and reaching higher peak titers than all other viruses tested. T1L, T3C$, r1Reovirus, and r2Reovirus had similar replication kinetics at days 2 and 3 post infection. T3D replication kinetics were slower, with lower viral yields, than all other viruses tested. Interestingly, although T3C$ only differs from T3D by 22 amino acids, its replication kinetics are more similar to T1L and the reassortant reoviruses than T3D. These data indicate that although reassortant reoviruses establish infection in MDA-MB-231 cells more efficiently than parental reoviruses, replication kinetics are similar to T1L but significantly enhanced compared to T3D.

r1Reovirus and r2Reovirus impact TNBC cell viability with faster kinetics than parental reoviruses.

Type 3 reoviruses induce cell death more efficiently than Type 1 reoviruses *in vitro* and *in vivo* and T3C$ is currently in clinical trials to test its efficacy as an oncolytic against a variety of cancers (32, 41). To determine the efficacy of viral-induced cytotoxicity in TNBC cells, MDA-MB-231 cells were adsorbed with mock, T1L, T3D, T3C$, r1Reovirus, or r2Reovirus at an MOI of 500 PFU/cell, or treated with staurosporine as a positive control, and assessed for cell viability for 7 days (FIG 5A). Compared to mock-infected cells, all reoviruses tested impaired cell viability, with reassortant reoviruses impairing cell viability with the fastest kinetics. In reassortant reovirus-infected cells, cell viability peaked at day 2 post infection, reaching levels similar to staurosporine by day 5 post infection. Cell viability peaked at day 3 post infection in T1L-, T3D-, and T3C$-infected cells reaching staurosporine levels by day 5 with T1L and day 6 with T3C$. At day 3 post infection, cell viability is significantly impaired in reassortant reovirus-infected cells, but not other reoviruses tested (FIG 5A). Overall, the impact on cell viability by reassortant viruses was 1 day ahead of T1L and

T3C$ and 2-3 days ahead of T3D. To determine if similar effects on cell viability could be observed in another TNBC cell line, MDA-MB-436 cells were infected with mock, T1L, T3D, T3C$, or r2Reovirus and assessed for cell viability over 6 days (FIG 5B). Similar to that observed in MDA-MB-231 cells, r2Reovirus induced cell death with significantly faster kinetics than either parental T1L or T3D, or T3C$. At day 4 post infection, r2Reovirus was the only virus tested to significantly impair MDA-MB-436 cell viability (FIG 5B). These data show that reassortant viruses negatively affect cell viability of TNBC cells more efficiently than parental reoviruses and the oncolytic T3C$ strain. These data also suggest that T3D is not efficient at inducing cell death in at least a subset of TNBC cells.

To determine if r1Reovirus and r2Reovirus differ from parental reoviruses in their ability to impair cell viability of non-TNBC cells, L929 cells were adsorbed with mock, T1L, T3D, T3C$, r1Reovirus, or r2Reovirus at an MOI of 500 PFU/cell and assessed for cell viability over a 3 day time course (FIG 5C). In contrast to that observed in MDA-MB-231 cells, all reoviruses tested impaired cell viability with relatively similar kinetics except for T3C$, which impaired L929 cell viability with significantly faster kinetics. These data indicate that reassortant viruses induce cell death with faster kinetics than parental reoviruses in TNBC cells and to a lesser extent in L929 cells. Given r2Reovirus had enhanced infectivity and cytotoxicity in MDA-MB-231 compared to parental viruses and r1Reovirus has a genomically unstable S2 gene segment, experiments in the rest of this study were performed with r2Reovirus.

Identification of small molecules that impact reovirus infectivity of MDA-MB-231 cells.

The efficacy of reovirus as a mono-oncolytic therapeutic has been limited. Combinatorial therapeutics can enhance efficacy by targeting different pathways that lead to enhanced cancer cell death (42). To identify small molecule inhibitors that enhance the oncolytic potential of reovirus, a

high-throughput screen to assess the effect of small molecules from the NIH Clinical Collection I and II (NCC) on reovirus infectivity was performed. The NCC is composed of compounds that have been through Phase I-III clinical trials. To test the effects on reovirus infectivity of compounds in the NCC, MDA-MB-231 cells were pre-treated with vehicle (DMSO), 4 μM E64-d, or 10 μM NCC compounds for 1 h. r2Reovirus was added to cells at an MOI of 20 PFU/cell, incubated for 20 h post infection in the presence of DMSO, 2 μM E64-d, or 5 μM NCC compounds, and scored for infectivity by indirect immunofluorescence using reovirus-specific antiserum (FIG 6A, Table S2). Of the 700 compounds in the NCC, 20 increased reovirus infectivity whereas 17 decreased infectivity (FIG 6B). Six microtubule-inhibiting compounds impaired reovirus infectivity, corroborating a need for microtubule function in reovirus cell entry (43). The sodium ATPase pump inhibitor digoxin and two serotonin antagonists also impaired reovirus infection, corroborating a role for the sodium ATPase pump and serotonin receptors in reovirus infection (44, 45). Four topoisomerase inhibitors, doxorubicin, epirubicin, etoposide (topoisomerase II inhibitors) and topotecan (topoisomerase I inhibitor), significantly enhanced reovirus infectivity. Topoisomerase inhibitors can sensitize TNBC cells to cell death but it is unknown how they impact reovirus-mediated cell death (46).

Topoisomerase inhibitors enhance reovirus infection of MDA-MB-231 cells without altering viral replication.

To determine if topoisomerase inhibitors affect reovirus infection of TNBC cells, MDA-MB-231 cells were treated with increasing concentrations of doxorubicin, epirubicin, and topotecan for 1 h at 37°C, infected with mock or r2Reovirus at an MOI of 100 PFU/cell, and scored for infectivity by indirect immunofluorescence using reovirus-specific antiserum (FIG 7). Reovirus infectivity increased slightly when cells were treated with 0.1 μM and more significantly when treated

with 1.0 μM with all three drugs. Treatment of cells with 10 μM doxorubicin or epirubicin decreased infectivity compared to 1.0 μM treatment, likely due to cellular cytotoxicity. In contrast, treatment of cells with 10 μM topotecan enhanced reovirus infectivity more than any other concentration tested. To determine if topoisomerase inhibitors affect reovirus replication in TNBC cells, MDA-MB-231 cells were treated with vehicle (DMSO), 1 μM doxorubicin, epirubicin, or topotecan, adsorbed with mock or r2Reovirus at an MOI of 10 PFU/cell, and assessed for replication over a 3 day time course (FIG 8). Treatment of cells with doxorubicin or epirubicin slightly decreased viral titers by day 3 post infection compared to DMSO. Treatment of cells with topotecan slightly affected viral titers at day 0, but replication kinetics were similar to all other conditions at days 1-3, with slightly higher viral yields at day 3.These data indicate that topoisomerase inhibitors augment reovirus infectivity in a concentration-dependent manner while not significantly altering the ability of reovirus to replicate in these cells.

Topoisomerase inhibitors enhance reovirus-mediated cell killing of MDA-MB-231 cells.

To determine if topoisomerase inhibitors confer additive or synergistic effects on reovirus-mediated cytotoxicity, MDA-MB-231 cells were treated with vehicle (DMSO) or increasing concentrations of doxorubicin, epirubicin, or topotecan for 1 h at 37°C, infected with r2Reovirus at an MOI of 200 PFU/cell, and assessed for cell viability over 3 days (FIG 9). Treatment with 0.1 μM of all three drugs did not significantly impact cell viability in the presence or absence of r2Reovirus. In the absence of virus, 1.0 μM doxorubicin and epirubicin impaired cell viability to similar levels as virus alone. Addition of reovirus moderately enhanced cytotoxicity compared to either agent alone. These effects can be especially observed at day 3 post infection (FIG 9B). Treatment with 10 μM doxorubicin or epirubicin had significant cytotoxic properties in the absence of reovirus. In contrast, 1.0 μM topotecan had significantly diminished cell viability in the absence of reovirus, and addition

of reovirus conferred an additive effect on the cytotoxic effects of both topotecan and reovirus. A synergistic cytotoxic effect was observed when reovirus was combined with 10 μM topotecan compared to either agent alone. Together, these data indicate that the combination of topoisomerase inhibitors with reovirus, especially topotecan, enhances the cytopathic properties of drugs and virus in a TNBC cell line.

Activation of DNA damage repair and innate immune signaling pathways following reovirus infection with topoisomerase inhibitors.

Reovirus infection activates innate immune signaling that results in the production of interferon (IFN) (8, 47). Topoisomerase inhibitors, but not reovirus, induce DNA damage repair pathways and can induce innate immune signaling (48). To determine if reovirus infection of TNBC cells impacts DNA damage repair and innate immune pathways, MDA-MB-231 cells were treated with DMSO, doxorubicin, epirubicin, or topotecan for 1 h at 37°C, infected with mock or r2Reovirus, whole cell lysates were collected at 0, 1, and 2 days post infection, and immunoblotted for phosphorylated and total STAT1, STAT2, STAT3, ATM, and p53 (FIG 10A). Reovirus infection in the presence of topotecan resulted in increased levels of phosphorylated STAT1 and STAT2 at day 1 post infection (FIG 10B). Total levels of STAT1 and STAT2 were slightly elevated in cells treated with doxorubicin, epirubicin, and topotecan compared to DMSO. STAT3 is constitutively activated in 40% of breast cancers and is associated with epithelial to mesenchymal transition (49, 50). Phosphorylated STAT3 was detected in the absence of reovirus regardless of the presence of topoisomerase inhibitors. Infection resulted in decreased levels of phosphorylated STAT3 at 1 and 2 dpi also independent of doxorubicin, epirubicin, or topotecan. These data indicate that reovirus infection of MDA-MB-231 cells promotes activation of innate immune pathways and that infection in the presence of topotecan, but not doxorubicin or epirubicin, enhances the activation of both

STAT1 and STAT2. Reovirus infection also dampens the activation of STAT3 independent of topoisomerase inhibitors.

Reovirus infection in the absence of topoisomerase inhibitors slightly affected phosphorylated and total levels of ATM and p53, with phosphorylated ATM levels trending upwards over the times tested (FIG 10C). Treatment of cells with topoisomerase inhibitors in the absence of reovirus increased levels of phosphorylated ATM and p53 compared to DMSO-treated cells at all time points tested. The activation of ATM and p53 by topoisomerase inhibitors was not affected by the presence of reovirus. These data suggest that reovirus does not affect the activation of DNA damage signaling activated by topoisomerase inhibitors.

Reovirus infection of TNBC cells results in increased levels of Type III interferon.

To assess if the increased levels of phosphorylated STAT1 and STAT2 correlate with IFN production during reovirus infection, MDA-MB-231 cells were treated with DMSO, doxorubicin, epirubicin, or topotecan for 1 h at 37°C, infected with r2Reovirus at an MOI of 100 PFU/cell, and RNA and supernatants were collected at 0, 8, 12, 24, and 48 h post infection (FIG 11). Reovirus mRNA levels were largely unaffected by the presence or absence of topoisomerase inhibitors up to 12 h post infection and slightly increased in doxorubicin and epirubicin at 24 and 48 h post infection compared to DMSO and topotecan (FIG 11A), confirming that topoisomerase inhibitors do not significantly affect reovirus replication. Despite robust infection, negligible levels of *IFNB1* mRNA were observed in the presence or absence topoisomerase inhibitors (FIG 11B). In contrast, significant levels of *IFNL1* mRNA were observed starting at 8 h post infection and up to 48 h post infection in infected cells (FIG 11C). Also, in infected cells *IFNL1* mRNA levels were higher in DMSO- and topotecan-treated cells at 8 and 12 h post infection than in doxorubicin- and epirubicin-treated cells, with the latter peaking at 24 h post infection. Interestingly, robust levels of

IFNL1 mRNA were observed at 24 h and 48 h in uninfected cells treated with doxorubicin and epirubicin. To determine if increasing levels of *IFNL1* mRNA result in increasing levels of protein, IFN-λ levels were assessed by ELISA (FIG 11D). Secreted IFN-λ was detected only in infected cells, except for low levels at 48 h in uninfected cells. IFN-λ was first observed at 12 h post infection only in epirubicin-treated cells. By 24 h post infection, IFN-λ was observed at similar levels in cells treated with DMSO, doxorubicin, and topotecan, but not epirubicin. At 48 h post infection, high levels of IFN-λ were observed in all infected conditions, with the highest levels observed in topotecan-treated cells. These data further support that topoisomerase inhibitors do not affect overall reovirus replication kinetics and that reovirus infection of MDA-MB-231 cells results in increased levels of Type III, but not Type I, IFN mRNA and protein. Although topoisomerase inhibitors had a modest effect in the induction of *IFNL1* mRNA following reovirus infection, the presence of topotecan had the largest effect on the levels of secreted IFN-λ .

Type III IFNs do not affect cell viability of TNBC cells.

Infection of MDA-MB-231 cells results in the production of Type III IFN. To determine if Type I or Type III IFNs impact cell viability of TNBC cells, MDA-MB-231 cells were treated with DMSO, increasing amounts of recombinant human IFN-λ or IFN-β, or 1 μM doxorubicin, or infected with r2Reovirus at an MOI of 100 PFU/cell, and assessed for cell viability over 3 days (FIG 12A). Treatment of cells with IFN-λ did not affect cell viability. In contrast, treatment of cells with IFN-β decreased cell viability in a dose-dependent manner, with cell viability levels reaching those see during reovirus infection with the highest dose tested. To determine if MDA-MB-231 cells can sense Type I and Type III IFNs, cells were untreated or treated with increasing amounts of IFN-λ or IFN-β, and assessed for the activation status of STAT1 and STAT2 after 1 h (FIG 12B). Compared to untreated cells, phosphorylated STAT1 and STAT2 were observed following

treatment with both IFN-λ or IFN-β, suggesting that MDA-MB-231 cells can respond to Type I and Type III IFNs. These data suggest that while infection of MDA-MB-231 cells results in robust production of Type III IFN, the cytotoxic effects of reovirus infection are not directly due to antiproliferative effects of the IFN-λ produced by these TNBC cells.

Discussion

Reovirus has an inherent preference to replicate in tumor cells, making it ideally suited for use in oncolytic therapy (14, 15). Reovirus can be delivered to patients via intratumoral and intravenous administration and can be effective in combination therapy (13). A Type 3 reovirus (T3C$) is currently in Phase I-II clinical trials against a variety of cancers in combination with several drugs (clinicaltrials.gov: NCT01622543, NCT01656538). In this study, we generated novel reassortant reoviruses with enhanced replicative properties in TNBC cells by coinfection of a TNBC cell line with prototype strains T1L, T2J, and T3D and serial passage. Reassortant reoviruses attach to cells with similar efficiency as T1L, whereas Type 3 reoviruses attach with enhanced efficacy. T1L uses GM2 glycans to attach to cells whereas T3D interacts with α2,3-linked sialic acid (38, 51). High expression of α2,3-sialic acid in breast cancer is associated with greater metastatic potential (52), suggesting the slight enhancement in attachment observed with Type 3 reoviruses could be due to high levels of α2,3-sialic acid present on the surface of MDA-MB-231 cells.

Reassortant viruses did not have mutations in σ 1 and the most predominant viruses following serial passaging all had a Type 1 σ1. These data suggest that carbohydrate binding did not drive selection of the reassortant viruses. JAM-A is expressed in normal mammary epithelial cells and high JAM-A expression in breast cancer patients correlates with worse survival and increased recurrence (53, 54). MDA-MB-231 cells express JAM-A (54), although relatively low JAM-A levels may be responsible for the lower infectivity observed by all reoviruses tested in comparison to

infection in L929 cells. These data suggest that receptor engagement is not responsible for the enhanced infectivity observed with the reassortant viruses.

During cell entry, reovirus traverses to endosomes where cathepsin proteases cleave outer capsid protein σ3, forming an infectious subvirion particle (ISVP) (40, 55). Both reassortants have a nonsynonymous mutation in the σ3-encoding S4 gene segment that results in a V49I substitution. This mutation has not been identified to impact reovirus disassembly kinetics, but it is possible it could expedite viral cell entry kinetics. However, reassortant viruses were equally sensitive to E64-d treatment as parental viruses. Although reassortant viruses infected MDA-MB-231 cells more efficiently than T1L, T3D, and T3C$, replication kinetics of the reassortant viruses were similar except for T3D, which had slower replication kinetics. These data indicate that Type 1 reoviruses replicate with enhanced kinetics compared to T3D, but that genetic differences between T3D and T3C$ are sufficient to allow T3C$ to replicate as efficiently as Type 1 viruses. These data also suggest that the enhanced cytotoxic properties of the reassortant viruses over parental viruses are not due to enhanced replication kinetics in MDA-MB-231 cells.

The reovirus L3, S2, and S3 gene segments have distinct roles in reovirus replication. The L3-encoded λ1 protein is a major inner-capsid protein that has phosphohydrolase activity and participates in viral transcription (56, 57). The S2-encoded σ2 protein is essential for the assembly of viral cores (58). The S3-encoded nonstructural protein σNS is required for viral factory formation (59). The similarity in replication efficiency observed between T1L and the reassortant viruses suggests the A160T mutation in L3 and I250V mutation in S3 (found in both reassortants) and the P161T in S3 (in r1Reovirus only) do not impact overall replication efficiency. However, it is possible that point mutations in these gene segments in the reassortant viruses impact the activity of the viral proteins that result in enhanced infectivity or cytotoxicity in the context of TNBC cells. Further

characterization of the point mutations found in the reassortant viruses will help elucidate their impact on viral fitness.

Of all the viruses tested in MDA-MB-231 cells, r1Reovirus and r2Reovirus impaired cell viability with the fastest kinetics, and only T3D was severely deficient in killing these cells. The poor induction of cell death by T3D may be related to its dampened replication in these cells. Differences in the induction of apoptosis by reovirus strains segregate with the M2 and S1 gene segments (32). Apoptosis is activated by fragments of the M2-encoded μ1 protein generated during reovirus cell entry (27, 31, 32, 60, 61). The σ1 protein impacts reovirus infectivity by enhancing reovirus attachment to cells (62). S1 is genetically linked to reovirus induction of apoptosis through the activities of both σ1 and σ1s, although it is unclear if the effects of σ1s on the induction of cell death are independent of its ability to regulate viral protein synthesis and induce cell cycle arrest (63, 64). We did not observe significant levels of cell cycle arrest in MDA-MB-231 cells infected with reassortant reoviruses (data not shown). It is unclear if the enhanced cytopathic properties of reassortant viruses in the context of TNBC cells maps to the T3D M2 gene segment, the various nonsynonymous changes, or a combination of both.

Screening small molecules from the NIH Clinical Collection identified 20 molecules that increase infectivity and 17 molecules that decreased infectivity in MDA-MB-231 cells. Six microtubule-inhibiting drugs, digoxin, and two serotonin antagonists affected reovirus infectivity, corroborating the role of microtubules, the sodium-potassium ATPase pump, and serotonin receptors in reovirus infection (43-45). Of the 17 molecules that enhanced infectivity, 4 are topoisomerase I (topotecan) or II (doxorubicin, epirubicin, and etoposide) inhibitors. Treatment of cells with topoisomerase inhibitors resulted in increased infectivity, with no effect on virus attachment (data not shown) or viral replication, except for slight increases in viral RNA at 24 and 48 h post infection. Topoisomerase inhibitors promote DNA double-strand breaks leading to cell

death (65-68). Reovirus infection does not induce DNA double-strand breaks and promotes cell death through the induction of extrinsic and intrinsic apoptosis or necroptosis (22, 23, 27, 32, 69, 70). It is possible that topoisomerase inhibitors positively affect uptake of viral particles during cell entry that results in enhanced infectivity and that doxorubicin and epirubicin further impact a step late in the viral life cycle that results in enhanced transcription of viral RNA. It is also possible that the additive cytotoxicity observed in MDA-MB-231 cells when both reovirus and topoisomerase inhibitors are present is through the activation of complementary cell death pathways.

Reovirus infection does not impair the DNA double strand break response activated by treatment with topoisomerase inhibitors. Late during infection in the presence of topoisomerase inhibitors, levels of phosphorylated and total p53 were lower than in uninfected cells. It remains to be determined if the effects of reovirus infection on p53 are at the transcriptional, translational, or post-translational level. Reovirus infection can induce higher levels of activated MDM2, which leads to p53 degradation (71). In the context of reovirus infection, it is possible that topoisomerase inhibitors promote p53 stabilization through impairing the activation of MDM2 by the virus. It is also possible the effects on total p53 at late times post infection are due to viral-dependent host translational shutoff. In support of this, total levels of STAT1, STAT2, STAT3, and ATM were also lower at late times of infection.

Reovirus infection of MDA-MB-231 cells resulted in robust expression of Type III, but not Type I, IFN mRNA and protein. Infection in the presence of topoisomerase inhibitors did not significantly affect levels of *IFNL1* mRNA. Interestingly, doxorubicin and epirubicin treatment in the absence of infection results in the induction of *IFNL1* mRNA starting at 24 h reaching similar levels to those detected in virus-infected cells by 48 h. Induction of DNA double strand breaks by topoisomerase inhibitors can result in p53-dependent regulation of Type I IFN through a STING-dependent but cGAS-independent pathway (48). MDA-MB-231 cells express STING (data not

shown), suggesting that topoisomerase inhibitors could be inducing transcription of Type III IFN downstream of the induction of the DNA damage response through a similar mechanism. However, topoisomerase inhibitors did not induce Type I IFN transcription in the presence or absence of reovirus.

Levels of IFN-λ were first observed at 12-24 h post infection in the presence or absence of topoisomerase inhibitors, with the highest levels of IFN-λ detected at 48 h post infection in the presence of topotecan. IFNλ1, IFNλ2, and IFNλ3 are expressed in breast cancer cells, although their role in mediating innate immunity in these cells is not well characterized (72). Type I and Type III IFN are transcriptionally regulated by the transcription factor IRF3 (73, 74). Reovirus can antagonize IFN production by sequestering IRF3 to viral inclusions (75) and infection of gut epithelial cells *in vitro* and *in vivo* results in upregulated levels of IFN-λ mRNA (75-77). It is possible that in MDA-MB-231 cells reovirus is unable to sequester IRF3 to viral inclusions, resulting in robust production of Type III IFN. Reovirus infection of TNBC cells resulted in high levels of secreted IFN-λ, with over 200 pg/ml detected at 48 h post infection in the presence or absence of topoisomerase inhibitors. Levels of IFN-λ in the presence of topotecan at 48 h post infection reached over 800 pg/ml, levels that are higher than that observed in dendritic cells that have been exposed to a RIG-I agonist (78). It is unclear why topotecan, but not doxorubicin or epirubicin result in significantly higher IFN-λ levels, especially considering that *IFNL1* mRNA levels were not different in infected cells in the presence of the different topoisomerase inhibitors. Interestingly, in the absence of reovirus, IFN-λ had no effect on MDA-MB-231 cell viability, while IFN-λ decreased cell viability in a concentration dependent manner. However, MDA-MB-231 cells responded to Type I and Type III IFN treatment, indicating these cells have functional receptors to detect and activate signaling pathways downstream of ligand engagement. MDA-MB-231 cells can express low basal levels and are responsive to Type I IFNs (79-81). The large levels of Type III IFN detected in

MDA-MB-231 cells, and lack of Type I IFN, indicates that STAT activation observed in these cells is likely in response to the interaction of IFN-λ with its receptors.

Despite the robust induction of Type III IFN in response to infection, robust levels of activated STAT1 and STAT2 were only detected in the presence of topotecan. Low levels of activated STAT1 were observed in infected cells in the absence of topoisomerase inhibitors, but no STAT activation was observed in the presence of doxorubicin or epirubicin. It is possible that the low levels of activated STAT1 and STAT2 in infected MDA-MB-231 cells are a result of impaired sensing of IFN-λ due to low level expression of the IFN-λ receptor. It is also possible that treatment of cells with topotecan may sensitize cells to IFN-λ through the upregulation of the IFN-λ receptor. Surprisingly, despite high levels of activated STAT1 and STAT2 following reovirus infection of topotecan-treated cells, reovirus infectivity and replication remained unimpaired.

In this study, we generated reoviruses with unique infective and cytotoxic properties by forward genetics following coinfection with three different serotype reoviruses. The novel genetic composition of the reassortant viruses could inform future studies on viral factors that promote infection and killing of cells by reovirus. Through high-throughput screening we identified topoisomerase inhibitors as a class of drug that enhances infection and the cytotoxic properties of reovirus in the context of TNBC. We also show that infection of a breast cancer cell line leads to the robust production of Type III, but not Type I, IFN. This study presents evidence for the pairing of reassortant reoviruses generated by forward genetics with topoisomerase inhibitors identified by high-throughput screening as a promising therapeutic against TNBC.

Materials and Methods

Cells, viruses, and antibodies

MDA-MB-231 cells (gift from Jennifer Pietenpol, Vanderbilt University) and MDA-MB-436 cells (ATCC HTB-130) were grown in Dulbecco's Modified Eagle's Medium (DMEM) supplemented with 10% fetal bovine serum (FBS) (Life Technologies), 100 U per ml penicillin and streptomycin (Life Technologies). Spinner-adapted L929 cells (Terry Dermody, University of Pittsburgh) were grown in Joklik's modified MEM with 5% FBS, 2 mM L- glutamine (Life Technologies), penicillin and streptomycin, and 0.25 mg per ml amphotericin B (Life Technologies).

Reovirus strains Type 1 Lang (T1L) and Type 3 Dearing (T3D) working stocks were prepared following rescue with reovirus cDNAs in BHK-T7 cells (gift from Terry Dermody, University of Pittsburgh), followed by plaque purification, and passage in L929 cells (82). Reovirus type 2 Jones (T2J) is a laboratory strain and Type 3 Cashdollar (T3C$) is a distinct Type 3 reovirus (83). Purified virions were prepared using second-passage L929 cell lysate stocks. Virus was purified from infected cell lysates by Vertrel XF (TMC Industries Inc.) extraction and CsCl gradient centrifugation as described (84). The band corresponding to the density of reovirus particles (1.36 g/cm^3) was collected and dialyzed exhaustively against virion storage buffer (150 mM NaCl, 15 mM MgCl2, 10 mM Tris-HCl [pH 7.4]). Reovirus particle concentration was determined from the equivalence of 1 unit of optical density at 260 nm to 2.1×10^{12} particles (85). Viral titers were determined by plaque assay using L929 cells (86). Reovirus virions were labeled with succinimidyl ester Alexa Fluor 488 (A488) (Life Technologies) as described (43, 87).

Reovirus polyclonal rabbit antiserum raised against reovirus strains T1L and T3D was purified as described (88) and cross-adsorbed for MDA-MB-231 cells. Secondary IRDye 680 and

800 antibodies (LI-COR Biosciences) and goat anti-rabbit Alexa Fluor 488 (A488) (Life Technologies).

Serial passage of T1L, T2J, and T3D in MDA-MB-231 cells

MDA-MB-231 cells were adsorbed with T1L, T2J, and T3D at a multiplicity of infection (MOI) of 1 PFU/cell for 1 h at room temperature and incubated for 48 h at 37°C in MDA-MB-231 cell media. Cells were freeze-thawed three times, fresh MDA-MB-231 cells were infected with 500 μl of freeze-thawed cell supernatant, and incubated for 48 h at 37°C. Serial passage was repeated 20 times and individual viral titers were obtained by plaque isolation following plaque assay in L929 cells.

Electrophoretic mobility of reovirus

5×10^{10} particles of purified reovirus or freeze-thawed supernatants containing reovirus mixed with 2X SDS-Sample Buffer (20% Glycerol, 100 mM Tris-HCl [pH 6.8], 0.4% SDS, and 3 mg Bromophenol Blue) were separated by SDS-PAGE using 4-20% gradient polyacrylamide gels (Bio-Rad Laboratories) at 10 mAmps for 16 h. The gel was stained with 5 μg/ml ethidium bromide for 20 min and imaged using a Chemidoc XRS+ (Bio-Rad).

Next Generation Sequencing of Reovirus

RNA from viral preparations of T1L, T2J, T3D, r1Reovirus, and r2Reovirus were obtained using an RNeasy RNA purification kit (Qiagen). Ten nanograms of viral RNA was used as input for cDNA synthesis using the Clontech SMARTer Stranded Total RNA-Seq Kit v2 (Pico Input, Mammalian) according to the manufacturer's instructions. Libraries were validated by capillary electrophoresis on an Agilent 4200 TapeStation, pooled, and sequenced on an Illumina HiSeq3000

with 100bp paired end reads averaging 13 million reads/sample, yielding an average depth of coverage > 1000 reads. Reads were trimmed of adapter sequence using Trimmomatic (version 0.36, http://www.usadellab.org/cms/?page=trimmomatic) using the TruSeq3-PE-2 paired end adapter reference. Trimmed reads from each sample were aligned to all of the parental strain reference sequences using the Burrows-Wheeler Aligner (BWA version 0.7.10-r789, http://bio-bwa.sourceforge.net/). Deduplication was performed with Picard tools (version 1.74(1243), https://broadinstitute.github.io/picard/), and variation was called, again for each sample against all the parental strain references, using the GATK pipeline's (version 3.4, https://software.broadinstitute.org/gatk/) HaplotypeCaller with ploidy set to 1 and other default parameters. The resultant Variant Call Files (.vcf) were examined for sample similarity/variation from the parental reference strains.

Flow cytometric analysis of cell-surface reovirus

MDA-MB-231 cells were adsorbed with 5×10^3-5×10^4 particles per cell of A633-labeled virus for 1 h at room temperature. Cells were washed with PBS, detached with Cellstripper (Cellgro) for 10 min at 37°C, quenched and washed with PBS containing 2% FBS. Cells were fixed in 1% EM-grade paraformaldehyde (Electron Microscopy Sciences). Mean fluorescence intensity (MFI) was assessed using a CytoFLEX flow cytometer (Beckman Coulter) and quantified using FlowJo software.

Reovirus infectivity assay

Reovirus infectivity was assessed by indirect immunofluorescence (23). MDA-MB-231 and L929 cells were adsorbed with reovirus at a range of MOIs for 1 h at room temperature, washed with PBS, and incubated in media for 16-24 h at 37°C. To assess the effects of topoisomerase

inhibitors on reovirus infectivity, cells were pretreated with topoisomerase inhibitors or E64-d for 1 h at 37°C, reovirus was added to cells, and incubated for 18-24 h at 37°C. Cells were fixed with ice-cold methanol and stored at -20°C for at least 30 min. Methanol was removed, cells were washed twice with PBS, and blocked with PBS containing 1% BSA for 15 min at room temperature. Cells were stained with reovirus-specific polyclonal antiserum (1:2000) for 1 h at room temperature, washed twice with PBS, stained with goat anti-rabbit Alexa 488 (1:1000) for 1 h at room temperature, counterstained with 0.5 ng/ml DAPI for 5 min at room temperature, and washed twice with PBS. Immunofluorescence was detected using a Lionheart FX Automated Microscope (Biotek) with a 4x-PLFL phase objective (NA 0.13), and percent infectivity was determined (reovirus positive cells/DAPI positive cells) using Gen5 software (Biotek).

Reovirus replication assay

MDA-MB-231 cells were adsorbed with reovirus at a MOI of 10 PFU/cell for 1 h at room temperature, washed with PBS, and incubated for 0-3 days in MDA-MB-231 media at 37°C. To determine the effects of topoisomerase inhibitors on reovirus replication, MDA-MB-231 cells were treated with vehicle or topoisomerase inhibitors for 1 h at 37°C, media was removed, cells were adsorbed with reovirus at an MOI of 10 PFU/cell for 1 h at room temperature, washed with PBS, and incubated for 0-3 days with complete media containing vehicle or topoisomerase inhibitors at 37°C. Cells were freeze-thawed three times and viral titers were determined by plaque assay using L929 cells. Viral yields were calculated by dividing viral titers by the viral titer from day 0.

Cell viability assay

Cell viability was assessed by measuring metabolic activity using Presto Blue reagent (Invitrogen). L929, MDA-MB-231, and MDA-MB-436 cells were adsorbed with reovirus at a range

of MOIs for 1 h at room temperature or treated with 1 μM staurosporine, washed with PBS, and incubated for 0-7 days at 37°C. To determine the effects of topoisomerase inhibitors on cell viability, cells were pretreated with increasing concentrations of topoisomerase inhibitors for 1 h at 37°C, reovirus was added to cells, and incubated in the presence of the inhibitors for 0-3 days. To determine the effect of recombinant IFNs on cell viability, MDA-MB-231 cells were treated with 10-5000 IU/ml human IFN-λ (Peprotech) or 10-1000 ng/ml IFN-β (Peprotech), 1 μ M doxorubicin, or infected with reovirus at an MOI of 100 PFU/cell and assessed for cell viability for 0-3 days. Presto Blue was added at each time point for 30 min at 37°C and fluorescence (540 nm excitation/590 nm emission) was measured with a Synergy HT plate reader (Biotek).

Screening of NIH Clinical Collection Small Molecule Inhibitors

The NIH Clinical Collection was obtained from the NIH Roadmap Molecular Libraries Screening Centers Network. MDA-MB-231 cells were treated with DMSO, 4 μM E64-d, or 10 μM of compounds from the NIH Clinical Collection for 1 h at 37°C. Media (mock) or reovirus was added to cells at an MOI of 20 PFU/cell, and incubated for 20 h at 37°C. Cells were fixed and scored for infectivity by indirect immunofluorescence as described previously. Z scores for each well were calculated using the following formula: Z score = (a-b)/c, where a is the percent infectivity (infected cells/number of cells), b is the median percent infectivity for each plate, and c is the standard deviation of percent infectivity for each plate. Z scores of $-2 > x < 2.0$ were considered significant. Data for all compounds in screen are provided in Table S2.

Immunoblotting for DNA damage response and innate immune molecules

MDA-MB-231 cells were treated with DMSO or 2 μM topoisomerase inhibitors for 1 h at 37°C, infected with mock or reovirus at an MOI of 100 PFU/cell, and incubated for 0-2 days at

37°C. To assess the ability of IFNs to stimulate immune signaling, MDA-MB-231 cells were treated with 10 and 100 ng/ml of IFN-λ or 100 and 1000 IU/ml IFN-β for 1 h at 37°C. Whole cell lysates were prepared using RIPA buffer (20 mM Tris-HCl [pH 7.5], 150 mM NaCl, 1 mM EDTA, 1% NP-40, 0.1% sodium dodecyl sulfate, 0.1% sodium deoxycholate) and fresh Protease Inhibitor Cocktail (P8340, Sigma-Aldrich), Phosphatase Inhibitor Cocktail 2 (P5726, Sigma-Aldrich), 1 mM sodium vanadate, and 1 mM phenylmethylsulfonyl fluoride (PMSF) and protein concentration was determined using the DC protein assay (Bio-Rad). Whole cell lysates were resolved by SDS-PAGE in 4-20% gradient Mini-PROTEAN TGX gels (Bio-Rad) and transferred to 0.2 μm pore size nitrocellulose membranes (Bio-Rad). Membranes were incubated for 1 h in blocking buffer (Tris-buffered saline [TBS] with 5% powdered milk), incubated with primary antibodies specific for phospho-STAT1 (Y701, clone D4A7 #7649), -STAT2 (Y690, clone D3P2P, #88410), -STAT3 (Y705, clone D3A7, #9145), -ATM(S1981, clone 10H11.E12, #4526), -p53(S15, #9284), total STAT1 (clone D3A7, #9145), STAT2 (clone D9J7L, #72604), STAT3 (clone 124H6, #9139), ATM (clone D2E2, #2873), p53 (clone 1C12, #2524), and GAPDH (clone GA1R, MA5-15738), and reovirus polyclonal antiserum overnight at 4°C. Antibodies are from Cell Signaling Technology except for GAPDH, ThermoFisher. Membranes were washed with TBS-T (TBS with 0.1% Tween 20) and incubated with secondary antibodies conjugated to IRDye 680 or IRDye 800. Membranes were imaged using a LiCor Odyssey CLx and processed in ImageStudio (LI-COR Biosciences).

qPCR assessment of Type 1 and 3 interferon transcript levels

MDA-MB-231 cells were treated with DMSO or 2 μM topoisomerase inhibitors for 1 h at 37°C, infected with mock or r2Reovirus at an MOI of 100 PFU/cell, and incubated for 0, 8, 12, 24, and 48 h. RNA was isolated using a QIAGEN RNeasy kit with on-column DNase digestion. cDNAs were generated using 500 ng of RNA and random primers with the High-Capacity cDNA

Reverse Transcription Kit (ThermoFisher) in a SimpliAmp Thermal Cycler (ThermoFisher). cDNA was diluted 1:5 in nuclease-free water and qPCR reactions were performed in MicroAmp Fast Optical 96-Well Reaction Plates (Applied Biosystems) using PrimeTime qPCR assays (IDT) for *IFNB1*, *IFNL1*, *HPRT1*, and a custom assay for the reovirus S1 gene segment (Probe: 5'-/56-FAM/TCAATGCTG/ZEN/TCGAACCACGAGTTGA/3IABkFQ/-3'; Primer 1: 5'-CGAGTCAGGTCACGCAATTA-3'; Primer 2: 5'-GGATGTTCGTCCAGTGAGATTAG-3') using a 7500 Fast Real-Time PCR System (Applied Biosystems) and accompanying software to analyze qPCR data.

IFNλ ELISA

MDA-MB-231 cells were treated with DMSO or 2 μM topoisomerase inhibitors for 1 h at 37°C, infected with mock or r2Reovirus at an MOI of 100 PFU/cell, and incubated for 0, 8, 12, 24, and 48 h. Cell supernatants were collected and levels of IFN-λ were determined with the IFN-lambda 1/3 DuoSet ELISA kit (R&D Systems). Plates were read on a Synergy HT plate reader (Biotek) using 450 nm for sample detection and 540 nm for wavelength correction.

Statistical analysis

Mean values for quadruplicate experiments were compared using one or two-way analysis of variance (ANOVA) with Dunnett's or Tukey's multiple-comparisons test (Graph Pad Prism). *P* values of < 0.05 were considered statistically significant.

Data Availability

Individual mutations identified in reassortant viruses are listed in Table S1. The read files for this study have been deposited with the NCBI Sequence Read Archive (SRA) and are available via accession PRJNA561538.

Acknowledgements

This work was supported by funding from the Children's Healthcare of Atlanta and the Pediatric Research Institute and Winship Comprehensive Cancer Institute #IRG-14-188-01 from the American Cancer Society (B.A.M.). Flow cytometry experiments were performed in the Emory Pediatrics Flow Cytometry Core (UL1TR002378). Imaging was performed at the Emory Integrated Cellular Imaging Core (2P30CA138292-04 and the Emory Pediatrics Institute). The Yerkes NHP Genomics Core is supported in part by NIH P51 OD011132. The funders had no role in the study design, data collection and analysis, decision to publish, or preparation of manuscript.

Figures and Tables

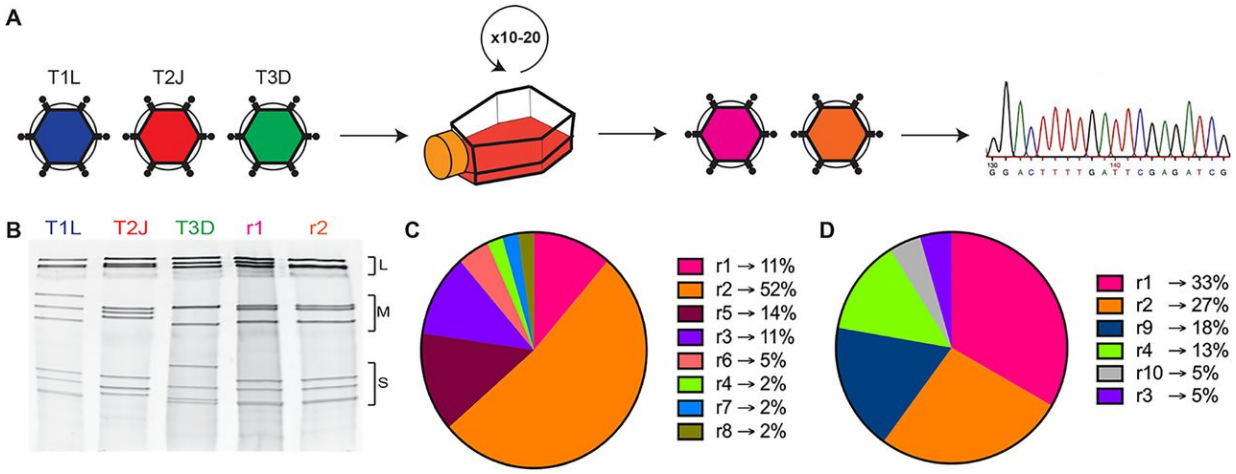

FIG 1. Generation of reoviruses by forward genetics in MDA-MB-231 cells. (A) Triple-negative breast cancer MDA-MB-231 cells were co-infected with T1L, T2J, and T3D and serially passaged ten or twenty times. Virus isolates were obtained following plaque assay on L929 cells and sequenced by Illumina Next-Generation Sequencing. (B) Polyacrylamide gel electrophoresis of reovirus parental strains T1L, T2J, and T3D and r1Reovirus (r1) and r2Reovirus (r2). Strains are differentiated by migration patterns of three large (L), three medium (M), and four small (S) gene segments. (C) Percentage of viral isolates with a specific electropherotype following 10 serial passages in MDA-MB-231 cells (n = 44). r1Reovirus (pink) accounts for 11% of isolates while r2Reovirus (orange) accounts for 52%. (D) Percentage of viral isolates with a specific electropherotype following 20 serial passages in MDA-MB-231 cells (n = 45). r1Reovirus (pink) accounts for 33% of isolates while r2Reovirus (orange) accounts for 27%.

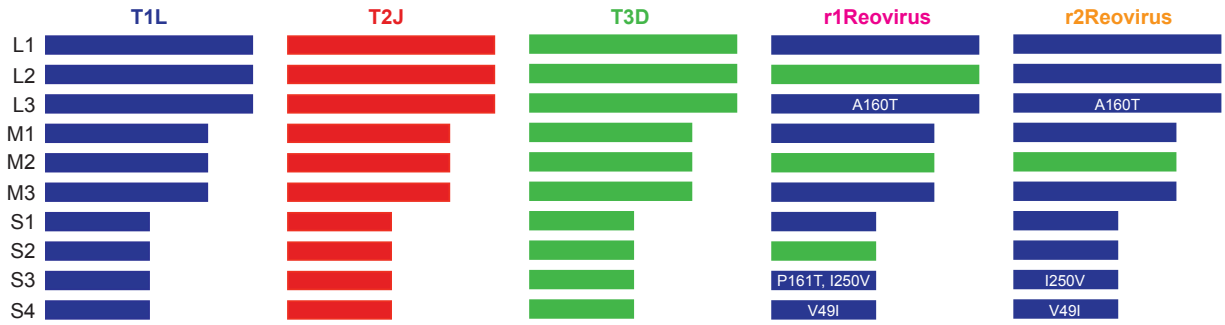

FIG 2. Genetic composition of r1Reovirus and r2Reovirus. The genetic composition of parental and reassortant r1Reovirus and r2Reovirus was determined by Illumina Next-Generation sequencing. r1Reovirus has seven gene segments from T1L and three from T3D (S2, M2, L2) and four nonsynonymous point mutations (L3 A160T, S3 P161T, I250V, and S4 V49I). r2Reovirus has nine gene segments from T1L and one from T3D (M2) and three nonsynonymous point mutations (L3 A160T, S3 I250V, and S4 V49I). Both r1Reovirus and r2Reovirus have several synonymous point mutations.

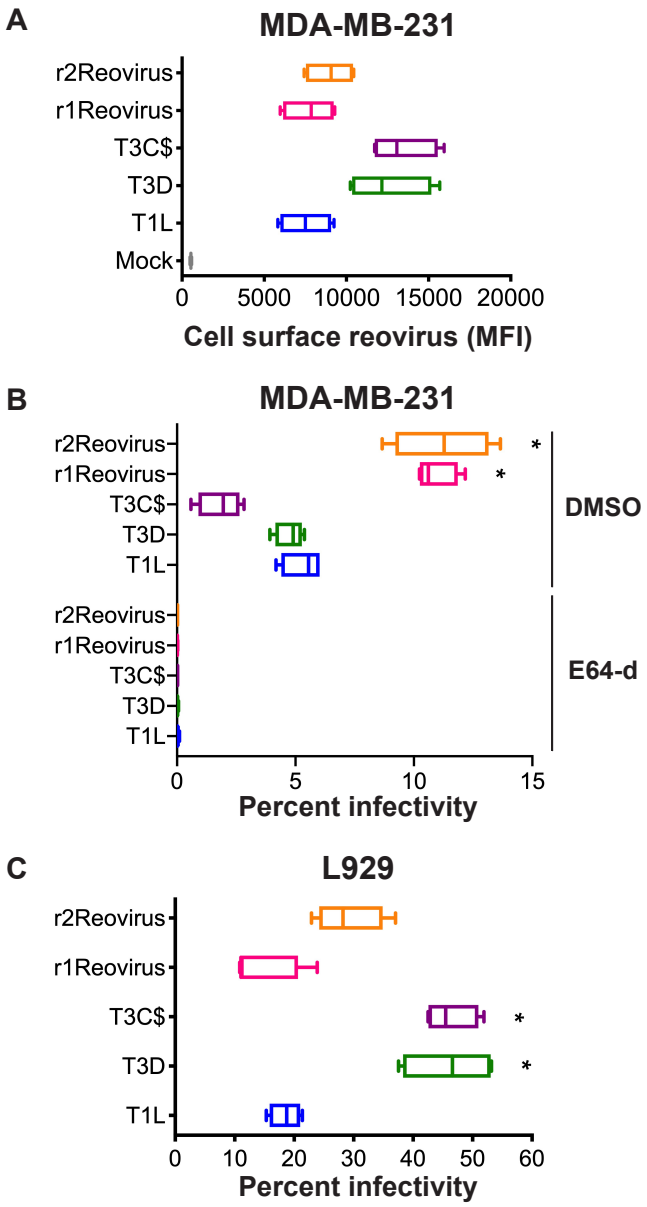

FIG 3. Attachment and infectivity of MDA-MB-231 cells by reassortant reoviruses. (A) MDA-MB-231 cells were adsorbed with A633-labeled T1L, T3D, T3C$, or reassortant reoviruses at an MOI of $5x10^4$ particles/cell and assessed for cell-surface reovirus by flow cytometry. Results are expressed as box and whisker plots of cell surface reovirus mean fluorescence intensity (MFI) for quadruplicate independent experiments. (B) MDA-MB-231 cells were treated with DMSO or 4 μM E64-d and adsorbed with T1L, T3D, T3C$, or reassortant reoviruses at an MOI of 100 PFU/cell and assessed

for infectivity after 18 h by indirect immunofluorescence using reovirus-specific antiserum. (C) L929 cells were adsorbed with T1L, T3D, T3C$, or reassortant reoviruses at an MOI of 5 PFU/cell and assessed for infectivity after 18 h by indirect immunofluorescence using reovirus-specific antiserum. Results are expressed as box and whisker plots of percent infectivity for quadruplicate independent experiments. *, $P < 0.0005$ in comparison to T1L by two-way ANOVA with Tukey's multiple comparisons test.

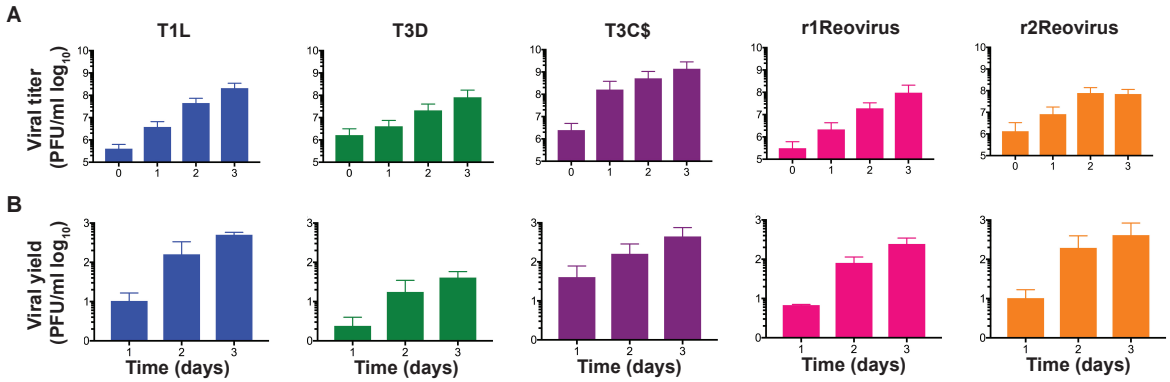

FIG 4. Reassortant viruses replicate with similar kinetics than T1L and T3C$, but faster than T3D, in MDA-MB-231 cells. T1L, T3D, T3C$, r1Reovirus, and r2Reovirus were adsorbed at an MOI of 10 PFU/cell and (A) viral titers and (B) viral yields were determined by plaque assay on L929 cells at 0-3 days post infection. The results are presented as (A) mean viral titers (± SEM) or (B) mean viral yields (± SEM) compared to day 0 post infection.

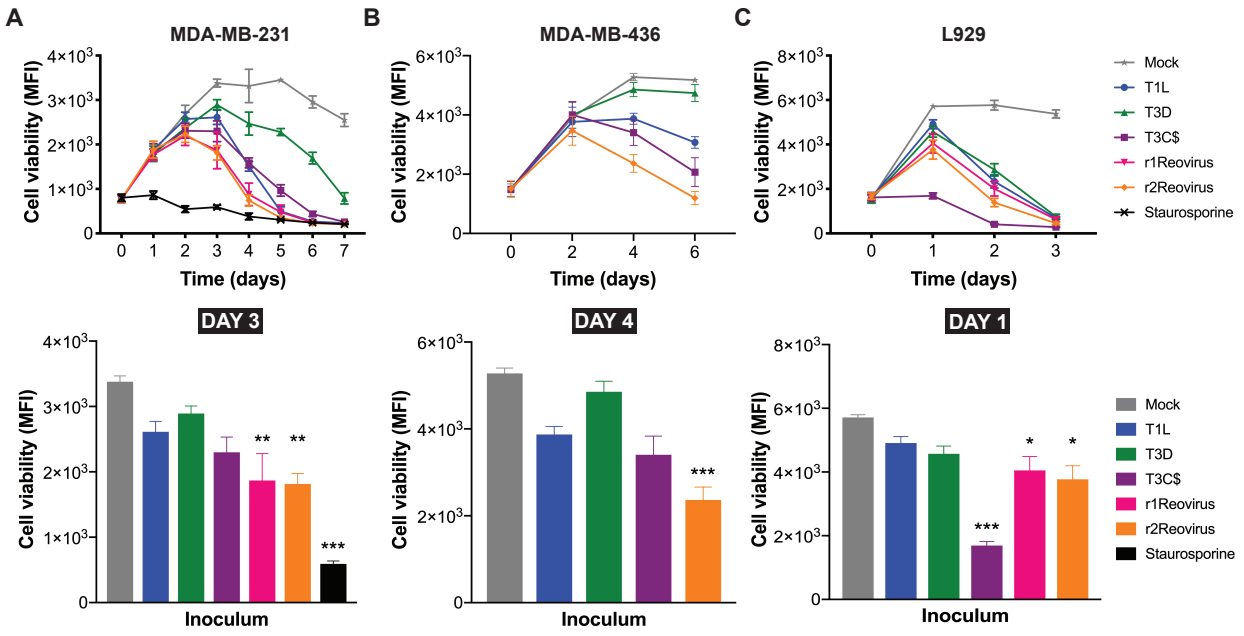

FIG 5. Impact on cell viability of TNBC cells and L929 cells following reovirus infection. (A) MDA-MB-231, (B) MDA-MB-436, and (C) L929 cells were adsorbed with T1L, T3D, T3C$, r1Reovirus, or r2Reovirus at an MOI of 500 PFU/ml or treated with 1 μM staurosporine and cell viability was assessed at times shown. Results are presented as mean fluorescence intensity (MFI) and SEM for four independent experiments. Bottom panel, cell viability for all cell lines in (A-C) for days 3, 4, and 1 post-infection. Error bars represent SEM. *, $P < 0.01$, **, $P \leq 0.001$, ***, $P \leq 0.0001$ in comparison to T1L by two-way ANOVA with Tukey's multiple comparisons test.

A

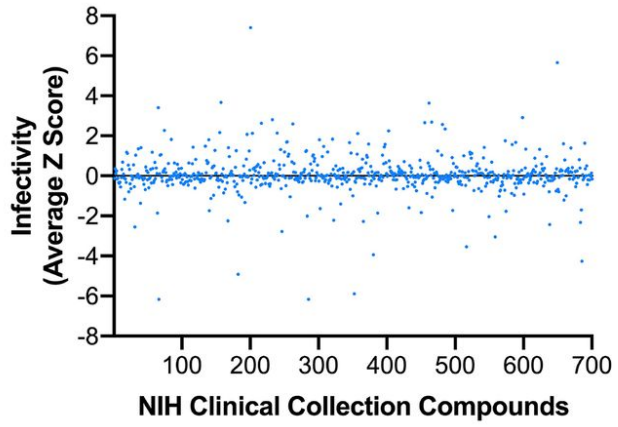

B

Compound Name	Target or Mode of Action	Run 1	Run 2	Average
Doxorubicin hydrochloride	Topoisomerase II Inhibitor	7.98	6.84	7.41
Topotecan hydrochloride	Topoisomerase I Inhibitor	5.38	5.94	5.66
Dactinomycin	DNA	3.18	4.16	3.67
Oligomycin A	ATPase Inhibitor	2.21	5.05	3.63
Azelastine hydrochloride	Histamine H1 Receptor Antagonist	2.98	3.85	3.41
Simvastatin	3-hydroxy-3-methyl-glutaryl-CoA Reductase	2.53	3.31	2.92
Etoposide	Topoisomerase II Inhibitor	3.35	2.26	2.81
Ondansetron	Serotonin 3 Receptor (5-HTR3) Antagonist	2.77	2.60	2.69
Nobiletin	MMP Inhibitor	2.12	3.19	2.66
Epirubicin hydrochloride	Topoisomerase II Inhibitor	3.24	2.02	2.63
Fluvastatin	3-hydroxy-3-methyl-glutaryl-CoA Reductase	2.45	2.75	2.60
Palonosetron hydrochloride	Serotonin 3 Receptor (5-HTR3) Antagonist	2.39	2.73	2.56
Paroxetine maleate	Serotonin Transporter	2.29	2.39	2.34
Benproperine phosphate	Cough Suppressor	2.22	2.33	2.27
Mevastatin	3-hydroxy-3-methyl-glutaryl-CoA Reductase	2.15	2.35	2.25
Cytarabine	Nucleoside Analogue	2.00	2.34	2.17
Fenofibrate	PPAR Alpha	1.87	2.41	2.14
Droperidol	Dopamine-2 Receptor Antagonist	2.76	1.49	2.13
Lovastatin	3-hydroxy-3-methyl-glutaryl-CoA Reductase	1.76	2.46	2.11
Donepezil hydrochloride	Acetylcholinesterase inhibitor	2.15	2.00	2.07

Compound Name	Target or Mode of Action	Run 1	Run 2	Average
Azithromycin	50S & 70S Ribosomes	-6.19	-6.15	-6.17
Homoharringtonine	80S Ribosome Subunit	-5.84	-6.50	-6.17
Loperamide hydrochloride	Opioid-receptor Agonist	-5.49	-6.30	-5.89
Digoxin	Na K ATPase Pump	-4.49	-5.36	-4.92
Vinorelbine tartrate	Microtubules	-3.86	-4.66	-4.26
Mercaptopurine	Purine Metabolism Inhibitor	-3.99	-3.89	-3.94
Podofilox	Microtubules	-3.45	-3.62	-3.54
Raloxifene hydrochloride	Estrogen Receptor Agonist	-2.30	-3.81	-3.05
Flubendazole	Microtubules	-3.53	-2.03	-2.78
Albendazole	Microtubules	-2.46	-2.64	-2.55
Thiothixene	Dopamine Antagonist	-2.16	-2.73	-2.44
Vincristine sulfate	Microtubules	-2.36	-2.31	-2.33
Mebendazole	Microtubules	-2.77	-1.78	-2.27
Desloratadine	Histamine H1 Receptor	-1.87	-2.60	-2.24
Itraconazole	Fungal P450	-2.85	-1.59	-2.22
Pyrimethamine	Folic Acid Antagonist	-2.11	-1.95	-2.03
Hexachlorophene	Glutamate Dehydrogenase	-2.21	-1.82	-2.01

FIG 6. Screening of NIH Clinical Collection small molecules for reovirus infectivity. MDA-MB-231 cells were treated with vehicle (DMSO), 4 μM E64-d, or 10 μM compounds from the NIH Clinical collection for 1 h, infected with r2Reovirus at an MOI of 20 PFU/cell in the presence of DMSO, 2 μM E64-d, or 5 μM compounds from the NIH Clinical collection for 20 h. Cells were scored for infectivity by indirect immunofluorescence using reovirus-specific antisera. (A) Data are shown as infectivity from average Z-scores for compounds in the NIH Clinical Collection for duplicate experiments. (B) Compounds from the NIH Clinical Collection that increase (green, top table) or decrease (red, bottom table) infectivity by 2 Z-scores or more. Data are shown for each experimental replicate (Run).

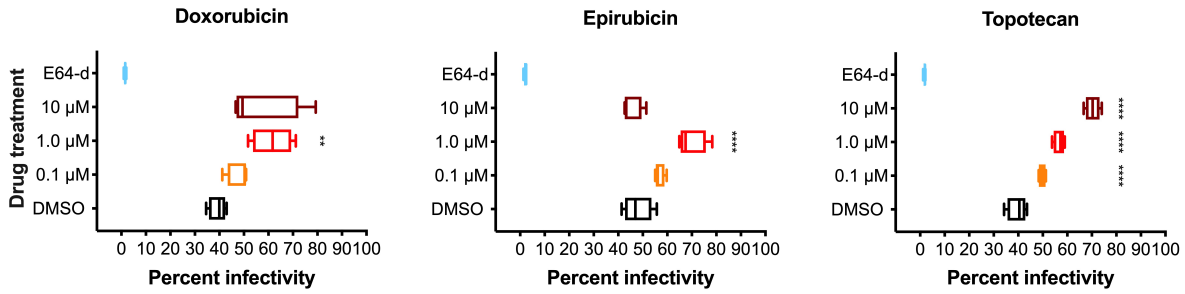

FIG 7. Topoisomerase inhibitors enhance reovirus infection of TNBC cells. MDA-MB-231 cells were treated for 1 h with vehicle (DMSO), 8 μM E64-d, or increasing concentrations doxorubicin, epirubicin, or topotecan and infected with r2Reovirus at an MOI of 100 PFU/cell for 20 h. Cells were assessed for infectivity by indirect immunofluorescence using reovirus-specific antisera. Data are shown as percent infectivity for quadruplicate independent experiments. **, $P \leq 0.01$, ***, $P < 0.001$, ****, $P < 0.0001$ in comparison to DMSO by one-way ANOVA with Dunnett's multiple comparisons test.

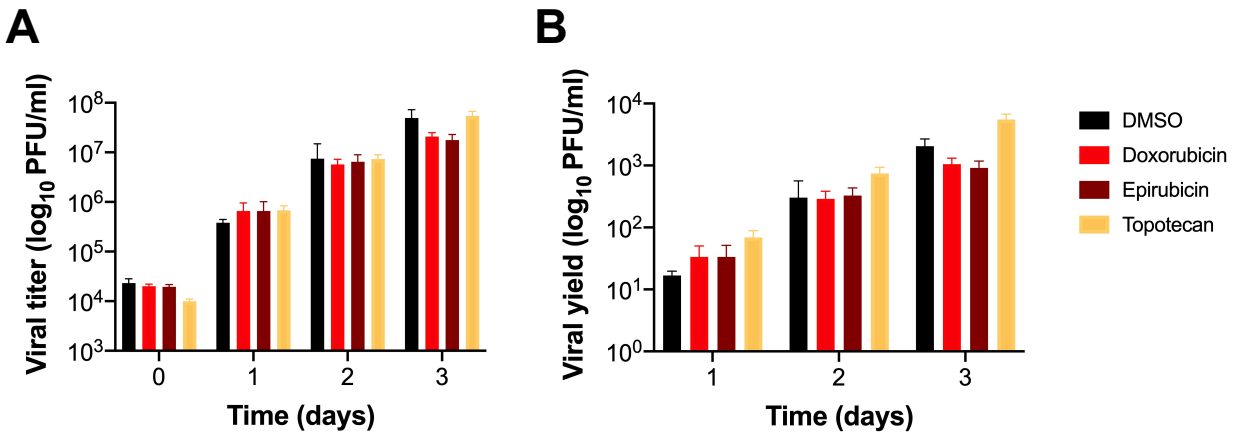

FIG 8. Topoisomerase inhibitor drugs do not impair r2Reovirus replication in MDA-MB-231 cells. MDA-MB-231 cells were treated with vehicle (DMSO), 1 μM topoisomerase inhibitors, adsorbed with r2Reovirus at an MOI of 10 PFU/cell, and assessed for viral replication by plaque assay on L929 cells at days 0-3 post infection. Results are presented as (A) mean viral titers (±SEM) and (B) mean viral yields (±SEM) from day 0.

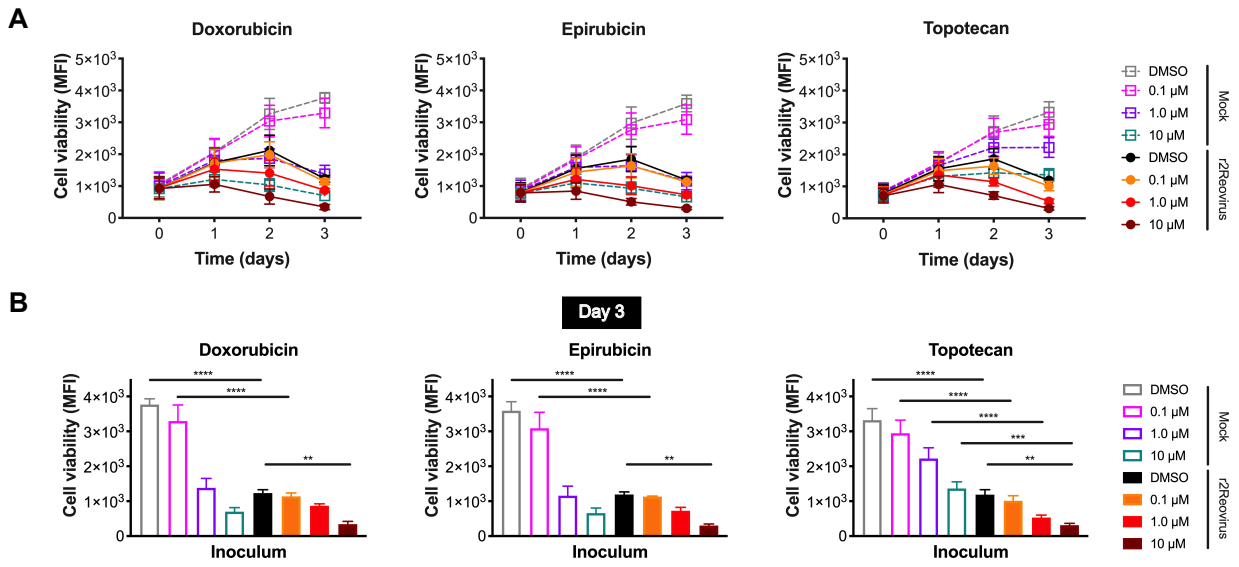

FIG 9. Cell viability of MDA-MB-231 cells is impaired by reovirus and topoisomerase inhibitors. (A) MDA-MB-231 cells were treated with vehicle (DMSO) or increasing concentrations of doxorubicin, epirubicin, or topotecan for 1 h, infected with r2Reovirus at an MOI of 200 PFU/cell, and assessed for cell viability at days 0-3 post infection. Data are shown as mean fluorescence intensity (MFI) for quadruplicate independent experiments. (B) Cell viability for all conditions in (A) for day 3 post infection. Error bars represent SEM. **, $P < 0.01$, ***, $P < 0.001$ by one-way ANOVA with Tukey's multiple comparisons test.

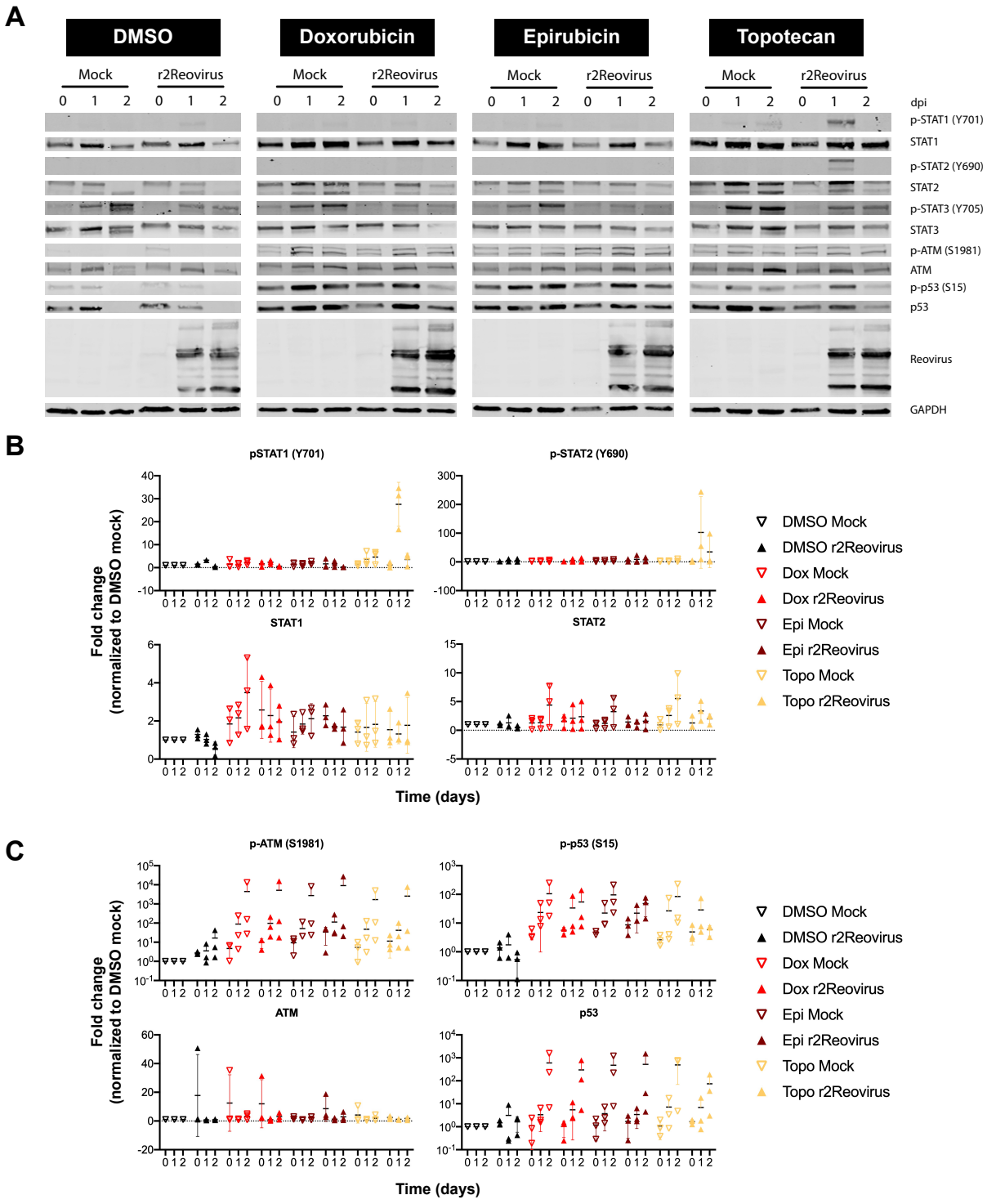

FIG 10. Reovirus activates STAT1 signaling and topoisomerase inhibitors activate DNA damage response pathways. (A) MDA-MB-231 cells were treated with vehicle (DMSO) or 2 μM

doxorubicin, epirubicin, or topotecan for 1 h, infected with reovirus at an MOI of 100 PFU/cell, and incubated with DMSO or 1 μM topoisomerase inhibitors for 0-2 days post infection. Whole cell lysates were resolved by SDS-PAGE and immunoblotted with antibodies specific for phosphorylated and total STAT1, STAT2, STAT3, ATM, p53 and GAPDH and reovirus. Residues recognized by phosphorylation-specific antibodies are shown in parenthesis. (B) Quantitative densitometry of immunoblots from three independent experiments. All data are normalized to GAPDH and DMSO Mock for each corresponding day. Error bars = SEM.

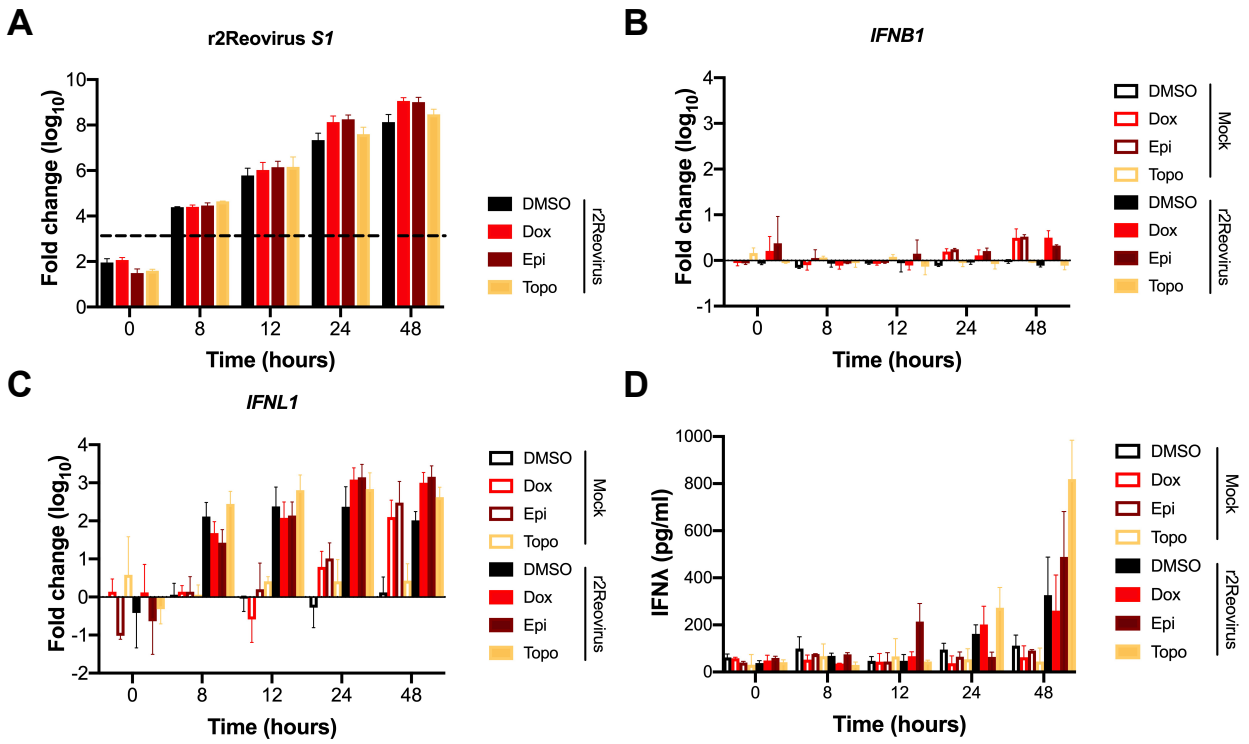

FIG 11. Topoisomerase inhibitors and r2Reovirus induce higher levels of IFNL1 over time than either agent alone. MDA-MB-231 cells were treated with vehicle (DMSO) or 2 μM doxorubicin, epirubicin, or topotecan, infected with mock or r2Reovirus at an MOI of 100 PFU/cell. RNA was isolated from cells at times shown and qPCR was performed to assess mRNA levels of (A) *IFNB1*, (B) *IFNL1*, and (C) reovirus *S1*. Dashed line in (C) represents background baseline levels observed in mock. Data are shown as fold change normalized to a housekeeping gene for duplicate independent experiments. Error bars = SEM. (D) Levels of IFN-λ in cell supernatants were detected by ELISA. Data are shown as pg/ml of IFN-λ for duplicate independent experiments.

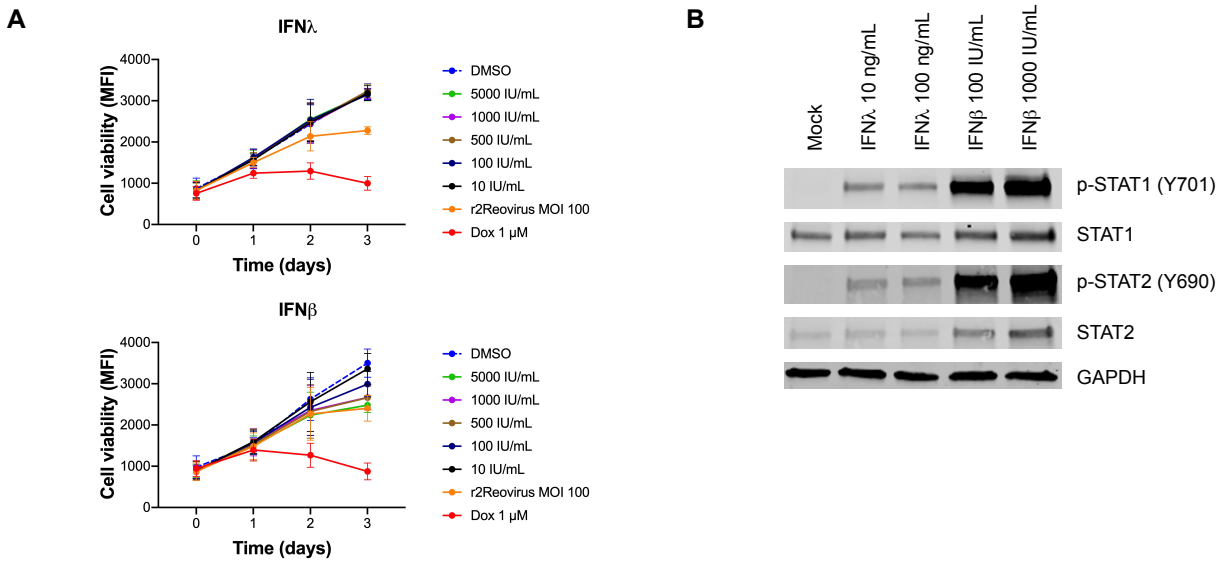

FIG 12. IFN-λ does not impact MDA-MB-231 cellular proliferation but activates STATs. (A) MDA-MB-231 cells were treated with DMSO, increasing amounts of recombinant human IFN-λ, recombinant human IFN-β, or 1 μM doxorubicin, or infected with r2Reovirus at an MOI of 100 PFU/cell for 1 h and assessed for cell viability at times shown. Data are shown as average mean fluorescent intensity (MFI) for quadruplicate independent experiments. Error bars = SEM. (B) MDA-MB-31 were untreated or treated with increasing amounts of recombinant human IFN-λ or IFN-β for 1h. Whole cell lysates were resolved by SDS-PAGE and immunoblotted with antibodies specific for phosphorylated and total STAT1, STAT2, and GAPDH. Residues recognized by phosphorylation-specific antibodies are shown in parenthesis.

References

1. Abramson VG, Lehmann BD, Ballinger TJ, Pietenpol JA. 2015. Subtyping of triple-negative breast cancer: implications for therapy. Cancer 121:8-16.
2. Lehmann BD, Bauer JA, Chen X, Sanders ME, Chakravarthy AB, Shyr Y, Pietenpol JA. 2011. Identification of human triple-negative breast cancer subtypes and preclinical models for selection of targeted therapies. J Clin Invest 121:2750-67.
3. Wahba HA, El-Hadaad HA. 2015. Current approaches in treatment of triple-negative breast cancer. Cancer Biol Med 12:106-16.
4. Zeichner SB, Terawaki H, Gogineni K. 2016. A Review of Systemic Treatment in Metastatic Triple-Negative Breast Cancer. Breast Cancer (Auckl) 10:25-36.
5. Dock G. 1904. The Influence of Complicating Diseases Upon Leukemia. Am J Med Sci 127:563-592.
6. Cattaneo R, Miest T, Shashkova EV, Barry MA. 2008. Reprogrammed viruses as cancer therapeutics: targeted, armed and shielded. Nat Rev Microbiol 6:529-40.
7. Bell J, McFadden G. 2014. Viruses for tumor therapy. Cell Host Microbe 15:260-5.
8. Phillips MB, Stuart JD, Rodriguez Stewart RM, Berry JT, Mainou BA, Boehme KW. 2018. Current understanding of reovirus oncolysis mechanisms. Oncolytic Virother 7:53-63.
9. Brown MC, Holl EK, Boczkowski D, Dobrikova E, Mosaheb M, Chandramohan V, Bigner DD, Gromeier M, Nair SK. 2017. Cancer immunotherapy with recombinant poliovirus induces IFN-dominant activation of dendritic cells and tumor antigen-specific CTLs. Sci Transl Med 9.
10. El-Sherbiny YM, Holmes TD, Wetherill LF, Black EV, Wilson EB, Phillips SL, Scott GB, Adair RA, Dave R, Scott KJ, Morgan RS, Coffey M, Toogood GJ, Melcher AA, Cook GP. 2015. Controlled infection with a therapeutic virus defines the activation kinetics of human natural killer cells in vivo. Clin Exp Immunol 180:98-107.
11. Kelly KR, Espitia CM, Zhao W, Wu K, Visconte V, Anwer F, Calton CM, Carew JS, Nawrocki ST. 2018. Oncolytic reovirus sensitizes multiple myeloma cells to anti-PD-L1 therapy. Leukemia 32:230-233.
12. Iordanov MS, Ryabinina OP, Schneider P, Magun BE. 2005. Two mechanisms of caspase 9 processing in double-stranded RNA- and virus-triggered apoptosis. Apoptosis 10:153-66.
13. Rajani K, Parrish C, Kottke T, Thompson J, Zaidi S, Ilett L, Shim KG, Diaz RM, Pandha H, Harrington K, Coffey M, Melcher A, Vile R. 2016. Combination Therapy With Reovirus and Anti-PD-1 Blockade Controls Tumor Growth Through Innate and Adaptive Immune Responses. Mol Ther 24:166-74.
14. Duncan MR, Stanish SM, Cox DC. 1978. Differential sensitivity of normal and transformed human cells to reovirus infection. J Virol 28:444-9.
15. Kemp V, Hoeben RC, van den Wollenberg DJ. 2015. Exploring Reovirus Plasticity for Improving Its Use as Oncolytic Virus. Viruses 8.
16. Shatkin AJ, Sipe JD, Loh P. 1968. Separation of ten reovirus genome segments by polyacrylamide gel electrophoresis. J Virol 2:986-91.
17. Dermody TS, Parker J, Sherry B. 2013. Orthoreoviruses, p 1304-1346. *In* Knipe DM, Howley PM (ed), Fields Virology, Sixth ed, vol 2. Lippincott Williams & Wilkins, Philadelphia.
18. Sabin AB. 1959. Reoviruses. A new group of respiratory and enteric viruses formerly classified as ECHO type 10 is described. Science 130:1387-9.
19. Ouattara LA, Barin F, Barthez MA, Bonnaud B, Roingeard P, Goudeau A, Castelnau P, Vernet G, Paranhos-Baccala G, Komurian-Pradel F. 2011. Novel human reovirus isolated from children with acute necrotizing encephalopathy. Emerg Infect Dis 17:1436-44.

20. Tai JH, Williams JV, Edwards KM, Wright PF, Crowe JE, Jr., Dermody TS. 2005. Prevalence of reovirus-specific antibodies in young children in Nashville, Tennessee. J Infect Dis 191:1221-4.
21. Bouziat R, Hinterleitner R, Brown JJ, Stencel-Baerenwald JE, Ikizler M, Mayassi T, Meisel M, Kim SM, Discepolo V, Pruijssers AJ, Ernest JD, Iskarpatyoti JA, Costes LM, Lawrence I, Palanski BA, Varma M, Zurenski MA, Khomandiak S, McAllister N, Aravamudhan P, Boehme KW, Hu F, Samsom JN, Reinecker HC, Kupfer SS, Guandalini S, Semrad CE, Abadie V, Khosla C, Barreiro LB, Xavier RJ, Ng A, Dermody TS, Jabri B. 2017. Reovirus infection triggers inflammatory responses to dietary antigens and development of celiac disease. Science 356:44-50.
22. Berger AK, Danthi P. 2013. Reovirus activates a caspase-independent cell death pathway. MBio 4:e00178-13.
23. Berger AK, Hiller BE, Thete D, Snyder AJ, Perez E, Jr., Upton JW, Danthi P. 2017. Viral RNA at Two Stages of Reovirus Infection Is Required for the Induction of Necroptosis. J Virol 91.
24. Brown JJ, Short SP, Stencel-Baerenwald J, Urbanek K, Pruijssers AJ, McAllister N, Ikizler M, Taylor G, Aravamudhan P, Khomandiak S, Jabri B, Williams CS, Dermody TS. 2018. Reovirus-Induced Apoptosis in the Intestine Limits Establishment of Enteric Infection. J Virol 92.
25. Clarke P, Beckham JD, Leser JS, Hoyt CC, Tyler KL. 2009. Fas-mediated apoptotic signaling in the mouse brain following reovirus infection. J Virol 83:6161-70.
26. Clarke P, Meintzer SM, Spalding AC, Johnson GL, Tyler KL. 2001. Caspase 8-dependent sensitization of cancer cells to TRAIL-induced apoptosis following reovirus-infection. Oncogene 20:6910-9.
27. Danthi P, Coffey CM, Parker JS, Abel TW, Dermody TS. 2008. Independent regulation of reovirus membrane penetration and apoptosis by the mu1 phi domain. PLoS Pathog 4:e1000248.
28. Pruijssers AJ, Hengel H, Abel TW, Dermody TS. 2013. Apoptosis induction influences reovirus replication and virulence in newborn mice. J Virol 87:12980-9.
29. Simon EJ, Howells MA, Stuart JD, Boehme KW. 2017. Serotype-Specific Killing of Large Cell Carcinoma Cells by Reovirus. Viruses 9.
30. Connolly JL, Barton ES, Dermody TS. 2001. Reovirus binding to cell surface sialic acid potentiates virus-induced apoptosis. J Virol 75:4029-39.
31. Danthi P, Hansberger MW, Campbell JA, Forrest JC, Dermody TS. 2006. JAM-A-independent, antibody-mediated uptake of reovirus into cells leads to apoptosis. J Virol 80:1261-70.
32. Tyler KL, Squier MK, Rodgers SE, Schneider BE, Oberhaus SM, Grdina TA, Cohen JJ, Dermody TS. 1995. Differences in the capacity of reovirus strains to induce apoptosis are determined by the viral attachment protein sigma 1. J Virol 69:6972-9.
33. Nibert ML, Margraf RL, Coombs KM. 1996. Nonrandom segregation of parental alleles in reovirus reassortants. J Virol 70:7295-300.
34. Wenske EA, Chanock SJ, Krata L, Fields BN. 1985. Genetic reassortment of mammalian reoviruses in mice. J Virol 56:613-6.
35. Barton ES, Forrest JC, Connolly JL, Chappell JD, Liu Y, Schnell FJ, Nusrat A, Parkos CA, Dermody TS. 2001. Junction adhesion molecule is a receptor for reovirus. Cell 104:441-51.
36. Kirchner E, Guglielmi KM, Strauss HM, Dermody TS, Stehle T. 2008. Structure of reovirus sigma1 in complex with its receptor junctional adhesion molecule-A. PLoS Pathog 4:e1000235.
37. Konopka-Anstadt JL, Mainou BA, Sutherland DM, Sekine Y, Strittmatter SM, Dermody TS. 2014. The Nogo receptor NgR1 mediates infection by mammalian reovirus. Cell Host Microbe 15:681-91.
38. Reiss K, Stencel JE, Liu Y, Blaum BS, Reiter DM, Feizi T, Dermody TS, Stehle T. 2012. The GM2 glycan serves as a functional coreceptor for serotype 1 reovirus. PLoS Pathog 8:e1003078.

39. Reiter DM, Frierson JM, Halvorson EE, Kobayashi T, Dermody TS, Stehle T. 2011. Crystal structure of reovirus attachment protein sigma1 in complex with sialylated oligosaccharides. PLoS Pathog 7:e1002166.
40. Baer GS, Dermody TS. 1997. Mutations in reovirus outer-capsid protein sigma3 selected during persistent infections of L cells confer resistance to protease inhibitor E64. J Virol 71:4921-8.
41. Oberhaus SM, Smith RL, Clayton GH, Dermody TS, Tyler KL. 1997. Reovirus infection and tissue injury in the mouse central nervous system are associated with apoptosis. J Virol 71:2100-6.
42. Lee MY, Zhang S, Lin SH, Chea J, Wang X, LeRoy C, Wong A, Zhang Z, Lee EY. 2012. Regulation of human DNA polymerase delta in the cellular responses to DNA damage. Environ Mol Mutagen 53:683-98.
43. Mainou BA, Zamora PF, Ashbrook AW, Dorset DC, Kim KS, Dermody TS. 2013. Reovirus cell entry requires functional microtubules. MBio 4.
44. Ashbrook AW, Lentscher AJ, Zamora PF, Silva LA, May NA, Bauer JA, Morrison TE, Dermody TS. 2016. Antagonism of the Sodium-Potassium ATPase Impairs Chikungunya Virus Infection. MBio 7.
45. Mainou BA, Ashbrook AW, Smith EC, Dorset DC, Denison MR, Dermody TS. 2015. Serotonin Receptor Agonist 5-Nonyloxytryptamine Alters the Kinetics of Reovirus Cell Entry. J Virol 89:8701-12.
46. Das S, Tripathi N, Siddharth S, Nayak A, Nayak D, Sethy C, Bharatam PV, Kundu CN. 2017. Etoposide and doxorubicin enhance the sensitivity of triple negative breast cancers through modulation of TRAIL-DR5 axis. Apoptosis 22:1205-1224.
47. Sherry B, Torres J, Blum MA. 1998. Reovirus induction of and sensitivity to beta interferon in cardiac myocyte cultures correlate with induction of myocarditis and are determined by viral core proteins. J Virol 72:1314-23.
48. Dunphy G, Flannery SM, Almine JF, Connolly DJ, Paulus C, Jonsson KL, Jakobsen MR, Nevels MM, Bowie AG, Unterholzner L. 2018. Non-canonical Activation of the DNA Sensing Adaptor STING by ATM and IFI16 Mediates NF-kappaB Signaling after Nuclear DNA Damage. Mol Cell 71:745-760 e5.
49. Alvarez JV, Febbo PG, Ramaswamy S, Loda M, Richardson A, Frank DA. 2005. Identification of a genetic signature of activated signal transducer and activator of transcription 3 in human tumors. Cancer Res 65:5054-62.
50. Banerjee K, Resat H. 2016. Constitutive activation of STAT3 in breast cancer cells: A review. Int J Cancer 138:2570-8.
51. Barton ES, Connolly JL, Forrest JC, Chappell JD, Dermody TS. 2001. Utilization of sialic acid as a coreceptor enhances reovirus attachment by multistep adhesion strengthening. J Biol Chem 276:2200-11.
52. Cui H, Lin Y, Yue L, Zhao X, Liu J. 2011. Differential expression of the alpha2,3-sialic acid residues in breast cancer is associated with metastatic potential. Oncol Rep 25:1365-71.
53. McSherry EA, McGee SF, Jirstrom K, Doyle EM, Brennan DJ, Landberg G, Dervan PA, Hopkins AM, Gallagher WM. 2009. JAM-A expression positively correlates with poor prognosis in breast cancer patients. Int J Cancer 125:1343-51.
54. Naik MU, Naik TU, Suckow AT, Duncan MK, Naik UP. 2008. Attenuation of junctional adhesion molecule-A is a contributing factor for breast cancer cell invasion. Cancer Res 68:2194-203.
55. Ebert DH, Deussing J, Peters C, Dermody TS. 2002. Cathepsin L and cathepsin B mediate reovirus disassembly in murine fibroblast cells. J Biol Chem 277:24609-17.
56. Noble S, Nibert ML. 1997. Characterization of an ATPase activity in reovirus cores and its genetic association with core-shell protein lambda1. J Virol 71:2182-91.

57. Drayna D, Fields BN. 1982. Activation and characterization of the reovirus transcriptase: genetic analysis. J Virol 41:110-8.
58. Coombs KM, Mak SC, Petrycky-Cox LD. 1994. Studies of the major reovirus core protein sigma 2: reversion of the assembly-defective mutant tsC447 is an intragenic process and involves back mutation of Asp-383 to Asn. J Virol 68:177-86.
59. Becker MM, Goral MI, Hazelton PR, Baer GS, Rodgers SE, Brown EG, Coombs KM, Dermody TS. 2001. Reovirus sigmaNS protein is required for nucleation of viral assembly complexes and formation of viral inclusions. J Virol 75:1459-75.
60. Tyler KL, Squier MK, Brown AL, Pike B, Willis D, Oberhaus SM, Dermody TS, Cohen JJ. 1996. Linkage between reovirus-induced apoptosis and inhibition of cellular DNA synthesis: role of the S1 and M2 genes. J Virol 70:7984-91.
61. Rodgers SE, Barton ES, Oberhaus SM, Pike B, Gibson CA, Tyler KL, Dermody TS. 1997. Reovirus-induced apoptosis of MDCK cells is not linked to viral yield and is blocked by Bcl-2. J Virol 71:2540-6.
62. Thete D, Snyder AJ, Mainou BA, Danthi P. 2016. Reovirus mu1 Protein Affects Infectivity by Altering Virus-Receptor Interactions. J Virol 90:10951-10962.
63. Boehme KW, Hammer K, Tollefson WC, Konopka-Anstadt JL, Kobayashi T, Dermody TS. 2013. Nonstructural protein sigma1s mediates reovirus-induced cell cycle arrest and apoptosis. J Virol 87:12967-79.
64. Phillips MB, Stuart JD, Simon EJ, Boehme KW. 2018. Nonstructural Protein sigma1s Is Required for Optimal Reovirus Protein Expression. J Virol 92.
65. Arcamone F, Penco S, Vigevani A, Redaelli S, Franchi G, DiMarco A, Casazza AM, Dasdia T, Formelli F, Necco A, Soranzo C. 1975. Synthesis and antitumor properties of new glycosides of daunomycinone and adriamycinone. J Med Chem 18:703-7.
66. Burris HA, 3rd, Hanauske AR, Johnson RK, Marshall MH, Kuhn JG, Hilsenbeck SG, Von Hoff DD. 1992. Activity of topotecan, a new topoisomerase I inhibitor, against human tumor colony-forming units in vitro. J Natl Cancer Inst 84:1816-20.
67. Hsiang YH, Hertzberg R, Hecht S, Liu LF. 1985. Camptothecin induces protein-linked DNA breaks via mammalian DNA topoisomerase I. J Biol Chem 260:14873-8.
68. Ross WE, Bradley MO. 1981. DNA double-stranded breaks in mammalian cells after exposure to intercalating agents. Biochim Biophys Acta 654:129-34.
69. Danthi P, Kobayashi T, Holm GH, Hansberger MW, Abel TW, Dermody TS. 2008. Reovirus apoptosis and virulence are regulated by host cell membrane penetration efficiency. J Virol 82:161-72.
70. Danthi P, Pruijssers AJ, Berger AK, Holm GH, Zinkel SS, Dermody TS. 2010. Bid regulates the pathogenesis of neurotropic reovirus. PLoS Pathog 6:e1000980.
71. Zhang X, Wu H, Liu C, Tian J, Qu L. 2015. PI3K/Akt/p53 pathway inhibits reovirus infection. Infect Genet Evol 34:415-22.
72. Yang L, Wei J, He S. 2010. Integrative genomic analyses on interferon-lambdas and their roles in cancer prediction. Int J Mol Med 25:299-304.
73. Onoguchi K, Yoneyama M, Takemura A, Akira S, Taniguchi T, Namiki H, Fujita T. 2007. Viral infections activate types I and III interferon genes through a common mechanism. J Biol Chem 282:7576-81.
74. Schafer SL, Lin R, Moore PA, Hiscott J, Pitha PM. 1998. Regulation of type I interferon gene expression by interferon regulatory factor-3. J Biol Chem 273:2714-20.
75. Stanifer ML, Kischnick C, Rippert A, Albrecht D, Boulant S. 2017. Reovirus inhibits interferon production by sequestering IRF3 into viral factories. Sci Rep 7:10873.

76. Pervolaraki K, Rastgou Talemi S, Albrecht D, Bormann F, Bamford C, Mendoza JL, Garcia KC, McLauchlan J, Hofer T, Stanifer ML, Boulant S. 2018. Differential induction of interferon stimulated genes between type I and type III interferons is independent of interferon receptor abundance. PLoS Pathog 14:e1007420.
77. Baldridge MT, Lee S, Brown JJ, McAllister N, Urbanek K, Dermody TS, Nice TJ, Virgin HW. 2017. Expression of Ifnlr1 on Intestinal Epithelial Cells Is Critical to the Antiviral Effects of Interferon Lambda against Norovirus and Reovirus. J Virol 91.
78. Bowen JR, Quicke KM, Maddur MS, O'Neal JT, McDonald CE, Fedorova NB, Puri V, Shabman RS, Pulendran B, Suthar MS. 2017. Zika Virus Antagonizes Type I Interferon Responses during Infection of Human Dendritic Cells. PLoS Pathog 13:e1006164.
79. Kang JX, Liu J, Wang J, He C, Li FP. 2005. The extract of huanglian, a medicinal herb, induces cell growth arrest and apoptosis by upregulation of interferon-beta and TNF-alpha in human breast cancer cells. Carcinogenesis 26:1934-9.
80. Lindner DJ, Kolla V, Kalvakolanu DV, Borden EC. 1997. Tamoxifen enhances interferon-regulated gene expression in breast cancer cells. Mol Cell Biochem 167:169-77.
81. Yoon N, Park MS, Shigemoto T, Peltier G, Lee RH. 2016. Activated human mesenchymal stem/stromal cells suppress metastatic features of MDA-MB-231 cells by secreting IFN-beta. Cell Death Dis 7:e2191.
82. Kobayashi T, Antar AA, Boehme KW, Danthi P, Eby EA, Guglielmi KM, Holm GH, Johnson EM, Maginnis MS, Naik S, Skelton WB, Wetzel JD, Wilson GJ, Chappell JD, Dermody TS. 2007. A plasmid-based reverse genetics system for animal double-stranded RNA viruses. Cell Host Microbe 1:147-57.
83. Cashdollar LW, Chmelo R, Esparza J, Hudson GR, Joklik WK. 1984. Molecular cloning of the complete genome of reovirus serotype 3. Virology 133:191-6.
84. Furlong DB, Nibert ML, Fields BN. 1988. Sigma 1 protein of mammalian reoviruses extends from the surfaces of viral particles. J Virol 62:246-56.
85. Smith RE, Zweerink HJ, Joklik WK. 1969. Polypeptide components of virions, top component and cores of reovirus type 3. Virology 39:791-810.
86. Virgin HW, Dermody TS, Tyler KL. 1998. Cellular and humoral immunity to reovirus infection. Curr Top Microbiol Immunol 233:147-61.
87. Mainou BA, Dermody TS. 2012. Transport to late endosomes is required for efficient reovirus infection. J Virol 86:8346-58.
88. Virgin HWt, Bassel-Duby R, Fields BN, Tyler KL. 1988. Antibody protects against lethal infection with the neurally spreading reovirus type 3 (Dearing). J Virol 62:4594-604.

Supplemental Information

I. Synonymous mutations

Gene segments	R1Reovirus	R2Reovirus
L1	N/A	N/A
L2	N/A	N/A
L3	G491A (A160T)	G491A (A160T)
M1	N/A	N/A
M2	N/A	N/A
M3	N/A	N/A
S1	N/A	N/A
S2	G1294A (after coding region) See table IV	N/A
S3	C508A (P161T) A775G (I250V) T1170G (after coding region)	A775G (I250V)
S4	G177A (V49I)	G177A (V49I)

II. Non-synonymous mutations

Gene segment	r1Reovirus	r2Reovirus
L1	N/A	N/A
L2	N/A	A318G
L3	C2059T G2062C	C2059T G2062C T3550C
M1	T229C C919T	T229C C919T
M2	N/A	N/A
M3	N/A	N/A
S1	N/A	N/A
S2	See table III	N/A
S3	N/A	N/A
S4	N/A	N/A

III. Synonymous mutations in r1Reovirus S2 gene segment

Mutation	Percentage
G54A	45% A, 55% G
C84T	64% C, 36% T
C87T	64% C, 36% T
A90G	64% A, 36% G
C91T	65% C, 35% G

T96G	65% T, 35%G
C108T	64% C, 35% T
T114C	33% C, 66% T
A123G	67% A, 33% G
A537G	57% A, 42% G
T564C	56% T, 44% C
C573T	59% C, 41% T
T834C	69% T, 31% C
C858T	65% C, 35% T
T939C	67% T, 33% C
A945G	55% A, 45% G
A951G	55% A, 45% G
G954T	55% G, 45% T
C972T	49% C, 51% T
T981C	51% C, 48% T
T990C	50% C, 50% T
A996G	52% A, 48% G
T997C	49% C, 51% T
G1005T	48% G, 52% T
G1011A	51% A, 49% G
A1015C	47% A, 52% C
T1035C	50% C, 49% T
G1044A	45% A, 55% G
G1047A	46% A, 54% G
T1059A	49% A, 51% T
C1062T	52% C, 48% T
C1068T	51% C, 49% T
G1080A	51% A, 49% G
G1107A	51% A, 49% G
G1257A	65% A, 35% G
T1274A	65% A, 35% G

IV. Non-synonymous mutations in r1Reovirus S2 gene segment

Mutation	**Percentage**
G1087A (V357I)	51% A, 49% G
C1174A (H386N)	54% A, 46% C

Table S1. List of Synonymous and Nonsynonymous Mutations in r1Reovirus and r2Reovirus

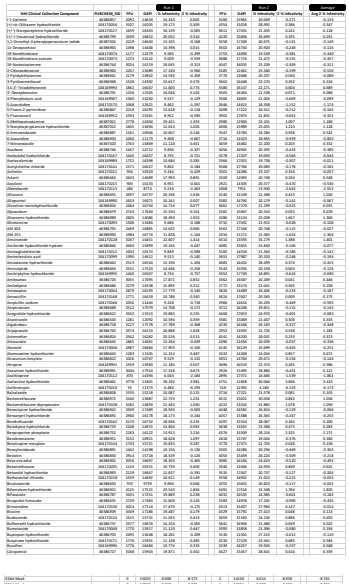

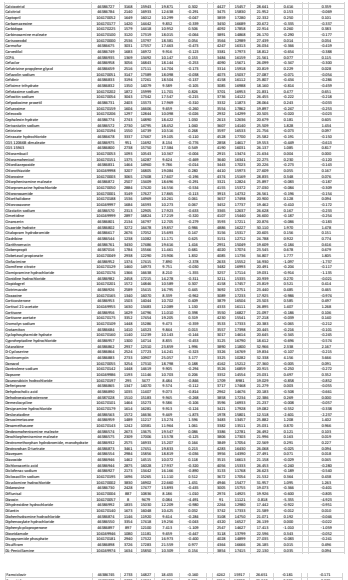

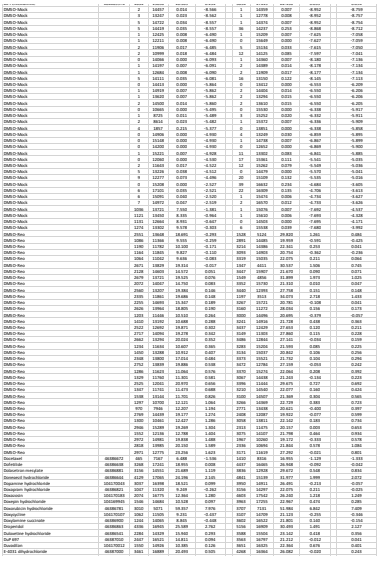

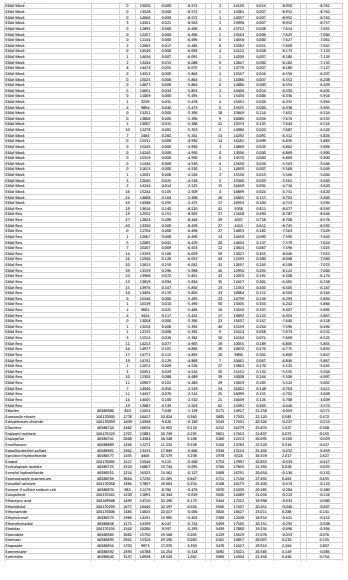

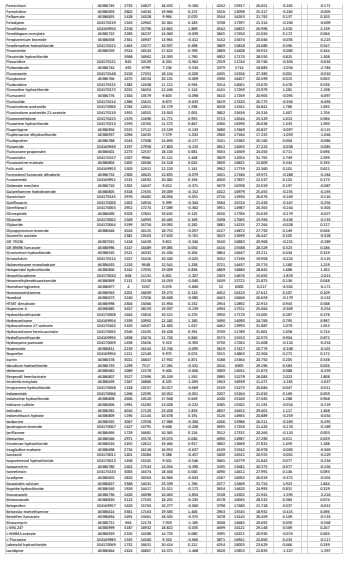

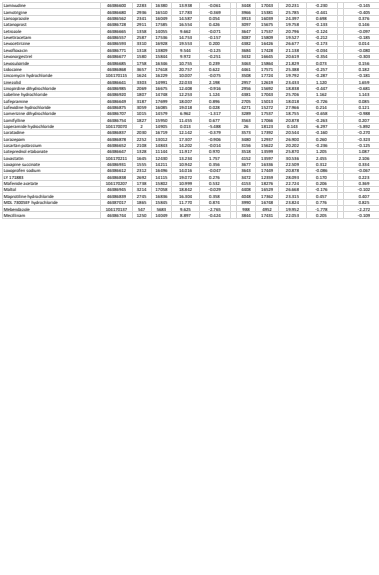

Table S2. Data from screening of reovirus infectivity using the NIH Clinical Collection. Data are shown for two independent experiments (Runs). For each run, reovirus focus forming units (FFU), number of cells (DAPI), percent infectivity ([FFU/DAPI]*100), and Z-score based on percent infectivity (Z percent infectivity) were calculated. Z scores for each well were calculated using the following formula: Z score = (a-b)/c, where a is the percent infectivity (infected cells/number of cells), b is the median percent infectivity for each plate, and c is the standard deviation of percent infectivity for each plate. The average Z-score for both runs is also provided (Avg Z % Infectivity). Name for individual compounds and their PubChem ID numbers are provided.

Chapter II: Non-canonical cell death by reassortant reovirus

Roxana M. Rodríguez Stewart[1,2], Vishnu Raghuram[1], Jameson T.L. Berry[1,2], and Bernardo A. Mainou[2,3*]

Emory University,[1] Department of Pediatrics,[2] Emory University School of Medicine, Atlanta, GA 30322, Children's Healthcare of Atlanta[3], Atlanta, GA, 30322

* To whom correspondence should be addressed: Emory University School of Medicine, Department of Pediatrics, ECC 564, 2015 Uppergate Drive, Atlanta, GA 30322. Tel.: (404) 727-1605. Fax: (404) 727-9223. E-mail: bernardo.mainou@emory.edu.

Running Title: Non-canonical cell death by reassortant reovirus

The work of this chapter has been submitted to the Journal of Virology.

The work of this chapter was uploaded to bioRxiv on May 21, 2020.

Citation:

2. **Rodríguez Stewart RM**, Raghuram V, Berry JTL, Mainou BA. Non-canonical cell death by reassortant reovirus. 21 May 2020. bioRxiv, doi: https://doi.org/10.1101/2020.05.20.107706.

Abstract

Triple-negative breast cancer (TNBC) constitutes 12% of all breast cancer and is associated with worse prognosis compared to other subtypes of breast cancer. Current therapies are limited to cytotoxic chemotherapy, radiation, and surgery, leaving a need for targeted therapeutics to improve outcomes for TNBC patients. Mammalian orthoreovirus (reovirus) is a nonenveloped, segmented, dsRNA virus in the *Reoviridae* family. Reovirus preferentially kills transformed cells and is in clinical trials to assess its efficacy against several types of cancer. We previously engineered a reassortant reovirus, r2Reovirus, that infects TNBC cells more efficiently and induces cell death with faster kinetics than parental reoviruses. In this study, we sought to understand the mechanisms by which r2Reovirus induces cell death in TNBC cells. We show that r2Reovirus infection of TNBC cells of a mesenchymal-stem like (MSL) lineage downregulates the MAPK/ERK pathway and induces non-conventional cell death that is caspase dependent, but caspase 3-independent. Infection of different MSL lineage TNBC cells with r2Reovirus results in caspase 3-dependent cell death. We map the enhanced oncolytic properties of r2Reovirus in TNBC to epistatic interactions between the Type 3 Dearing M2 gene segment and Type 1 Lang genes. These findings suggest that the genetic composition of the host cell impacts the mechanism of reovirus-induced cell death in TNBC. Together, our data show that understanding host and virus determinants of cell death can identify novel properties and interactions between host and viral gene products that can be exploited for the development of improved viral oncolytics.

Importance

Triple negative breast cancer (TNBC) is unresponsive to hormone therapies, leaving patients afflicted with this disease with limited treatment options. We previously engineered an oncolytic reovirus (r2Reovirus) with enhanced infective and cytotoxic properties in TNBC cells. However, how r2Reovirus promotes TNBC cell death is not known. In this study, we show that reassortant r2Reovirus can promote non-conventional caspase-dependent but caspase 3-independent cell death and that the mechanism of cell death depends on the genetic composition of the host cell. We also map the enhanced oncolytic properties of r2Reovirus in TNBC to interactions between a Type 3 M2 gene segment and Type 1 genes. Our data show that understanding the interplay between the host cell environment and the genetic composition of oncolytic viruses is crucial for the development of efficacious viral oncolytics.

Introduction

Breast cancer is the leading cause of cancer in women and second leading cause of death by cancer in women in the United States (https://seer.cancer.gov/). Triple-negative breast cancer (TNBC) constitutes 10-15% of breast cancer diagnoses, has a higher rate of relapse, and lower survival after metastasis than other types of breast cancer (1). TNBC is characterized by its lack of expression of estrogen receptor (ER), progesterone receptor (PR), and human epidermal growth factor receptor 2 (HER-2). These characteristics render TNBC cells unresponsive to hormone therapies that have been efficacious in treating other types of breast cancer (2, 3).

Mammalian orthoreovirus (reovirus) is a segmented double-stranded RNA (dsRNA) virus in the *Reoviridae* family (4). Reovirus has three large (L1, L2, L3), three medium (M1, M2, M3), and four small (S1, S2, S3, S4) gene segments that encode 8 structural and 3 non-structural proteins (33, 41). There are three reovirus serotypes (types 1, 2, and 3) determined by the recognition of the S1-

enconded σ1 attachment protein by neutralizing antibodies (4, 32). In humans, reovirus infection usually occurs during childhood, though infection is generally asymptomatic (4-7). Additionally, reovirus preferentially replicates and kills tumor cells (8-11). Because of these features, a lab adapted type 3 reovirus is currently in Phase I-III clinical trials to test its efficacy against a variety of cancers (https://clinicaltrials.gov). However, little is known about the biology of reovirus infection in TNBC.

TNBC cells are categorized into subtypes based on their genetic composition (1, 14). Cells in the mesenchymal stem-like (MSL) subtype, including MDA-MB-231 and MDA-MB-436 cells, are characterized by enriched expression of genes involved in motility, cellular differentiation, and growth factor pathways (14, 202-209). The K-Ras G13D and B-Raf G464V B-Raf mutations found in MDA-MB-231 cells result in an upregulated Ras pathway (122, 123). Constitutively active Ras mutations have been identified in many human tumors and signaling through Ras increases tumor cell proliferation and survival in some cancers (118-121). B-Raf regulates the Raf–mitogen-activated protein kinase (MAPK)/extracellular signal-regulated kinase (ERK) pathway by phosphorylation of MEK 1/2, which activates the kinase (125). MAPK/ERK signaling promotes cancer cell proliferation, survival, and metastasis (126). Small-molecule inhibitors that target various steps of the MAPK/ERK pathway are currently in clinical trials to test their efficacy against several cancers (210).

Activated Ras signaling regulates various aspects of reovirus biology, including virus uncoating, infectivity, replication, and release from infected cells (10, 11, 24, 110, 112-117). However, reovirus can also infect and kill cancer cells independent of Ras activation (64, 127-129). In some cells, reovirus downregulates Ras signaling during infection, inducing programmed cell death (131). Reovirus can induce cell death by apoptosis, necroptosis, cell cycle arrest or autophagy (55, 56, 101, 114, 164-174, 211). Reovirus can trigger apoptosis through recognition of viral nucleic

acid by cellular pattern recognition receptors and subsequent activation of caspase 8, Bid cleavage, and disruption of the mitochondrial membrane. This results in cytochrome c release, caspase 9 activation, and activation of executioner caspases 3 and 7 (4, 55-58, 101, 164, 165, 168, 170, 180, 184-188). Reovirus can also induce caspase-independent cell death through induction of RIPK3 and MLKL-dependent necroptosis (166, 167, 172). The mode of cell death induced by reovirus appears to be largely dependent on the host cell.

We previously engineered an oncolytic reovirus with enhanced infective and cytotoxic properties in TNBC (r2Reovirus) (63). Oncolytic r2Reovirus is a reassortant virus with 9 gene segments from serotype 1 Lang (T1L) reovirus and a serotype 3 Dearing (T3D) M2 gene segment, as well as several synonymous and non-synonymous point mutations. Strain-specific differences in infectivity, replication, and induction of cell death indicate a vital role of specific viral factors in defining the host cell response and outcome of infection (52-54) (55-59). It is not known how r2Reovirus promotes TNBC cell death or the contribution of specific viral factors to the enhanced oncolytic properties of the virus.

In this study, we sought to better understand how reovirus induces programmed cell death in a subtype of TNBC and the viral factors associated with this phenotype. We show that reassortant r2Reovirus can promote TNBC cell death by inhibiting MAPK/ERK signaling and inducing a non-conventional cell death that is caspase dependent, but caspase 3-independent conditional on the genetic composition of the host cell. These data suggest that the genetic composition of the host cell can greatly impact the type of cell death induced by reovirus. We also show that the enhanced oncolytic properties of r2Reovirus in TNBC likely map to the presence of a T3D M2 gene segment in the context of an otherwise T1L virus. Together, our data show that an improved understanding of host cell and virus interactions can identify biological properties and interactions between viral

gene products to better understand how viruses promote cell death and exploited for the development of improved viral oncolytics.

Results

r2Reovirus impairs MAPK/ERK signaling.

We previously generated a reassortant reovirus with enhanced infective and cytotoxic properties in TNBC cells (63). The mechanisms through which this virus promotes TNBC cell death is not known. It is also largely unclear how reoviruses promote TNBC cell death. The MDA-MB-231 TNBC cell line has an upregulated Ras pathway from mutations in Ras (G13D) and B-Raf (G464V) (122). To determine the effect of parental reoviruses (T1L and T3D) and r2Reovirus on MAPK/ERK, MDA-MB-231 cells were infected with mock, T1L, T3D, or r2Reovirus at an MOI of 500 PFU/cell or treated with 10 μM MEK1/2 inhibitor U0126. Whole cell lysates were collected at 0, 1, and 2 days post-infection (dpi) and probed for phosphorylated and total MEK1/2 and ERK1/2 by immunoblot (Fig. 1A). Infection with T1L and T3D did not affect the levels of phosphorylated MEK1/2 or ERK1/2 when compared to uninfected cells (mock) at the times tested (Fig. 1B). In cells infected with r2Reovirus, levels of phospho- and total MEK1/2 and total ERK1/2 were slightly lower than mock and levels of phospho-ERK1/2 were significantly lower at 2 dpi than mock. These data suggest that infection with r2Reovirus, but not T1L nor T3D, results in downregulation of MAPK/ERK pathway in these cells.

To determine the effect of inhibiting MAPK/ERK signaling on reovirus-infected MDA-MB-231 cell viability, cells were treated with increasing concentrations of U0126 for 1 h, adsorbed with mock, T1L, T3D, or r2Reovirus at an MOI of 100 PFU/cell or 50 μM etoposide as a positive control, and cell viability was assessed over 6 days (Fig. 2A). Similar to that observed previously (63), r2Reovirus impaired cell viability with faster kinetics than T1L and T3D did not impact cell viability.

Treatment of cells with U0126 alone resulted in a dose-dependent cytostatic effect on cell viability, with cell viability leveling at 2 dpi when treated with 10 mM U0126 (red line). This was expected as MAPK/ERK signaling is necessary for cell proliferation in these cells (212-218). Treatment with 0.1 μM U0126 had no significant effect on cell viability in the presence or absence of reovirus. Infection of cells with T3D in addition to U0126 did not significantly impact U0126-induced cytotoxicity. Infection with T1L in the presence of U0126 enhanced the cytotoxicity kinetics, with infection in the presence of 5 or 10 mM U0126 having an additive effect on cytotoxicity (Fig. 2B). Similar to that observed with T1L, Infection of cells with r2Reovirus in the presence of U0126 enhanced the kinetics of cytotoxicity, with 10 mM U0126 having a significant combinatorial effect on cytotoxicity induced by the drug and virus alone. These data show that inactivation of MEK-ERK signaling in MDA-MB-231 cells impairs cellular proliferation without having a cytotoxic effect on cells and that in the context of infection with T3D, does not promote viral cell killing. While inactivation of this pathway in the context of infection with T1L or r2Reovirus enhances the cytotoxic effect of the virus, a statistically significant impairment on cell viability was only observed in the presence of r2Reovirus and 10 mM U0126. Together, these data show r2Reovirus downregulates MAPK/ERK signaling and infection with a serotype 1 reovirus in the presence of a MEK inhibitor enhances the kinetics of viral-mediated cytotoxicity in these cells.

Induction of cell death by r2Reovirus is partially dependent on caspases.

Inhibition of MAPK/ERK signaling can result in the induction of apoptosis (131, 219-222) and reovirus can induce apoptosis *in vitro* and *in vivo* (4, 55-58, 101, 164, 165, 168, 170, 180, 184-188). To determine if r2Reovirus induces caspase-dependent cell death in TNBC cells, MDA-MB-231 cells were treated with vehicle (DMSO) or 25 μM pan-caspase inhibitor Q-VD-OPH for 1 h, infected with mock or r2Reovirus at an MOI of 500 PFU/cell, and assessed for cell death by

annexin V-fluorescein isothiocyanate (FITC)/propidium iodide (PI) staining over 3 days (Fig. 3A). Following r2Reovirus infection, 35.43% of infected cells were annexin V+/PI+ by 2 dpi and 49.24% by 3 dpi. Infection in the presence of Q-VD-OPH decreased the percentage of annexin V+/PI+ cells to 19.09% at 2 dpi and 30.79% by 3 dpi. In etoposide-treated cells, 48.39% of cells were annexin V+/PI+ by day 2 post treatment and 78.12% by day 3 post treatment. Q-VD-OPH treatment decreased the percentage of annexin V+/PI+ to 10% by day 2 post treatment and 20% by day 3 post treatment. Q-VD-OPH also increased the number of annexin V-/PI- cells during infection or etoposide treatment, especially at 2 dpi. Interestingly, we did not observe a significant number of annexin V+/PI- cells under any condition tested. These data show that the pan caspase inhibitor Q-VD-OPH dampens, but does not fully block, r2Reovirus-induced cell death.

To further assess if r2Reovirus is dependent on caspases to promote cell death, MDA-MB-231 cells were treated with DMSO or 25 μM Q-VD-OPH for 1 h, infected with mock or r2Reovirus at an MOI of 500 PFU/cell or treated with 50 mM etoposide, and cell viability was assessed over 6 days (Fig. 3B). Infection of cells with r2Reovirus in the presence of Q-VD-OPH significantly impacted viral-induced cytotoxicity at 4 and 6 dpi, with cell viability over two times greater compared to infection in the absence of the drug. These data show that inhibition of caspase activity results in a significant, but not total, reduction of viral-mediated cell death.

Reovirus does not affect mitochondrial permeability during infection of MDA-MB-231 cells.

Reovirus can induce extrinsic and intrinsic apoptosis (4, 55-58, 101, 164, 165, 168, 170, 180, 184-188). During intrinsic apoptosis, mitochondrial membrane permeabilization leads to loss of mitochondrial transmembrane potential, and release of cytochrome c into the cytoplasm (188, 223-226). To assess if reovirus infection of MDA-MB-231 cells impacts mitochondrial membrane potential, cells were infected with mock, T1L, T3D or r2Reovirus at an MOI of 500 PFU/cell or

treated with DMSO or 50 μM etoposide and analyzed by flow cytometry over a 3 day time course of infection using tetramethylrhodamine, ethyl ester (TMRE), a positively-charged dye that accumulates in the mitochondria (Fig. 4A). Infection with T1L or T3D did not significantly affect mitochondrial membrane potential at any of the times tested, while infection with r2Reovirus slightly reduced mitochondrial membrane potential at 3 dpi. Treatment with etoposide significantly reduced mitochondrial membrane permeabilization at all times tested, with stark changes at days 2 and 3 post treatment. These results suggest reovirus induces cell death in MDA-MB-231 cells without major disruption of the mitochondrial membrane.

Cytochrome c release from the mitochondria is a key event that can lead to apoptosome formation and subsequent caspase 3 activation. It is possible for cytochrome c to be released from the mitochondria without impacting mitochondrial membrane integrity (227-229). To determine if cytochrome c is released following reovirus infection of MDA-MB-231 cells, cells were infected with mock, T1L, T3D, or r2Reovirus at an MOI of 500 PFU/ml or treated with 50 μM etoposide and assessed for intracellular localization of cytochrome c (green), mitochondria (red), or reovirus antigen (blue) by confocal microscopy at 3 dpi (Fig. 4B). In uninfected cells, cytochrome c largely co-localized with mitochondria. In etoposide-treated cells, cytochrome c localized to areas surrounding swollen mitochondria. In cells infected with T1L, T3D, and r2Reovirus, cytochrome c largely co-localized with mitochondria with no observable swollen mitochondria. These data indicate that during reovirus infection of MDA-MB-231 cells, cytochrome c remains largely associated with mitochondria. Together with TMRE data, these results show that reovirus induces MDA-MB-231 cell death independent of disruption of mitochondrial membrane potential and cytochrome c release.

Infection with serotype 1 reoviruses increases caspase 9 activity.

We next assessed the activation status of caspase 9, a component of the apoptosome that can be activated independent of cytochrome c release in a caspase 8-dependent manner (184, 230). MDA-MB-231 cells were adsorbed with mock, T1L, T3D or r2Reovirus at an MOI of 500 PFU/cell or treated with DMSO or 50 μM etoposide for 1 h, and assessed for caspase 9 activity over a 3 day time course of infection (Fig. 5A). Infection with T1L and r2Reovirus significantly induced caspase 9 activation, with caspase 9 activity levels increasing by 2 dpi and reaching up to 2-fold over mock by 3 dpi. Infection with T3D and treatment with etoposide did not impact caspase 9 activation at the times tested. To measure the requirement of caspase 9 activity in r2Reovirus-mediated cell death of MDA-MB-231 cells, cells were treated with DMSO, 25 μM caspase 9 inhibitor z-LEHD-fmk, or 25 μM Q-VD-OPH for 1 h, infected with mock or r2Reovirus at an MOI of 500 PFU/cell or treated with 10 mM doxorubicin, and assessed for cell viability over 6 days (Fig. 5B). As observed previously, treatment of cells with the pan-caspase inhibitor (Q-VD-OPH) partially blocked reovirus-induced cytotoxicity. Treatment of cells with the caspase 9 inhibitor (z-LEHD-fmk) reduced virus-induced cytotoxicity, albeit not to the same extent as the pan-caspase inhibitor. Together these data show that although infection with T1L and r2Reovirus does not affect mitochondrial membrane potential or promote release of cytochrome c, infection promotes caspase 9 activation. These data also show that although activation of caspase 9 is not solely responsible for viral-mediated cytotoxicity in MDA-MB-231 cells, caspase 9 activation is necessary for the full cytotoxic effects of serotype 1 infection in these cells.

r2Reovirus blocks caspase 3/7 activity in a replication-dependent manner.

Caspase 9 activates caspase 3 and 7 during intrinsic apoptosis (231-233). To determine if caspase 3 is activated during reovirus infection of MDA-MB-231 cells, cells were infected with

mock, T1L, T3D or r2Reovirus at an MOI of 500 PFU/cell or treated with 50 μM etoposide, and caspase 3/7 activity was assessed over a 3 day time course of infection (Fig. 6A). Caspase 3/7 activity was not observed in MDA-MB-231 cells infected with mock, T1L, T3D, or r2Reovirus during the times tested. Caspase 3/7 activity was also not observed in cells infected with T1L, T3D, or r2Reovirus at days 4-6 post-infection (data not shown). Treatment of cells with etoposide induced robust caspase 3/7 activity by day 2 post treatment. These data show that etoposide can activate caspase 3 in MDA-MB-231 cells, although in a caspase 9-independent manner. Interestingly, infection with T1L or r2Reovirus does not lead to activation of caspase 3 despite robust caspase 9 activation. These data also show that in MDA-MB-231 cells caspase 3 can be activated.

To determine if reovirus can impact the activation of caspases 3 and 7, MDA-MB-231 cells were infected with mock, T1L, T3D, or r2Reovirus for 1 day, treated with DMSO or 50 μM etoposide, and assessed for caspase 3/7 activity 2 days post etoposide treatment (Fig. 6B). As previously seen, infection with reovirus did not induce caspase 3/7 activity, whereas etoposide treatment resulted in robust caspase 3/7 activation. Infection of cells with T1L or T3D prior to etoposide treatment did not significantly affect etoposide-induced activation of caspase 3/7. In contrast, infection with r2Reovirus prior to etoposide treatment fully blocked etoposide-induced caspase 3/7 activation. To determine if the ability of r2Reovirus to impair etoposide-induced caspase 3/7 activation is dependent on viral replication, MDA-MB-231 cells were infected with mock or UV-inactivated T1L, T3D, or r2Reovirus one day prior to etoposide treatment, and caspase 3/7 activity was assessed 2 days post etoposide treatment (Fig. 6C). In contrast to that observed with replicating virus, infection of cells with UV-inactivated T1L, T3D, or r2Reovirus did not affect etoposide-induced caspase 3/7 activation. Interestingly, infection with UV-inactivated T1L, T3D, and r2Reovirus resulted in a small, but consistent activation of caspase 3/7 compared to uninfected

cells. These results indicate that r2Reovirus blocks etoposide-induced caspase 3/7 activation in MDA-MB-231 cells in a replication-dependent manner.

PARP-1 cleavage during reovirus infection results in a cleavage fragment that does not correspond to caspase 3 proteolysis.

Poly (ADP-ribose) polymerase (PARP-1) is involved in many cellular processes, including DNA repair, genomic stability, and programmed cell death (234-237). During apoptosis, PARP-1 is cleaved into an 89 kDa fragment by caspase 3 (189) (238-240). PARP-1 can also be cleaved by various proteases during non-apoptotic cell death (189). To assess if PARP-1 is cleaved during reovirus-infection of MDA-MB-231 cells, cells were infected with mock, T1L, T3D or r2Reovirus at an MOI of 500 PFU/cell or treated with 50 μM etoposide, and whole cell lysates were collected at 0, 1, and 2 dpi. Lysates were resolved by SDS-PAGE and immunoblotted with antisera specific for PARP-1, reovirus, and tubulin (Fig. 7). Etoposide treatment resulted in an 89 kDa PARP-1 cleavage fragment at day 2 post treatment, consistent with etoposide activation of caspase 3. In contrast, infection with T1L and r2Reovirus resulted in a 70 kDa PARP-1 cleavage fragment while infection with T3D, which does not impair MDA-MB-231 cell viability, did not result in PARP-1 proteolysis. Treatment with caspase 3 inhibitor (Q-VD-OPH) did not reduce PARP-1 cleavage following reovirus infection (data not shown). Calpains, cathepsins, granzyme A and B, and matrix metalloprotease 2 (MMP-2) can proteolytically cleave PARP into fragments of the molecular weight observed during reovirus infection (189). These data suggest that during T1L and r2Reovirus infection of MDA-MB-231 cells PARP-1 is cleaved by a protease other than caspase 3.

Reovirus infection of MDA-MB-436 cells promotes caspase 3/7 activation and cell death.

r2Reovirus induces cell death with enhanced kinetics in TNBC cells, including MDA-MB-436 cells, a mesenchymal-stem like (MSL) subtype TNBC cell line with different mutations than MDA-MB-231 cells (14, 63). To assess if host heterogeneity affects the mode of cell death induced by reovirus, r2Reovirus oncolysis was tested in MDA-MB-436 cells. To determine if reovirus cell death induction is caspase dependent, MDA-MB-436 cells were treated with DMSO or 25 μM pan-caspase inhibitor Q-VD-OPH for 1 h, infected with mock or r2Reovirus at an MOI of 500 PFU/cell or treated with 50 μM etoposide, and assessed for cell viability over 6 days (Fig. 8A). Infection with r2Reovirus impaired MDA-MB-436 cell viability, with significant cytotoxicity observed by day 4 pi. Treatment of cells with Q-VD-OPH significantly reduced reovirus-mediated cytotoxicity, although cell viability levels were not fully restored to those observed in mock. To determine if r2Reovirus infection of MDA-MB-436 cells impacts mitochondrial membrane potential, cells were infected with mock or r2Reovirus or treated with DMSO or 50 μM etoposide, and assessed for TMRE levels by flow cytometry over 3 days (Fig. 8B). At 2 and 3 dpi, there is a significant decrease in mitochondrial membrane potential in r2Reovirus-infected cells, and to a lesser degree in etoposide-treated cells. To assess if r2Reovirus infection of MDA-MB-436 cells promotes caspase 3/7 activation, cells were infected with mock or r2Reovirus for at an MOI of 500 PFU/cell or treated with DMSO or 50 μM etoposide, and caspase 3/7 activity was assessed over 3 days (Fig. 8C). In contrast to that observed in MDA-MB-231 cells, r2Reovirus infection induced significant caspase 3/7 activation by 1 dpi, with sustained activation over the times tested. Etoposide induced a slight increase in caspase 3/7 activation, but to a lesser degree than reovirus, mirroring that observed by cell viability and TMRE staining. These results show r2Reovirus infection of MDA-MB-436 cells robustly disrupts the mitochondrial membrane and promotes caspase 3/7 activation. These data also show etoposide is not as effective at inducing cell death in MDA-MB-436 cells compared to MDA-

MB-231 cells. Together, these data show that the mechanism of cell death induced by r2Reovirus is host cell context-dependent and independent of the ability of the virus to activate caspase 3.

Enhanced r2Reovirus oncolysis maps to the T3D M2 gene segment.

The reassortant r2Reovirus is composed of 9 T1L gene segments and an M2 gene segment from T3D in addition to several synonymous and non-synonymous point mutations (63). To determine the contribution of the M2 gene segment to r2Reovirus oncolysis in TNBC cells, reoviruses were engineered by reverse genetics with T1L and T3D M2 gene segment swaps in otherwise isogenic backgrounds (52, 56, 96, 99). To confirm the presence of swapped M2 gene segments, the genetic composition of parental T1L and T3D reoviruses, r2Reovirus, and T1L-T3M2 and T3D-T1M2 was assessed by SDS-gel electrophoresis (Fig. 9A). The electromobility of the reovirus gene segments confirmed that T1L and T3D-T1M2 contain a T1L M2 gene segment, whereas T3D, r2Reovirus, and T1L-T3M2 contain a T3D M2 gene segment (asterisks).

To assess the role of the M2 gene segment in reovirus-induced cytotoxicity of TNBC cells, MDA-MB-231 (Fig. 9B) and MDA-MB-436 cells (Fig. 9C) were infected with mock, T1L, T3D, T1L-T3M2, T3D-T1M2, or r2Reovirus at an MOI of 500 PFU/cell or treated with DMSO, 50 μM etoposide (MDA-MB-231), or 1 μM staurosporine (MDA-MB-436), and assessed for cell viability over 6 days. In both cell lines, T1L-T3M2 impaired cell viability with similar kinetics as r2Reovirus and with faster kinetics than T1L, especially in MDA-MB-436 cells. In contrast, T3D-T1M2 and T3D did not significantly impact cell viability in either MDA-MB-231 or MDA-MB-436 cells. To assess if cytopathic differences observed with the recombinant viruses were a result of differences in infectivity, MDA-MB-231 cells were infected with mock, T1L, T3D, T1L-T3M2 or T3D-T1M2. T1L-T3M2 infected MDA-MB-231 cells at a slightly higher rate than T1L and T3D, while T3D-T1M2 had slightly diminished infectivity when compared to the parental viruses (data not shown).

These data indicate that the T3D M2 gene segment is sufficient to enhance the cytotoxic properties of an otherwise T1L virus, without significant impact on infectivity. These data also indicate that the enhanced cytotoxic properties of r2Reovirus map to the T3D M2 gene segment and that mutations found in r2Reovirus likely have little or no effect on the virus' enhanced oncolysis. Further, the addition of the T1L M2 gene segment to an otherwise T3D virus does not affect the infective or cytopathic properties of the virus. Additionally, even though r2Reovirus induces cell death by different modes in MDA-MB-231 and MDA-MB-436 cells, enhanced cell death induction by the reassortant virus maps to the same viral factor in both cell lines.

To determine if the M2 gene segment impacts the activation of caspase 3/7 following etoposide treatment, MDA-MB-231 cells were infected with mock, T1L, T3D, T1L-T3M2, T3D-T1M2, or r2Reovirus at an MOI of 500 PFU/cell for 1 day, treated with DMSO or 50 μM etoposide, and assessed for caspase 3/7 activity 2 days post etoposide treatment (Fig. 9D). As observed previously, infection with all the reoviruses tested did not induce caspase 3/7 activation and treatment of cells with etoposide resulted in robust activation of caspase 3/7. Infection with T1L-T3M2 or r2Reovirus prior to etoposide treatment robustly impaired caspase 3/7 activation. Conversely, infection with T1L, T3D, or T3D-T1M2 did not impact etoposide-induced caspase 3/7 activation. These results indicate that the ability for r2Reovirus to block etoposide-induced caspase 3/7 activation maps to the T3D M2 gene segment.

Discussion

Reassortant r2Reovirus infects TNBC cells more efficiently and induces cell death with enhanced kinetics when compared to prototypic strains of reovirus, including the oncolytic reovirus currently in clinical trials. r2Reovirus was obtained from co-infection of MDA-MB-231 cells with T1L, Type 2 Jones (T2J), and T3D followed by serial passaging. r2Reovirus has 9 gene segments

from T1L, an M2 gene segment from T3D, and several synonymous and non-synonymous point mutations (63). In this study, we sought to better understand how r2Reovirus, and reoviruses in general, promote TNBC cell death. We focused on MDA-MB-231 cells, a TNBC cell line belonging to the MSL subtype (14). There are limited treatment options against TNBC and the MSL subtype is associated with enrichment of genes involved in cell motility, cellular differentiation, and growth factor signaling pathways (1-3, 14). MDA-MB-231 cells have mutations in *BRAF*, *CDKN2A*, *KRAS*, *NF2*, *TP53*, and *PDGFRA* genes (14). Mutations in *BRAF* (G464V) and *KRAS* (G13D) result in constitutive activation of MAPK/ERK signaling, promoting survival, proliferation, cell cycle progression, and cell growth (122, 241). Constitutive activation of MAP/ERK is found in several cancers (119-122, 241-244). Constitutive Ras activation can enhance reovirus oncolysis by affecting multiple steps of the viral replication cycle, including enhancing virus uncoating and disassembly, negative regulation of retinoic acid-inducible gene I (RIG-I) signaling and impairing PKR activation, increasing progeny, and enhancing viral spread (24, 117, 245). In some cells, reovirus downregulation of MAP/ERK results in induction of apoptosis (131). In the context of MDA-MB-231 cells, r2Reovirus, but not T1L or T3D, decreased activation of MAPK/ERK signaling. The observed downregulation of MEK 1/2 and ERK 1/2 activation suggests r2Reovirus inhibits this pathway by either directly targeting MEK 1/2 or upstream of MEK 1/2 on Ras and B-Raf, or B-Raf alone. The combination of r2Reovirus and MEK inhibitor U0126 resulted in increased cell death compared to inhibitor or virus alone, highlighting the importance of this pathway in serotype 1 reovirus-mediated cell killing of TNBC cells. The lack of enhancement of cell death by U0126 when combined with T3D suggests that downregulation of MAPK/ERK signaling is not sufficient to promote virus killing.

Downregulation of MAPK/ERK signaling can lead to apoptosis and reovirus can induce programmed cell death by intrinsic and extrinsic apoptosis or necroptosis (55, 56, 101, 114, 131,

164-172). We did not observe an effect on r2Reovirus-induced cell death in the presence of a RIPK3 inhibitor (data not shown), suggesting that reovirus does not promote TNBC cell death by necroptosis. Infection of MDA-MB-231 and MDA-MB-436 cells in the presence of a pan-caspase inhibitor resulted in a significant, but not complete, reduction of virus-mediated cytotoxicity, indicating the need for caspases to promote cell death. During reovirus-induced apoptosis, caspase 8-cleaved Bid translocates to mitochondria, cytochrome c is released following mitochondrial membrane permeabilization, resulting in caspase 9 and caspase 3 activation (4, 55-58, 101, 164, 165, 168, 170, 180, 184-188). In MDA-MB-231 cells, etoposide treatment disrupted mitochondrial membrane potential and promoted cytochrome c release from mitochondria. In reovirus-infected MDA-MB-231 cells, the mitochondrial membrane was largely unaffected and cytochrome c was not released. Despite the lack of disruption of the mitochondrial membrane during reovirus infection, caspase 9 was significantly activated during infection with T1L and r2Reovirus. Caspase 9 can be activated in a cytochrome c-independent manner via caspase 8-activation of caspase 3, which in turn cleaves and activates caspase 9 (184, 230). These results indicate that at least in the context of MDA-MB-231 cells, caspase 9 activation is a property of serotype 1 reoviruses, but not serotype 3 reoviruses. The lack of activation of caspase 3 during reovirus infection suggests a novel mechanism for caspase 9 activation, with the possibility of a viral protein directly activating caspase 9. These findings suggest that in MDA-MB-231 cells, reovirus promotes programmed cell death through a non-canonical pathway.

Activation of caspase 9 can subsequently activate caspase 3 and caspase 7 (231-233). In reovirus-infected MDA-MB-231 cells, caspase 3/7 activity was not observed. Reovirus infection can result in secretion of tumor necrosis factor (TNF)-associated death-inducing ligand (TRAIL), activation of nuclear factor kappa-light-chain-enhancer of activated B cells (NF-κB), and induction of apoptosis (164, 171, 180). There are conflicting data on secretion and sensitivity to TRAIL in

MDA-MB-231 cells (246-251). It is possible the lack of effects on the mitochondrial membrane during reovirus infection are linked to MDA-MB-231 cells being insensitive to TRAIL. However, we also observed that r2Reovirus blocks caspase 3/7 activation following etoposide treatment and that this effect is dependent on viral replication.

We show that the ability of r2Reovirus to block caspase 3/7 activation maps to the T3D M2 gene segment. Interestingly, this phenotype is only observed when the T3D M2 gene segment is expressed in the context of T1L, as infection with T3D did not block caspase 3/7 activation. This suggests an epistatic effect of T3D M2 with a T1L-encoded gene. Expression of the T3D-M2 gene segment in the context of an otherwise T1L virus also promoted cell death of MDA-MB-231 and MDA-MB-436 cells with similar kinetics as r2Reovirus and faster kinetics compared to T1L. These data suggest the enhanced cytopathic effects of r2Reovirus in TNBC cells is largely linked to the expression of the T3D M2 gene segment in the context of an otherwise T1L virus, with the point mutations present in r2Reovirus having little or no effect on enhanced oncolysis. T1L-T3M2 reovirus has enhanced attachment and infectivity in L929 and HeLa cells likely due to an interaction between the T3D M2 gene encoded μ1 protein and the T1L attachment protein σ1 (99). In various cells, the S1 and M2 genes are also key factors in reovirus-induced inhibition of cellular DNA synthesis and programmed cell death (55, 57))(58, 101, 102). Though not significant, T1L-T3M2 infected MDA-MB-231 cells at a slightly higher rate than T1L, while T3D-T1M2 showed diminished infectivity when compared to T3D (data not shown). It is possible that in TNBC cells, the interaction between T3D m1 and T1L s1 promote enhanced oncolysis. These findings further highlight the epistatic effects of reovirus genes in various aspects of reovirus biology.

Several viruses exploit host cell caspases, including caspase 3, to promote viral replication (252-255). Avian reovirus utilizes caspase 3 to proteolytically process viral nonstructural protein μNS, which is involved in the formation of viral factories (256). Mammalian reovirus recruits host

proteins to viral factories, including cytoskeletal elements, cellular chaperones, intrinsic immune system proteins, as well as the endoplasmic reticulum (ER) and ER-Golgi intermediate compartment (86, 257-260). It is possible reovirus recruits caspase 3 to viral factories to aid in a step in the replication cycle. Viral protein synthesis and expression of m1 is required to block necroptosis in L929 cells (172). While we did not observe induction of necroptosis in TNBC cells (data not shown), it is possible that newly synthesized m1 in conjunction with a T1L gene product blocks caspase 3/7 activation, which results in unconventional cell death in these cells.

During programmed cell death, PARP-1 can be proteolytically cleaved by various proteases (189). As such, PARP-1 cleavage is commonly used as a downstream marker of programmed cell death. Etoposide treatment of MDA-MB-231 cells resulted in an 89 kDa cleaved PARP-1 fragment that is characteristic of caspase 3 cleavage during apoptotic cell death (189, 261) (238-240). Infection with T3D did not result in PARP-1 proteolytic cleavage, which concurs with T3D not promoting cytopathic effects during infection of MDA-MB-231 cells. Infection with T1L or r2Reovirus resulted in a 70 kDa cleaved PARP-1 fragment. Proteases, including calpains, cathepsins, E64-d, Granzyme A and B, and MMP-2 can proteolytically cleave PARP into cleavage fragments of this molecular weight (189). Infection in the presence of a calpain inhibitor blocked PARP-1 cleavage, but the calpain inhibitor also blocked infectivity (data not shown). In addition, treatment with caspase 3 inhibitor did not result in reduced PARP-1 cleavage (data not shown). These results suggest proteolysis of PARP-1 during T1L and r2Reovirus infection is mediated by an enzyme other than caspase 3. These data further suggest that serotype 1 reoviruses promote caspase 3-independent programmed cell death in MDA-MB-231 cells.

The mechanism by which r2Reovirus promotes cell death of another TNBC cell line, MDA-MB-436, was assessed to better understand how host cell heterogeneity impacts virus induced cell death. MDA-MB-436 cells have mutated *BRCA1* and *TP53* genes, and BRAF and KRAS do not

have mutations, creating a different cellular environment compared to MDA-MB-231 cells (14). In contrast to that observed in MDA-MB-231 cells, r2Reovirus infection of MDA-MB-436 cells decreases mitochondrial membrane potential and increases caspase 3/7 activity, suggestive of canonical apoptosis. These data suggest that although both TNBC cell lines are more susceptible to r2Reovirus-mediated cell death than parental reoviruses, infection promotes different types of cell death in each cell line. These results suggest that the host cell environment plays a key role in the type of cell death promoted following reovirus infection and that the type of cell death induced by the virus can be independent of the viral genetic composition.

In conclusion, this study identifies a non-conventional virus-induced cell death mechanism in TNBC cells driven by a reassortant oncolytic reovirus. We further map the enhanced cytopathic properties of this reassortant reovirus in TNBC cells to an epistatic effect of the T3D M2 gene with a T1L viral gene product. Better understanding of the interplay between the genetic composition of oncolytic viruses and the host cell environment is crucial for the development of improved reoviruses for oncolytic therapy.

Materials and Methods

Cells, viruses, and antibodies

MDA-MB-231 cells (gift from Jennifer Pietenpol, Vanderbilt University) and MDA-MB-436 cells (ATCC® HTB-130™) were grown in Dulbecco's Modified Eagle's Medium (DMEM) supplemented with 10% fetal bovine serum (FBS) (Life Technologies), 100 U per ml penicillin and streptomycin (Life Technologies). Spinner-adapted L929 cells (gift from Terry Dermody, University of Pittsburgh) were grown in Joklik's modified minimal essential medium (MEM) with 5% FBS, 2 mM L-glutamine (Life Technologies), penicillin and streptomycin, and 0.25 mg per ml amphotericin B (Life Technologies).

Reovirus strains Type 1 Lang (T1L) and Type 3 Dearing (T3D) working stocks were prepared following rescue with reovirus cDNAs in BHK-T7 cells (gift from Terry Dermody, University of Pittsburgh), followed by plaque purification, and passage in L929 cells (95). r2Reovirus is a reassortant strain obtained from co-infection of MDA-MB-231 cells with T1L, T2J, and T3D reovirus strains followed by serial passage in these cells. (63). T1L-T3M2 and T3D-T1M2 (gift from Pranav Danthi, Indiana University (262)) were obtained through reovirus reverse genetics (95). Purified virions were prepared using second-passage L929 cell lysate stocks. Virus was purified from infected cell lysates by Vertrel XF (TMC Industries Inc.) extraction and CsCl gradient centrifugation as described (263). The band corresponding to the density of reovirus particles (1.36 g/cm^3) was collected and dialyzed exhaustively against virion storage buffer (150 mM NaCl, 15 mM MgCl2, 10 mM Tris-HCl [pH 7.4]). Reovirus particle concentration was determined from the equivalence of 1 unit of optical density at 260 nm to 2.1×10^{12} particles (264). Viral titers were determined by plaque assay using L929 cells (265, 266).

Reovirus polyclonal rabbit antiserum raised against reovirus strains T1L and T3D was purified as described (267) and cross-adsorbed for MDA-MB-231 cells. Secondary IRDye 680 and 800 antibodies (LI-COR Biosciences) and goat anti-rabbit Alexa Fluor 405 (A405) (Life Technologies).

Immunoblotting to assess activation of MAPK/ERK signaling and proteins involved in apoptosis pathway

MDA-MB-231 cells and MDA-MB-436 cells were adsorbed with T1L, T3D, and r2Reovirus at an MOI of 500 PFU/cell for 1 h at room temperature or treated with DMSO or 10 μM U0126, washed with PBS, and incubated for 0-2 days at 37°C. Whole cell lysates were prepared using RIPA buffer (20 mM Tris-HCl [pH 7.5], 150 mM NaCl, 1 mM EDTA, 1% NP-40, 0.1% sodium dodecyl

sulfate, 0.1% sodium deoxycholate) and fresh Protease Inhibitor Cocktail (P8340, Sigma-Aldrich), Phosphatase Inhibitor Cocktail 2 (P5726, Sigma-Aldrich), 1 mM sodium vanadate, and 1 mM phenylmethylsulfonyl fluoride (PMSF) and collected at times shown. Protein concentration was determined using the DC protein assay (Bio-Rad), measuring absorbance at 695nm in a Synergy HT or Synergy H1 Plate Reader (Biotek). Whole cell lysates were resolved by SDS-PAGE in 4-20% gradient Mini-PROTEAN TGX gels (Bio-Rad) and transferred to 0.2 μm pore size nitrocellulose membranes (Bio-Rad). Membranes were incubated for 1 h in blocking buffer (Tris-buffered saline [TBS] with 5% powdered milk), incubated with primary antibodies specific for phospho–ERK 1/2 (Thr202/Tyr204, #9101) and –MEK 1/2 (Ser217/221, clone 41G9, #9154), total ERK 1/2 (#9102) and MEK (#9122), PARP (clone 46D11, #9532), caspase 3 (clone D3R6Y, #14220), reovirus polyclonal antiserum, and α-tubulin (clone DM1A, #3873) overnight at 4°C. Antibodies are from Cell Signaling Technology. Membranes were washed with TBS-T (TBS with 0.1% Tween 20) and incubated with secondary antibodies conjugated to IRDye 680 or IRDye 800 (LI-COR Biosciences). Membranes were imaged using a LiCor Odyssey CLx. Images were processed and band density measured in ImageStudio (LI-COR Biosciences).

Cell viability assay

Metabolic activity was used as a measurement of cell viability by using Presto Blue reagent (Invitrogen). MDA-MB-231 and MDA-MB-436 cells were untreated or treated with DMSO, increasing concentrations of MEK1/2 inhibitor U0126 or 25 μM pan-caspase inhibitor Q-VD-OPH for 1 h at room temperature and adsorbed with reovirus at an MOI of 500 PFU/cell for 1 h at room temperature or treated with 50 μM etoposide. Cells were washed with PBS and incubated for 0-6 days at 37°C in the absence or presence of DMSO, U0126 or Q-VD-OPH. Presto Blue (Thermo Fisher Scientific) was added at each time point for 30 min at 37°C and fluorescence (540 nm

excitation/590 nm emission) was measured using black 96-well plates with clear bottom (Corning, 3904) with a Synergy HT or Synergy H1 plate reader (Biotek).

Flow cytometric analysis of reovirus cell death

Cell viability was assessed by measuring FITC-labeled Annexin V (BioVision) (525/40 nm) and propidium iodide (690/50 nm) fluorescence using flow cytometry. MDA-MB-231 cells were pretreated with vehicle (DMSO) or 25 μM pan-caspase inhibitor Q-VD-OPH for 1 h at room temperature prior to being adsorbed with T1L, T3D, and r2Reovirus at an MOI of 500 PFU/cell for 1 h at room temperature or treated with 50 μM etoposide, washed with PBS, and incubated for 1-3 days at 37°C in the presence of DMSO or Q-VD-OPH. Cells were collected at each time point and resuspended in Annexin Cocktail (1X Annexin Buffer [10 mM HEPES, 0.14 M NaCl, and 2.5 mM $CaCl_2$ in water], Annexin V-FITC, and propidium iodide). Mean fluorescence intensity (MFI) was assessed using a CytoFLEX flow cytometer (Beckman Coulter) and quantified using FlowJo software (BD Biosciences).

Flow cytometric analysis of mitochondrial membrane potential

Mitochondrial membrane potential was measured by using tetramethylrhodamine, ethyl ester (TMRE) (Abcam). MDA-MB-231 and MDA-MB-436 cells were adsorbed with reovirus at an MOI of 500 PFU/cell or treated with 50 μM etoposide for 1 h at room temperature, washed with PBS, and incubated at 37°C for 1-3 days post-infection. Cells were stained with 100 nM TMRE at 37°C for 1 h at each time point. Cells were collected and resuspended in PBS containing 2% FBS. MFI was assessed using a CytoFLEX flow cytometer (Beckman Coulter) and quantified using FlowJo software (BD Biosciences).

Confocal microscopy to assess cytochrome c intracellular localization

MDA-MB-231 cells plated on #1.5 glass coverslips were adsorbed with T1L, T3D or r2Reovirus at an MOI of 100 PFU/cell or treated with 50 μM etoposide for 1 h at room temperature, washed with PBS, and incubated at 37°C for 0-4 days post-infection. At each time point, cells were collected and incubated with media containing 300 nM MitoTracker Red-CMX Ros (Thermo Fisher) for 1 h at 37°C. Stained cells were fixed with 4% paraformaldehyde (PFA) in PBS for 20 min at room temperature. PFA was quenched with equal volume of 0.1 M glycine, cells were washed with PBS and stored at 4°C. Cells were treated with 0.1% Triton X100 and washed with PBS-BGT (PBS/0.5% BSA/0.1% Glycine/0.05% Tween 20), incubated with reovirus polyclonal antiserum for 1 h at room temperature, and washed with PBS-BGT. Cells were incubated with secondary antibody (Alexa 405, Thermo Fisher Scientific) and AlexaFluor488-conjugated cytochrome C monoclonal antibody (BD Pharmingen, cat. 560263), washed with PBS-BGT and mounted on coverslips with Aqua Poly/Mount (Polysciences Inc.). Cells were imaged by confocal microscopy using Olympus IX81 laser-scanning confocal microscope using a PlanApo N 60× oil objective with a 1.42 numerical aperture (NA). Pinhole size was the same for all fluorophores. Single sections of 0.44 μm thickness from a Z-stack are presented. Whole images were only adjusted for brightness and contrast.

Measuring caspase 9 activity

Caspase 9 activity was measured by using Caspase-9 Colorimetric Assay Kit (Biovision). MDA-MB-231 cells were adsorbed with T1L, T3D, and r2Reovirus at an MOI of 500 PFU/cell for 1 h at room temperature or treated with 50 μM etoposide, washed with PBS, and incubated for 1-3 days at 37°C. Caspase 9 activity was measured at each time point using manufacturer's instructions

and reading absorbance in a clear 96-well plate (Greiner) with a Synergy HT or Synergy H1 plate reader (Biotek).

Measuring caspase 3/7 activity

Caspase 3/7 activity was measured by using Caspase Glo reagent (Promega). MDA-MB-231 and MDA-MB-436 cells were adsorbed with reovirus at an MOI of 500 PFU/cell for 1 h at room temperature or treated with 50 μM etoposide, washed with PBS, and incubated for 1-3 days at 37°C. Alternatively, MDA-MB-231 cells were adsorbed with reovirus at an MOI of 500 PFU/cell for 1 h at room temperature, washed with PBS, incubated at 37°C, and treated with 50 μM etoposide 1 day post-infection. Caspase 3/7 activity was measured at each time point by incubating cells in equal amounts of Caspase Glo solution and cell media for 30 min at RT and reading luminescence in a white 96-well plate (Greiner) with a Synergy HT or Synergy H1 plate reader (Biotek).

Electrophoretic mobility of reovirus

5×10^{10} particles of purified reovirus were mixed with 2× SDS sample buffer (20% glycerol, 100mM Tris-HCl [pH 6.8], 0.4% SDS, and 3 mg bromophenol blue) and separated by SDS-PAGE using 4-to-20% gradient polyacrylamide gels (Bio-Rad Laboratories) at 10 mAmps for 16 h. The gel was stained with 5 μg/ml ethidium bromide for 20 min and imaged using the ChemiDoc XRS+ system (Bio-Rad).

Statistical analysis

Mean values for independent experiments were compared using one or two-way analysis of variance (ANOVA) with Tukey's or Dunnett's multiple-comparison test (Graph Pad Prism). *P* values of < 0.05 were considered statistically significant.

Acknowledgements

We would like to thank Jessie Wozniak and Nicholas Harbin for careful review of the manuscript and useful suggestions. This work was supported by funding from the Children's Healthcare of Atlanta and the Pediatric Research Institute, Winship Comprehensive Cancer Institute #IRG-14-188-01 from the American Cancer Society, and the National Institutes of Health (R01 AI146260) (B.A.M.). Flow cytometry experiments were performed in the Emory Pediatrics Flow Cytometry Core (UL1TR002378). Imaging was performed at the Emory Integrated Cellular Imaging Core (2P30 CA138292-04 and the Emory Pediatrics Institute). The funders had no role in the study design, data collection and analysis, decision to publish, or preparation of manuscript.

Figures

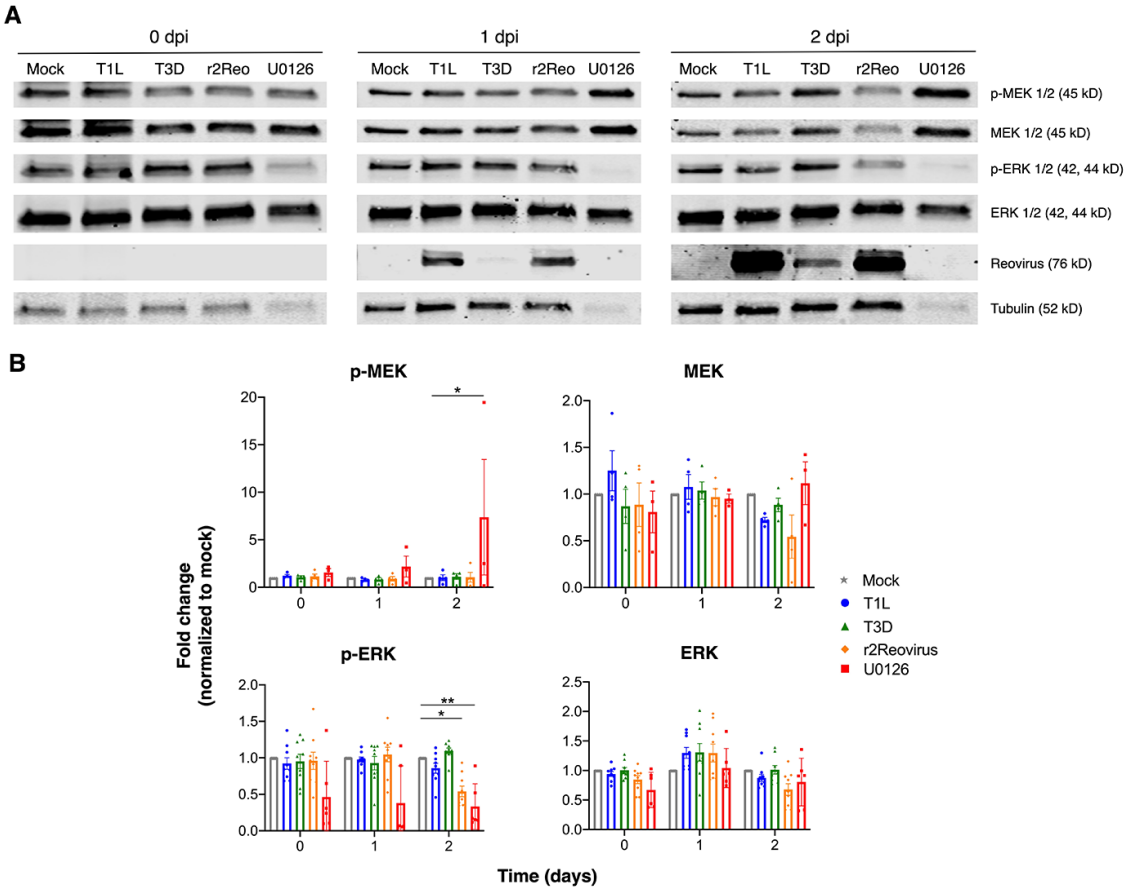

FIG 1. r2Reovirus downregulates MAPK/ERK signaling. MDA-MB-231 cells were adsorbed with mock, T1L, T3D, or r2Reovirus (r2Reo) at an MOI of 500 PFU/cell or treated with 10 μM U0126 for 1 h. A) Whole cell lysates were collected at 0-2 dpi, resolved by SDS-PAGE, and immunoblotted with antibodies specific for phosphorylated and total MEK and ERK, reovirus, and tubulin. Representative data of independent experiments shown. B) Quantitation of band intensity from five independent experiments for phosphorylated MEK (p-MEK) and total MEK and nine independent experiments for phosphorylated ERK (p-ERK) and total ERK and SEM. Data are normalized to mock. *, $P \leq 0.002$; **, $P < 0.0001$ in comparison to mock at each time point, as determined by two-way ANOVA with Tukey's multiple-comparison test.

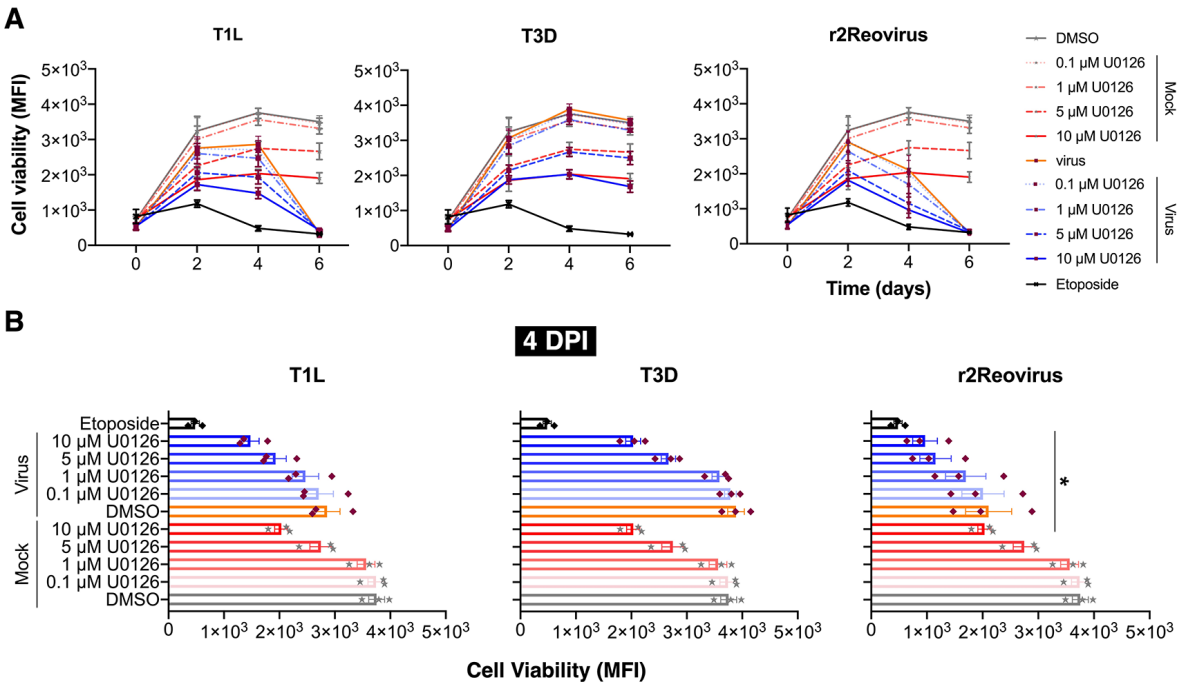

FIG 2. Inhibition of MEK activity increases cytotoxicity induced by T1L and r2Reovirus. MDA-MB-231 cells were treated for 1 h with vehicle (DMSO) or increasing concentrations of U0126 and adsorbed with mock, T1L, T3D or r2Reovirus at an MOI of 100 PFU/ml or treated with 50 μM etoposide for 1 h. A) Cell viability was assessed at times shown. Results are presented as mean fluorescence intensity (MFI) and SEM for three independent experiments. B) Cell viability for data shown in A for day 4 pi. *, $P \leq 0.04$; **, $P = 0.001$; ***, $P \leq 0.005$ in comparison to virus alone, as determined by two-way ANOVA with Tukey's multiple-comparison test.

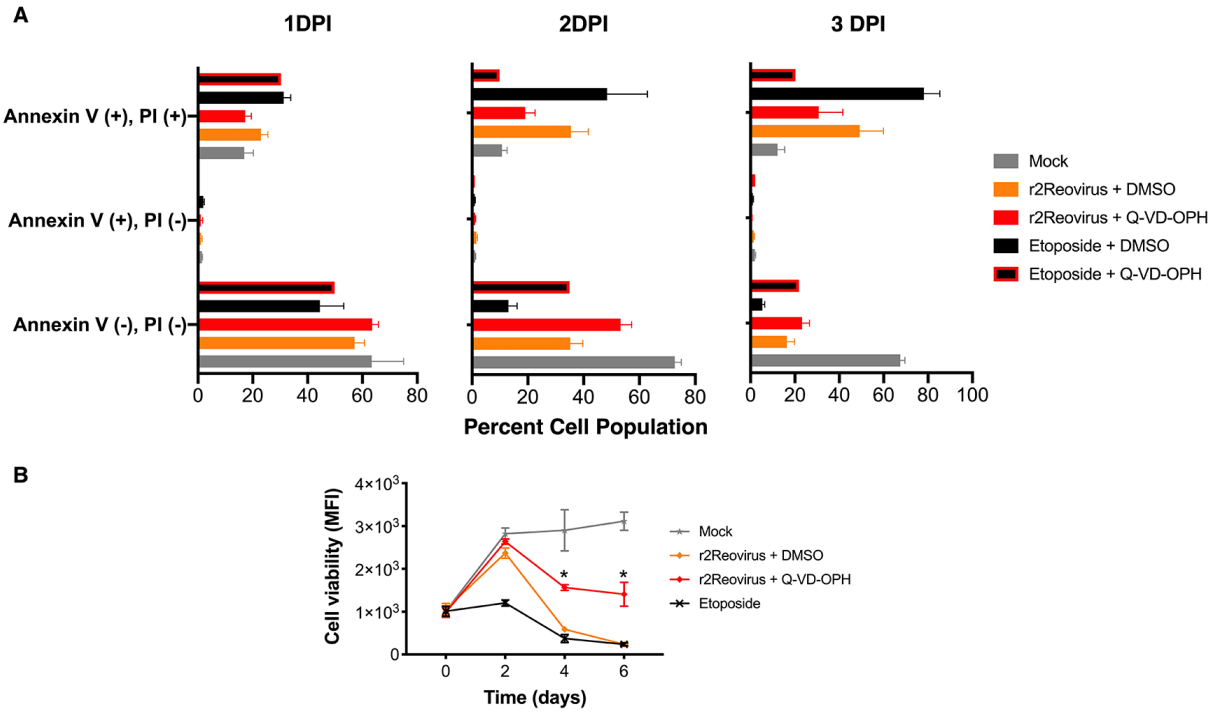

FIG 3. r2Reovirus induced cell death is partially dependent on caspases. MDA-MB-231 cells were treated for 1 h with vehicle (DMSO) or 25 μM caspase inhibitor Q-VD-OPH and adsorbed with mock or r2Reovirus at an MOI of 500 PFU/ml or treated with 50 μM etoposide for 1 h. A) Cells were assessed for annexin V and PI levels by flow cytometry at times shown. Data shown as percentage of cells that are AV-/PI-, AV+/PI- or AV+/PI+. B) Cell viability was assessed at the times shown. Results are shown as mean fluorescence intensity (MFI) and SEM for three independent experiments. *, $P \leq 0.0002$ in comparison to r2Reovirus, as determined by two-way ANOVA with Tukey's multiple-comparison test.

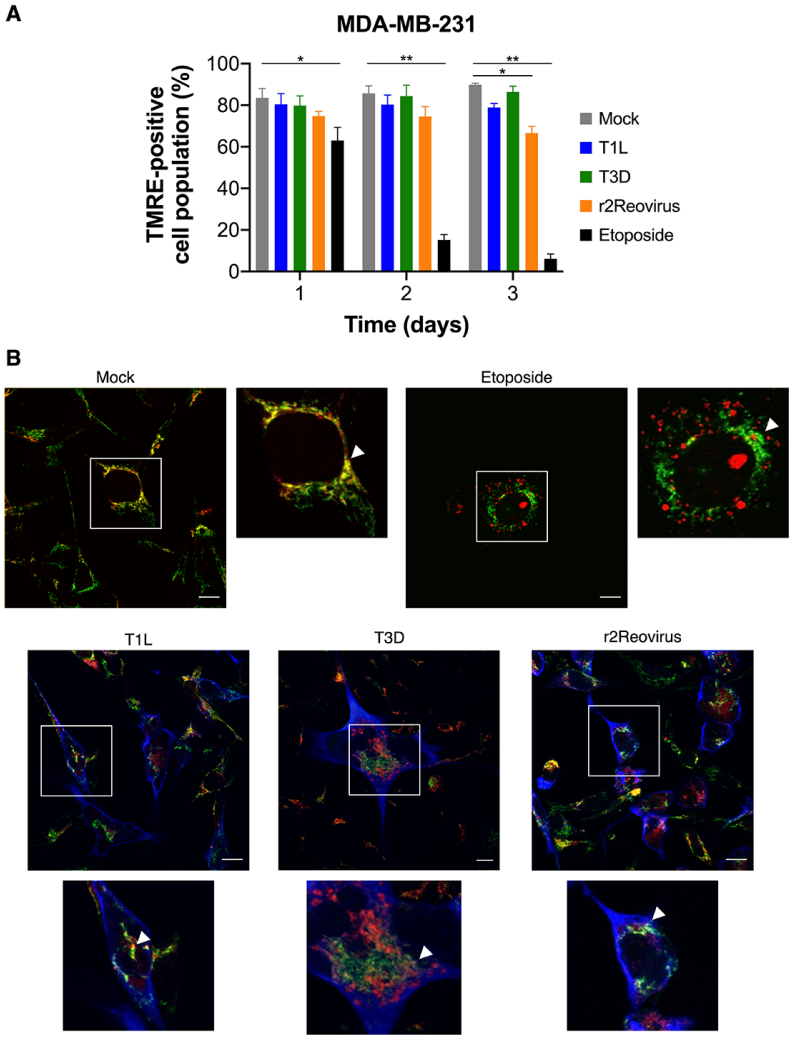

FIG 4. Reovirus does not affect the mitochondria during infection of MDA-MB-231 cells. MDA-MB-231 cells were adsorbed with mock, T1L, T3D, and r2Reovirus for 1 h at an MOI of 500 PFU/cell or treated with 50 μM etoposide. A) Cells were assessed for levels of tetramethylrhodamine, ethyl ester (TMRE) by flow cytometry at times shown. Results are presented as the percentage of TMRE-positive cells and SEM for three independent experiments. *, $P \leq 0.008$; **, $P < 0.0001$. B) Cells were fixed at 3 dpi and stained with antibodies specific for reovirus (blue) or cytochrome c (green) or with MitoTracker to visualize the mitochondria (red). Images are representative of two independent experiments. Scale bar, 10 μm.

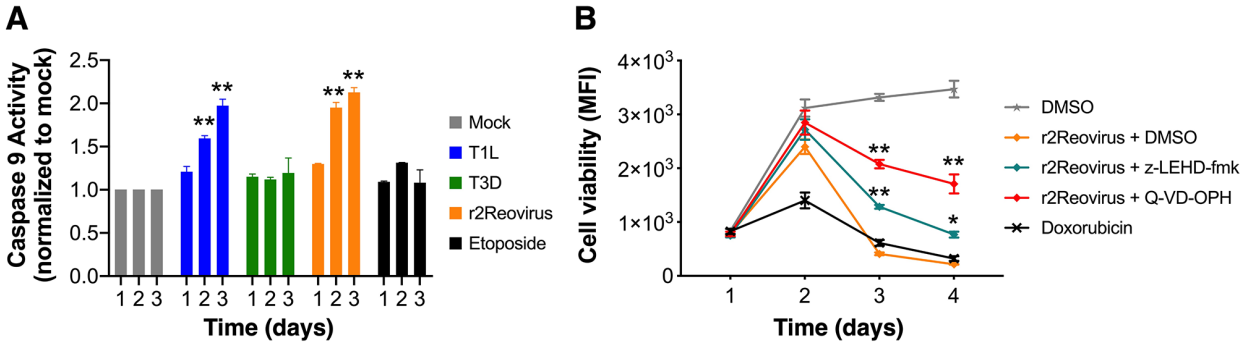

FIG 5. Caspase 9 is activated but not necessary for reovirus-mediated cell death. A) MDA-MB-231 cells were infected with mock, T1L, T3D or r2Reovirus at an MOI of 500 PFU/cell or treated with 50 μM etoposide for 1 h. Cells were assessed for caspase 9 activity at times shown. Results are shown for caspase 9 activity normalized to mock at each time point and SEM for three independent experiments. B) MDA-MB-231 cells were treated with vehicle (DMSO), 25 μM caspase 9 inhibitor z-LEHD-fmk or 25 μM pan-caspase inhibitor Q-VD-OPH and adsorbed with mock or r2Reovirus at an MOI of 500 PFU/cell or treated with 10 μM doxorubicin for 1 h. Cell viability was assessed at times shown. Results are presented as mean fluorescence intensity (MFI) and SEM for three independent experiments. *, $P = 0.003$; **, $P < 0.0001$ in comparison to A) mock and B) r2Reovirus, as determined by two-way ANOVA with Tukey's multiple-comparison test.

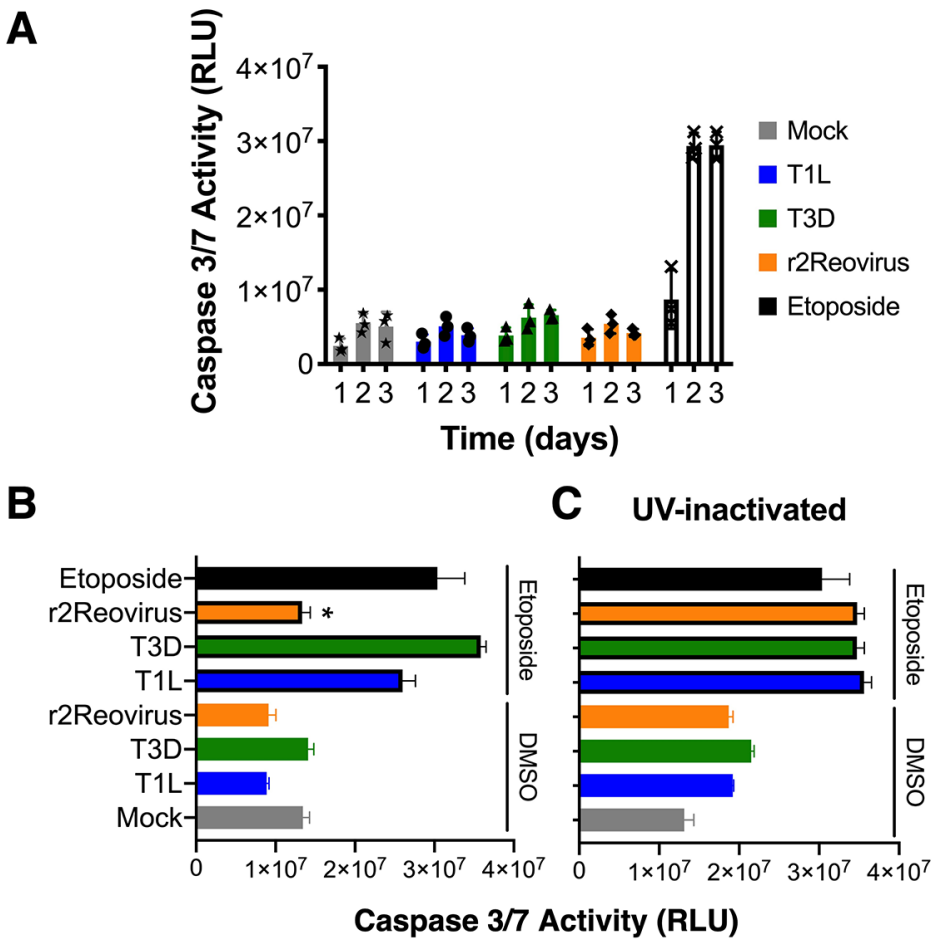

FIG 6. r2Reovirus blocks etoposide-induced caspase 3/7 activity in a replication-dependent manner. A) MDA-MB-231 cells were infected with mock, T1L, T3D or r2Reovirus at an MOI of 500 PFU/cell or treated with 50 μM etoposide for 1 h. Caspase 3/7 activity was measured at times shown in relative luminometer units (RLU) and SEM for three independent experiments. Cells were infected with mock, B) untreated or C) UV-inactivated reovirus at an MOI of 500 PFU/cell, treated with DMSO or 50 μM etoposide 1 dpi, and assessed for caspase 3/7 activity 3 dpi in relative luminometer units (RLU) and SEM for three independent experiments. *, $P < 0.0001$ in comparison to etoposide, as determined by one-way ANOVA with Dunnett's multiple-comparison test.

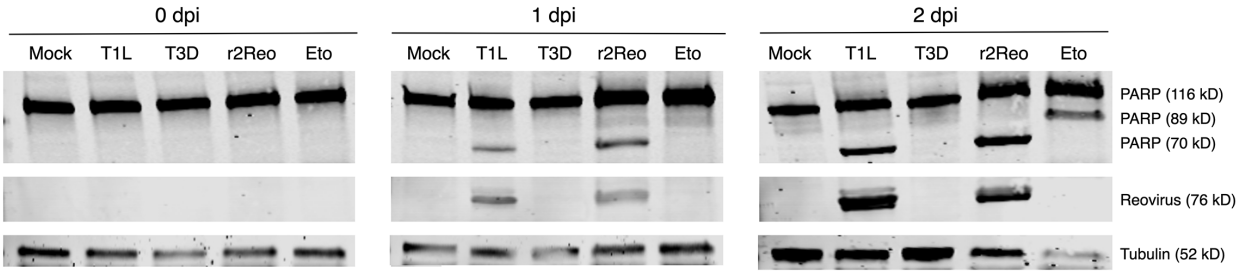

FIG 7. Differential PARP cleavage in reovirus-infected cells. MDA-MB-231 cells were adsorbed with mock, T1L, T3D, or r2Reovirus (r2Reo) at an MOI of 500 PFU/cell or treated with 50 μM etoposide (eto) for 1 h. Whole cell lysates were collected at 0-2 dpi, resolved by SDS-PAGE, and immunoblotted with antibodies specific for PARP, reovirus, and tubulin. Representative experiment of nineteen.

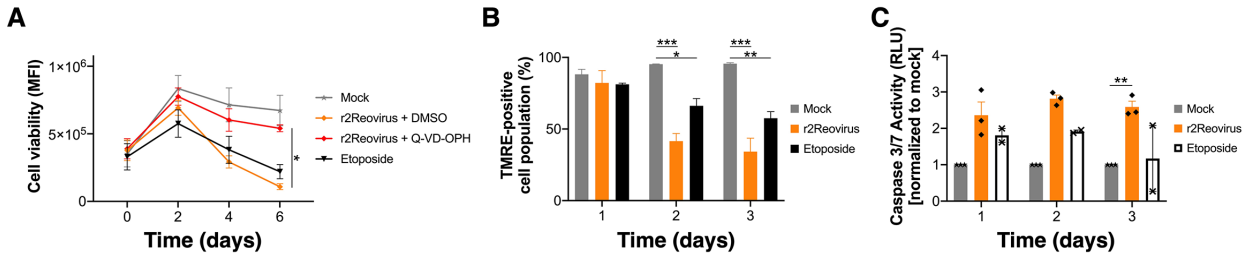

FIG 8. Caspase 3-dependent cell death is observed in MDA-MB-436 cells. A) MDA-MB-436 cells were treated for 1 h with vehicle (DMSO) or 25 μM caspase inhibitor Q-VD-OPH and adsorbed with mock or r2Reovirus at an MOI of 500 PFU/ml for 1 h. Cells were assessed for cell viability over times shown. B, C) MDA-MB-436 cells were infected with mock or r2Reovirus at an MOI of 500 PFU/cell or treated with 50 μM etoposide for 1 h. B) Cells were assessed for TMRE levels by flow cytometry at times shown. Results are presented as the percentage of cells that are TMRE-positive and SEM for three independent experiments. C) Caspase 3/7 activity was measured at times shown. Results are shown as relative luminometer units (RLU) and SEM and normalized to mock for three independent experiments. *, $P \leq 0.05$; **, $P \leq 0.008$; ***, $P < 0.0001$ as determined by two-way ANOVA with Tukey's multiple-comparison test.

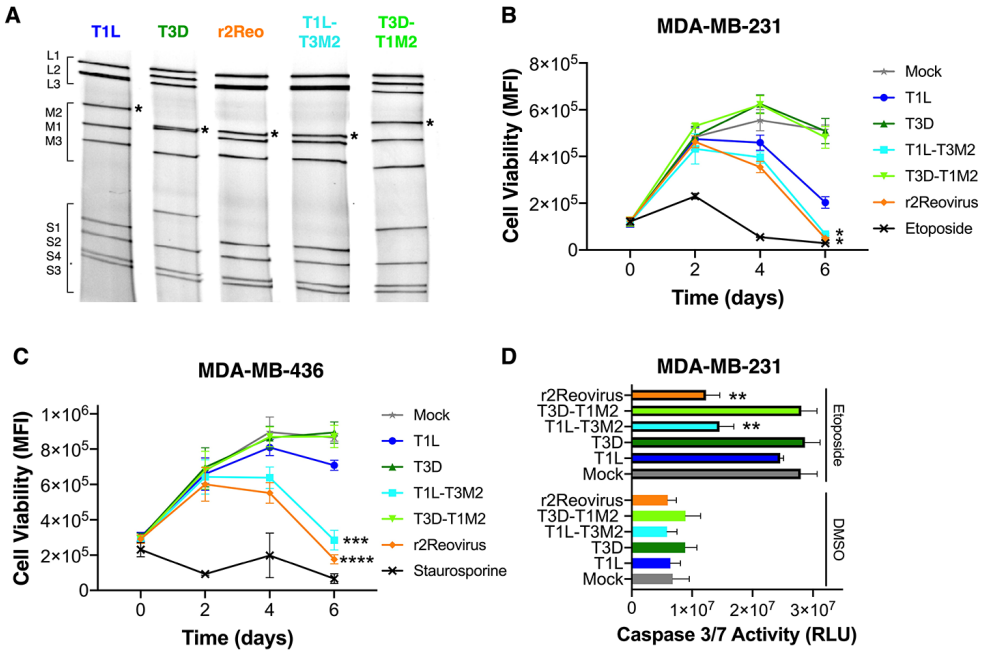

FIG 9. Impact of the M2 gene segment in virus-induced cytotoxicity of TNBC cells. A) SDS-PAGE gel electrophoresis of T1L, T3D, r2Reovirus (r2Reo), and recombinants T1L-T3M2 and T3D-T1M2. Strains are differentiated by migration patterns of three large (L), three medium (M), and four small (S) gene segments. Asterisk denotes M2 gene segment. B) MDA-MB-231 cells were infected with mock, T1L, T3D, T1L-T3M2, T3D-T1M2 or r2Reovirus at an MOI of 500 PFU/cell and treated with vehicle (DMSO) or 50 μM etoposide 1 day post-infection. Caspase 3/7 activity was measured 3 days post-infection. Data are shown as relative luminometer units (RLU) and SEM for three independent experiments. C) MDA-MB-231 and D) MDA-MB-436 cells were infected with mock, T1L, T3D, T1L-T3M2, T3D-T1M2 or r2Reovirus at an MOI of 500 PFU/cell or treated with C) 50 μM etoposide or D) 1 μM staurosporine for 1 h. Cell viability was assessed at times shown. Results are presented as mean fluorescence intensity (MFI) and SEM for three independent experiments. *, $P \leq 0.04$; **, $P = 0.009$; ***, $P = 0.0003$; ****, $P < 0.0001$ in comparison to T1L, as determined by two-way ANOVA with Tukey's multiple-comparison test.

References

1. Abramson VG, Lehmann BD, Ballinger TJ, Pietenpol JA. 2015. Subtyping of triple-negative breast cancer: implications for therapy. Cancer 121:8-16.
2. Wahba HA, El-Hadaad HA. 2015. Current approaches in treatment of triple-negative breast cancer. Cancer Biol Med 12:106-16.
3. Zeichner SB, Terawaki H, Gogineni K. 2016. A Review of Systemic Treatment in Metastatic Triple-Negative Breast Cancer. Breast Cancer (Auckl) 10:25-36.
4. Sherry TSDJSLPB. 2013. Orthoreoviruses. Fields Virology, 6th Edition 2.
5. Millward S, Graham AF. 1970. Structural studies on reovirus: discontinuities in the genome. Proc Natl Acad Sci U S A 65:422-9.
6. Shatkin AJ, Sipe JD, Loh P. 1968. Separation of ten reovirus genome segments by polyacrylamide gel electrophoresis. J Virol 2:986-91.
7. Sabin AB. 1959. Reoviruses. A new group of respiratory and enteric viruses formerly classified as ECHO type 10 is described. Science 130:1387-9.
8. Bouziat R, Hinterleitner R, Brown JJ, Stencel-Baerenwald JE, Ikizler M, Mayassi T, Meisel M, Kim SM, Discepolo V, Pruijssers AJ, Ernest JD, Iskarpatyoti JA, Costes LM, Lawrence I, Palanski BA, Varma M, Zurenski MA, Khomandiak S, McAllister N, Aravamudhan P, Boehme KW, Hu F, Samsom JN, Reinecker HC, Kupfer SS, Guandalini S, Semrad CE, Abadie V, Khosla C, Barreiro LB, Xavier RJ, Ng A, Dermody TS, Jabri B. 2017. Reovirus infection triggers inflammatory responses to dietary antigens and development of celiac disease. Science 356:44-50.
9. Tai JH, Williams JV, Edwards KM, Wright PF, Crowe JE, Jr., Dermody TS. 2005. Prevalence of reovirus-specific antibodies in young children in Nashville, Tennessee. J Infect Dis 191:1221-4.
10. Ouattara LA, Barin F, Barthez MA, Bonnaud B, Roingeard P, Goudeau A, Castelnau P, Vernet G, Paranhos-Baccala G, Komurian-Pradel F. 2011. Novel human reovirus isolated from children with acute necrotizing encephalopathy. Emerg Infect Dis 17:1436-44.
11. Duncan MR, Stanish SM, Cox DC. 1978. Differential sensitivity of normal and transformed human cells to reovirus infection. J Virol 28:444-9.
12. Kemp V, Hoeben RC, van den Wollenberg DJ. 2015. Exploring Reovirus Plasticity for Improving Its Use as Oncolytic Virus. Viruses 8.
13. Coffey MC, Strong JE, Forsyth PA, Lee PW. 1998. Reovirus therapy of tumors with activated Ras pathway. Science 282:1332-4.
14. Strong JE, Coffey MC, Tang D, Sabinin P, Lee PW. 1998. The molecular basis of viral oncolysis: usurpation of the Ras signaling pathway by reovirus. EMBO J 17:3351-62.
15. Lehmann BD, Bauer JA, Chen X, Sanders ME, Chakravarthy AB, Shyr Y, Pietenpol JA. 2011. Identification of human triple-negative breast cancer subtypes and preclinical models for selection of targeted therapies. J Clin Invest 121:2750-67.
16. Baker DJ, Childs BG, Durik M, Wijers ME, Sieben CJ, Zhong J, Saltness RA, Jeganathan KB, Verzosa GC, Pezeshki A, Khazaie K, Miller JD, van Deursen JM. 2016. Naturally occurring p16(Ink4a)-positive cells shorten healthy lifespan. Nature 530:184-9.
17. Canepa ET, Scassa ME, Ceruti JM, Marazita MC, Carcagno AL, Sirkin PF, Ogara MF. 2007. INK4 proteins, a family of mammalian CDK inhibitors with novel biological functions. IUBMB Life 59:419-26.
18. Agrawal N, Frederick MJ, Pickering CR, Bettegowda C, Chang K, Li RJ, Fakhry C, Xie TX, Zhang J, Wang J, Zhang N, El-Naggar AK, Jasser SA, Weinstein JN, Trevino L, Drummond JA, Muzny DM, Wu Y, Wood LD, Hruban RH, Westra WH, Koch WM, Califano JA, Gibbs RA, Sidransky D, Vogelstein B, Velculescu VE, Papadopoulos N, Wheeler DA, Kinzler KW, Myers

JN. 2011. Exome sequencing of head and neck squamous cell carcinoma reveals inactivating mutations in NOTCH1. Science 333:1154-7.
19. Stransky N, Egloff AM, Tward AD, Kostic AD, Cibulskis K, Sivachenko A, Kryukov GV, Lawrence MS, Sougnez C, McKenna A, Shefler E, Ramos AH, Stojanov P, Carter SL, Voet D, Cortes ML, Auclair D, Berger MF, Saksena G, Guiducci C, Onofrio RC, Parkin M, Romkes M, Weissfeld JL, Seethala RR, Wang L, Rangel-Escareno C, Fernandez-Lopez JC, Hidalgo-Miranda A, Melendez-Zajgla J, Winckler W, Ardlie K, Gabriel SB, Meyerson M, Lander ES, Getz G, Golub TR, Garraway LA, Grandis JR. 2011. The mutational landscape of head and neck squamous cell carcinoma. Science 333:1157-60.
20. Reed AL, Califano J, Cairns P, Westra WH, Jones RM, Koch W, Ahrendt S, Eby Y, Sewell D, Nawroz H, Bartek J, Sidransky D. 1996. High frequency of p16 (CDKN2/MTS-1/INK4A) inactivation in head and neck squamous cell carcinoma. Cancer Res 56:3630-3.
21. Morgan DO. 1995. Principles of CDK regulation. Nature 374:131-4.
22. Oseini AM, Roberts LR. 2009. PDGFRalpha: a new therapeutic target in the treatment of hepatocellular carcinoma? Expert Opin Ther Targets 13:443-54.
23. Loyo M, Li RJ, Bettegowda C, Pickering CR, Frederick MJ, Myers JN, Agrawal N. 2013. Lessons learned from next-generation sequencing in head and neck cancer. Head Neck 35:454-63.
24. Hollestelle A, Elstrodt F, Nagel JH, Kallemeijn WW, Schutte M. 2007. Phosphatidylinositol-3-OH kinase or RAS pathway mutations in human breast cancer cell lines. Mol Cancer Res 5:195-201.
25. Yao Z, Torres NM, Tao A, Gao Y, Luo L, Li Q, de Stanchina E, Abdel-Wahab O, Solit DB, Poulikakos PI, Rosen N. 2015. BRAF Mutants Evade ERK-Dependent Feedback by Different Mechanisms that Determine Their Sensitivity to Pharmacologic Inhibition. Cancer Cell 28:370-83.
26. Daud A, Bastian BC. 2012. Beyond BRAF in melanoma. Curr Top Microbiol Immunol 355:99-117.
27. Calvo F, Agudo-Ibanez L, Crespo P. 2010. The Ras-ERK pathway: understanding site-specific signaling provides hope of new anti-tumor therapies. Bioessays 32:412-21.
28. Malumbres M, Barbacid M. 2003. RAS oncogenes: the first 30 years. Nat Rev Cancer 3:459-65.
29. Gou HF, Li X, Qiu M, Cheng K, Li LH, Dong H, Chen Y, Tang Y, Gao F, Zhao F, Men HT, Ge J, Su JM, Xu F, Bi F, Gao JJ, Liu JY. 2013. Epidermal growth factor receptor (EGFR)-RAS signaling pathway in penile squamous cell carcinoma. PLoS One 8:e62175.
30. Catling AD, Schaeffer HJ, Reuter CW, Reddy GR, Weber MJ. 1995. A proline-rich sequence unique to MEK1 and MEK2 is required for raf binding and regulates MEK function. Mol Cell Biol 15:5214-25.
31. Guo YJ, Pan WW, Liu SB, Shen ZF, Xu Y, Hu LL. 2020. ERK/MAPK signalling pathway and tumorigenesis. Exp Ther Med 19:1997-2007.
32. Sebolt-Leopold JS, Herrera R. 2004. Targeting the mitogen-activated protein kinase cascade to treat cancer. Nat Rev Cancer 4:937-47.
33. Norman KL, Hirasawa K, Yang AD, Shields MA, Lee PW. 2004. Reovirus oncolysis: the Ras/RalGEF/p38 pathway dictates host cell permissiveness to reovirus infection. Proc Natl Acad Sci U S A 101:11099-104.
34. Marcato P, Shmulevitz M, Pan D, Stoltz D, Lee PW. 2007. Ras transformation mediates reovirus oncolysis by enhancing virus uncoating, particle infectivity, and apoptosis-dependent release. Mol Ther 15:1522-30.
35. Phillips MB, Stuart JD, Rodriguez Stewart RM, Berry JT, Mainou BA, Boehme KW. 2018. Current understanding of reovirus oncolysis mechanisms. Oncolytic Virother 7:53-63.

36.Maitra R, Seetharam R, Tesfa L, Augustine TA, Klampfer L, Coffey MC, Mariadason JM, Goel S. 2014. Oncolytic reovirus preferentially induces apoptosis in KRAS mutant colorectal cancer cells, and synergizes with irinotecan. Oncotarget 5:2807-19.
37.Kelly KR, Espitia CM, Mahalingam D, Oyajobi BO, Coffey M, Giles FJ, Carew JS, Nawrocki ST. 2012. Reovirus therapy stimulates endoplasmic reticular stress, NOXA induction, and augments bortezomib-mediated apoptosis in multiple myeloma. Oncogene 31:3023-38.
38.Shmulevitz M, Pan LZ, Garant K, Pan D, Lee PW. 2010. Oncogenic Ras promotes reovirus spread by suppressing IFN-beta production through negative regulation of RIG-I signaling. Cancer Res 70:4912-21.
39.Garant KA, Shmulevitz M, Pan L, Daigle RM, Ahn DG, Gujar SA, Lee PW. 2016. Oncolytic reovirus induces intracellular redistribution of Ras to promote apoptosis and progeny virus release. Oncogene 35:771-82.
40.Gong J, Mita MM. 2014. Activated ras signaling pathways and reovirus oncolysis: an update on the mechanism of preferential reovirus replication in cancer cells. Front Oncol 4:167.
41.Song L, Ohnuma T, Gelman IH, Holland JF. 2009. Reovirus infection of cancer cells is not due to activated Ras pathway. Cancer Gene Ther 16:382.
42.Twigger K, Roulstone V, Kyula J, Karapanagiotou EM, Syrigos KN, Morgan R, White C, Bhide S, Nuovo G, Coffey M, Thompson B, Jebar A, Errington F, Melcher AA, Vile RG, Pandha HS, Harrington KJ. 2012. Reovirus exerts potent oncolytic effects in head and neck cancer cell lines that are independent of signalling in the EGFR pathway. BMC Cancer 12:368.
43.Simon EJ, Howells MA, Stuart JD, Boehme KW. 2017. Serotype-Specific Killing of Large Cell Carcinoma Cells by Reovirus. Viruses 9.
44.Thirukkumaran CM, Shi ZQ, Luider J, Kopciuk K, Gao H, Bahlis N, Neri P, Pho M, Stewart D, Mansoor A, Morris DG. 2012. Reovirus as a viable therapeutic option for the treatment of multiple myeloma. Clin Cancer Res 18:4962-72.
45.Hwang CC, Igase M, Okuda M, Coffey M, Noguchi S, Mizuno T. 2019. Reovirus changes the expression of anti-apoptotic and proapoptotic proteins with the c-kit downregulation in canine mast cell tumor cell lines. Biochem Biophys Res Commun 517:233-237.
46.Tyler KL, Squier MK, Rodgers SE, Schneider BE, Oberhaus SM, Grdina TA, Cohen JJ, Dermody TS. 1995. Differences in the capacity of reovirus strains to induce apoptosis are determined by the viral attachment protein sigma 1. J Virol 69:6972-9.
47.Connolly JL, Rodgers SE, Clarke P, Ballard DW, Kerr LD, Tyler KL, Dermody TS. 2000. Reovirus-induced apoptosis requires activation of transcription factor NF-kappaB. J Virol 74:2981-9.
48.Clarke P, Debiasi RL, Goody R, Hoyt CC, Richardson-Burns S, Tyler KL. 2005. Mechanisms of reovirus-induced cell death and tissue injury: role of apoptosis and virus-induced perturbation of host-cell signaling and transcription factor activation. Viral Immunol 18:89-115.
49.Tyler KL, Squier MK, Brown AL, Pike B, Willis D, Oberhaus SM, Dermody TS, Cohen JJ. 1996. Linkage between reovirus-induced apoptosis and inhibition of cellular DNA synthesis: role of the S1 and M2 genes. J Virol 70:7984-91.
50.Berger AK, Hiller BE, Thete D, Snyder AJ, Perez E, Jr., Upton JW, Danthi P. 2017. Viral RNA at Two Stages of Reovirus Infection Is Required for the Induction of Necroptosis. J Virol 91.
51.Berger AK, Danthi P. 2013. Reovirus activates a caspase-independent cell death pathway. MBio 4:e00178-13.
52.Boehme KW, Hammer K, Tollefson WC, Konopka-Anstadt JL, Kobayashi T, Dermody TS. 2013. Nonstructural protein sigma1s mediates reovirus-induced cell cycle arrest and apoptosis. J Virol 87:12967-79.

53.Igase M, Shibutani S, Kurogouchi Y, Fujiki N, Hwang CC, Coffey M, Noguchi S, Nemoto Y, Mizuno T. 2019. Combination Therapy with Reovirus and ATM Inhibitor Enhances Cell Death and Virus Replication in Canine Melanoma. Mol Ther Oncolytics 15:49-59.
54.Holm GH, Zurney J, Tumilasci V, Leveille S, Danthi P, Hiscott J, Sherry B, Dermody TS. 2007. Retinoic acid-inducible gene-I and interferon-beta promoter stimulator-1 augment proapoptotic responses following mammalian reovirus infection via interferon regulatory factor-3. J Biol Chem 282:21953-61.
55.Danthi P, Hansberger MW, Campbell JA, Forrest JC, Dermody TS. 2006. JAM-A-independent, antibody-mediated uptake of reovirus into cells leads to apoptosis. J Virol 80:1261-70.
56.Hansberger MW, Campbell JA, Danthi P, Arrate P, Pennington KN, Marcu KB, Ballard DW, Dermody TS. 2007. IkappaB kinase subunits alpha and gamma are required for activation of NF-kappaB and induction of apoptosis by mammalian reovirus. J Virol 81:1360-71.
57.Roebke KE, Danthi P. 2019. Cell Entry-Independent Role for the Reovirus mu1 Protein in Regulating Necroptosis and the Accumulation of Viral Gene Products. J Virol 93.
58.Chiu HC, Richart S, Lin FY, Hsu WL, Liu HJ. 2014. The interplay of reovirus with autophagy. Biomed Res Int 2014:483657.
59.Clarke P, Tyler KL. 2003. Reovirus-induced apoptosis: A minireview. Apoptosis 8:141-50.
60.Poggioli GJ, Keefer C, Connolly JL, Dermody TS, Tyler KL. 2000. Reovirus-induced G(2)/M cell cycle arrest requires sigma1s and occurs in the absence of apoptosis. J Virol 74:9562-70.
61.Clarke P, Meintzer SM, Gibson S, Widmann C, Garrington TP, Johnson GL, Tyler KL. 2000. Reovirus-induced apoptosis is mediated by TRAIL. J Virol 74:8135-9.
62.Iordanov MS, Ryabinina OP, Schneider P, Magun BE. 2005. Two mechanisms of caspase 9 processing in double-stranded RNA- and virus-triggered apoptosis. Apoptosis 10:153-66.
63.Rodgers SE, Barton ES, Oberhaus SM, Pike B, Gibson CA, Tyler KL, Dermody TS. 1997. Reovirus-induced apoptosis of MDCK cells is not linked to viral yield and is blocked by Bcl-2. J Virol 71:2540-6.
64.Connolly JL, Barton ES, Dermody TS. 2001. Reovirus binding to cell surface sialic acid potentiates virus-induced apoptosis. J Virol 75:4029-39.
65.Beckham JD, Tuttle KD, Tyler KL. 2010. Caspase-3 activation is required for reovirus-induced encephalitis in vivo. J Neurovirol 16:306-17.
66.Danthi P, Pruijssers AJ, Berger AK, Holm GH, Zinkel SS, Dermody TS. 2010. Bid regulates the pathogenesis of neurotropic reovirus. PLoS Pathog 6:e1000980.
67.Kominsky DJ, Bickel RJ, Tyler KL. 2002. Reovirus-induced apoptosis requires both death receptor- and mitochondrial-mediated caspase-dependent pathways of cell death. Cell Death Differ 9:926-33.
68.Kominsky DJ, Bickel RJ, Tyler KL. 2002. Reovirus-induced apoptosis requires mitochondrial release of Smac/DIABLO and involves reduction of cellular inhibitor of apoptosis protein levels. J Virol 76:11414-24.
69.Rodriguez Stewart RM, Berry JTL, Berger AK, Yoon SB, Hirsch AL, Guberman JA, Patel NB, Tharp GK, Bosinger SE, Mainou BA. 2019. Enhanced Killing of Triple-Negative Breast Cancer Cells by Reassortant Reovirus and Topoisomerase Inhibitors. J Virol 93.
70.Snyder AJ, Wang JC, Danthi P. 2019. Components of the Reovirus Capsid Differentially Contribute to Stability. J Virol 93.
71.Roner MR, Mutsoli C. 2007. The use of monoreassortants and reverse genetics to map reovirus lysis of a ras-transformed cell line. J Virol Methods 139:132-42.
72.Sharpe AH, Fields BN. 1982. Reovirus inhibition of cellular RNA and protein synthesis: role of the S4 gene. Virology 122:381-91.

73.Kim M, Garant KA, zur Nieden NI, Alain T, Loken SD, Urbanski SJ, Forsyth PA, Rancourt DE, Lee PW, Johnston RN. 2011. Attenuated reovirus displays oncolysis with reduced host toxicity. Br J Cancer 104:290-9.
74.Jiang L, Wang Y, Liu G, Liu H, Zhu F, Ji H, Li B. 2018. C-Phycocyanin exerts anti-cancer effects via the MAPK signaling pathway in MDA-MB-231 cells. Cancer Cell Int 18:12.
75.Chen Y, Wang X, Cao C, Wang X, Liang S, Peng C, Fu L, He G. 2017. Inhibition of HSP90 sensitizes a novel Raf/ERK dual inhibitor CY-9d in triple-negative breast cancer cells. Oncotarget 8:104193-104205.
76.Fernandez IF, Blanco S, Lozano J, Lazo PA. 2010. VRK2 inhibits mitogen-activated protein kinase signaling and inversely correlates with ErbB2 in human breast cancer. Mol Cell Biol 30:4687-97.
77.Fukazawa H, Noguchi K, Murakami Y, Uehara Y. 2002. Mitogen-activated protein/extracellular signal-regulated kinase kinase (MEK) inhibitors restore anoikis sensitivity in human breast cancer cell lines with a constitutively activated extracellular-regulated kinase (ERK) pathway. Mol Cancer Ther 1:303-9.
78.Oh AS, Lorant LA, Holloway JN, Miller DL, Kern FG, El-Ashry D. 2001. Hyperactivation of MAPK induces loss of ERalpha expression in breast cancer cells. Mol Endocrinol 15:1344-59.
79.Li Y, Liang R, Zhang X, Wang J, Shan C, Liu S, Li L, Zhang S. 2019. Copper Chaperone for Superoxide Dismutase Promotes Breast Cancer Cell Proliferation and Migration via ROS-Mediated MAPK/ERK Signaling. Front Pharmacol 10:356.
80.Gu XD, Xu LL, Zhao H, Gu JZ, Xie XH. 2017. Cantharidin suppressed breast cancer MDA-MB-231 cell growth and migration by inhibiting MAPK signaling pathway. Braz J Med Biol Res 50:e5920.
81.Lu Z, Xu S. 2006. ERK1/2 MAP kinases in cell survival and apoptosis. IUBMB Life 58:621-31.
82.Qiao D, Stratagouleas ED, Martinez JD. 2001. Activation and role of mitogen-activated protein kinases in deoxycholic acid-induced apoptosis. Carcinogenesis 22:35-41.
83.Mirzoeva OK, Das D, Heiser LM, Bhattacharya S, Siwak D, Gendelman R, Bayani N, Wang NJ, Neve RM, Guan Y, Hu Z, Knight Z, Feiler HS, Gascard P, Parvin B, Spellman PT, Shokat KM, Wyrobek AJ, Bissell MJ, McCormick F, Kuo WL, Mills GB, Gray JW, Korn WM. 2009. Basal subtype and MAPK/ERK kinase (MEK)-phosphoinositide 3-kinase feedback signaling determine susceptibility of breast cancer cells to MEK inhibition. Cancer Res 69:565-72.
84.Ye J, Li A, Liu Q, Wang X, Zhou J. 2005. Inhibition of mitogen-activated protein kinase kinase enhances apoptosis induced by arsenic trioxide in human breast cancer MCF-7 cells. Clin Exp Pharmacol Physiol 32:1042-8.
85.Wang C, Youle RJ. 2009. The role of mitochondria in apoptosis*. Annu Rev Genet 43:95-118.
86.Garrido C, Galluzzi L, Brunet M, Puig PE, Didelot C, Kroemer G. 2006. Mechanisms of cytochrome c release from mitochondria. Cell Death Differ 13:1423-33.
87.Tait SW, Green DR. 2013. Mitochondrial regulation of cell death. Cold Spring Harb Perspect Biol 5.
88.Finucane DM, Bossy-Wetzel E, Waterhouse NJ, Cotter TG, Green DR. 1999. Bax-induced caspase activation and apoptosis via cytochrome c release from mitochondria is inhibitable by Bcl-xL. J Biol Chem 274:2225-33.
89.Waterhouse NJ, Goldstein JC, von Ahsen O, Schuler M, Newmeyer DD, Green DR. 2001. Cytochrome c maintains mitochondrial transmembrane potential and ATP generation after outer mitochondrial membrane permeabilization during the apoptotic process. J Cell Biol 153:319-28.
90.Von Ahsen O, Waterhouse NJ, Kuwana T, Newmeyer DD, Green DR. 2000. The 'harmless' release of cytochrome c. Cell Death Differ 7:1192-9.

91. Ricci JE, Munoz-Pinedo C, Fitzgerald P, Bailly-Maitre B, Perkins GA, Yadava N, Scheffler IE, Ellisman MH, Green DR. 2004. Disruption of mitochondrial function during apoptosis is mediated by caspase cleavage of the p75 subunit of complex I of the electron transport chain. Cell 117:773-86.
92. McComb S, Chan PK, Guinot A, Hartmannsdottir H, Jenni S, Dobay MP, Bourquin JP, Bornhauser BC. 2019. Efficient apoptosis requires feedback amplification of upstream apoptotic signals by effector caspase-3 or -7. Sci Adv 5:eaau9433.
93. Brentnall M, Rodriguez-Menocal L, De Guevara RL, Cepero E, Boise LH. 2013. Caspase-9, caspase-3 and caspase-7 have distinct roles during intrinsic apoptosis. BMC Cell Biol 14:32.
94. Inoue S, Browne G, Melino G, Cohen GM. 2009. Ordering of caspases in cells undergoing apoptosis by the intrinsic pathway. Cell Death Differ 16:1053-61.
95. Lavrik IN, Golks A, Krammer PH. 2005. Caspases: pharmacological manipulation of cell death. J Clin Invest 115:2665-72.
96. Morales J, Li L, Fattah FJ, Dong Y, Bey EA, Patel M, Gao J, Boothman DA. 2014. Review of poly (ADP-ribose) polymerase (PARP) mechanisms of action and rationale for targeting in cancer and other diseases. Crit Rev Eukaryot Gene Expr 24:15-28.
97. Bouchard VJ, Rouleau M, Poirier GG. 2003. PARP-1, a determinant of cell survival in response to DNA damage. Exp Hematol 31:446-54.
98. Weaver AN, Yang ES. 2013. Beyond DNA Repair: Additional Functions of PARP-1 in Cancer. Front Oncol 3:290.
99. Sousa FG, Matuo R, Soares DG, Escargueil AE, Henriques JA, Larsen AK, Saffi J. 2012. PARPs and the DNA damage response. Carcinogenesis 33:1433-40.
100. Chaitanya GV, Steven AJ, Babu PP. 2010. PARP-1 cleavage fragments: signatures of cell-death proteases in neurodegeneration. Cell Commun Signal 8:31.
101. Boulares AH, Yakovlev AG, Ivanova V, Stoica BA, Wang G, Iyer S, Smulson M. 1999. Role of poly(ADP-ribose) polymerase (PARP) cleavage in apoptosis. Caspase 3-resistant PARP mutant increases rates of apoptosis in transfected cells. J Biol Chem 274:22932-40.
102. Simbulan-Rosenthal CM, Rosenthal DS, Iyer S, Boulares H, Smulson ME. 1999. Involvement of PARP and poly(ADP-ribosyl)ation in the early stages of apoptosis and DNA replication. Mol Cell Biochem 193:137-48.
103. Kaufmann SH, Desnoyers S, Ottaviano Y, Davidson NE, Poirier GG. 1993. Specific proteolytic cleavage of poly(ADP-ribose) polymerase: an early marker of chemotherapy-induced apoptosis. Cancer Res 53:3976-85.
104. Komoto S, Kawagishi T, Kobayashi T, Ikizler M, Iskarpatyoti J, Dermody TS, Taniguchi K. 2014. A plasmid-based reverse genetics system for mammalian orthoreoviruses driven by a plasmid-encoded T7 RNA polymerase. J Virol Methods 196:36-9.
105. Thete D, Snyder AJ, Mainou BA, Danthi P. 2016. Reovirus mu1 Protein Affects Infectivity by Altering Virus-Receptor Interactions. J Virol 90:10951-10962.
106. Occhi G, Barollo S, Regazzo D, Bertazza L, Galuppini F, Guzzardo V, Jaffrain-Rea ML, Vianello F, Ciato D, Ceccato F, Watutantrige-Fernando S, Bisognin A, Bortoluzzi S, Pennelli G, Boscaro M, Scaroni C, Mian C. 2015. A constitutive active MAPK/ERK pathway due to BRAFV600E positively regulates AHR pathway in PTC. Oncotarget 6:32104-14.
107. Steinmetz R, Wagoner HA, Zeng P, Hammond JR, Hannon TS, Meyers JL, Pescovitz OH. 2004. Mechanisms regulating the constitutive activation of the extracellular signal-regulated kinase (ERK) signaling pathway in ovarian cancer and the effect of ribonucleic acid interference for ERK1/2 on cancer cell proliferation. Mol Endocrinol 18:2570-82.
108. Burotto M, Chiou VL, Lee JM, Kohn EC. 2014. The MAPK pathway across different malignancies: a new perspective. Cancer 120:3446-56.

109. Dhillon AS, Hagan S, Rath O, Kolch W. 2007. MAP kinase signalling pathways in cancer. Oncogene 26:3279-90.
110. Fernandes J. 2016. Oncogenes: The Passport for Viral Oncolysis Through PKR Inhibition. Biomark Cancer 8:101-10.
111. Aroui S, Brahim S, Hamelin J, De Waard M, Breard J, Kenani A. 2009. Conjugation of doxorubicin to cell penetrating peptides sensitizes human breast MDA-MB 231 cancer cells to endogenous TRAIL-induced apoptosis. Apoptosis 14:1352-65.
112. Butler LM, Liapis V, Bouralexis S, Welldon K, Hay S, Thai le M, Labrinidis A, Tilley WD, Findlay DM, Evdokiou A. 2006. The histone deacetylase inhibitor, suberoylanilide hydroxamic acid, overcomes resistance of human breast cancer cells to Apo2L/TRAIL. Int J Cancer 119:944-54.
113. Lagadec C, Adriaenssens E, Toillon RA, Chopin V, Romon R, Van Coppenolle F, Hondermarck H, Le Bourhis X. 2008. Tamoxifen and TRAIL synergistically induce apoptosis in breast cancer cells. Oncogene 27:1472-7.
114. Melendez ME, Silva-Oliveira RJ, Silva Almeida Vicente AL, Rebolho Batista Arantes LM, Carolina de Carvalho A, Epstein AL, Reis RM, Carvalho AL. 2018. Construction and characterization of a new TRAIL soluble form, active at picomolar concentrations. Oncotarget 9:27233-27241.
115. Rahman M, Davis SR, Pumphrey JG, Bao J, Nau MM, Meltzer PS, Lipkowitz S. 2009. TRAIL induces apoptosis in triple-negative breast cancer cells with a mesenchymal phenotype. Breast Cancer Res Treat 113:217-30.
116. Park C, Moon DO, Ryu CH, Choi B, Lee W, Kim GY, Choi Y. 2008. Beta-sitosterol sensitizes MDA-MB-231 cells to TRAIL-induced apoptosis. Acta Pharmacol Sin 29:341-8.
117. Danthi P, Coffey CM, Parker JS, Abel TW, Dermody TS. 2008. Independent regulation of reovirus membrane penetration and apoptosis by the mu1 phi domain. PLoS Pathog 4:e1000248.
118. Galvan V, Brandimarti R, Roizman B. 1999. Herpes simplex virus 1 blocks caspase-3-independent and caspase-dependent pathways to cell death. J Virol 73:3219-26.
119. Richard A, Tulasne D. 2012. Caspase cleavage of viral proteins, another way for viruses to make the best of apoptosis. Cell Death Dis 3:e277.
120. Tabtieng T, Degterev A, Gaglia MM. 2018. Caspase-Dependent Suppression of Type I Interferon Signaling Promotes Kaposi's Sarcoma-Associated Herpesvirus Lytic Replication. J Virol 92.
121. Connolly PF, Fearnhead HO. 2017. Viral hijacking of host caspases: an emerging category of pathogen-host interactions. Cell Death Differ 24:1401-1410.
122. Rodriguez-Grille J, Busch LK, Martinez-Costas J, Benavente J. 2014. Avian reovirus-triggered apoptosis enhances both virus spread and the processing of the viral nonstructural muNS protein. Virology 462-463:49-59.
123. Kaufer S, Coffey CM, Parker JS. 2012. The cellular chaperone hsc70 is specifically recruited to reovirus viral factories independently of its chaperone function. J Virol 86:1079-89.
124. Stanifer ML, Kischnick C, Rippert A, Albrecht D, Boulant S. 2017. Reovirus inhibits interferon production by sequestering IRF3 into viral factories. Sci Rep 7:10873.
125. Tenorio R, Fernandez de Castro I, Knowlton JJ, Zamora PF, Lee CH, Mainou BA, Dermody TS, Risco C. 2018. Reovirus sigmaNS and muNS Proteins Remodel the Endoplasmic Reticulum to Build Replication Neo-Organelles. mBio 9.
126. Fernandez de Castro I, Zamora PF, Ooms L, Fernandez JJ, Lai CM, Mainou BA, Dermody TS, Risco C. 2014. Reovirus forms neo-organelles for progeny particle assembly within reorganized cell membranes. mBio 5.

127. Parker JS, Broering TJ, Kim J, Higgins DE, Nibert ML. 2002. Reovirus core protein mu2 determines the filamentous morphology of viral inclusion bodies by interacting with and stabilizing microtubules. J Virol 76:4483-96.
128. Castri P, Lee YJ, Ponzio T, Maric D, Spatz M, Bembry J, Hallenbeck J. 2014. Poly(ADP-ribose) polymerase-1 and its cleavage products differentially modulate cellular protection through NF-kappaB-dependent signaling. Biochim Biophys Acta 1843:640-51.
129. Kobayashi T, Antar AA, Boehme KW, Danthi P, Eby EA, Guglielmi KM, Holm GH, Johnson EM, Maginnis MS, Naik S, Skelton WB, Wetzel JD, Wilson GJ, Chappell JD, Dermody TS. 2007. A plasmid-based reverse genetics system for animal double-stranded RNA viruses. Cell Host Microbe 1:147-57.
130. Sarkar P, Danthi P. 2010. Determinants of strain-specific differences in efficiency of reovirus entry. J Virol 84:12723-32.
131. Furlong DB, Nibert ML, Fields BN. 1988. Sigma 1 protein of mammalian reoviruses extends from the surfaces of viral particles. J Virol 62:246-56.
132. Smith RE, Zweerink HJ, Joklik WK. 1969. Polypeptide components of virions, top component and cores of reovirus type 3. Virology 39:791-810.
133. Mainou BA, Zamora PF, Ashbrook AW, Dorset DC, Kim KS, Dermody TS. 2013. Reovirus cell entry requires functional microtubules. mBio 4.
134. Mainou BA, Dermody TS. 2012. Transport to late endosomes is required for efficient reovirus infection. J Virol 86:8346-58.
135. Virgin HWt, Bassel-Duby R, Fields BN, Tyler KL. 1988. Antibody protects against lethal infection with the neurally spreading reovirus type 3 (Dearing). J Virol 62:4594-604.

Chapter IV: Discussion

Reovirus infection is usually asymptomatic and the virus has an inherent preference to replicate in transformed cells while eliciting immune responses (1-8). This confers great potential as an oncolytic. These inherent oncolytic properties can be exploited to create improved therapies against cancers with limited treatment options, such as TNBC. In chapter II of this dissertation, we generated novel reassortant reoviruses, r1Reovirus and r2Reovirus, with enhanced oncolytic properties in TNBC cells by forward genetics following coinfection with prototype strains of three different reovirus serotypes (T1L, T2J, and T3D). r1Reovirus is composed of seven gene segments from T1L and three from T3D (L2, M2, and S2), while r2Reovirus is composed of nine gene segments from T1L and one from T3D (M2). In addition, both viruses have previously unidentified synonymous and nonsynonymous point mutations. These data show coinfection and serial passaging in TNBC cells can be used for the generation of reassortant reoviruses with novel genetic compositions.

Both reassortant viruses exhibited phenotypic differences from parental T1L and T3D strains. Attachment of r1Reovirus and r2Reovirus to MDA-MB-231 and HCC1937 cells was similar to T1L. This was not surprising given they all share the same S1 gene segment, which encodes the σ1 attachment protein (1, 9). This indicates that we did not select for viruses with enhanced attachment properties and that other genetic changes found in r1Reovirus and r2Reovirus do not impact the ability of these viruses to attach to cells. Both reassortant viruses have enhanced infective properties when compared to parental reovirus strains in MDA-MB-231 cells. In HCC1937 cells, r2Reovirus, but not r1Reovirus, showed enhanced infective capacity compared to both parental reoviruses. This suggests that the genetic changes found in r2Reovirus confer enhanced infection in TNBC cells at a step after attachment. Interestingly, T3D and r1Reovirus infection of HCC1937

cells was similar. This suggests additional T3D-derived gene segments found in r1Reovirus might be driving infection in these cells.

A T1L reovirus with a T3D M2 gene segment (T1L-T3M2) attaches and infects L929 cells more efficiently than parental T1L virus, showing an epistatic effect between T1L S1-encoded σ1 attachment protein and non-adjacent T3D M2-encoded μ1 protein (10). r2Reovirus infection of L929 cells was slightly, though not significantly, enhanced compared to T1L and r1Reovirus infection. This suggests that the genetic changes found in r2Reovirus confer a slight enhancement of infection in L929 cells and that additional changes found in r1Reovirus might revert enhancement of reovirus infection in some contexts. Previous studies performed in L929 cells showing an epistatic effect between T1L σ1 and T3D μ1 proteins suggest the slight enhancement in infectivity observed with r2Reovirus is conferred by the genetic reassortment and the additional mutations have little or no effect on viral infection. These data indicate that r2Reovirus infection of TNBC cells, but not L929 cells, is significantly enhanced when compared with parental reoviruses. This also suggests that additional mutations found in r1Reovirus but not r2Reovirus revert r1Reovirus infection potential of non-MDA-MB-231 cells similar to that of parental reoviruses. Interestingly, all non-synonymous point mutations present in r2Reovirus are also present in r1Reovirus, so enhancement of infectivity of r2Reovirus over r1Reovirus is not a result of mutations present in r2Reovirus. In fact, r1Reovirus has more mutations than r2Reovirus and it has an unstable S2 gene segment, with single-residue variations that range from 35% to 65%. The unstable S2 gene segment could hinder its infectivity potential in non-MDA-MB-231 cells. Proteolytic disassembly of the virion during cell entry is a critical determinant of susceptibility to reovirus infection. Mutations observed in reassortant reoviruses gene segments could make the structural proteins they encode, major inner-capsid protein λ1 and major outer-capsid σ3, more susceptible to proteolytic cleavage, leading to faster entry kinetics and thus higher infectivity in MDA-MB-231 cells (11).

Enhanced r2Reovirus infectivity in TNBC cells but not L929 cells could be a result of availability of host factors involved in viral entry such as β1 integrin, calpains, cathepsins, Src kinase or proteases involved in virion disassembly. β1 integrin is found in high levels in TNBC cells and can regulate migration, invasion, and epithelial-mesenchymal transition (EMT) (12). Calpain-1 is also significantly expressed in TNBC tissues (13) and Src kinase is being investigated as a potential target for the treatment of TNBC partly due to higher expression of Src in TNBC cells when compared to non-TNBC cells (14). Both reassortant viruses displayed enhanced cytotoxic properties when compared to parental reovirus strains in HeLa, L929, MDA-MB-231, and MDA-MB-436 cells. These data indicate that enhanced kinetics of reassortant viruses does not isolate to just TNBC cells. Additionally, although all reoviruses tested induce a cytostatic effect in HCC1937 cells, peak cell viability in r2Reovirus-infected cells is lower when compared to other viruses. Studies have attributed the capacity of reovirus to inhibit cellular DNA synthesis and induce cell death to S1 and M2 gene segments (15-17).

The combination of oncolytic viruses with radiotherapy and chemotherapeutic drugs, including carboplatin, docetaxel, and paclitaxel, has proven more successful than administration of virus alone in a variety of clinical trials (https://clinicaltrials.gov)(18-21); consequently, we attempted to identify small-molecule inhibitors that enhance the oncolytic potential of reovirus. A high-throughput screen assessing the effect of small molecules from NIH Clinical Collections I and II (NCC) on reovirus infectivity identified four topoisomerase inhibitors (doxorubicin, epirubicin, etoposide, and topotecan) that significantly enhanced reovirus infectivity. Administered alone as chemotherapeutic treatment, topoisomerase inhibitors cause DNA double-strand breaks during DNA replication, and many cells belonging to the TNBC subtype have a defective DNA double-strand break repair machinery (22). Further testing showed these topoisomerase inhibitors enhanced reovirus infection of MDA-MB-231 cells without altering viral replication. This suggests that

topoisomerase inhibitors positively affect the uptake of viral particles during cell entry, which results in enhanced infectivity and thus cytotoxicity. It is also possible that the additive cytotoxicity observed in MDA-MB-231 cells when both reovirus and topoisomerase inhibitors are present is mediated through the activation of complementary cell death pathways. Additionally, topoisomerase inhibitors did not hinder reovirus induction of type III interferon and reovirus did not affect the activation of DNA damage signaling by topoisomerase inhibitors, suggesting an effective combinatorial effect between reovirus and topoisomerase inhibitors. In summary, chapter II shows coinfection and forward genetics in MDA-MB-231 cells can result in reassortant reoviruses with enhanced infectivity and cytotoxicity in TNBC cells. Additionally, the pairing of reassortant viruses with topoisomerase inhibitors is a promising therapeutic against TNBC.

Chapter II demonstrated r2Reovirus by itself and in combination with chemotherapeutic drugs is a potential enhanced therapeutic against triple-negative breast cancer. Extending further studies to non-TNBC cell lines will help elucidate its effectiveness as an oncolytic agent against other types of cancer. Additional studies can include the assessment of synergistic effects of r2Reovirus in combination with chemotherapeutic drugs additional to those tested in chapter II. Results obtained in chapter II increase the knowledge base about the use of forward genetics for the generation of reassortant viruses with enhanced oncolysis in a subset of cancer cells. These methods can be used to obtain novel reassortant reoviruses with enhanced oncolysis in other cancer cell types. Because T1L-T3M2 has shown to induce enhanced cell death in a variety of cell lines, there is a high probability this gene reassortment would be obtained after serial passage in other cells. However, additional mutations or reassortment of additional gene segments might arise. It could be hypothesized that in cells more prone to undergo cell cycle arrest, the S1 gene segment from T3D, which encodes the nonstructural σ1s protein involved in induction of cell cycle arrest, would be selected for (23). Ras signaling suppresses protein kinase R (PKR) function and PKR mediates

activation of IFN-β following recognition of dsRNA during virus infection (24). MDA-MB-231 cells have an upregulated Ras pathway, leading to reduced PKR expression and IFN-β gene induction (25, 26). In cells with a non-mutant Ras, there would be higher PKR activation and type I IFN secretion, so forward genetics in these cells could generate a reassortant reovirus with a μ2 protein-encoding M1 gene segment from T1L, which is more efficient at suppressing type I IFN than T3D μ2 protein (8, 27, 28). Knowledge obtained from chapter II can also be extended to other viruses with reassortment capabilities, such as oncolytic influenza viruses. These novel findings demonstrate forward genetics can provide a better oncolytic and pairing this virus with chemotherapeutic drugs can provide a better, more targeted therapeutic.

The development of r2Reovirus as an enhanced oncolytic therapy against TNBC requires further understanding of the mechanism of cell death induction. Understanding of viral and host determinants of reovirus oncolysis is crucial in understanding cytopathic efficiency of the virus in different cancer cells. Additionally, by understanding what viral factors and host targets are involved in reovirus oncolysis, we can make more informed decisions on reovirus-drug pairings for enhanced synergistic effects. Despite many studies seeking to understand reovirus tropism for cancer cells, the inherent preference of reovirus for replicating in transformed cells is not fully understood. Increased permissiveness to reovirus infection, enhancement of various aspects of reovirus replication, and increased reovirus-driven cell death induction has been attributed to increased Ras activity in a variety of cell lines (7, 8, 28-35). However, reovirus can induce Ras-independent cell death and cells transformed in the absence of activated Ras pathways also are susceptible to reovirus oncolysis (36-39). More so, downregulation of major pathways downstream of Ras, such as MAPK/ERK and PI3K/AKT pathways, can result in enhanced reovirus replication and cell death induction (40, 41). MDA-MB-231 cell mutations in *BRAF* (G464V) and *KRAS* (G13D) result in an upregulated Ras pathway and constitutive activation of MAPK/ERK signaling, promoting survival, proliferation, cell

cycle progression, and cell growth (42-44). r2Reovirus downregulates MAPK/ERK signaling in these cells and inhibition of this pathway results in increased r2Reovirus-induced cell death. This effect on the MAPK/ERK pathway was not observed in T1L- or T3D-infected cells.

MAPK/ERK signaling regulates many downstream transcriptional responses to extracellular signals, including growth factors, hormones, cytokines, and environmental stresses. Through this modulation, MAPK/ERK signaling regulates a multitude of cellular functions such as DNA binding, protein stability, cellular localization, transactivation or repression, and nucleosome structure (45). ERK downstream targets are located in both the cytoplasm and nucleus. Two well-known cytoplasmic targets are c-fos and c-jun, that upon dimerization form the Ap-1 complex, translocate to the nucleus, and control multiple cellular processes including differentiation, proliferation, and apoptosis (46). A widely studied nuclear target is the oncogene c-myc. c-myc is involved in transformation of cells by stimulating genes involved in expression of many pro-proliferative genes, including protein biosynthesis, cancer metabolism, transcription factors, and cell cycle genes while inhibiting expression of tumor suppressor genes (47, 48). ERK is a kinase that activates c-fos, c-jun, and c-myc via phosphorylation, so activation of ERK leads to their increased gene expression. Interestingly, even though r2Reovirus infection led to a decrease of p-ERK in MDA-MB-231 cells, infection also resulted in increased mRNA levels of of c-fos, c-jun, and c-myc transcription and a slight increase in Ap-1 protein levels in MDA-MB-231 cells. In MDA-MB-436 cells, no increase was observed in MYC nor Ap-1 protein levels. c-fos, c-jun, and c-myc can be activated by alternate kinases, so the disconnect observed between downregulation of ERK and activation of transcription factors downstream of ERK in MDA-MB-231 cells could be due to activated alternative pathways upon r2Reovirus infection.

Downregulation of MAPK/ERK signaling can lead to apoptosis and reovirus induces programmed cell death by intrinsic and extrinsic apoptosis, autophagy, cell cycle arrest, and

necroptosis in a variety of cell lines (16, 17, 33, 40, 49-58). Infection of MDA-MB-231 cells in the presence of a pan-caspase inhibitor resulted in partial reduction of virus-mediated cytotoxicity, suggesting reovirus utilizes caspases for cell death induction. During canonical reovirus-induced apoptosis, caspase 8 cleaves Bid, leading to translocation of Bid to mitochondria, resulting in mitochondrial membrane permeabilization, cytochrome c release, and caspase 9 activation. Lastly, caspase 9 cleaves caspase 3, leading to its activation and PARP-1 cleavage (1, 15-17, 49, 50, 53, 55, 57, 59-65). In reovirus-infected MDA-MB-231 cells, caspase 9 was significantly activated during infection with T1L and r2Reovirus. However, the mitochondrial membrane potential was not disrupted and cytochrome c was not released. Additionally, none of the viruses tested induced caspase 3/7 activity at any of the assessed time points (1-6 dpi). This suggests serotype 1 reovirus infection elicits a previously unknown role for caspase 9 that does not involve activation of caspase 3. Concordant with lack of caspase 3/7 activation upon reovirus infection, PARP-1 cleavage observed during T1L and r2Reovirus infection resulted in a 70 kD fragment, instead of the 89 kD fragment observed when PARP-1 is cleaved by caspase 3 in cells undergoing apoptosis. Treatment with caspase 3 inhibitor had no effect on the 70 kD PARP-1 fragment observed in reovirus-infected cells. These data suggest PARP-1 is being cleaved in a caspase 3-independent manner in reovirus serotype 1-infected cells. These findings suggest that in MDA-MB-231 cells, reovirus promotes programmed cell death in a non-canonical, caspase 3-independent manner. Calpains, cathepsins, granzyme A and B, and matrix metalloprotease 2 (MMP-2) can proteolytically cleave PARP into fragments of this molecular weight in cells undergoing other types of programmed cell death (66). Inhibitors of Granzyme B and MMP-2 inhibitors have no effect on r2Reovirus induction of cell death, while calpain and cathepsin inhibitors decrease cytotoxicity induction by r2Reovirus. However, calpains and cathepsins are necessary for reovirus entry (1, 64, 67, 68) and their inhibition also results in decreased r2Reovirus infection of MDA-MB-231 cells. These data suggest decreased

cytotoxicity observed in the presence of calpain and cathepsin inhibitors is a result of drug-dependent decreased virus infection. Additionally, cathepsin inhibitor E64d alone resulted in increased viability of uninfected cells. Interestingly, as a cysteine protease inhibitor, treatment with E64d is expected to decrease cell proliferation (69, 70). These results suggest decreased r2Reovirus-induced cytotoxicity observed in the presence of calpain and cathepsin inhibitors might be compromised by other viral and cellular factors.

Viral replication is not necessary for reovirus induction of apoptosis, while necroptosis induction requires newly synthesized viral dsRNA (51, 52, 54, 71). In MDA-MB-231 cells, UV-inactivated T1L and r2Reovirus induce cell death with significantly slower kinetics than replicating T1L and r2Reovirus. These results show replication of T1L and r2Reovirus is necessary for the full cytotoxic effects of serotype 1 infection in these cells. RIPK3 and its substrate MLKL are required for necroptosis induction (51, 52, 54, 72). Inhibition of RIPK3 had no effect on r2Reovirus-induced MDA-MB-231 cell death, suggesting that although replication is required for full induction of MDA-MB-231 cell death, reovirus does not induce necroptosis in these cells. r2Reovirus-infected cells show similar cell cycle progression to that of uninfected cells, showing r2Reovirus does not induce MDA-MB-231 cell cycle arrest.

The lack of apoptosis and necroptosis induction in reovirus-infected cells could be due to lack of specific host factors necessary for induction of these cell death pathways. Even though reovirus does not induce apoptosis in MDA-MB-231 cells, etoposide treatment results in mitochondrial membrane potential disruption, cytochrome c release from the mitochondria, and caspase 3/7 activity that results in an 89 kD PARP-1 cleavage fragment. This shows MDA-MB-231 cells can undergo apoptosis, so the inability of reovirus to induce apoptosis in these cells is reovirus-related. Reovirus relies on tumor necrosis factor (TNF)-associated death-inducing ligand (TRAIL) secretion and activation of nuclear factor kappa-light-chain-enhancer of activated B cells (NF-kB)

activation for apoptosis induction (49, 58, 59). There are conflicting data on secretion and sensitivity or resistance to TRAIL and TRAIL-induced apoptosis in MDA-MB-231 cells (73-78). It is possible the lack of apoptotic signaling during reovirus infection are linked to MDA-MB-231 cells being insensitive to TRAIL. Alternately, it is possible NF-kB is not being secreted in these cells. Because NF-kB is required for apoptosis and necroptosis induction, as well as type I IFN secretion, lack of NF-kB secretion would explain why none of these pathways are activated during reovirus infection of MDA-MB-231 cells (ref).

r2Reovirus, but not T1L or T3D, displays an inhibitory effect on etoposide-induced caspase 3/7 activity in a replication-dependent manner. Additionally, MDA-MB-231 cells infection with UV-inactivated reoviruses resulted in a faint 89 kD cleavage, indicative of caspase 3 cleavage. These data suggest non-replicating reovirus induces activation of caspase 3/7, albeit to a small extent, upon cell entry and inhibition of caspase 3/7 activity is observed once reovirus undergoes replication. Interestingly, caspase 3 knockout in MDA-MB-231 cells resulted in decreased cell death induction by T1L, T3D, and r2Reovirus. This suggests inhibition of caspase 3 is necessary for r2Reovirus cell death induction of MDA-MB-231 cells. Several viruses exploit host cell caspases to facilitate viral replication (79-82) and reovirus recruits a variety of host proteins to viral factories (83-87). Reovirus could be recruiting caspase 3 to viral factories to aid in replication. Viral protein synthesis and expression of μ1 is required to block cell death induction in other cells (54). In MDA-MB-231 cells, newly synthesized viral proteins could be necessary for the inhibition of caspase 3/7, resulting in unconventional cell death.

MDA-MB-436 cells are TNBC cells belonging to the MSL subtype. Caspase dependency, mitochondrial membrane potential disruption, and an increase in caspase 3/7 activity in r2Reovirus-infected MDA-MB-436 cells suggests the reassortant reovirus induces canonical apoptosis in these cells. r2Reovirus also disrupted mitochondrial membrane potential and induced caspase 3/7 activity

in HeLa cells. Caspase 3-dependent cell death in HeLa and MDA-MB-436 cells, in contrast to caspase 3-independent cell death in MDA-MB-231 cells, shows the mechanism of cell death induced by r2Reovirus is host cell-dependent. These results along with observations from chapter II, in which r2Reovirus induced cell death with enhanced kinetics in both MDA-MB-231 and MDA-MB-436 cells, suggest r2Reovirus can affect cell viability with enhanced kinetics, albeit by different mechanisms, independent of cell heterogeneity. These properties make r2Reovirus a versatile therapeutic. r2Reovirus inhibits cellular proliferation pathways and has a cytopathic effect in MDA-MB-231 and MDA-MB-436 cells. Both cell lines belong to the MSL subtype and are heavily dependent on enriched proliferation genes (88). Alternately, r2Reovirus has a cytostatic effect in BL1 subtype HCC1937 cells, which have deficient DNA damage repair due to a 5382C insertion mutation in the *BRCA1* gene and a S168A silencing mutation in the *MDC1* gene (89). *BRCA1*-deficient breast cancer cell lines are resistant to MEK inhibitors (90). The inability of 2Reovirus to induce cell death in HCC1937 cells could be due to the resistance of this cell line to inhibitors of proliferative signaling. Additionally, the S168A silencing mutation in the *MDC1* gene has been linked to less apoptosis induction (91). However, r2Reovirus infection might be initiating a cellular stress response which causes HCC1937 cells to halt cellular proliferation and undergo cell cycle arrest. Although the MDA-MB-436 cells also have a mutation in *BRCA1*, the dependency of this cell line on proliferation genes might make it more susceptible to the anti-proliferative effects of r2Reovirus. Knowing it can mold its cytopathic (as seen in MDA-MB-231 and MDA-MB-436 cells) or cytostatic (as seen in HCC1937 cells) effects to the genetic background of the infected cell makes this reassortant reovirus a good prospective oncolytic against different types of cancer.

Understanding viral determinants necessary for enhanced oncolysis is crucial for the development of a more targeted therapeutic. Reassortment of gene segments between different reovirus serotypes results in viruses with enhanced infective and cytotoxic properties in different cell

lines (1, 10, 17, 92-94). This raises the possibility of creating an oncolytic virus with enhanced killing kinetics to traditional, lab adapted, reovirus strains. As discussed in chapter II, r2Reovirus is a T1L reovirus with a T3D M2 gene segment and several synonymous and nonsynonymous point mutations. Studies performed with recombinant viruses T1L-T3M2 and T3D-T1M2 mapped enhanced oncolysis of r2Reovirus to the T3D M2 gene segment in a T1L virus. T1L-T3M2 induced cell death with similar kinetics as r2Reovirus in MDA-MB-231 and MDA-MB-436 cells, which shows T3D M2 in an otherwise T1L virus is sufficient for enhanced cell death induction of r2Reovirus and that other mutations present in this virus have little or no effect as it relates to cytotoxicity. Furthermore, r2Reovirus and T1L-T3M2 resulted in similar inhibition of etoposide-induced caspase 3/7 activity. These data show the T3D M2 gene segment in an otherwise T1L virus is sufficient for inhibition of caspase 3/7 activity in MDA-MB-231 cells and enhanced cell death induction in both MSL TNBC cell lines studied. The lack of inhibition of caspase 3/7 activity and enhancement of cell death induction by T3D suggests an epistatic effect of the T3D M2 gene segment with one or more T1L gene segments.

The novel genetic composition of r2Reovirus could inform future studies on viral factors that promote enhanced infection and killing of transformed cells. Further studies on the novel function of the μ1 protein in inhibiting caspase 3 will aid in understanding the mechanism by which this protein, by itself or through interactions with other proteins, blocks caspase 3 activity. Additional studies are also needed to understand the importance and implications of caspase 3 inhibition in reovirus cell death induction in TNBC cells. Because this is a replication-dependent effect, it is possible a reduction in caspase 3/7 activity is observed after caspase 3 is recruited to viral factories as replication aid. This would also explain why caspase 3 knockout results in ablation of reovirus-induced cell death. Alternately, reovirus might need to block initial low levels of apoptosis being induced upon reovirus entry for it to be able to induce a replication-dependent non-

conventional cell death. Lastly, while r2Reovirus does not induce MDA-MB-231 cell death by apoptosis, cell cycle arrest nor necroptosis, it induces apoptosis in MDA-MB-436 cells and has a cytostatic effect in HCC1937 cells. Understanding the mechanisms by which r2Reovirus induces cytopathic or cytostatic effects in these TNBC cells will greatly aid in the identification of host cell factors necessary for reovirus induction of cell death in TNBC cells.

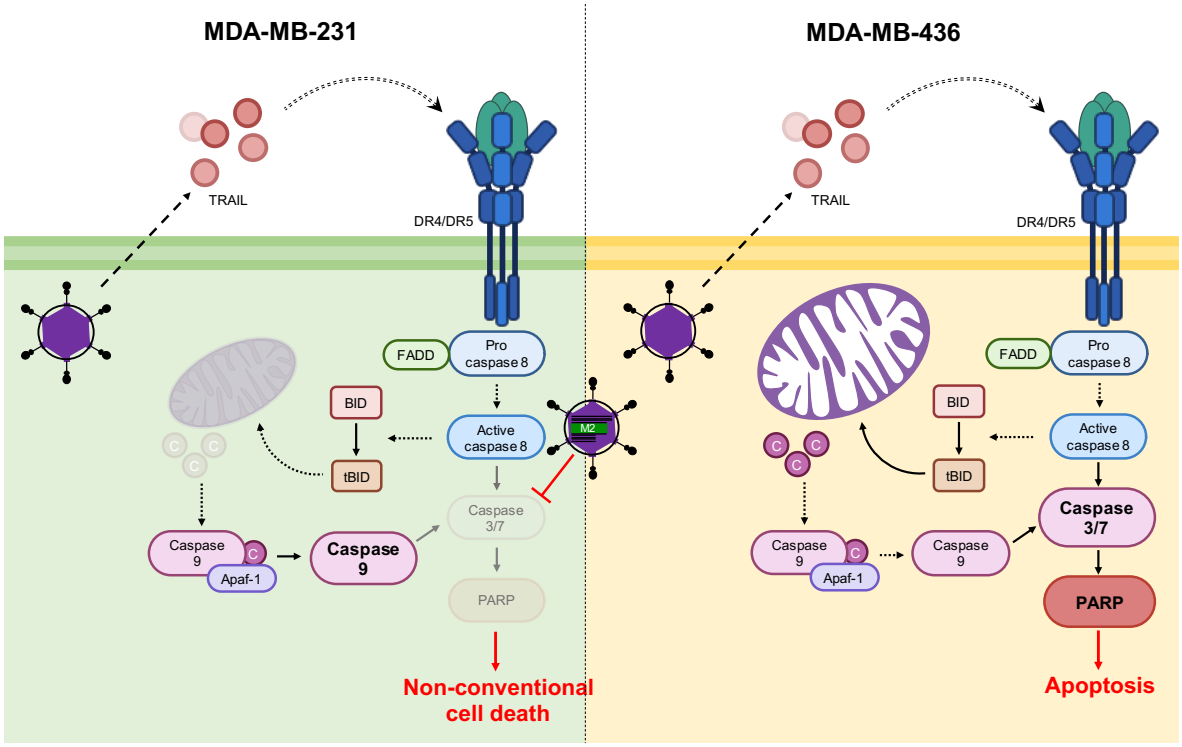

Fig. 1. r2Reovirus induces caspase-dependent, caspase 3-independent non-conventional cell death in MDA-MB-231 cells, while inducing caspase 3-dependent apoptosis in MDA-MB-436 cells. r2Reovirus induces cell death in MDA-MB-231 cells independent of mitochondrial membrane potential disruption, cytochrome c release, and caspase 3/7 activity. r2Reovirus infection results in activation of caspase 9, but μ1-dependent inhibition of caspase 3/7 activity in these cells and differential PARP cleavage. In MDA-MB-436 cells, r2Reovirus elicits mitochondrial membrane potential disruption and caspase 3/7 activation, resulting in apoptosis induction. Faded images are

pathway components that are not observed, dotted lines are unknown portions of the pathway, and enlarged bolded proteins and organelles are observed in r2Reovirus cell death induction of that cell line.

Chapter III demonstrated r2Reovirus can induce non-conventional cell death in a caspase-dependent, caspase 3-independent manner in some cells, while inducing conventional apoptosis in other cells of the same TNBC subtype. Additionally, it suggests an unknown role for caspase 9 independent of caspase 3 activation. Interestingly, r2Reovirus induces enhanced cytopathic or cytostatic effects compared to parental reoviruses in all cell lines tested, albeit by different mechanisms. Further studies assessing what host factors drive r2Reovirus induction of cell death will help evaluate the oncolytic potential of reovirus in different cancer cell types. Additionally, understanding the mechanism by which reovirus induces cell death in different cells will aid in the identification of drugs that synergize cell death by inhibiting distinct cell proliferative pathways or inducing parallel cell death pathways.

Chapter III also mapped reovirus oncolytic efficacy to the T3D M2 gene segment and found a novel role for this gene segment in blocking caspase 3/7 activity in a replication-dependent manner. This gene segment is implicated in apoptosis induction in a variety of cell lines and, to our knowledge, this is the first time it has been shown to be involved in inhibiting caspase 3/7 activity. Further studies incorporating the nonsynonymous mutations present in r2Reovirus into a T1L virus in the presence and absence of the T3D M2 gene segment might shed light on the role and importance of genetic mutations present in r2Reovirus. Understanding the impact of independent viral components on different aspects of reovirus biology in TNBC cells is necessary for the development of a more targeted and enhanced oncolytic virus. Increased caspase 3/7 activity following r2Reovirus infection in HCC1937, HeLa S3, L929, and MDA-MB-436 suggests the

caspase 3/7 inhibitory effect observed during r2Reovirus infection is specific to MDA-MB-231 cells. More studies are needed to assess the purpose and implications of caspase 3/7 activity inhibition and its link to enhanced reovirus oncolysis. The fact that r2Reovirus blocks caspase 3, but does not induce cell death in MDA-MB-231 caspase 3-/- cells raises questions on the importance of this protease in reovirus infectivity and induction of cell death of MDA-MB-231 cells.

r2Reovirus enhanced cytotoxicity in both MDA-MB-231 cells and MDA-MB-436 cells, while it blocked caspase 3/7 activity in MDA-MB-231 cells but induced caspase 3/7 activity in MDA-MB-436 cells, suggesting there might be a disconnect between inhibition of caspase 3/7 activity and enhanced r2Reovirus-driven induction of cell death. Because the T3D M2 gene segment is linked to both caspase 3/7 activity inhibition and enhancement of cell death, this raises the question of μ1's role in driving enhancement of virus-driven cell death in both cell lines. Together, knowledge of what host and viral factors determine the extent and mode of reovirus cell death induction can be exploited to engineer viruses that more specifically target host factors of interest. Once all viral factors and their roles in conferring enhanced oncolysis in different cell lines are elucidated, r2Reovirus can be used as a model for engineering viruses with enhanced cytotoxic effects in cells with specific genomic mutations.

The goal of these studies was to make a more targeted and efficacious therapeutic against TNBC and understand viral and cellular factors involved in enhanced oncolysis. These studies demonstrate the possibility of generating reoviruses with unique infective and cytotoxic properties by forward genetics following coinfection with reoviruses of three different serotypes. Additionally, we identified topoisomerase inhibitors as a class of drugs that enhances infection and the cytotoxic properties of reovirus in the context of TNBC. This study shows pairing reassortant reoviruses generated by forward genetics with topoisomerase inhibitors is a promising therapeutic against TNBC. This knowledge can lead to future projects studying the combinatorial effects of different

drugs with reassortant reoviruses. For combinatorial therapeutics to be effective, it is necessary to understand host and viral factors involved in cell death induction, and how these can complement drug targeting of specific host cell factors. A second study identified a non-conventional caspase-dependent, caspase 3-independent r2Reovirus-induced cell death mechanism in TNBC cells and mapped the enhanced cytopathic properties of this reassortant reovirus in TNBC cells to an epistatic effect of the T3D M2 gene in a T1L virus. These studies show that understanding the interplay between the host cell environment and the genetic composition of oncolytic viruses is crucial for the development of improved viral oncolytics. Additional studies of how reassortant reoviruses target and kill TNBC cells will further improve our understanding of host mechanisms and viral components used by reovirus to impair TNBC cell growth. In summary, we engineered reassortant reovirus with enhanced non-canonical, cell-dependent oncolytic properties in TNBC cells that map to specific viral factors. Results from these and future studies will result in an improved viral oncolytic therapeutic that will provide better quality of life and survival prognosis for TNBC patients.

References

1. Sherry TSDJSLPB. 2013. Orthoreoviruses. Fields Virology, 6th Edition 2.
2. Bouziat R, Hinterleitner R, Brown JJ, Stencel-Baerenwald JE, Ikizler M, Mayassi T, Meisel M, Kim SM, Discepolo V, Pruijssers AJ, Ernest JD, Iskarpatyoti JA, Costes LM, Lawrence I, Palanski BA, Varma M, Zurenski MA, Khomandiak S, McAllister N, Aravamudhan P, Boehme KW, Hu F, Samsom JN, Reinecker HC, Kupfer SS, Guandalini S, Semrad CE, Abadie V, Khosla C, Barreiro LB, Xavier RJ, Ng A, Dermody TS, Jabri B. 2017. Reovirus infection triggers inflammatory responses to dietary antigens and development of celiac disease. Science 356:44-50.
3. Tai JH, Williams JV, Edwards KM, Wright PF, Crowe JE, Jr., Dermody TS. 2005. Prevalence of reovirus-specific antibodies in young children in Nashville, Tennessee. J Infect Dis 191:1221-4.
4. Ouattara LA, Barin F, Barthez MA, Bonnaud B, Roingeard P, Goudeau A, Castelnau P, Vernet G, Paranhos-Baccala G, Komurian-Pradel F. 2011. Novel human reovirus isolated from children with acute necrotizing encephalopathy. Emerg Infect Dis 17:1436-44.
5. Duncan MR, Stanish SM, Cox DC. 1978. Differential sensitivity of normal and transformed human cells to reovirus infection. J Virol 28:444-9.
6. Kemp V, Hoeben RC, van den Wollenberg DJ. 2015. Exploring Reovirus Plasticity for Improving Its Use as Oncolytic Virus. Viruses 8.
7. Coffey MC, Strong JE, Forsyth PA, Lee PW. 1998. Reovirus therapy of tumors with activated Ras pathway. Science 282:1332-4.
8. Strong JE, Coffey MC, Tang D, Sabinin P, Lee PW. 1998. The molecular basis of viral oncolysis: usurpation of the Ras signaling pathway by reovirus. EMBO J 17:3351-62.
9. Sabin AB. 1959. Reoviruses. A new group of respiratory and enteric viruses formerly classified as ECHO type 10 is described. Science 130:1387-9.
10. Thete D, Snyder AJ, Mainou BA, Danthi P. 2016. Reovirus mu1 Protein Affects Infectivity by Altering Virus-Receptor Interactions. J Virol 90:10951-10962.
11. Ebert DH, Deussing J, Peters C, Dermody TS. 2002. Cathepsin L and cathepsin B mediate reovirus disassembly in murine fibroblast cells. J Biol Chem 277:24609-17.
12. Yin HL, Wu CC, Lin CH, Chai CY, Hou MF, Chang SJ, Tsai HP, Hung WC, Pan MR, Luo CW. 2016. beta1 Integrin as a Prognostic and Predictive Marker in Triple-Negative Breast Cancer. Int J Mol Sci 17.
13. Al-Bahlani SM, Al-Rashdi RM, Kumar S, Al-Sinawi SS, Al-Bahri MA, Shalaby AA. 2017. Calpain-1 Expression in Triple-Negative Breast Cancer: A Potential Prognostic Factor Independent of the Proliferative/Apoptotic Index. Biomed Res Int 2017:9290425.
14. Tryfonopoulos D, Walsh S, Collins DM, Flanagan L, Quinn C, Corkery B, McDermott EW, Evoy D, Pierce A, O'Donovan N, Crown J, Duffy MJ. 2011. Src: a potential target for the treatment of triple-negative breast cancer. Ann Oncol 22:2234-40.
15. Connolly JL, Barton ES, Dermody TS. 2001. Reovirus binding to cell surface sialic acid potentiates virus-induced apoptosis. J Virol 75:4029-39.
16. Tyler KL, Squier MK, Rodgers SE, Schneider BE, Oberhaus SM, Grdina TA, Cohen JJ, Dermody TS. 1995. Differences in the capacity of reovirus strains to induce apoptosis are determined by the viral attachment protein sigma 1. J Virol 69:6972-9.
17. Tyler KL, Squier MK, Brown AL, Pike B, Willis D, Oberhaus SM, Dermody TS, Cohen JJ. 1996. Linkage between reovirus-induced apoptosis and inhibition of cellular DNA synthesis: role of the S1 and M2 genes. J Virol 70:7984-91.

18. Rajani K, Parrish C, Kottke T, Thompson J, Zaidi S, Ilett L, Shim KG, Diaz RM, Pandha H, Harrington K, Coffey M, Melcher A, Vile R. 2016. Combination Therapy With Reovirus and Anti-PD-1 Blockade Controls Tumor Growth Through Innate and Adaptive Immune Responses. Mol Ther 24:166-74.
19. Comins C, Spicer J, Protheroe A, Roulstone V, Twigger K, White CM, Vile R, Melcher A, Coffey MC, Mettinger KL, Nuovo G, Cohn DE, Phelps M, Harrington KJ, Pandha HS. 2010. REO-10: a phase I study of intravenous reovirus and docetaxel in patients with advanced cancer. Clin Cancer Res 16:5564-72.
20. Karapanagiotou EM, Roulstone V, Twigger K, Ball M, Tanay M, Nutting C, Newbold K, Gore ME, Larkin J, Syrigos KN, Coffey M, Thompson B, Mettinger K, Vile RG, Pandha HS, Hall GD, Melcher AA, Chester J, Harrington KJ. 2012. Phase I/II trial of carboplatin and paclitaxel chemotherapy in combination with intravenous oncolytic reovirus in patients with advanced malignancies. Clin Cancer Res 18:2080-9.
21. Clements D, Helson E, Gujar SA, Lee PW. 2014. Reovirus in cancer therapy: an evidence-based review. Oncolytic Virother 3:69-82.
22. Coussy F, El-Botty R, Chateau-Joubert S, Dahmani A, Montaudon E, Leboucher S, Morisset L, Painsec P, Sourd L, Huguet L, Nemati F, Servely JL, Larcher T, Vacher S, Briaux A, Reyes C, La Rosa P, Lucotte G, Popova T, Foidart P, Sounni NE, Noel A, Decaudin D, Fuhrmann L, Salomon A, Reyal F, Mueller C, Ter Brugge P, Jonkers J, Poupon MF, Stern MH, Bieche I, Pommier Y, Marangoni E. 2020. BRCAness, SLFN11, and RB1 loss predict response to topoisomerase I inhibitors in triple-negative breast cancers. Sci Transl Med 12.
23. Poggioli GJ, Keefer C, Connolly JL, Dermody TS, Tyler KL. 2000. Reovirus-induced G(2)/M cell cycle arrest requires sigma1s and occurs in the absence of apoptosis. J Virol 74:9562-70.
24. Schulz O, Pichlmair A, Rehwinkel J, Rogers NC, Scheuner D, Kato H, Takeuchi O, Akira S, Kaufman RJ, Reis e Sousa C. 2010. Protein kinase R contributes to immunity against specific viruses by regulating interferon mRNA integrity. Cell Host Microbe 7:354-61.
25. McAllister CS, Taghavi N, Samuel CE. 2012. Protein kinase PKR amplification of interferon beta induction occurs through initiation factor eIF-2alpha-mediated translational control. J Biol Chem 287:36384-92.
26. Smith KD, Mezhir JJ, Bickenbach K, Veerapong J, Charron J, Posner MC, Roizman B, Weichselbaum RR. 2006. Activated MEK suppresses activation of PKR and enables efficient replication and in vivo oncolysis by Deltagamma(1)34.5 mutants of herpes simplex virus 1. J Virol 80:1110-20.
27. Rudd P, Lemay G. 2005. Correlation between interferon sensitivity of reovirus isolates and ability to discriminate between normal and Ras-transformed cells. J Gen Virol 86:1489-97.
28. Gong J, Mita MM. 2014. Activated ras signaling pathways and reovirus oncolysis: an update on the mechanism of preferential reovirus replication in cancer cells. Front Oncol 4:167.
29. Norman KL, Hirasawa K, Yang AD, Shields MA, Lee PW. 2004. Reovirus oncolysis: the Ras/RalGEF/p38 pathway dictates host cell permissiveness to reovirus infection. Proc Natl Acad Sci U S A 101:11099-104.
30. Marcato P, Shmulevitz M, Pan D, Stoltz D, Lee PW. 2007. Ras transformation mediates reovirus oncolysis by enhancing virus uncoating, particle infectivity, and apoptosis-dependent release. Mol Ther 15:1522-30.
31. Phillips MB, Stuart JD, Rodriguez Stewart RM, Berry JT, Mainou BA, Boehme KW. 2018. Current understanding of reovirus oncolysis mechanisms. Oncolytic Virother 7:53-63.

32. Shmulevitz M, Pan LZ, Garant K, Pan D, Lee PW. 2010. Oncogenic Ras promotes reovirus spread by suppressing IFN-beta production through negative regulation of RIG-I signaling. Cancer Res 70:4912-21.
33. Maitra R, Seetharam R, Tesfa L, Augustine TA, Klampfer L, Coffey MC, Mariadason JM, Goel S. 2014. Oncolytic reovirus preferentially induces apoptosis in KRAS mutant colorectal cancer cells, and synergizes with irinotecan. Oncotarget 5:2807-19.
34. Kelly KR, Espitia CM, Mahalingam D, Oyajobi BO, Coffey M, Giles FJ, Carew JS, Nawrocki ST. 2012. Reovirus therapy stimulates endoplasmic reticular stress, NOXA induction, and augments bortezomib-mediated apoptosis in multiple myeloma. Oncogene 31:3023-38.
35. Garant KA, Shmulevitz M, Pan L, Daigle RM, Ahn DG, Gujar SA, Lee PW. 2016. Oncolytic reovirus induces intracellular redistribution of Ras to promote apoptosis and progeny virus release. Oncogene 35:771-82.
36. Song L, Ohnuma T, Gelman IH, Holland JF. 2009. Reovirus infection of cancer cells is not due to activated Ras pathway. Cancer Gene Ther 16:382.
37. Twigger K, Roulstone V, Kyula J, Karapanagiotou EM, Syrigos KN, Morgan R, White C, Bhide S, Nuovo G, Coffey M, Thompson B, Jebar A, Errington F, Melcher AA, Vile RG, Pandha HS, Harrington KJ. 2012. Reovirus exerts potent oncolytic effects in head and neck cancer cell lines that are independent of signalling in the EGFR pathway. BMC Cancer 12:368.
38. Simon EJ, Howells MA, Stuart JD, Boehme KW. 2017. Serotype-Specific Killing of Large Cell Carcinoma Cells by Reovirus. Viruses 9.
39. Thirukkumaran CM, Shi ZQ, Luider J, Kopciuk K, Gao H, Bahlis N, Neri P, Pho M, Stewart D, Mansoor A, Morris DG. 2012. Reovirus as a viable therapeutic option for the treatment of multiple myeloma. Clin Cancer Res 18:4962-72.
40. Hwang CC, Igase M, Okuda M, Coffey M, Noguchi S, Mizuno T. 2019. Reovirus changes the expression of anti-apoptotic and proapoptotic proteins with the c-kit downregulation in canine mast cell tumor cell lines. Biochem Biophys Res Commun 517:233-237.
41. Tian J, Zhang X, Wu H, Liu C, Li Z, Hu X, Su S, Wang LF, Qu L. 2015. Blocking the PI3K/AKT pathway enhances mammalian reovirus replication by repressing IFN-stimulated genes. Front Microbiol 6:886.
42. Hollestelle A, Elstrodt F, Nagel JH, Kallemeijn WW, Schutte M. 2007. Phosphatidylinositol-3-OH kinase or RAS pathway mutations in human breast cancer cell lines. Mol Cancer Res 5:195-201.
43. Yao Z, Torres NM, Tao A, Gao Y, Luo L, Li Q, de Stanchina E, Abdel-Wahab O, Solit DB, Poulikakos PI, Rosen N. 2015. BRAF Mutants Evade ERK-Dependent Feedback by Different Mechanisms that Determine Their Sensitivity to Pharmacologic Inhibition. Cancer Cell 28:370-83.
44. Occhi G, Barollo S, Regazzo D, Bertazza L, Galuppini F, Guzzardo V, Jaffrain-Rea ML, Vianello F, Ciato D, Ceccato F, Watutantrige-Fernando S, Bisognin A, Bortoluzzi S, Pennelli G, Boscaro M, Scaroni C, Mian C. 2015. A constitutive active MAPK/ERK pathway due to BRAFV600E positively regulates AHR pathway in PTC. Oncotarget 6:32104-14.
45. Whitmarsh AJ. 2007. Regulation of gene transcription by mitogen-activated protein kinase signaling pathways. Biochim Biophys Acta 1773:1285-98.
46. Ameyar M, Wisniewska M, Weitzman JB. 2003. A role for AP-1 in apoptosis: the case for and against. Biochimie 85:747-52.
47. Eilers M, Eisenman RN. 2008. Myc's broad reach. Genes Dev 22:2755-66.

48. Miller DM, Thomas SD, Islam A, Muench D, Sedoris K. 2012. c-Myc and cancer metabolism. Clin Cancer Res 18:5546-53.
49. Connolly JL, Rodgers SE, Clarke P, Ballard DW, Kerr LD, Tyler KL, Dermody TS. 2000. Reovirus-induced apoptosis requires activation of transcription factor NF-kappaB. J Virol 74:2981-9.
50. Clarke P, Debiasi RL, Goody R, Hoyt CC, Richardson-Burns S, Tyler KL. 2005. Mechanisms of reovirus-induced cell death and tissue injury: role of apoptosis and virus-induced perturbation of host-cell signaling and transcription factor activation. Viral Immunol 18:89-115.
51. Berger AK, Danthi P. 2013. Reovirus activates a caspase-independent cell death pathway. MBio 4:e00178-13.
52. Berger AK, Hiller BE, Thete D, Snyder AJ, Perez E, Jr., Upton JW, Danthi P. 2017. Viral RNA at Two Stages of Reovirus Infection Is Required for the Induction of Necroptosis. J Virol 91.
53. Danthi P, Hansberger MW, Campbell JA, Forrest JC, Dermody TS. 2006. JAM-A-independent, antibody-mediated uptake of reovirus into cells leads to apoptosis. J Virol 80:1261-70.
54. Roebke KE, Danthi P. 2019. Cell Entry-Independent Role for the Reovirus mu1 Protein in Regulating Necroptosis and the Accumulation of Viral Gene Products. J Virol 93.
55. Boehme KW, Hammer K, Tollefson WC, Konopka-Anstadt JL, Kobayashi T, Dermody TS. 2013. Nonstructural protein sigma1s mediates reovirus-induced cell cycle arrest and apoptosis. J Virol 87:12967-79.
56. Igase M, Shibutani S, Kurogouchi Y, Fujiki N, Hwang CC, Coffey M, Noguchi S, Nemoto Y, Mizuno T. 2019. Combination Therapy with Reovirus and ATM Inhibitor Enhances Cell Death and Virus Replication in Canine Melanoma. Mol Ther Oncolytics 15:49-59.
57. Holm GH, Zurney J, Tumilasci V, Leveille S, Danthi P, Hiscott J, Sherry B, Dermody TS. 2007. Retinoic acid-inducible gene-I and interferon-beta promoter stimulator-1 augment proapoptotic responses following mammalian reovirus infection via interferon regulatory factor-3. J Biol Chem 282:21953-61.
58. Hansberger MW, Campbell JA, Danthi P, Arrate P, Pennington KN, Marcu KB, Ballard DW, Dermody TS. 2007. IkappaB kinase subunits alpha and gamma are required for activation of NF-kappaB and induction of apoptosis by mammalian reovirus. J Virol 81:1360-71.
59. Clarke P, Meintzer SM, Gibson S, Widmann C, Garrington TP, Johnson GL, Tyler KL. 2000. Reovirus-induced apoptosis is mediated by TRAIL. J Virol 74:8135-9.
60. Iordanov MS, Ryabinina OP, Schneider P, Magun BE. 2005. Two mechanisms of caspase 9 processing in double-stranded RNA- and virus-triggered apoptosis. Apoptosis 10:153-66.
61. Rodgers SE, Barton ES, Oberhaus SM, Pike B, Gibson CA, Tyler KL, Dermody TS. 1997. Reovirus-induced apoptosis of MDCK cells is not linked to viral yield and is blocked by Bcl-2. J Virol 71:2540-6.
62. Beckham JD, Tuttle KD, Tyler KL. 2010. Caspase-3 activation is required for reovirus-induced encephalitis in vivo. J Neurovirol 16:306-17.
63. Danthi P, Pruijssers AJ, Berger AK, Holm GH, Zinkel SS, Dermody TS. 2010. Bid regulates the pathogenesis of neurotropic reovirus. PLoS Pathog 6:e1000980.
64. Kominsky DJ, Bickel RJ, Tyler KL. 2002. Reovirus-induced apoptosis requires both death receptor- and mitochondrial-mediated caspase-dependent pathways of cell death. Cell Death Differ 9:926-33.

65. Kominsky DJ, Bickel RJ, Tyler KL. 2002. Reovirus-induced apoptosis requires mitochondrial release of Smac/DIABLO and involves reduction of cellular inhibitor of apoptosis protein levels. J Virol 76:11414-24.
66. Chaitanya GV, Steven AJ, Babu PP. 2010. PARP-1 cleavage fragments: signatures of cell-death proteases in neurodegeneration. Cell Commun Signal 8:31.
67. Danthi P, Holm GH, Stehle T, Dermody TS. 2013. Reovirus receptors, cell entry, and proapoptotic signaling. Adv Exp Med Biol 790:42-71.
68. DeBiasi RL, Edelstein CL, Sherry B, Tyler KL. 2001. Calpain inhibition protects against virus-induced apoptotic myocardial injury. J Virol 75:351-61.
69. Murray EJ, Grisanti MS, Bentley GV, Murray SS. 1997. E64d, a membrane-permeable cysteine protease inhibitor, attenuates the effects of parathyroid hormone on osteoblasts in vitro. Metabolism 46:1090-4.
70. Jung M, Lee J, Seo HY, Lim JS, Kim EK. 2015. Cathepsin inhibition-induced lysosomal dysfunction enhances pancreatic beta-cell apoptosis in high glucose. PLoS One 10:e0116972.
71. Clarke P, Meintzer SM, Moffitt LA, Tyler KL. 2003. Two distinct phases of virus-induced nuclear factor kappa B regulation enhance tumor necrosis factor-related apoptosis-inducing ligand-mediated apoptosis in virus-infected cells. J Biol Chem 278:18092-100.
72. Degterev A, Huang Z, Boyce M, Li Y, Jagtap P, Mizushima N, Cuny GD, Mitchison TJ, Moskowitz MA, Yuan J. 2005. Chemical inhibitor of nonapoptotic cell death with therapeutic potential for ischemic brain injury. Nat Chem Biol 1:112-9.
73. Aroui S, Brahim S, Hamelin J, De Waard M, Breard J, Kenani A. 2009. Conjugation of doxorubicin to cell penetrating peptides sensitizes human breast MDA-MB 231 cancer cells to endogenous TRAIL-induced apoptosis. Apoptosis 14:1352-65.
74. Butler LM, Liapis V, Bouralexis S, Welldon K, Hay S, Thai le M, Labrinidis A, Tilley WD, Findlay DM, Evdokiou A. 2006. The histone deacetylase inhibitor, suberoylanilide hydroxamic acid, overcomes resistance of human breast cancer cells to Apo2L/TRAIL. Int J Cancer 119:944-54.
75. Lagadec C, Adriaenssens E, Toillon RA, Chopin V, Romon R, Van Coppenolle F, Hondermarck H, Le Bourhis X. 2008. Tamoxifen and TRAIL synergistically induce apoptosis in breast cancer cells. Oncogene 27:1472-7.
76. Melendez ME, Silva-Oliveira RJ, Silva Almeida Vicente AL, Rebolho Batista Arantes LM, Carolina de Carvalho A, Epstein AL, Reis RM, Carvalho AL. 2018. Construction and characterization of a new TRAIL soluble form, active at picomolar concentrations. Oncotarget 9:27233-27241.
77. Rahman M, Davis SR, Pumphrey JG, Bao J, Nau MM, Meltzer PS, Lipkowitz S. 2009. TRAIL induces apoptosis in triple-negative breast cancer cells with a mesenchymal phenotype. Breast Cancer Res Treat 113:217-30.
78. Park C, Moon DO, Ryu CH, Choi B, Lee W, Kim GY, Choi Y. 2008. Beta-sitosterol sensitizes MDA-MB-231 cells to TRAIL-induced apoptosis. Acta Pharmacol Sin 29:341-8.
79. Galvan V, Brandimarti R, Roizman B. 1999. Herpes simplex virus 1 blocks caspase-3-independent and caspase-dependent pathways to cell death. J Virol 73:3219-26.
80. Richard A, Tulasne D. 2012. Caspase cleavage of viral proteins, another way for viruses to make the best of apoptosis. Cell Death Dis 3:e277.
81. Tabtieng T, Degterev A, Gaglia MM. 2018. Caspase-Dependent Suppression of Type I Interferon Signaling Promotes Kaposi's Sarcoma-Associated Herpesvirus Lytic Replication. J Virol 92.
82. Connolly PF, Fearnhead HO. 2017. Viral hijacking of host caspases: an emerging category of pathogen-host interactions. Cell Death Differ 24:1401-1410.

83. Kaufer S, Coffey CM, Parker JS. 2012. The cellular chaperone hsc70 is specifically recruited to reovirus viral factories independently of its chaperone function. J Virol 86:1079-89.
84. Stanifer ML, Kischnick C, Rippert A, Albrecht D, Boulant S. 2017. Reovirus inhibits interferon production by sequestering IRF3 into viral factories. Sci Rep 7:10873.
85. Tenorio R, Fernandez de Castro I, Knowlton JJ, Zamora PF, Lee CH, Mainou BA, Dermody TS, Risco C. 2018. Reovirus sigmaNS and muNS Proteins Remodel the Endoplasmic Reticulum to Build Replication Neo-Organelles. mBio 9.
86. Fernandez de Castro I, Zamora PF, Ooms L, Fernandez JJ, Lai CM, Mainou BA, Dermody TS, Risco C. 2014. Reovirus forms neo-organelles for progeny particle assembly within reorganized cell membranes. mBio 5.
87. Parker JS, Broering TJ, Kim J, Higgins DE, Nibert ML. 2002. Reovirus core protein mu2 determines the filamentous morphology of viral inclusion bodies by interacting with and stabilizing microtubules. J Virol 76:4483-96.
88. Lehmann BD, Bauer JA, Chen X, Sanders ME, Chakravarthy AB, Shyr Y, Pietenpol JA. 2011. Identification of human triple-negative breast cancer subtypes and preclinical models for selection of targeted therapies. J Clin Invest 121:2750-67.
89. Martinez-Outschoorn UE, Balliet R, Lin Z, Whitaker-Menezes D, Birbe RC, Bombonati A, Pavlides S, Lamb R, Sneddon S, Howell A, Sotgia F, Lisanti MP. 2012. BRCA1 mutations drive oxidative stress and glycolysis in the tumor microenvironment: implications for breast cancer prevention with antioxidant therapies. Cell Cycle 11:4402-13.
90. Gu Y, Helenius M, Vaananen K, Bulanova D, Saarela J, Sokolenko A, Martens J, Imyanitov E, Kuznetsov S. 2016. BRCA1-deficient breast cancer cell lines are resistant to MEK inhibitors and show distinct sensitivities to 6-thioguanine. Sci Rep 6:28217.
91. Jungmichel S, Stucki M. 2010. MDC1: The art of keeping things in focus. Chromosoma 119:337-49.
92. Thete D, Danthi P. 2018. Protein Mismatches Caused by Reassortment Influence Functions of the Reovirus Capsid. J Virol 92.
93. Snyder AJ, Wang JC, Danthi P. 2019. Components of the Reovirus Capsid Differentially Contribute to Stability. J Virol 93.
94. Danthi P, Kobayashi T, Holm GH, Hansberger MW, Abel TW, Dermody TS. 2008. Reovirus apoptosis and virulence are regulated by host cell membrane penetration efficiency. J Virol 82:161-72.

Chapter V: Appendix

Attachment, infection, and cytostatic effect of reovirus on HCC1937 cells

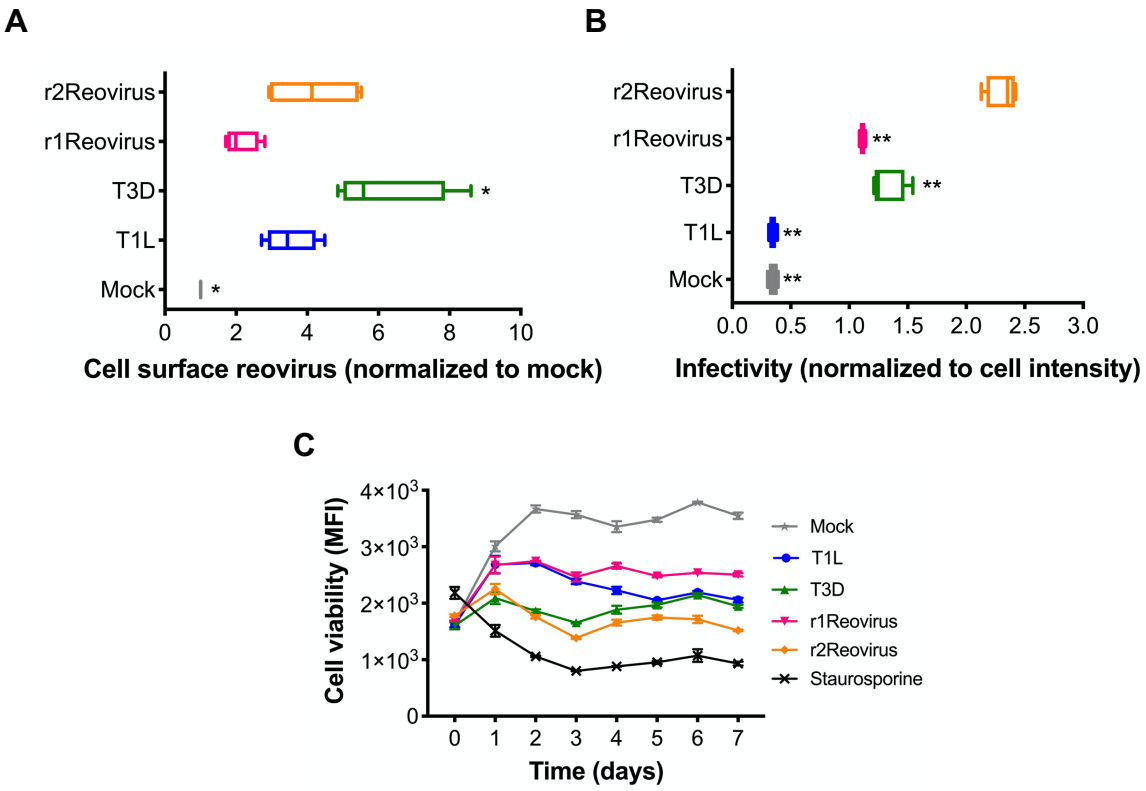

FIG 1. Attachment, infection, and cytostatic effect of reovirus on HCC1937 cells. A) HCC1937 cells were adsorbed with A633-labeled T1L, T3D, r1Reovirus or r2Reovirus at an MOI of 5×10^4 particles/cell and assessed for cell surface reovirus by flow cytometry. Results are expressed as box-and-whisker plots of cell surface reovirus mean fluorescence intensities (MFI) for quadruplicate independent experiments. B) Cells were adsorbed with T1L, T3D, r1Reovirus or r2Reovirus at an MOI of 25 PFU/cell and assessed for infectivity after 18 h by indirect immunofluorescence using reovirus-specific antiserum. C) Cells were adsorbed with T1L, T3D, r1Reovirus or r2Reovirus at an MOI of 500 PFU/cell or treated with 1 μM staurosporine and cell viability was assessed 0-7 dpi. Results are presented as MFI and SEM for three independent experiments. *, $P = 0.02$, ** P <

0.0001, in comparison to A) T1L and B) r2Reovirus, as determined by one-way ANOVA with Tukey's multiple-comparison test.

HCC1937 cells are a TNBC cell line belonging to the BL1 subtype. Mutations found in HCC1937 cells confer an enrichment of cell cycle and cell division components (14). Both reassortant viruses have similar attachment efficiency as T1L, while T3D has slightly higher attachment efficiency than all other reoviruses tested (Fig. 1A). r2Reovirus displays enhanced infectivity in HCC1937 cells, while r1Reovirus infects with similar kinetics as T3D and they all have enhanced infectivity when compared to T1L (Fig. 1B). These data show a disconnect between attachment and infection of reassortant viruses. Additionally, they show genetic reassortment and/or mutations present in r2Reovirus confer enhanced infective properties in HCC1937 cells compared to r1Reovirus. Different to cytopathic effects observed in reovirus-infected MDA-MB-231, MDA-MB-436, and L929 cells, all reoviruses tested induce a cytostatic effect in HCC1937 cells. However, peak cell viability in T3D and r2Reovirus-infected cells is lower when compared to other viruses. Cytostatic effects in HCC1937 cells could be driven by enrichment of cell cycle and cell division components in these cells. Reovirus induces cell cycle arrest in various cells lines (4, 168, 211, 286). Together, these data show genetic alterations found in reassortant viruses have no effect in attachment of these viruses to HCC1937 cells, while genetic reassortment and/or mutations present in r2Reovirus confer enhanced infectivity compared to all reoviruses tested and enhanced cytostatic properties similar to T3D in HCC1937 cells.

r2Reovirus induces enhanced caspase 3-dependent cell death in HeLa cells

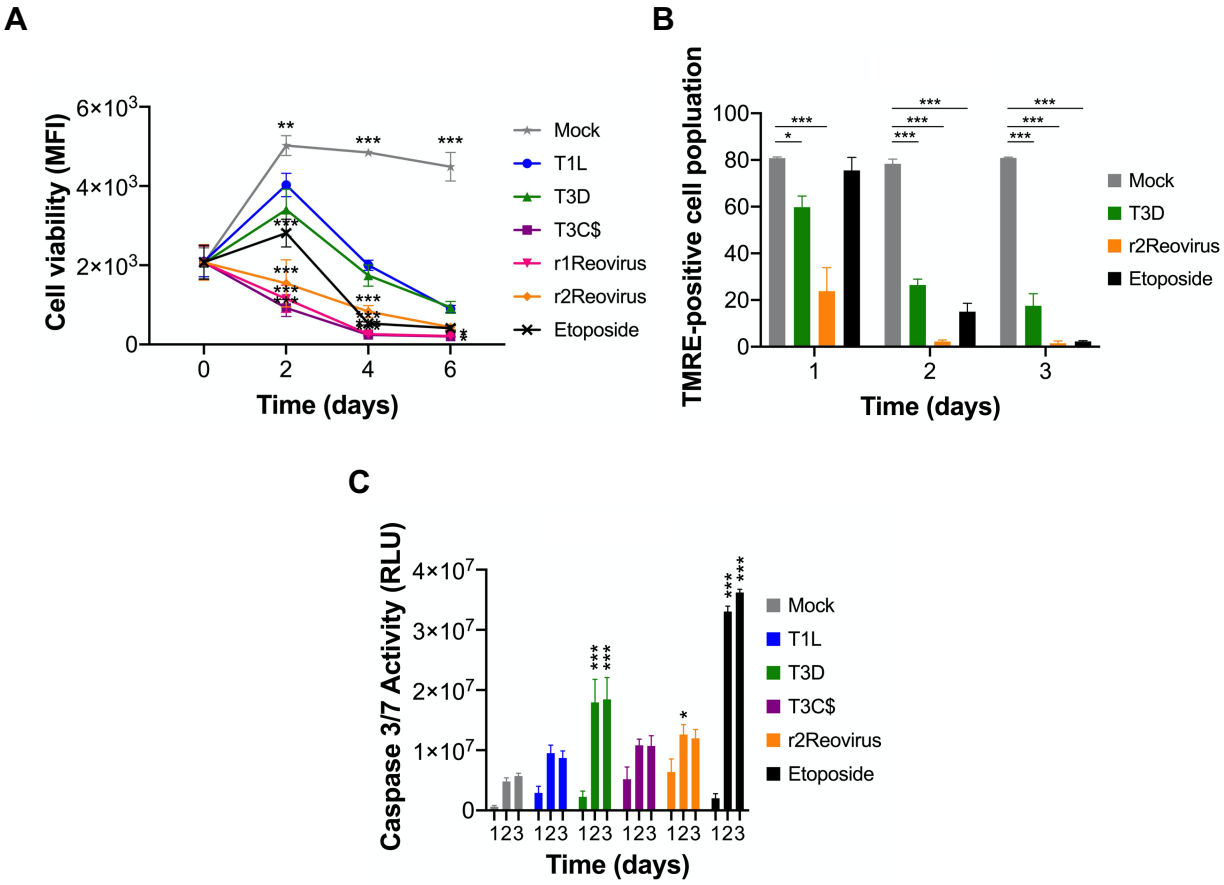

FIG 2. r2Reovirus induces enhanced caspase 3-dependent cell death in HeLa cells. A) HeLa cells were adsorbed with T1L, T3D, T3C$, r1Reovirus or r2Reovirus at an MOI of 500 PFU/cell or treated with 50 μM etoposide and cell viability was assessed at the times shown. Results are presented as MFI and SEM for four independent experiments. B) HeLa cells were adsorbed with mock, T3D or r2Reovirus for 1 h at an MOI of 500 PFU/cell or treated with 50 μM etoposide and assessed for levels of tetramethylrhodamine, ethyl ester (TMRE) by flow cytometry at times shown. Results are presented as the percentage of TMRE-positive cells and SEM for four independent experiments. C) HeLa cells were infected with mock, T1L, T3D, T3C$ or r2Reovirus at an MOI of 500 PFU/cell or treated with 50 μM etoposide for 1 h. Caspase 3/7 activity was measured at times shown in relative luminometer units (RLU) and SEM for three independent experiments. *, $P \leq$

0.03; **, $P = 0.0002$; ***, $P < 0.0001$ in comparison to A) r2Reovirus, B) mock, and C) T1L, as determined by two-way ANOVA with Tukey's multiple-comparison test.

Reovirus induction of apoptosis in HeLa cells requires intrinsic and extrinsic apoptosis factors, including disrupting mitochondrial membrane potential and induction of caspase 3/7 activity (4, 186, 287). To assess the cytotoxic effect of the reassortant reoviruses in these cells, HeLa cells were adsorbed with mock or reovirus or treated with etoposide and cell viability was assessed for 6 days. r1Reovirus and r2Reovirus induce cell death with similar kinetics to current oncolytic strain T3C$ and faster kinetics than parental T1L and T3D. To test the ability of reovirus to disrupt the mitochondrial membrane potential in HeLa cells, cells were adsorbed with mock, T3D or r2Reovirus or treated with etoposide and assessed for TMRE levels by flow cytometry at 1-3 dpi. r2Reovirus infection resulted in mitochondrial membrane disruption at a faster rate than T3D infection and etoposide treatment, with significant mitochondrial membrane potential disruption at 1 dpi. By 3 dpi, all three treatments had significantly disrupted mitochondrial membrane potential. To test if reovirus induces caspase 3/7 activity in HeLa cells, cells were infected with mock or reovirus or treated with etoposide and caspase 3/7 activity was measured 1-3 dpi. Infection with all reoviruses tested and etoposide treatment resulted in an increase in caspase 3/7 activity compared to mock as early as 2 dpi. Interestingly, although r2Reovirus induced cell death and disrupted the mitochondrial membrane potential with faster kinetics, T3D induced significantly more caspase 3/7 activity than other viruses tested by day 2 and 3 pi. Together, these results show that reassortant reoviruses induce cell death with faster kinetics than parental reoviruses and that infection of HeLa cells with parental and reassortant reoviruses result in mitochondria and caspase 3-dependent apoptosis induction.

Transcription factors downstream of ERK are upregulated in r2Reovirus-infected cells

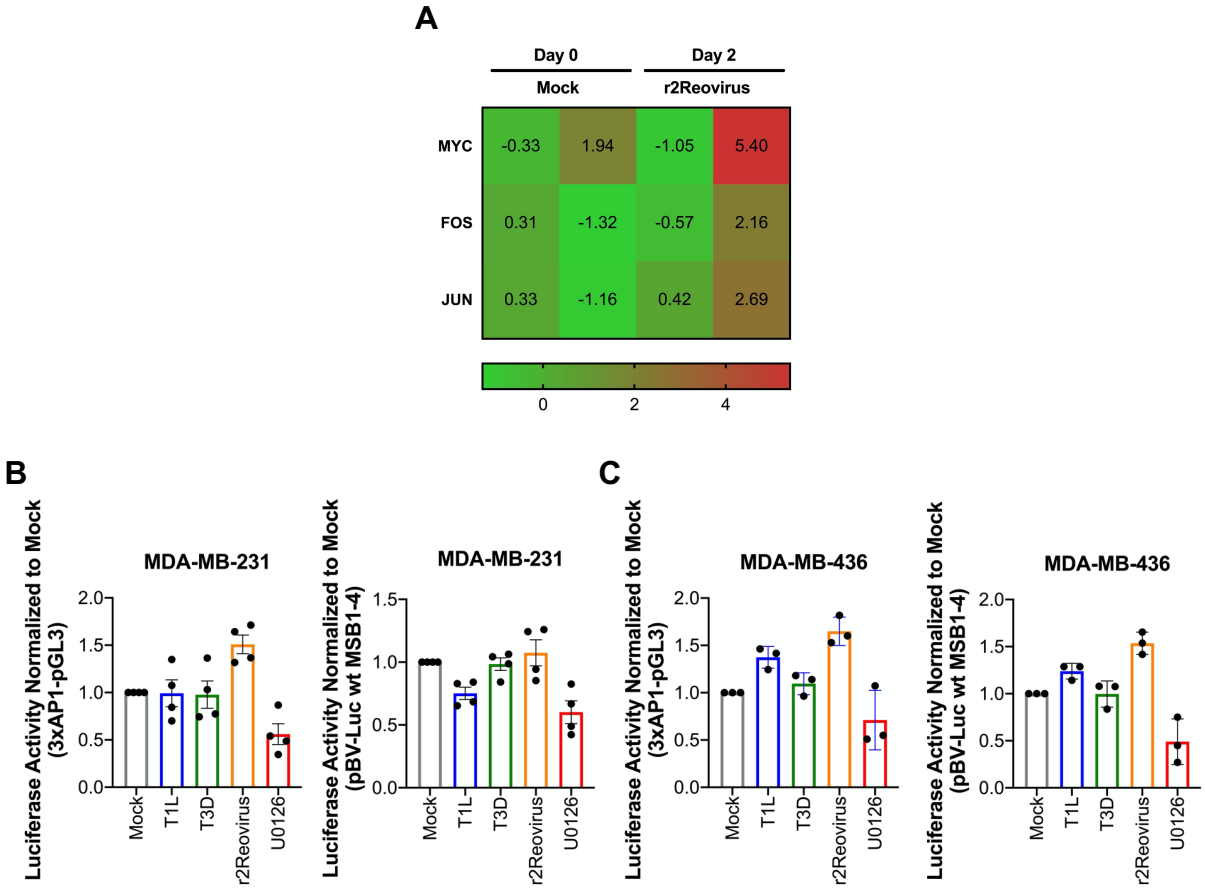

FIG 3. Transcription factors downstream of ERK are upregulated in r2Reovirus-infected cells. A) MDA-MB-231 cells were infected with mock or r2Reovirus at an MOI of 500 PFU/cell or for 1 h. RNA was isolated at times shown and mRNA was measured by NanoString Breast Cancer (BC) 360 panel. B) MDA-MB-231 and C) MDA-MB-436 cells were infected with mock, T1L, T3D or r2Reovirus at an MOI of 500 PFU/cell or treated with 10 μM U0126 for 1 h. AP1 and MYC activity were measured 2 dpi in luciferase activity and SEM for four (MDA-MB-231 cells) and three (MDA-MB-436 cells) independent experiments.

The MAPK/ERK pathway regulates many downstream transcriptional responses to extracellular signals, including growth factors, hormones, cytokines, and environmental stresses.

Through this mediation, they regulate a multitude of cellular functions such as DNA binding, protein stability, cellular localization, transactivation or repression, and nucleosome structure (274). In chapter III, we showed r2Reovirus downregulates MAPK/ERK signaling, so we tested the effect of r2Reovirus infection on downstream factors of ERK. ERK downstream targets are located in both, the cytoplasm and nucleus. Two well-known cytoplasmic targets are c-fos and c-jun, that upon dimerization form the Activator Protein-1 (Ap-1) complex, translocate to the nucleus, and initiate transcription of genes involved in proliferation, differentiation, and cell death (288). A widely studied nuclear target is c-myc, a transcription factor that activates expression of many pro-proliferative genes (289). Activation of ERK leads to an increased expression of c-fos, c-jun, and c-myc mRNA. Interestingly, even though r2Reovirus infection led to a decrease of p-ERK in MDA-MB-231 cells, it led to an increase of c-fos, c-jun, and c-myc transcription (Fig. 3A) and a slight increase in Ap-1 protein levels in MDA-MB-231 cells (Fig. 3B). In MDA-MB-436 cells, no increase was observed in MYC nor Ap-1 protein levels (Fig. 3C). c-fos and c-jun activation can be induced by a variety of stimuli (290, 291). The activity of c-fos is regulated post-translationally through phosphorylation by ERK, cdc2, PKA or PKC (292-294). c-jun can be autoregulated by its own product, Jun, or through phosphorylation by ERK or the Jun N-terminal kinase (JNK) pathway (295, 296). c-myc is activated upon various mitogenic signals such as serum stimulation or by wingless-activated (Wnt), Sonic hedgehog (Shh) or MAPK/ERK signaling (289, 297, 298). Since these transcription factors can be activated by a variety of kinases, the disconnect observed between downregulation of ERK and activation of transcription factors downstream of ERK could be due to activated alternate pathways upon r2Reovirus infection.

Inhibition of RIPK3 has no effect on cell death induction by r2Reovirus in MDA-MB-231 cells

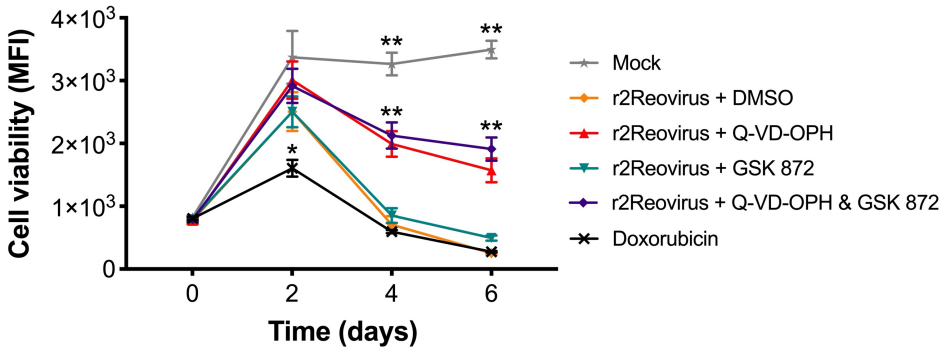

FIG 4. Inhibition of RIPK3 has no effect on cell death induction by r2Reovirus in MDA-MB-231 cells. MDA-MB-231 cells were treated for 1 h with vehicle (DMSO) or 3 μM R1PK3 inhibitor GSK872 or 25 μM caspase inhibitor Q-VD-OPH and adsorbed with r2Reovirus at an MOI of 500 PFU/ml or treated with 10 μM doxorubicin for 1 h. Cell viability was assessed at times shown. Results are presented as mean fluorescence intensity (MFI) and SEM for four independent experiments. *, $P = 0.008$; *, $P < 0.0001$ in comparison to r2Reovirus, as determined by two-way ANOVA with Tukey's multiple-comparison test.

The two major mechanisms of reovirus cell death induction are apoptosis and necroptosis (4, 102, 103, 164-168, 172, 179, 282, 299). Necroptosis, a caspase-independent cell death requiring the induction of RIPK3 and MLKL-dependent necroptosis, can occur in cells where apoptosis has been inhibited (166, 167, 172, 191). Induction of cell death by necroptosis was tested through inhibition of RIPK3 using GSK 872 in the presence and absence of Q-VD-OPH. Addition of GSK872 had no effect in r2Reovirus induction of cell death and combinatorial treatment of GSK 872 and Q-VD-OPH had similar effect to Q-VD-OPH treatment alone. These results suggest r2Reovirus is not inducing necroptosis in these cells.

r2Reovirus is not inducing cell cycle arrest in MDA-MB-231 cells

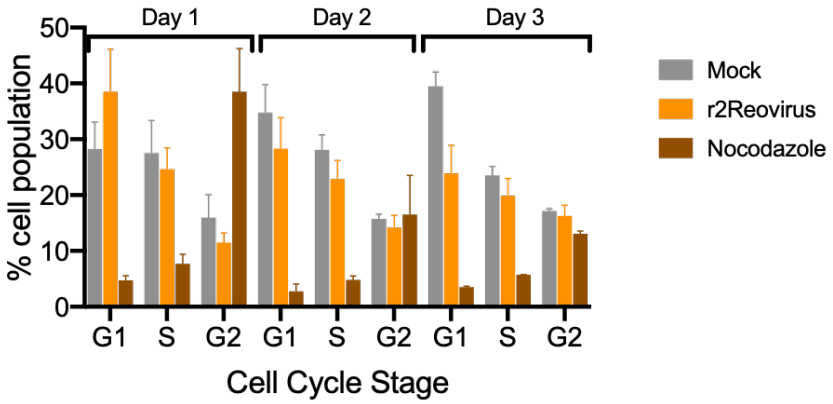

FIG 5. r2Reovirus does not induce cell cycle arrest in MDA-MB-231 cells. MDA-MB-231 cells were adsorbed with r2Reovirus at an MOI of 500 PFU/ml or treated with 1 μg/ml nocodazole for 1 h. Cell cycle was assessed by propidium iodide stain at times shown. Results are presented as mean fluorescence intensity (MFI) and SEM for four independent experiments.

The cell cycle is composed of interphase (G_1, S, and G_2 phases), followed by the mitotic phase (mitosis and cytokinesis), and G_0 phase. Reovirus infection can lead to cell cycle arrest during the G_1 phase and G_2/M phase of the cell cycle and disruption of the mitotic spindle apparatus, resulting in inhibition of cellular proliferation (4, 211). T3D induces cell cycle arrest to a greater extent than T1L in a variety of cell lines, a characteristic that segregates with the S1 gene segment (286). To assess if r2Reovirus induces cell cycle arrest in MDA-MB-231 cells, cells were infected with mock or r2Reovirus or treated with nocodazole and cell cycle progression was assessed 1-3 dpi. Cells treated with nocodazole were primarily in the G_2 phase starting at day 1 and throughout the days tested, while r2Reovirus-infected cells showed a similar cell cycle progression to that of uninfected (mock) cells. These results show that while nocodazole induces cell cycle arrest at the G_2 phase in these cells at 1dpi, r2Reovirus does not induce cell cycle arrest throughout any of the days tested.

Reovirus does not induce caspase 3/7 activity at later time points in MDA-MB-231 cells

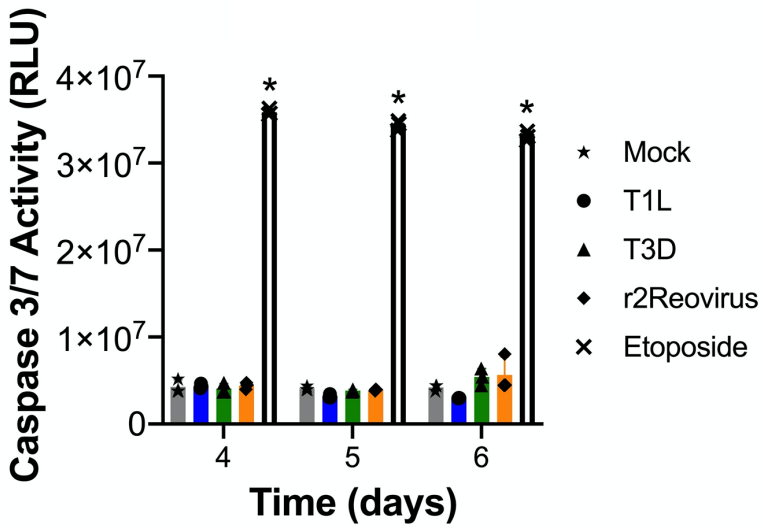

FIG 6. Reovirus does not induce caspase 3/7 activity at later time points in MDA-MB-231 cells. MDA-MB-231 cells were infected with mock, T1L, T3D, T3C$ or r2Reovirus at an MOI of 500 PFU/cell or treated with 50 μM etoposide for 1 h. Caspase 3/7 activity was measured at times shown in relative luminometer units (RLU) and SD for one experiment. *, $P < 0.0001$ in comparison to mock, as determined by two-way ANOVA with Tukey's multiple-comparison test.

Data from chapter III show caspase 3/7 activity was not observed in reovirus-infected MDA-MB-231 cells infected at 1-3 dpi. To determine if caspase 3 is activated during reovirus infection at later times, MDA-MB-231 cells were infected with mock, T1L, T3D, T3C$ or r2Reovirus or treated with etoposide and caspase 3/7 activity was assessed 4-6 dpi. These data indicate that while etoposide can activate caspase 3/7 activity in MDA-MB-231 cells, none of the viruses tested activate caspase 3/7 at later time points of infection. Taken together with results from chapter III, these results show reovirus does not activate caspase 3/7 at any point during infection. These results further suggest r2Reovirus cell death induction is caspase 3-independent.

Inhibition of caspase 3 does not affect PARP-1 cleavage

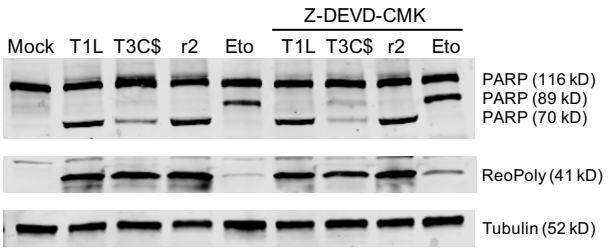

FIG 7. Inhibition of caspase 3 does not affect reovirus-induced PARP-1 cleavage. MDA-MB-231 cells were treated with vehicle (DMSO) or 25 μM caspase 3 inhibitor Z-DEVD-CMK and infected with mock, T1L, T3C$ or r2Reovirus (r2) at an MOI of 500 PFU/cell or treated with 50 μM etoposide. PARP-1 cleavage was assessed by western blot. Whole cell lysates were collected at 2 dpi, resolved by SDS-PAGE, and immunoblotted with antibodies specific for PARP-1, reovirus, and tubulin.

To assess if PARP-1 cleavage observed during reovirus infection is caspase 3-dependent, MDA-MB-231 cells were treated with vehicle (DMSO) or caspase 3 inhibitor Z-DEVD-CMK and infected with mock or reovirus or treated with etoposide. Etoposide treatment resulted in an 89 kD fragment. As seen in chapter III, a PARP-1 cleavage fragment of 70 kD was observed in cells infected with T1L, T3C$, and r2Reovirus. When treated with Z-DEVD-CMK, infection with T1L and r2Reovirus still resulted in a PARP-1 cleavage fragment of 70 kD. Treatment of T3C$-infected cells with Z-DEVD-CMK resulted in two PARP-1 faint bands of 70 and 89 kD. Z-DEVD-CMK treatment had no substantial effect on PARP-1 cleavage in etoposide-treated cells. These results show that inhibition of caspase 3 has no effect on T1L and r2Reovirus-induced PARP-1 cleavage and that inhibition of caspase 3 in T3C$-infected cells results in a slight decrease of PARP-1 cleavage into a 70 kD fragment and a slight increase in an 89 kD PARP-1 cleavage fragment. These data suggest that caspase 3 is not cleaving PARP-1 in serotype 1 reovirus-infected cells.

Effect of inhibitors of PARP-1 proteases on r2Reovirus cell death induction in MDA-MB-231 cells

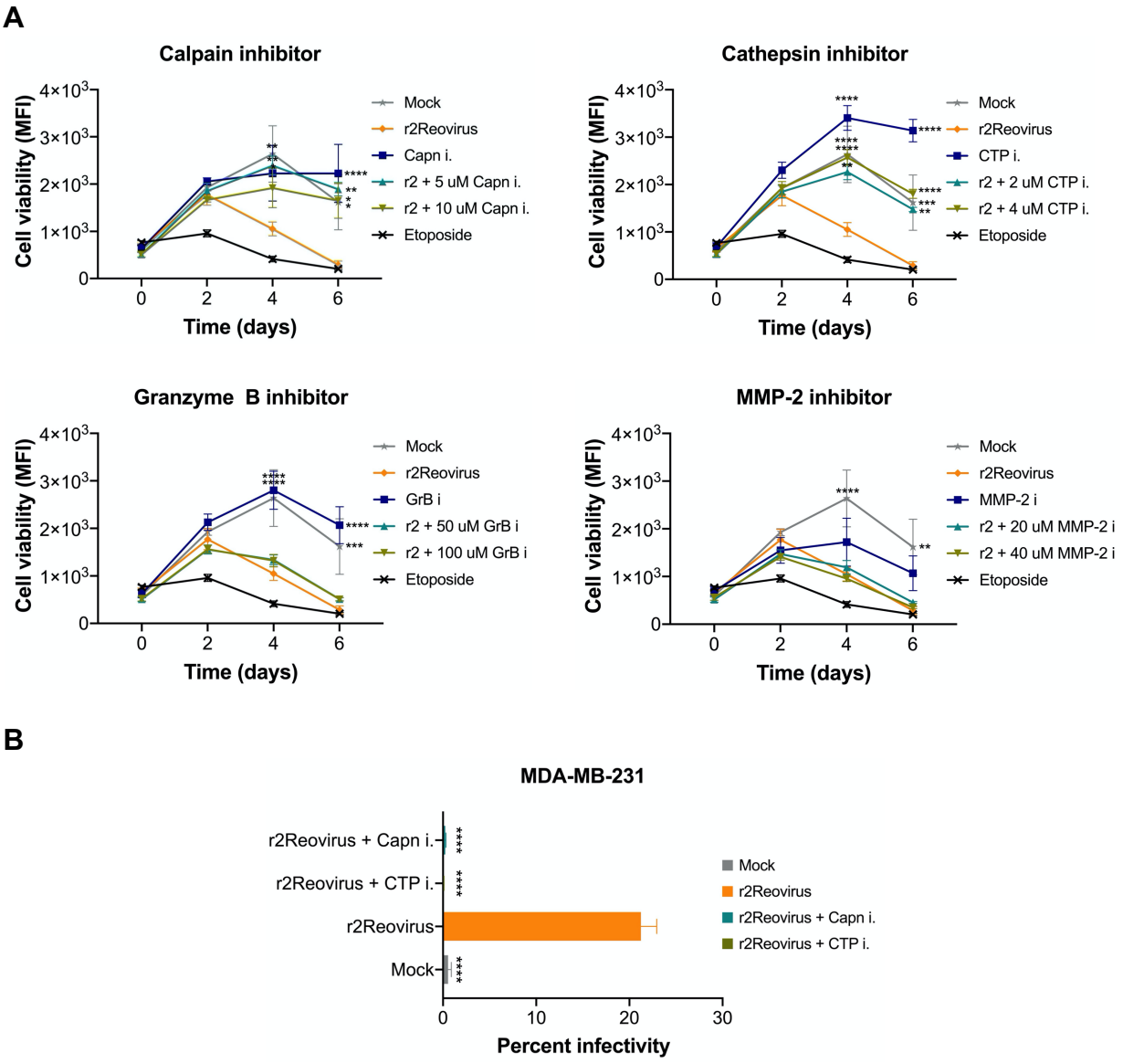

FIG 8. Effect of inhibitors of PARP-1 proteases on r2Reovirus cell death induction in MDA-MB-231 cells. A) MDA-MB-231 cells were treated for 1 h with vehicle (DMSO) or varying concentrations of PARP-1 protease inhibitors calpain (Capn), cathepsin (CTP), granzyme B (GrB), and matrix metalloproteinase-2 (MMP-2) and adsorbed with r2Reovirus at an MOI of 500 PFU/ml or treated with 50 μM etoposide for 1 h. Cell viability was assessed at times shown. Results are

presented as mean fluorescence intensity (MFI) and SEM for four independent experiments. B) MDA-MB-231 cells were treated for 1 h with vehicle (DMSO), 40 μM calpain inhibitor or 4 μM cathepsin inhibitor and adsorbed with r2Reovirus at an MOI of 500 PFU/ml and assessed for infectivity after 18 h by indirect immunofluorescence using reovirus-specific antiserum. Results are expressed as percent infectivity and SEM for three independent experiments. *, $P \leq 0.05$; **, $P = 0.002$; ***, $P \leq 0.0009$; ****, $P \leq 0.0001$ in comparison to r2Reovirus, as determined by A) two-way and B) one-way ANOVA with Tukey's multiple-comparison test.

Calpains, cathepsins, granzyme A and B, and matrix metalloprotease 2 (MMP-2) can proteolytically cleave PARP into fragments ranging from 55-74 kD, similar to that observed during reovirus infection (189). Cells were treated with DMSO or varying concentrations of inhibitors of PARP-1 proteases calpains, cathepsins, granzyme B, and MMP-2 and adsorbed with r2Reovirus or treated with etoposide and tested for cell viability over 6 dpi. Inhibition of calpain significantly decreased r2Reovirus cell death induction by day 6 pi at both concentrations tested. However, calpains are necessary for reovirus entry (4, 187, 278, 279) and inhibition of calpains also results in decreased r2Reovirus infectivity of MDA-MB-231 cells (Fig. 8B). While both concentrations assayed of cathepsin inhibitor E64d resulted in significant decrease of r2Reovirus-induced cell death by day 4 pi, the protease inhibitor alone resulted in increased viability of uninfected cells. Neither Granzyme B nor MMP-2 inhibitors had an effect at any of the concentrations tested on r2Reovirus cell death induction and MMP-2 inhibitor alone decreased cell viability of uninfected cells. These data show inhibitors of Granzyme B and MMP-2 inhibitors have no effect on r2Reovirus induction of cell death, while calpain and E64d inhibitors decrease cytotoxicity induction by r2Reovirus. However, effects observed by calpain and E64d inhibitors might be compromised by other viral and cellular factors.

UV-inactivated reoviruses induce cell death with slower kinetics than replicating reoviruses

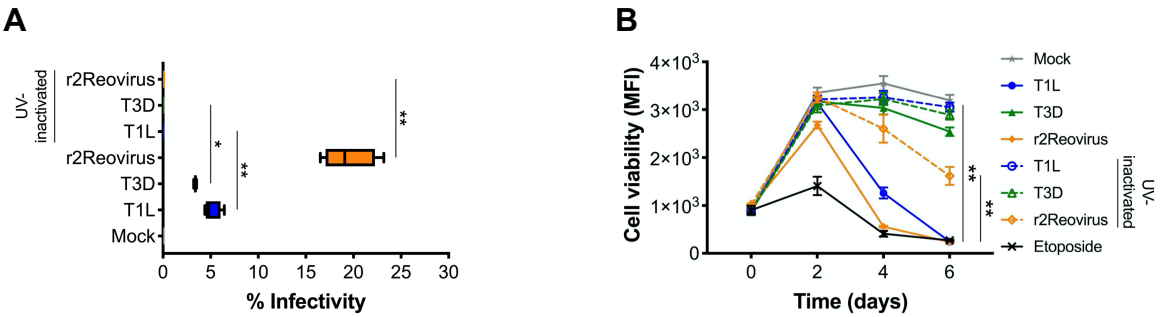

FIG 9. UV-inactivated reoviruses induce cell death with slower kinetics than replicating reoviruses. MDA-MB-231 cells were infected with untreated and UV-inactivated mock, T1L, T3D or r2Reovirus at an MOI of A) 100 PFU/cell or B) 500 PFU/cell or treated with 50 μM etoposide. Cells were assessed for A) infectivity after 18 h by indirect immunofluorescence using reovirus-specific antiserum and B) cell viability at times shown. A) Results are expressed as box-and-whisker plots of percent infectivity. B) Results are presented as mean fluorescence intensity (MFI) and SEM for four independent experiments. Dotted lines represent UV-inactivated viruses. *, $P = 0.005$; **, $P < 0.0001$ as determined by two-way ANOVA with Tukey's multiple-comparison test.

Viral replication is not necessary for reovirus induction of apoptosis, whereas newly synthesized dsRNA is required for reovirus induction of necroptosis (166, 167, 172, 282). UV-inactivation of reoviruses resulted in no infection of MDA-MB-231 cells (Fig. 9A). To assess if replication is necessary for reovirus induction of MDA-MB-231 cell death, cells were infected with mock or untreated and UV-inactivated reovirus or treated with etoposide (Fig. 9B). Results show non-replicating T1L and r2Reovirus induce cell death with significantly slower kinetics than replicating T1L and r2Reovirus. No significant difference was observed in cell viability of T3D-infected cells because T3D does not induce substantial cell death in these cells. These data suggest replication is necessary for the full cytotoxic effects of serotype 1 reovirus infection in these cells.

Differential PARP cleavage in reovirus-infected cells is replication-dependent

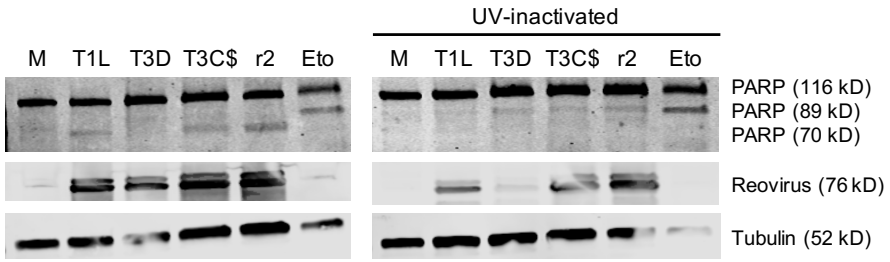

FIG 10. Differential PARP cleavage in reovirus-infected cells is not observed in cells infected with UV-inactivated viruses. MDA-MB-231 cells were adsorbed with untreated or UV-inactivated mock, T1L, T3D, or r2Reovirus (r2) at an MOI of 500 PFU/cell or treated with 50 μM etoposide (eto) for 1 h. Whole cell lysates were collected 2 dpi, resolved by SDS-PAGE, and immunoblotted with antibodies specific for PARP, reovirus, and tubulin.

To assess if differential PARP-1 cleavage observed in chapter III is replication-dependent, cells were infected with mock or untreated and UV-inactivated reovirus or treated with etoposide. Whole cell lysates were collected at 2 dpi and probed for PARP by immunoblot. As previously observed, etoposide treatment resulted in an 89 kDa PARP-1 cleavage fragment and infection with untreated T1L, T3C$, and r2Reovirus resulted in a 70 kDa PARP-1 cleavage fragment while infection with T3D did not result in PARP-1 proteolysis. Infection with UV-inactivated viruses did not result in a 70 kD PARP-1 cleavage fragment. In fact, infection with UV-inactivated T3D, T3C$, and r2Reovirus resulted in a faint 89 kD PARP-1 cleavage fragment. These data suggest that during infection of MDA-MB-231 cells by UV-inactivated viruses, PARP-1 is cleaved to a small extent by caspase 3, which in turn suggest reovirus infection can result in a small extent of apoptosis induction that is blocked upon viral replication.

Knockout of caspase 3 has no effect on reovirus cell death induction

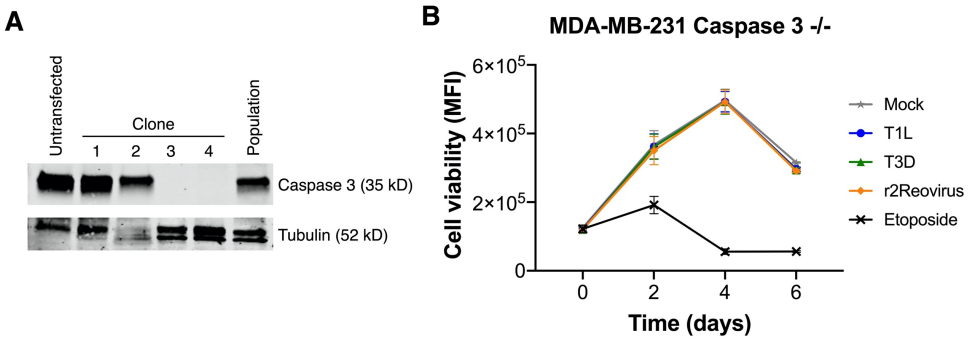

FIG 11. Knockout of caspase 3 has no effect on reovirus cell death induction. A) Caspase 3 was knocked out of MDA-MB-231 cells by CRISPR-Cas9 and assessed for complete knockout by western blot. Whole cell lysates of clones were collected, resolved by SDS-PAGE, and immunoblotted with antibodies specific for caspase 3 and tubulin. B) MDA-MB-231 caspase 3 -/- cells were infected with T1L, T3D, and r2Reovirus at an MOI of 500 PFU/cell or treated with 50 μM etoposide for 1 h. Cell viability was assessed at times shown.

Data from chapter III showed r2Reovirus blocks caspase 3/7 activity in a replication-dependent manner in MDA-MB-231 cells. To test the requirement of caspase 3 in r2Reovirus induction of MDA-MB-231 cells, caspase 3 was ablated in MDA-MB-231 cells by clustered regularly interspaced short palindromic repeats (CRISPR)/CRISPR associated protein 9 (Cas9) (Fig. 11A). MDA-MB-231 Caspase 3-/- cells were infected with mock or reovirus or treated with etoposide and assessed for cell viability over 6 dpi (Fig. 11B). Interestingly, even though r2Reovirus blocks caspase 3/7 activity upon infection, knocking out caspase 3 in MDA-MB-231 cells resulted in decreased cell death induction by all viruses tested. These data suggest caspase 3 is required for reovirus induction of cell death. Several viruses exploit host cell caspases, including caspase 3, to promote viral replication (252-255) and reovirus recruits various host proteins to viral factories (86, 257-260). Reovirus could be recruiting caspase 3 to viral factories to aid in replication.

Caspase inhibition results in decreased replication of r2Reovirus in MDA-MB-231 cells

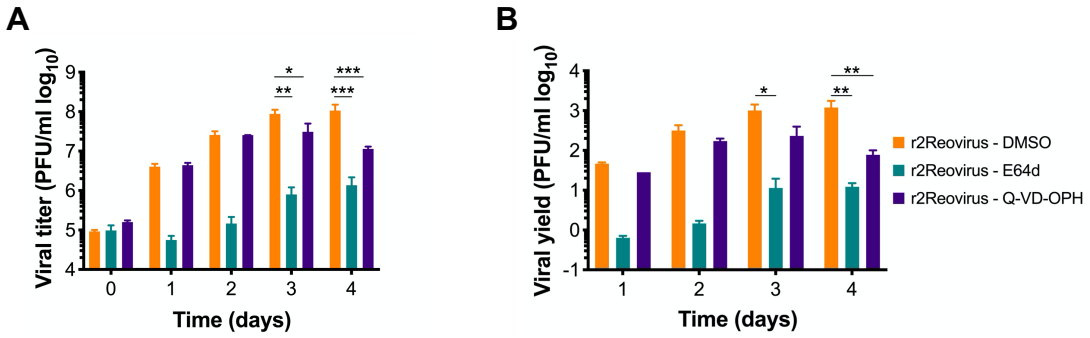

Fig 12. Caspase inhibition results in decreased replication of r2Reovirus in MDA-MB-231 cells. MDA-MB-231 cells were treated with vehicle (DMSO), 4 μM E64d or 25 μM Q-VD-OPH and adsorbed with r2Reovirus at an MOI of 10 PFU/cell, and (A) viral titers and (B) viral yields were determined by a plaque assay on L929 cells at 0 to 4 days post-infection. The results are presented as (A) mean viral titers (± standard errors of the means [SEM]) or (B) mean viral yields (± SEM) compared to values at day 0 post-infection. *, $P \leq 0.02$; **, $P \leq 0.006$; ***, $P \leq 0.0006$ in comparison to DMSO, as determined by two-way ANOVA with Tukey's multiple-comparison test.

Several viruses exploit host cell caspases to promote viral replication (252-255) and reovirus recruits various host proteins to viral factories (86, 257-260). MDA-MB-231 cells were treated with vehicle (DMSO), E64d or Q-VD-OPH and adsorbed with r2Reovirus to assess effect of caspases on viral replication. E64d is a cysteine protease inhibitor and reovirus entry is dependent on proteases, so E64d inhibits reovirus cell entry. By 3 dpi, treatment with E64d resulted in a 2-fold decrease in viral titer when compared to r2Reovirus-infected cells. Treatment with Q-VD-OPH resulted in a less, but significant, 1-fold reduction of replication starting at 3 dpi when compared to r2Reovirus-infected cells. These data show caspase inhibition results in a slight decrease of r2Reovirus replication in MDA-MB-231 cells, albeit at later times and to a lesser extent than inhibition of cysteine proteases.

References

1. Lehmann BD, Bauer JA, Chen X, Sanders ME, Chakravarthy AB, Shyr Y, Pietenpol JA. 2011. Identification of human triple-negative breast cancer subtypes and preclinical models for selection of targeted therapies. J Clin Invest 121:2750-67.
2. Boehme KW, Hammer K, Tollefson WC, Konopka-Anstadt JL, Kobayashi T, Dermody TS. 2013. Nonstructural protein sigma1s mediates reovirus-induced cell cycle arrest and apoptosis. J Virol 87:12967-79.
3. Poggioli GJ, DeBiasi RL, Bickel R, Jotte R, Spalding A, Johnson GL, Tyler KL. 2002. Reovirus-induced alterations in gene expression related to cell cycle regulation. J Virol 76:2585-94.
4. Poggioli GJ, Keefer C, Connolly JL, Dermody TS, Tyler KL. 2000. Reovirus-induced G(2)/M cell cycle arrest requires sigma1s and occurs in the absence of apoptosis. J Virol 74:9562-70.
5. Sherry TSDJSLPB. 2013. Orthoreoviruses. Fields Virology, 6th Edition 2.
6. DeBiasi RL, Robinson BA, Leser JS, Brown RD, Long CS, Clarke P. 2010. Critical role for death-receptor mediated apoptotic signaling in viral myocarditis. J Card Fail 16:901-10.
7. Danthi P, Pruijssers AJ, Berger AK, Holm GH, Zinkel SS, Dermody TS. 2010. Bid regulates the pathogenesis of neurotropic reovirus. PLoS Pathog 6:e1000980.
8. Whitmarsh AJ. 2007. Regulation of gene transcription by mitogen-activated protein kinase signaling pathways. Biochim Biophys Acta 1773:1285-98.
9. Garces de Los Fayos Alonso I, Liang HC, Turner SD, Lagger S, Merkel O, Kenner L. 2018. The Role of Activator Protein-1 (AP-1) Family Members in CD30-Positive Lymphomas. Cancers (Basel) 10.
10. Dang CV. 2012. MYC on the path to cancer. Cell 149:22-35.
11. Hu E, Mueller E, Oliviero S, Papaioannou VE, Johnson R, Spiegelman BM. 1994. Targeted disruption of the c-fos gene demonstrates c-fos-dependent and -independent pathways for gene expression stimulated by growth factors or oncogenes. EMBO J 13:3094-103.
12. Wisdom R, Johnson RS, Moore C. 1999. c-Jun regulates cell cycle progression and apoptosis by distinct mechanisms. EMBO J 18:188-97.
13. Gruda MC, Kovary K, Metz R, Bravo R. 1994. Regulation of Fra-1 and Fra-2 phosphorylation differs during the cell cycle of fibroblasts and phosphorylation in vitro by MAP kinase affects DNA binding activity. Oncogene 9:2537-47.
14. Hurd TW, Culbert AA, Webster KJ, Tavare JM. 2002. Dual role for mitogen-activated protein kinase (Erk) in insulin-dependent regulation of Fra-1 (fos-related antigen-1) transcription and phosphorylation. Biochem J 368:573-80.
15. Rosenberger SF, Finch JS, Gupta A, Bowden GT. 1999. Extracellular signal-regulated kinase 1/2-mediated phosphorylation of JunD and FosB is required for okadaic acid-induced activator protein 1 activation. J Biol Chem 274:1124-30.
16. Angel P, Hattori K, Smeal T, Karin M. 1988. The jun proto-oncogene is positively autoregulated by its product, Jun/AP-1. Cell 55:875-85.
17. Lopez-Bergami P, Huang C, Goydos JS, Yip D, Bar-Eli M, Herlyn M, Smalley KS, Mahale A, Eroshkin A, Aaronson S, Ronai Z. 2007. Rewired ERK-JNK signaling pathways in melanoma. Cancer Cell 11:447-60.
18. Roussel MF, Robinson GW. 2013. Role of MYC in Medulloblastoma. Cold Spring Harb Perspect Med 3.
19. Hsieh AL, Walton ZE, Altman BJ, Stine ZE, Dang CV. 2015. MYC and metabolism on the path to cancer. Semin Cell Dev Biol 43:11-21.

20. Roebke KE, Danthi P. 2019. Cell Entry-Independent Role for the Reovirus mu1 Protein in Regulating Necroptosis and the Accumulation of Viral Gene Products. J Virol 93.
21. Berger AK, Danthi P. 2013. Reovirus activates a caspase-independent cell death pathway. MBio 4:e00178-13.
22. Berger AK, Hiller BE, Thete D, Snyder AJ, Perez E, Jr., Upton JW, Danthi P. 2017. Viral RNA at Two Stages of Reovirus Infection Is Required for the Induction of Necroptosis. J Virol 91.
23. Clarke P, Richardson-Burns SM, DeBiasi RL, Tyler KL. 2005. Mechanisms of apoptosis during reovirus infection. Curr Top Microbiol Immunol 289:1-24.
24. Clarke P, Debiasi RL, Goody R, Hoyt CC, Richardson-Burns S, Tyler KL. 2005. Mechanisms of reovirus-induced cell death and tissue injury: role of apoptosis and virus-induced perturbation of host-cell signaling and transcription factor activation. Viral Immunol 18:89-115.
25. Connolly JL, Rodgers SE, Clarke P, Ballard DW, Kerr LD, Tyler KL, Dermody TS. 2000. Reovirus-induced apoptosis requires activation of transcription factor NF-kappaB. J Virol 74:2981-9.
26. Connolly JL, Dermody TS. 2002. Virion disassembly is required for apoptosis induced by reovirus. J Virol 76:1632-41.
27. Danthi P, Coffey CM, Parker JS, Abel TW, Dermody TS. 2008. Independent regulation of reovirus membrane penetration and apoptosis by the mu1 phi domain. PLoS Pathog 4:e1000248.
28. Danthi P, Kobayashi T, Holm GH, Hansberger MW, Abel TW, Dermody TS. 2008. Reovirus apoptosis and virulence are regulated by host cell membrane penetration efficiency. J Virol 82:161-72.
29. Clarke P, Meintzer SM, Moffitt LA, Tyler KL. 2003. Two distinct phases of virus-induced nuclear factor kappa B regulation enhance tumor necrosis factor-related apoptosis-inducing ligand-mediated apoptosis in virus-infected cells. J Biol Chem 278:18092-100.
30. Degterev A, Huang Z, Boyce M, Li Y, Jagtap P, Mizushima N, Cuny GD, Mitchison TJ, Moskowitz MA, Yuan J. 2005. Chemical inhibitor of nonapoptotic cell death with therapeutic potential for ischemic brain injury. Nat Chem Biol 1:112-9.
31. Chaitanya GV, Steven AJ, Babu PP. 2010. PARP-1 cleavage fragments: signatures of cell-death proteases in neurodegeneration. Cell Commun Signal 8:31.
32. Danthi P, Holm GH, Stehle T, Dermody TS. 2013. Reovirus receptors, cell entry, and proapoptotic signaling. Adv Exp Med Biol 790:42-71.
33. DeBiasi RL, Edelstein CL, Sherry B, Tyler KL. 2001. Calpain inhibition protects against virus-induced apoptotic myocardial injury. J Virol 75:351-61.
34. Kominsky DJ, Bickel RJ, Tyler KL. 2002. Reovirus-induced apoptosis requires both death receptor- and mitochondrial-mediated caspase-dependent pathways of cell death. Cell Death Differ 9:926-33.
35. Galvan V, Brandimarti R, Roizman B. 1999. Herpes simplex virus 1 blocks caspase-3-independent and caspase-dependent pathways to cell death. J Virol 73:3219-26.
36. Richard A, Tulasne D. 2012. Caspase cleavage of viral proteins, another way for viruses to make the best of apoptosis. Cell Death Dis 3:e277.
37. Tabtieng T, Degterev A, Gaglia MM. 2018. Caspase-Dependent Suppression of Type I Interferon Signaling Promotes Kaposi's Sarcoma-Associated Herpesvirus Lytic Replication. J Virol 92.
38. Connolly PF, Fearnhead HO. 2017. Viral hijacking of host caspases: an emerging category of pathogen-host interactions. Cell Death Differ 24:1401-1410.

39. Kaufer S, Coffey CM, Parker JS. 2012. The cellular chaperone hsc70 is specifically recruited to reovirus viral factories independently of its chaperone function. J Virol 86:1079-89.
40. Stanifer ML, Kischnick C, Rippert A, Albrecht D, Boulant S. 2017. Reovirus inhibits interferon production by sequestering IRF3 into viral factories. Sci Rep 7:10873.
41. Tenorio R, Fernandez de Castro I, Knowlton JJ, Zamora PF, Lee CH, Mainou BA, Dermody TS, Risco C. 2018. Reovirus sigmaNS and muNS Proteins Remodel the Endoplasmic Reticulum to Build Replication Neo-Organelles. mBio 9.
42. Fernandez de Castro I, Zamora PF, Ooms L, Fernandez JJ, Lai CM, Mainou BA, Dermody TS, Risco C. 2014. Reovirus forms neo-organelles for progeny particle assembly within reorganized cell membranes. mBio 5.
43. Parker JS, Broering TJ, Kim J, Higgins DE, Nibert ML. 2002. Reovirus core protein mu2 determines the filamentous morphology of viral inclusion bodies by interacting with and stabilizing microtubules. J Virol 76:4483-96.